Special Issue on
RECENT ADVANCES IN SYNTHESIS,
CHARACTERIZATION, AND APPLICATIONS
OF CHEMICALLY BONDED PHASES

Edited by MIETEK JARONIEC
Separation and Surface Science Center
Kent State University
Kent, Ohio

Subscribe Today!

Use the cards below to subscribe to the *Journal of Liquid Chromatography & Related Technologies* **or to recommend the journal to your library for acquisition.**

Order Form

Journal of Liquid Chromatography & Related Technologies

Please enter my subscription to Vol. 19, 20 Numbers, 1996 at the ☐ institutional rate of $1595.00; ☐ individual rate of $797.50 *Individual subscriptions must be prepaid in American currency by personal check or credit card. Please add $3.50 per issue (number) for shipping outside the U.S. For airmail to Europe, add $5.50 per issue; to Asia, add $6.50 per issue. Canadian customers please add 7% GST.*

_____ Please send me a proforma invoice.
_____ Check enclosed made payable to Marcel Dekker, Inc.
_____ Charge my: ☐ MasterCard ☐ Visa ☐ American Express

Card No._____ Exp. Date_____

Signature_____

Name_____

Address_____

City/State/Zip_____

Does your library subscribe to the *Journal of Liquid Chromatography & Related Technologies*? Just complete this card and submit it to your librarian or department head.

Attention: Librarian/Department Head: I have examined the *Journal of Liquid Chromatography & Related Technologies* and would like to recommend the journal for acquisition.

Signature_____ Date_____

Name_____ Department_____

Journal of Liquid Chromatography & Related Technologies
Volume 19, 20 Numbers, 1996: $1595.00
ISSN: 1082–6076   CODEN: JLCTFC

Sample copy and proforma invoice available upon request.

Please contact the Promotion Department at:

Marcel Dekker, Inc.
270 Madison Avenue
New York, NY 10016
(212) 696-9000 phone
(212) 685-4540 fax

Subscribe Today!

Use the cards below to subscribe to the *Journal of Liquid Chromatography & Related Technologies* or to recommend the journal to your library for acquisition.

Journal of Liquid Chromatography & Related Technologies

Editor: **JACK CAZES**
               Cherry Hill, New Jersey

The *Journal of Liquid Chromatography & Related Technologies* now publishes an outstanding selection of critical, peer-reviewed papers dealing with analytical, preparative and process-scale liquid chromatography of all types and related technologies such as TLC; capillary electrophoresis; supercritical fluid extraction and chromatography; membrane separation technology; field-flow techniques; and others. As new separation technologies are introduced, they will also be included in the journal. On a regular basis, special topical issues are devoted to specific technologies and applications. Book reviews, software reviews, and schedules of meetings, symposiums and expositions are also included.

Formerly the *Journal of Liquid Chromatography*

JOURNAL OF LIQUID CHROMATOGRAPHY & RELATED TECHNOLOGIES

This journal is also available on CD-ROM through ADONIS^{TM} beginning with the 1991 volume year. For information contact: ADONIS, Marketing Services, P.O. Box 17005, 1001 JA Amsterdam, The Netherlands, Tel: +31-20-626-2629, Fax: +31-20-626-1437.

The journals of Marcel Dekker, Inc. are available in microform from: University Microfilms, Inc., 300 North Zeeb Road, Ann Arbor, Michigan 48106-1346, Telephone: 800-521-0600; Fax: (313) 761-1203.

Contributions to this journal are published free of charge.

Effective with Volume 6, Number 11, this journal is printed on acid-free paper.

RECENT ADVANCES IN SYNTHESIS, CHARACTERIZATION, AND APPLICATIONS OF CHEMICALLY BONDED PHASES

Edited by

Mietek Jaroniec
Separation and Surface Science Center
Department of Chemistry
Kent State University
Kent, Ohio 44242

JOURNAL OF LIQUID CHROMATOGRAPHY & RELATED TECHNOLOGIES

Volume 19, Numbers 17 & 18, 1996

Special Issue on
Recent Advances in Synthesis, Characterization, and
Applications of Chemically Bonded Phases

CONTENTS

CONTENTS

NEW EDITORIAL ADDRESS

Please note the following new editorial address for the

Journal of Liquid Chromatography
& Related Technologies

Effective July 10, 1996,
all correspondence, including manuscripts,
should be sent to

JLC & RT
Post Office Box 970210
Coconut Creek, FL 33097

Correspondence must be sent via mail services that
can deliver mail to a US Postal Service mailbox.

Mail sent via courier services,
e.g., United Parcel, Federal Express, DHL, etc.
cannot be delivered to a post office box.
Correspondence sent via these services
may be returned to the sender.

SILYLATION OF THE SILICA SURFACE A REVIEW

P. Van Der Voort* and E. F. Vansant

University of Antwerpen (U.I.A.)
Department of Chemistry
Laboratory of Inorganic Chemistry
Universiteitsplein 1
B-2610 Wilrijk (Antwerpen), Belgium

ABSTRACT

Silylated silica surfaces have found many applications in the field of analytical chemistry (HPLC, Ion Exchange Chromatography, Size Exclusion Chromatography, GC), synthetic chemistry (heterogeneous catalysts, phase transfer catalysts), biochemistry (enzyme immobilization, affinity chromatography) and industries (composites, high-tech materials, semiconductor devices).

In all cases, the knowledge of their chemical composition and surface characteristics is of great importance for the understanding and eventual improvement of their performance.

This review presents a general description of the silica surface and a summary of the different modification techniques that have been developed to silylate oxide surfaces. The chlorosilylation of the silica surface (in liquid and gaseous phase) and the modification with aminosilanes are discussed in more detail, emphasizing the analysis techniques and skills that enable researchers to get a more profound insight into the reaction mechanisms and the nature and concentration of the created surface groups.

Table 1

Surface Silanol Types with their ^{29}Si CP MAS NMR and FTIR Peak Positions and Names
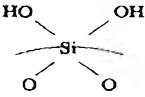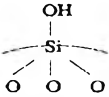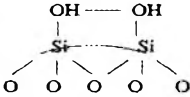
	Geminal	**Isolated**	**Vicinal**
Si-NMR	Q2	Q3	Q3
	-94 ppm	-100 ppm	-100 ppm
FTIR	3743 cm^{-1}	3743 cm^{-1}	3660 cm^{-1}
	free	free	bridged

1. The Surface of Silica - Quantification of the Silanol Types as a Function of Temperature

The ultimate particles which make up the silicas can be regarded as polymers of silicic acid, consisting of interlinked SiO_4 tetrahedra. At the surface, the structure terminates in either a *siloxane group* ($\equiv$Si-O-Si$\equiv$) with the oxygen on the surface, or one of several forms of *silanol groups* ($\equiv$Si-OH). The silanols can be divided into *isolated* groups (or *free silanols*), where the surface silicon atom has three bonds into the bulk structure and the fourth bond attached to a single OH group, and *vicinal silanols* (or *bridged silanols*), where two single silanol groups, attached to different silicon atoms, are close enough to hydrogen bond.

A third type of silanols, *geminal silanols*, consist of two hydroxyl groups, that are attached to one silicon atom. The geminal silanols are too close to hydrogen bond to each other,[2] whereas the free hydroxyl groups are too far separated. These different silanol types, together with their infrared and ^{29}Si NMR attributes are shown in Table 1.

Since silanols play an important role in all surface modifications, a thorough understanding of the absolute number of silanols and the relative distribution of the silanol types is very important. A very large number of publications has appeared on the distribution of these various silanol types as a function of pretreatment temperature of the silica. We have recently evaluated the most important of these models[1] and have come to an average distribution of silanol types, shown in Figure 1.

Silanol number (OH/nm^2)

In Vacuo
■ *total hydroxyls;* + *geminal silanols;* * *isolated silanols;* □ *vicinal silanols.*

Temperature (K)

Substrate
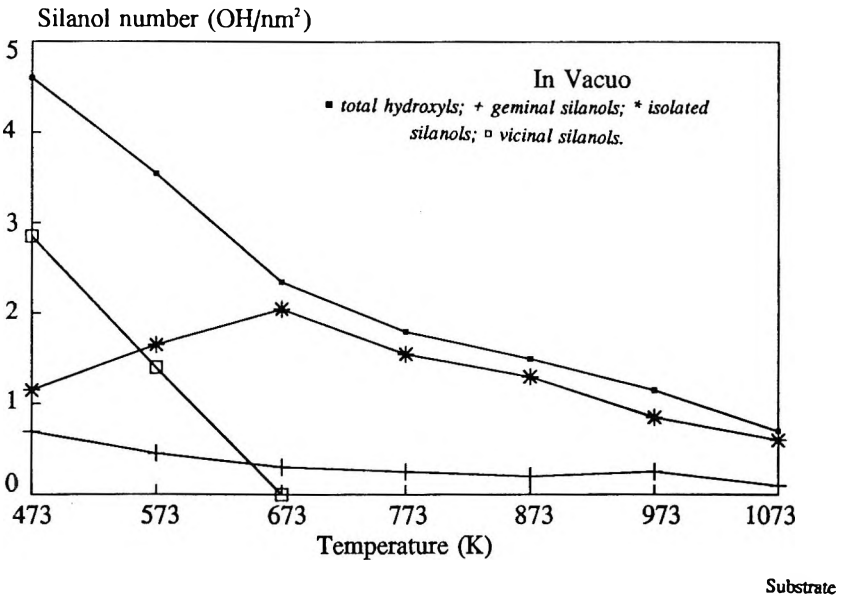
Figure 1. Silanol type distribution as a function of pretreatment temperature. In vacuo.

2. Silylation of the Silica Surface: Modification Procedures

In the selection of a chemical modification procedure, two criteria have to be considered.

(i) the aimed coating morphology; and

(ii) the scale on which the modification has to be performed.

The coating morphology includes layer thickness (mono- or multi-layer), the modification density (molecules/nm^2), the orientations of the surface molecules, and the type of interaction of the coating layer with the surface (relative amount physisorption/chemisorption).

The procedures used for the chemical modification of silica will be discussed using these criteria. This survey is restricted to the preparation of chemically modified silicas, used as a base material in the above-cited applications. Procedures are ordered according to the possibility to control the ultimately formed layer.
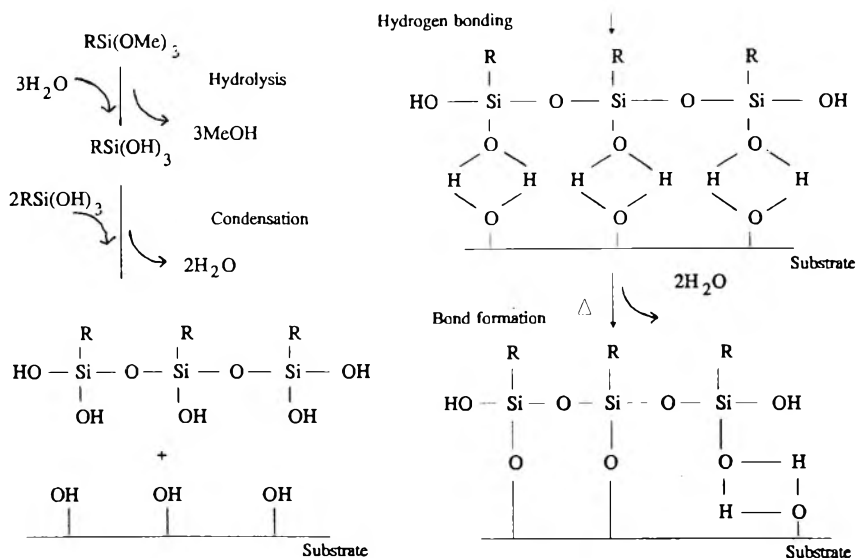
Figure 2. Mechanism of silane deposition in aqueous solvent.

Sol-gel

The incorporation of organofunctional groups on the silica surface may be effected during the synthesis of the silica material. The addition of organofunctional alkoxysilanes to the TEOS (tetraethoxysilane) solution in the sol-gel process, produces functionalized silica gels. This procedure does not allow a careful control of the resultant surface morphology. Since the relative amounts of silane and TEOS are the only variable parameters, neither layer thickness, nor modification density can be precisely tuned. This results in an irreproducible functionalization of the surface.

Aqueous Solvent

The preparation of organofunctional silica gels on an industrial scale is performed by liquid phase reaction. As a solvent, water, a water/ethanol or water/acetone mixture is used. Chlorosilanes or alkoxysilanes are used for this type of modification.

In the aqueous solvent, the silanes undergo hydrolysis and condensation before deposition on the surface[3] (Figure 2). In contact with water, halogen or alkoxy groups are hydrolyzed. The as-formed silanol groups go into hydrogen-bonding interactions with neighbouring hydrolyzed silane molecules and with surface silanol groups. Siloxane bonds are formed, with release of water. The coating molecules are polymerized horizontally as well as vertically. Thus, a three-dimensional polymeric silane network is formed on the silica surface.

The polymerization reactions are hard to control and a layer of unreproducible thickness results. The control is ameliorated with the addition of a variable amount of a polar organic solvent, such as ethanol or acetone. Ethanol/water mixtures in a 70%/30% ratio are commonly used.

Covalent bond formation is not an immediate process. Silane coating layers consist of physisorbed as well as chemisorbed molecules. Physisorbed molecules go into condensation only slowly and chemical stabilization of the coating layer requires a post-reaction curing step. In this step, the modified substrate is thermally treated at temperatures generally in the 353 - 473 °K range.

Organic solvent

If modification with chlorosilanes or alkoxysilanes is performed in completely dry conditions (dry organic solvent, dehydrated surface), hydrolysis is prevented. Chemical bonding with the substrate should result from the direct condensation of the chloro- or alkoxy groups with the surface silanols. From experiments using methoxymethylsilanes, Blitz[2] concluded that this direct condensation does not take place. Post-reaction curing only results in evaporation of the adsorbed molecules. Alkoxysilanes may only bond chemically to the silica surface if water is present at the interface. Thus adsorbed silane molecules are hydrolyzed before reaction with the surface. Hydrolysis, however also causes polymerization and, therefore, non-monolayer coverages are obtained.

Another way to realize the direct condensation is by using ammonia as a catalyst. Blitz and coworkers[5] studied the reactions of methoxymethylsilanes with silica in a dry toluene medium in the presence of ammonia. They found that high-temperature post-reaction curing is unnecessary for silylation to occur on the silica surfaces (either wet or dry) in the presence of ammonia. Monolayer or greater than monolayer surface coverage is obtained when ammonia is present and is about 12 times the surface coverage obtained in the absence of ammonia. In Figures 3 a and b, two possible mechanisms of ammonia catalysis are proposed.[6]
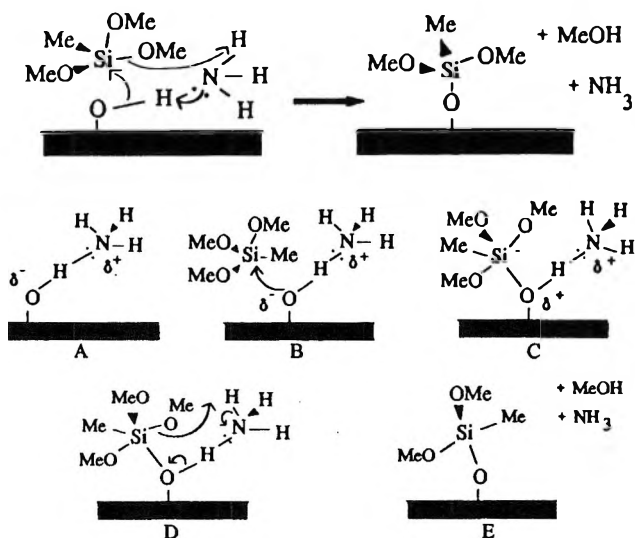
Figure 3. (a) Amine catalysis of silylation reaction, mechanism #1; (b) Amine catalysis of silylation reaction, mechanism #2.
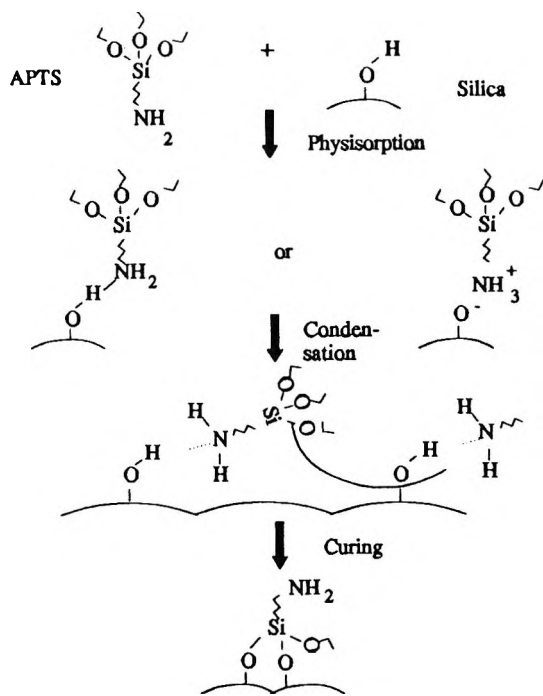
Figure 4. Modifcation of silica gel with APTS.

In the first mechanism (Figure 3a) the transition state involves the formation of a low-energetic six-membered ring. The second mechanism (Figure 3b) proceeds by the formation of a pentacoordinate intermediate, after nucleophilic attack of the ammonia at the silicon atom.

Aminosilanes contain the catalyzing amine function in the organic chain. The reaction of aminosilanes with silica gel in dry conditions is therefore self-catalyzed. They show direct condensation, even in completely dry conditions. Upon addition of the aminosilane to the silica substrate, the amine group may form hydrogen bonds or proton transfer complexes with the surface silanols. This results in a very fast adsorption, followed by direct condensation. This reaction mechanism of APTS (γ-aminopropyltriethoxysilane) with silica gel in dry conditions, is shown in Figure 4. After liquid phase reaction, the filtered substrate is cured in order to consolidate the modification layer.

Self-Assembled Monolayers

Among the liquid phase adsorption procedures, Self-Assembled Monolayers (SAMs) take a special place. This type of monolayer originated as an extension of Langmuir-Blodgett film technology.[7] In this latter technique, highly ordered films of large polar molecules are deposited on flat surfaces. Being obtained as insoluble ordered floating films on the surface of a liquid, Langmuir-Blodgett monolayer films are transferred onto solid supports, from the water-gas interface, by dipping or immersion of the substrate (Figure 5).

In the formation of SAMs, the film-forming molecules order themselves by chemical interaction with neighbouring molecules and with the substrate surface. This technique has been applied for a large variety of modifier/substrate combinations. Various sulphur compounds, such as alkanethiols and (di)sulfides have been deposited on metals such as silver, copper and gold; isocyanides on platinum and carboxylic acids on aluminum oxide and silver oxide.[8] Alkyltrichlorosilanes have been deposited on gold, mica, aluminum, tin oxide and silicon oxide. The latter combination is of interest here.

The main feature of the technique is the deposition of the coating molecules from organic solvent onto a cleaned hydrated surface. As a solvent dicyclohexyl, ethanol, n-hexadecane and n-heptane are used. In a typical synthesis procedure, the silica is first cleaned to remove all trace organic compounds. This cleaning step appears to be crucial in the formation of smooth, complete monolayers, especially on metal surfaces. Cleaning is performed by boiling in nitric acid or hydrogenperoxide/sulphuric acid ('piranha') solution. The cleaning step is followed by a careful rinse with distilled water and drying in a stream of dry nitrogen.
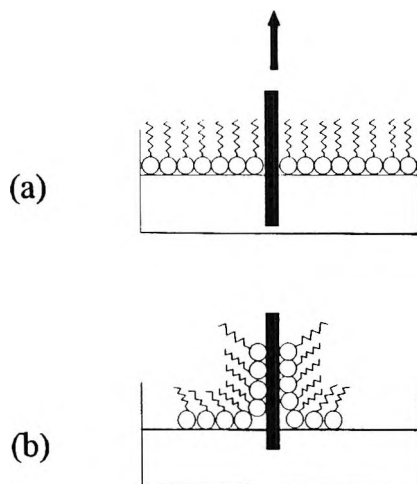
Figure 5. Langmuir-Blodgett film formation on a solid support by transfer of a film at liquid-gas interface (a) to solid-gas (b) interface.
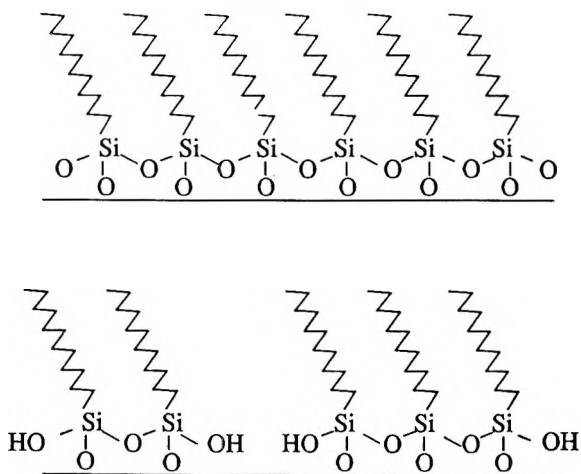
Figure 6. Schematic drawings of self-assembled monolayer (upper) and conventional monolayer. Taken from ref 11, with permission.

The silica may be rehydrated by exposure to air, with controlled humidity, shortly before use. Whereas the modification of flat solid substrates involves an immersion/retraction procedure, this is not possible for powdered substrates such as silica gel. Therefore, these are stirred in the reagent solution, filtered or decanted and rinsed with the pure solvent. Detailed descriptions of the reaction conditions may be found in the literature.[7,9,10]

The SAM is formed by using only the monolayer of surface water on the silica gel. Since no excess water is present, the polymerization reaction is strictly under control. Additionally, the water is present at the place where the surface bond has to be formed.

Thus-formed SAM's are densely packed, ordered films, attached to the surface with chemical bonds. Alkyl chains are aligned paralel in a densely packed fashion. The surface is fully covered, irrespective of the number of hydroxyl groups. Not all silane molecules are covalently linked to the surface. Le Grange et al.[9] evidenced that on a dehydrated surface that was exposed to moisture, 1 in 5 octadecylchlorosilane molecules is bonded to the surface. Due to this dense structure and full surface coverage, this type of layer is clearly different from other wet modification methods. In Figure 6 the structure of a self-assembled monolayer is compared to that of a conventional polymeric layer.

Wirth and Fatunmbi[11] defined the bonding of trifunctional silanes as self-assembly, when the bonding density of functional groups is made to be close-packed, approximately 8 μmol/m^2 (2.2 nm^2/chain). Conventional polymeric phases are no more than 5 μmol/m^2. Because of their close packing, these phases are very well suited for chromatographic separations, since all interference of surface hydroxyls is excluded. In order to avoid over-crowding of the alkyl chains, but to retain the advantages of molecular self-assembly, mixed phases of long and short chain alkyls have been prepared. As one of such possible combinations, C$_3$ chains have been mixed with C$_{18}$.[12]

Vapour-Phase Reactions

Modification of silica gel with volatile or gaseous compounds is performed in the vapour phase. Industrial-scale reactors and laboratory scale gas adsorption apparatus have been used. In the industrial field, fluidized bed and fluid mill reactors are of main importance.

For laboratory-scale modification, distinction has to be made between static and dynamic adsorption procedures. In a static procedure, the substrate is contacted with a known volume of gas at a well-defined pressure. The modifying gas may be

stationary or circulating in a closed loop. Modification in a static gas adsorption apparatus allows the careful control of all reaction parameters. Temperature and pressure can be controlled and easily measured. Adsorption kinetics may be determined by following the pressure as a function of the reaction time.

In the dynamic gas modification procedure, the reacting gas is passed through the substrate and dissipated. Temperature and gas flow may be controlled, with the limitation of pressure build-up at the substrate site. Relatively large amounts of gas may be passed through the sample.

The main difference between the two procedures is the type of control of the reaction mechanism. For static reactions, the reaction velocity is controlled thermodynamically. In this case, the velocity is mainly controlled by the equilibrium constants for the reactions at a given pressure. In the dynamic regime, on the other hand, a more intimate contact between reagent and substrate occurs. Moreover, gaseous reaction products are captured constantly and the overall process is under kinetic control. Detailed experiments on the difference in kinetics between the two processes have been performed by Yongan.[13]

Hydrolysis and condensation behaviour are analogous to modification procedures in dry organic solvent. However, controlled gas phase procedures allow a better control of reaction conditions, leading to a more reproducible coating layer. While the possibility to form true monolayered coatings from solution has been doubted,[14,15] gas phase modification is generally agreed to give monolayer modification.

3. Modification of the Silica Surface with (Alkyl)Chlorosilanes

Strangely enough, a unified approach to the reactions of chlorosilanes with the silica surface is lacking in the international literature. This is probably due to the different reaction procedures that have been used and the different applications of the modified silica surfaces.

The high vapour pressure of the (methyl)chlorosilanes allows for a vapour-phase reaction. Moreover, these reactions are usually performed on amorphous silica with a high surface area, which is very suitable for a detailed study of the surface species by means of FTIR, XPS and NMR.

The higher order alkylchlorosilanes (C_8 and C_{18}) have historically been treated in the same way as organosilanes. The reaction inevitably occurs in the liquid phase and is usually followed by a curing step. The extremely low surface of the silicon wafers and the deposited SiO_2 layers used for self-assembled-monolayers does not
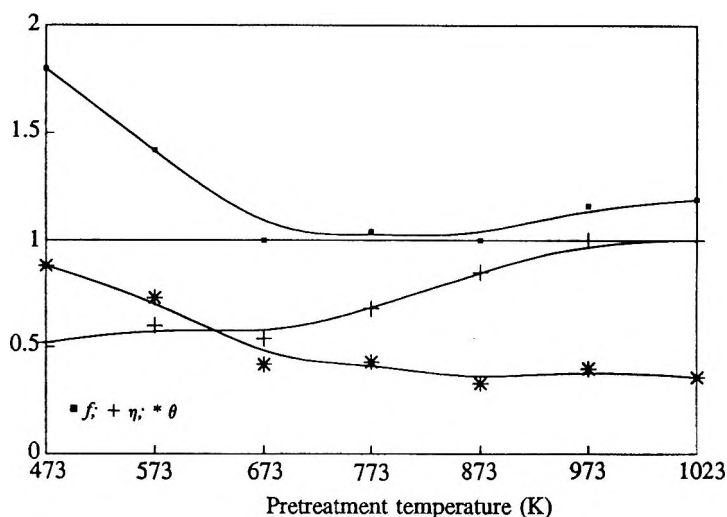
Figure 7. Effectiveness, surface coverage and stoichiometry factor for the reaction of silica gel with TCS. Reactions occured at 623 K for 1h.

allow a spectroscopic quantification of the surface species. A completely different type of analysis technique is used here mainly to determine the quality (roughness and uniformity), the adherence (parallel or at random) and the hydrophobicity of the coated layer. Often used techniques are AFM (Atomic Force Microscopy), ellipsometry and chromatography.

3.1. Vapour-Phase Reactions with (Methyl)Chlorosilanes

The reactions between (methyl)chlorosilanes and the surface of silica have been investigated by many researchers, primarily because of the utility of these reagents as coupling agents in polymer chemistry and as surface deactivating agents in chromatography.

Few studies are devoted to the reaction of silica with trichlorosilane (TCS). The earliest report, dealing specifically with the TCS modification of silica, is the one of Chuiko et al.[16] A silica, pretreated at 673 °K, was reacted with TCS vapour at room temperature. The authors observed a complete disappearance of the free hydroxyl groups, due to reaction (A).

$$\equiv Si - OH \quad + \quad \underset{Cl}{\overset{Cl}{\diagdown}}Si\underset{Cl}{\overset{H}{\diagup}} \quad \longrightarrow \quad \equiv Si - O - Si - H \underset{Cl}{\overset{Cl}{<}} \quad + HCl \qquad (A)$$

They claimed that, under these conditions, a bimolecular reaction with two silanols is not possible, due to steric reasons. The distance between 2 Cl groups in trichlorosilane is 0.33 nm, whereas the mean distance between 2 OH groups on a silica surface, annealed at 673 °K, is considerably larger.

Low[17] refined Chuiko's findings in 1981. He confirmed the statement that bimolecular reactions are not likely to occur at high pretreatment temperatures, but he suggested a secondary, (consecutive) reaction (B):

$$\begin{array}{l} \equiv Si - O - Si \overset{Cl}{\underset{Cl}{<}} H \\[2mm] \equiv Si - OH \end{array} \quad \longrightarrow \quad \begin{array}{l} \equiv Si - O \\ \qquad\qquad\diagdown \\ \qquad\qquad Si \\ \equiv Si - O \diagup \quad \diagdown Cl \end{array}\overset{H}{}\ + HCl \qquad (B)$$
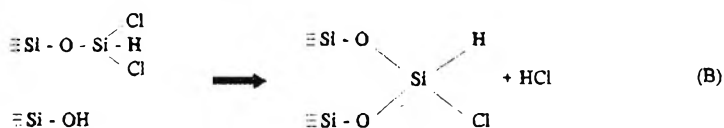
He also suggested a side reaction (C) with so-called *strained* siloxane bridges.

$$\begin{array}{l} \equiv Si \\ \qquad \diagdown \\ \qquad\quad O \\ \equiv Si \diagup \end{array} + \underset{Cl}{\overset{Cl}{\diagdown}}Si\underset{Cl}{\overset{H}{\diagup}} \quad \longrightarrow \quad \begin{array}{l} \equiv Si - Cl \\[2mm] \qquad\qquad Cl \\ \equiv Si - O - Si - H \\ \qquad\qquad Cl \end{array} \qquad (C)$$
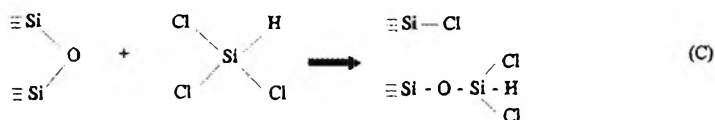
In the meantime, many articles were published on the reaction of methylchlorosilanes with silica. Especially the publications of Hair and co-workers[18-22] have gained widespread attention. Using infrared band integration of the hydroxyl region, and putting the normalized data into the integrated form of the rate equation, they found that all polyfunctional methylchlorosilanes followed a reaction order of 1.6 at a reaction temperature of 573 °K. This means that 60% of the silane reacts bifunctionally. The bimolecular reaction of trichlorosilane with silica is presented as reaction (D):

$$\begin{array}{l} \equiv Si - OH \\[4mm] \qquad\qquad + \\[4mm] \equiv Si - OH \end{array} \quad \underset{Cl}{\overset{Cl}{\diagdown}}Si\underset{Cl}{\overset{H}{\diagup}} \quad \longrightarrow \quad \begin{array}{l} \equiv Si - O \\ \qquad\qquad\diagdown \\ \qquad\qquad Si \\ \equiv Si - O \diagup \quad \diagdown Cl \end{array}\overset{H}{}\ + 2\ HCl \qquad (D)$$
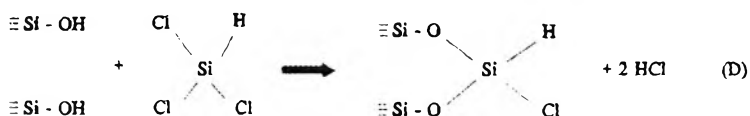
In addition to this reaction, they noticed a positive intercept in the fitting of the experimental data by the rate equation, and ascribed this effect to an initial fast reaction (E):

$$\equiv Si\text{-}OH \quad + \quad \underset{Cl \quad\nearrow\quad H}{\overset{Cl \quad\nwarrow\quad Cl}{Si}} \quad \longrightarrow \quad \equiv Si\text{-}Cl \quad + \quad \underset{Cl \quad\nearrow\quad H}{\overset{OH \quad\nwarrow\quad Cl}{Si}} \qquad (E)$$
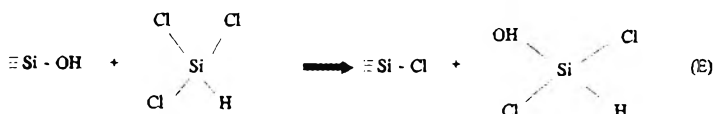
In his kinetic plots, Hair only considered a monomolecular reaction (A), and a bimolecular reaction (D). He never mentioned the secondary reaction (B) or the side reaction (C). Although his general conclusions on the stoichiometry of the reaction may be correct, it is not excluded that other reactions than the two he mentioned are involved.

Summarizing, the study of the chlorosilylation of the silica surface has given rise to five possible reaction mechanisms, that are believed to occur simultaneously or consecutively. In order to quantify all five mechanisms, the researcher needs at least five independently measurable and quantifyable parameters. However, there are often fewer independently measurable parameters than unknowns. In these cases, only semi-quantitative data can be obtained.

One possible way to optimize such a chemical modification, is to express the experimental data in terms of effectiveness, surface coverage and stoichiometry.

2.1.2. Effectiveness, Surface Coverage and Stoichiometry[23]

In the case of a chemical modification of silica, the ratio of the number of hydroxyl groups undergoing reaction ($n_{OH(r)}$) to the total number of initial hydroxyl groups ($n_{OH(t)}$) reflects the effectiveness factor η. If the specific surface area (S_{BET}) of the silica sample does not change during the reaction, the effectiveness factor can also be expressed as a ratio of the number of silanols per nm^2 (α_{OH}).

$$\eta = \frac{n_{OH_{(r)}}\left[mmol/g\right]}{n_{OH_{(t)}}\left[mmol/g\right]} = \frac{\alpha_{OH_{(r)}}\left[\#/nm^2\right]}{\alpha_{OH_{(t)}}\left[\#/nm^2\right]} \tag{1}$$

However, using η as the only parameter in the optimization can often be misleading, since the maximum degree of conversion is not only determined by the number of reacting hydroxyl groups, but also by the mean cross-sectional area (A_m)

of the reacted group (steric hindrance effects). The surface coverage (θ) is defined as the ratio of the actual bonded species on the surface to the maximum number of bonded species that is sterically possible.

$$\theta = \frac{\alpha_{exp}}{\alpha_{max}} = A_{m} \bullet \alpha_{exp} \tag{2}$$

Effectiveness and surface coverage are only indices for the amount of silanols that have reacted. Depending on the functionality of the modifier, various reaction mechanisms can take place.

A third parameter has to be introduced, yielding information on the different kinds of surface species. A factor f, reflecting the stoichiometry of the reaction, can be defined as:

$$f = \frac{n_{OH_{(r)}}}{n_{modifier_{(r)}}} = \frac{\alpha_{OH_{(r)}}}{\alpha_{modifier_{(r)}}} \tag{3}$$

For a monomolecular reaction, f is 1. For a completely bimolecular reaction, where 2 silanol molecules react with one molecule of modifier, $f = 2$.

Let us now apply these general formulae to the chemisorption of trichlorosilane on silica. Assuming that the reaction of trichlorosilane with silica gel only causes monodentate (reaction (A)) and bidentate (reactions (B) and (D)) species, the general formulae for effectiveness, surface coverage and stoichiometry can be rewritten in function of $OH_{(r)}$ (number of reacted silanols, quantified by FTIR spectroscopy[23-25] and Cl on the surface.

Since in the reaction (A), 1 silane linkage includes 2 Cl groups and for a bidentate species, 2 silane links include 1 Cl group, one can write:

$$\frac{Cl}{OH_{(r)}} = \frac{2MS + BS}{MS + 2BS} = \frac{2 - BS}{1 + BS} \tag{4}$$

where BS stands for the percentage of bidentate species and MS for the percentage of monodentate species. The monodentate species can be substituted in Equation (4), following the initial assumption that MS + BS = 1.

Rewriting Equation (4) as a function of BS, one obtains:

$$BS = \frac{2 - \dfrac{Cl}{OH_{(r)}}}{1 + \dfrac{Cl}{OH_{(r)}}}$$ (5)

Formula (3) for the stoichiometry factor can then be actualized for the TCS chemisorption as:

$$f = \frac{OH_{(r)}}{\left[(1 - BS) \bullet OH_{(r)}\right] + \left[BS \bullet \dfrac{OH_{(r)}}{2}\right]}$$ (6)

When optimizing the surface modification, the first important factor to consider is the effectiveness. The pretreatment temperature of the silica, the reaction temperature and reaction time must be controlled to yield an effectiveness of 1. Remaining hydroxyl groups on the surface of silica gel are highly undesirable, since they would cause uncontrollable side-effects in the following reaction steps.

Of all conditions, yielding an O of 1, those must be chosen which produce the highest amount of reactive chlorine groups. This means that the surface coverage must be as high as possible, and that the stoichiometry must approach unity.

Figure 7 shows the three parameters as a function of the pretreatment temperature of the silica. All reactions occurred at 623 °K for 1 h. The surface coverage curve is decreasing as a function of pretreatment temperature. A maximal surface coverage is only possible at pretreatment temperatures below 673 °K. However, as can be inferred from the figure, this situation is never achieved. Therefore, it is recommendable to study the effectiveness curve. An effectiveness of 1. a very important condition to avoid unreacted silanol groups, only occurs at pretreatment temperatures of 973 °K or higher. Based on these two curves, a pretreatment temperature of 973 °K seems to be the best choice: it is the lowest temperature (highest amount of reactable silanols) at which complete silylation occurs.

The stoichiometry curve can be subdivided into three regions. In the temperature region between 473 °K and 673 °K, bimolecular and/or secondary reactions are sterically possible. The stoichiometry factor of 1.6, found by Hair[21] for the reaction of silica, pretreated at 573 °K, with methyltrichlorosilane, is reflected in
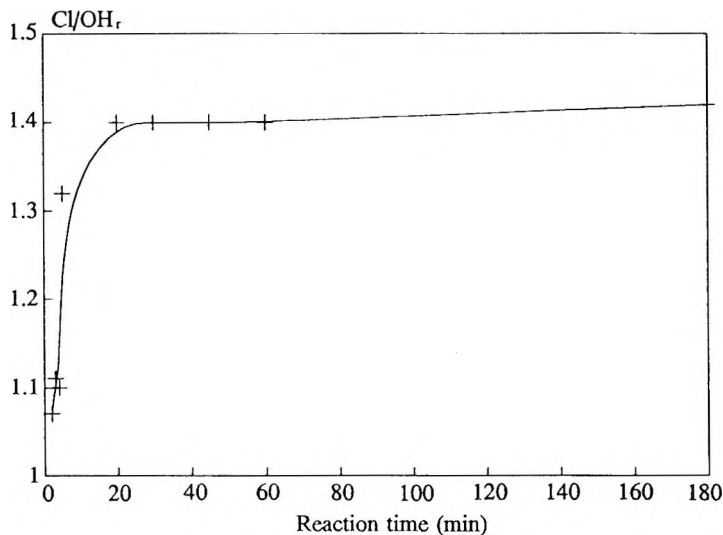
Figure 8. The ratio Cl over OH (reacted) for the reaction of Kieselgel 60 (pretreated at 973 K) with TCS (at 623 K) as a function of reaction time.

these experiments. Equation (6) proves to be a very useful formula for a relatively fast evaluation of the stoichiometry factor, provided that the initial condition (MS + BS = 1) is fulfilled. The question whether these secondary species originate from bimolecular or secondary reactions, cannot be solved by this curve. In the temperature region 673 °K-873 °K, the silanols are too far separated to be involved in secondary or bimolecular reactions. In this region the stoichiometry factor is obviously 1.

In the pretreatment region above 873 °K, the silanol loading on the surface is very low (cfr. Figure 1) and the formation of bidentate species is excluded for steric reasons.[23] In this temperature region, f has no longer a physical meaning, since the condition MS+BS=1 is no longer fulfilled, and side reactions (C) and (E) have to be considered.

Figure 8 shows the ratio Cl/OH$_r$ for the reaction on Kieselgel 60 (pretreated at 973 °K) with TCS at 623 °K at different reaction times. During the first 5 minutes of the reaction, this ratio is close to 1, meaning that 1 OH is replaced by 1 Cl group. It seems very unlikely that this value is due to a combination of primary and

secondary reactions.[23]   Therefore, this value is most probably caused by the reaction (E). This reaction indeed yields a Cl/OH value of 1. So, Figure 8 confirms Hair's statement that reaction (E) should be considered as a *fast initial reaction*.

Reaction with Strained Siloxane Bridges

The above does not mean that reaction (C) with the siloxane bridges does not occur. On the contrary, it is possible to present a number of arguments that suggest a reaction with strained siloxane bridges at high pretreatment temperature of the silica. Not only the *concentration* of the siloxane bridges increases with rising pretreatment temperatures, they also show an enhanced *reactivity*. It is assumed that with higher degassing temperatures, the remaining isolated hydroxyls are progressively removed and that various types of structural changes must occur, giving rise to the so-called *strained* siloxane bridges, which exhibit an enhanced activity. Morrow[26] stated that site is assumed to be an unsymmetrical siloxane bridge, containing an electron deficient silicon atom, which can act as a Lewis acid centre.

A relatively easy way to check the existence of a reaction with strained siloxane bridges is to replace and/or block all surface hydroxyl groups by a reaction with hexamethyldisilazane. In this way, we were able to prove that reaction with strained siloxane bridges occurs at reaction temperatures > 623 °K and pretreatment temperatures > 973 °K.[23]

3.2 Liquid-Phase Reaction with Alkylchlorosilanes (C_8 - C_{18})

The formation of monolayers by self-assembly of organochlorosilanes on various surfaces[27-30] and organosulfur compounds on gold[31,32] is well established. The durability of the self-assembled monolayer is highly dependent on the effectiveness of the anchoring to the surface. On gold, the attachment to the surface is due to an interaction of sulphur end groups with the gold surface. However, the nature of the attachment of the organochlorosilane with the surface is ill-defined.[33-35]

Octadecyltrichlorosilane ($C_{18}H_{37}SiCl_3$, henceforth denoted OTS) is the most common organosilane used for the formation of self-assembled monolayers and, when reacted with silica surface, finds extensive use as a bonded phase in liquid chromatography applications.[36] A common mechanism proposed for attachment of the chlorosilane to the surface[33,37] involves the hydrolysis of the chlorosilane groups with water which is already on the surface of the substrate.

The silanols which are formed then condense with the surface hydroxyls groups to form stable linkages to the substrate. In practice, a curing process is usually required to condense adjacent silanols attached to the organosilane to form a cross-linked 'mat' on the surface. Part of the difficulty in determining the nature of the attachment to the surface arises from the lack of direct spectral evidence, due to the low surface areas of the substrates.

In 1992 Tripp and Hair[38] unified the two chlorosilane approaches by reacting OTS with a high surface area amorphous silica gel, in order to probe spectroscopically the different surface species. Using a home-made *in situ* liquid infrared cell, they derived following conclusions:

> 1. OTS does not react with degassed silica at room temperature. The infrared band of the free hydroxyls shifts to 3690 cm^{-1} but does not change in intensity. This indicates that the chlorosilane is physisorbed (H-bridged) on the silica surface. Subsequent degassing removes all adsorbed species.

> This conclusion is not surprising. Also, (methyl)chlorosilanes do not react with the silica surface at room temperature. Reaction temperatures > 473 °K are required to achieve noticeable reaction. The boiling point of octadecyltrichlorosilane is 433 °K. It would be very interesting to see what happens at reflux temperature.

> 2. OTS does react slightly with 'wet' silica at room temperature, containing multilayers of water on the surface. The broad band at 3650 cm^{-1} decreases slightly, and a band at 3350 cm^{-1} arises, attributed to trisilanols.[39,40] Tripp and Hair[38] state that the first layer of water is strongly bonded to the surface and does not participate in the hydrolysis of the chlorosilane headgroup of the OTS molecule.

> Subsequent layers would be less strongly bonded to the surface and would be able to participate in direct hydrolysis of the OTS.

Since the hydrolysis and adsorption of the OTS occurs with the subsequent layers of water, an optimum level is necessary to form robust films: too little water results in the formation of an incomplete monolayer, whereas a thick water layer causes a polymerization of the OTS with the water, resulting in a very poor adherence to the silica surface.

Not only octadecyltrichlorosilane is unreactive towards dry silica at room temperature. This is also the case for the chlorosilanes and the methylchlorosilanes. It was stated earlier that the vapour phase reaction occurs at elevated temperatures (> 473 °K). This high-temperature constraint limits potential gas phase silanizing agents to those which have a high thermal stability and sufficient vapour pressure.

In practice, the common method for silanization of silica is to mix a chlorosilane with a hydrated silica in a suitable organic solvent. A common mechanism reported for this reaction is that the chlorosilane is first hydrolyzed by the water and this is followed by the condensation with the surface hydroxyl groups to form a strong Si-O-Si surface bond.[37]

If the starting silane contains a trichlorosilyl headgroup, then further condensation between adjacent silanes can occur, yielding a two-dimensional polysiloxane network. The occurrence of the first step, the hydrolysis of the chlorosilane to a silanol by the surface water is amply supported by the literature.[33,34,38,41]

At either the solid/gas or solid/liquid interface the chlorosilane does not adsorb onto a completely dehydrated silica and is hydrolyzed to the silanol with the surface water of a hydrated silica.

However, Tripp and Hair[42] have shown that the second critical step (i.e. condensation of the silanol with the surface hydroxyls groups) does not occur. At the solid/gas interface, the silanol adsorbs on the surface but does not undergo condensation or polymerization, whereas at the solid/liquid interface, the silanol polymerizes in solution and adsorbs on the surface.

In neither case there is a strong Si_s-O-Si bond formed with the substrate. It is the absence of Si_s-O-Si surface linkages that is responsible for the general lack of robustness of silanized surfaces prepared from solution.

In a subsequent publication, Tripp and Hair[43] describe a new method to chemically bind chlorosilanes to the surface under mild reaction conditions. In fact, there are two possible ways for a base-catalyzed chemisorption of chlorosilanes on silica.

One possible strategy is to use a base to promote the reaction of chlorosilanes with the surface silanols.

In essence, this reaction proceeds by a one-stage nucleophilic mechanism through the formation of a pentacoordinate silicon intermediate (reaction (F)).

$$R_3SiCl + Nu \longrightarrow \left[\begin{matrix} R \quad Cl \\ \searrow | \\ Si - R \\ \nearrow | \\ R \quad\; Nu \end{matrix} \right] \qquad\qquad (F)$$
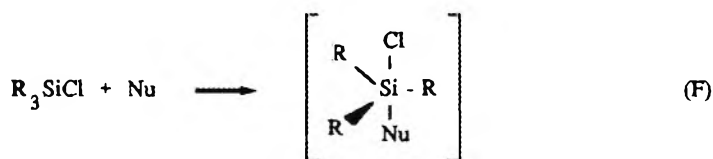
The Si-Cl bond is lengthened in the intermediate and is susceptible to attack by a second nucleophile:[44]

$$\left[\begin{matrix} R \quad Cl \\ \searrow | \\ Si - R \\ \nearrow | \\ R \quad\; Nu \end{matrix} \right] + \equiv Si\text{-}OH \longrightarrow \equiv Si\text{-}OSiR_3 + HCl + Nu \quad (G)$$
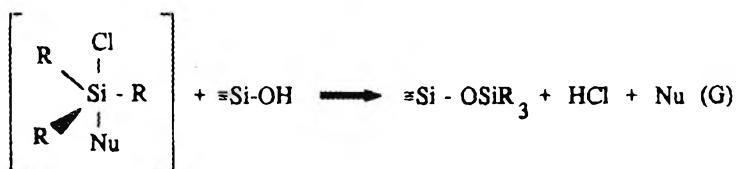
An alternative mechanism for the base-promoted reaction of silanes with silica has been described by Blitz et al.[45] In this mechanism, the base attacks directly to the surface silanols. The bonded amine renders the silanol more nucleophilic which then attacks the silicon atom of an approaching silane, giving rise to a pentacoordinate intermediate.

(H)
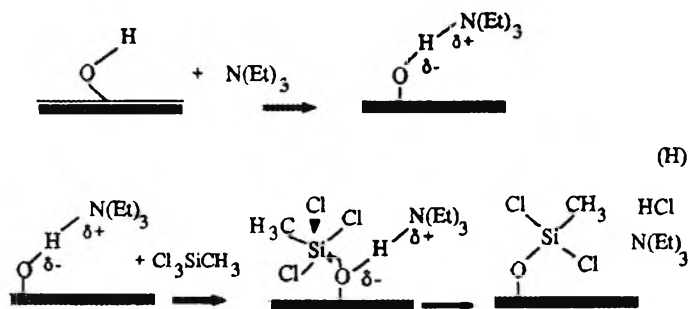
In both mechanisms a pentacoordinate intermediate is postulated. The main difference is that the pentacoordinate intermediate is formed by attachment of the amine to the chlorosilane in one case and by attachment to a surface Si-O group in the other. The main problem associated with base-catalized silanization is that it is very difficult to prevent polymerization of the silane in solution. Rapid polymerization of the chlorosilane occurs in solution unless extreme precautions are taken to exclude contact with residual water.

Thus, in a typical base-promoted silanization on silica, it is more likely that both polymerization and surface reaction occur to some extent. Both mechanisms can account for polymerization. The intermediate formed by attachment of the amine to the chlorosilane could react with nucleophiles (i.e., molecular water) other than the surface silanols. In the mechanism described by Blitz et al., the chlorosilane (either attached or in solution) could be hydrolyzed to the trisilanol by molecular water and the trisilanol offers an additional source of silanols for base attachment and subsequent polymerization. Polymerization often results in a thick silane layer on the surface that, in many cases, is undesirable.

Polymerization is not possible in the complete absence of water or when reactions are carried out using monochlorosilanes. However, trichlorosilanes are attractive because it is possible to increase the strength of the adsorbed silane layer through cross-linking between adjacent molecules. The other approach, the exclusion of trace quantities of water, especially in solution, is extremely difficult and costly.

In 1993, Tripp and Hair[43] described a method to promote the direct reaction of the chlorosilyl headgroup with the surface hydroxyls groups, using a nitrogen-containing base (triethylamine). In this method, polymerization is avoided because the base and chlorosilane are not added simultaneously but subsequentially in a two-step process.

4. Modification of the silica surface with Aminosilanes

For a fundamental understanding of the processes occurring during the modification, a distinction has to be made between processes taking place in the reaction step and in the post-reaction curing.

In the reaction phase, three types of interaction of the aminosilane molecule (in this case APTS, γ-aminopropyltriethoxysilane; $(CH_3CH_2O)_3Si-CH_2CH_2CH_2NH_2$) with the silica surface have been reported[46,47] (Figure 9). The amine may enter into a hydrogen bonding interaction with a surface hydroxyl group. The basic amine may abstract a proton from a silanol group and form an ionic bond. This type of interaction is much more stable than the first one. The hydrogen-bonded molecules may self-catalyze the condensation of the silicon side of the silane molecule. Thus, a covalent siloxane bond is formed.

In order to determine the extent of all three of the interaction types in the reaction phase, a leaching test was performed on a non-cured sample.[48,49] Upon stirring in ethanol, the weakly bonded silane molecules desorb and the amount is
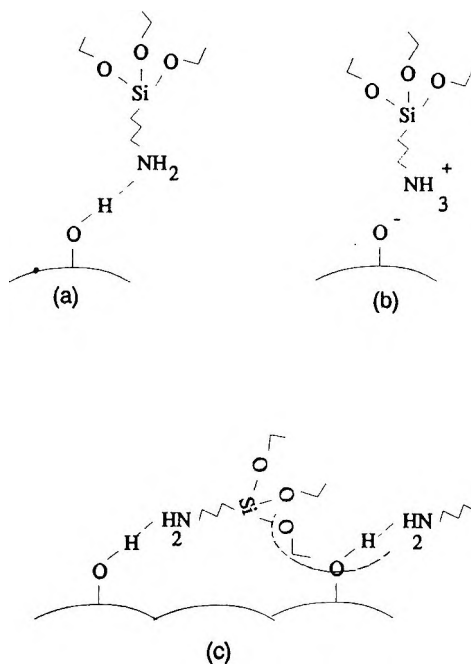
Figure 9. Surface - aminosilane interactions in the loading step, (a) hydrogen bonding, (b) proton transfer, (c) condensation to siloxane.
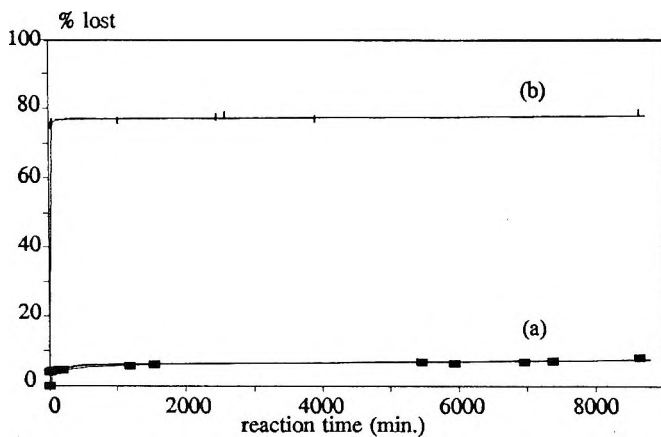
Figure 10. Ethanol leaching curves of uncured modified silica; (a) APTS, (b) n-butylamine.

Loading (mmol\g)
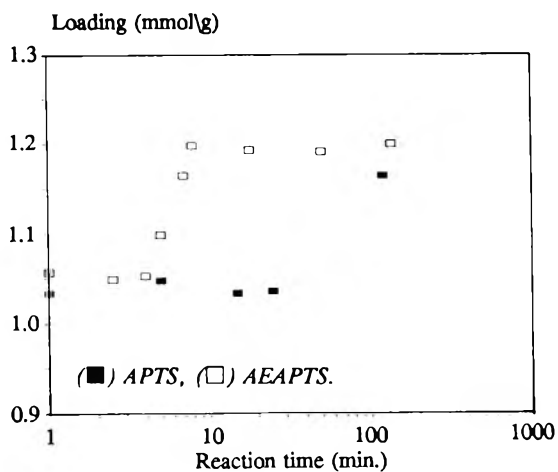
Figure 11. Silane loading on dried mesoporous silica gel as a function of reaction time.

C (molec/nm2)
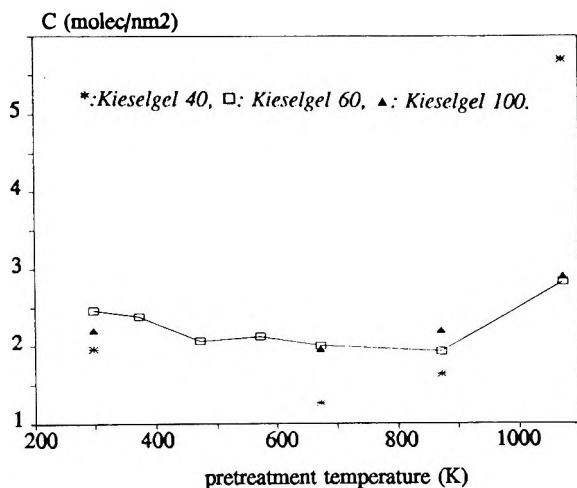
Figure 12. Total surface coverage of APTS modified silica gel, with variable pretreatment temperature.

measured quantitatively by means of a colour reaction with salicylic aldehyde.[50] Physisorbed molecules desorb, while ionic and covalently bound molecules are stable towards this ethanol leaching. In Figure 10, the relative percentages of silane lost from the surface is displayed as a function of leaching time.

From the APTS leaching curve (curve **a**), we obtain a relative amount of about 10% of the coating which is only physically bonded to the surface before curing.

In order to distinguish the ionic bonding from the covalent attachment, the same test was performed using n-butylamine (curve **b**). The amine group interaction of butylamine is similar to APTS, but there is no silicon atom present to form covalent linkages. 22% of the butylamine appears to be stable towards the ethanol leaching. Therefore, it was concluded that 22% of the coating is in ionic interaction with the surface. 10% is hydrogen bonded and 68% is covalently bonded after 2h of reaction at room temperature.

The course of the aminosilane deposition during the reaction phase was measured using free sampling analysis. After certain reaction times, samples are taken from the reaction mixture, which are then frozen to stop the reaction. After melting and separation, the amount of reacted silane is measured.

The reaction profiles of APTS and AEAPTS (N-β-aminoethyl-γ-aminopropyl-trimethoxysilane; $(CH_3O)_3SiCH_2CH_2CH_2NHCH_2CH_2NH_2$) are displayed in Figure 11. Both compounds reach an equilibrium adsorption within 1 min of reaction. This reflects the quick adsorption of the amine group, forming hydrogen bonds with the surface silanol groups.

For the AEAPTS, carrying two amine groups, a two-step adsorption is found. This indicates that an amine group of the organic chain remains free in the first step and is able to adsorb an additional layer of silane molecules. Since secondary amines are better acceptors for hydrogen bonds, it will be the primary amine function at the end of the organic chain that remains free. Upon adsorption of the secondary layer, an equilibrium situation is again reached.

For the monofunctional silane, the first equilibrium is followed by an additional adsorption, which does not have a step-wise profile. The equilibrium situation is related to the localized adsorption of silane molecules on the surface hydroxyl groups, thus forming a monolayer coating on the surface.

In order to study the effect of substrate related parameters, the pretreatment temperature of the silica substrate may be varied. In Figure 12, the total coverage, expressed as number of APTS molecules per nm^2, is displayed as a function of the pretreatment temperature.

The total coverage is a measure for both chemically and physically adsorbed silane species. The degree of surface hydration and hydroxylation, as well as the specific surface of the silica, varies with varying pretreatment temperature. In the low temperature region (< 473 °K) a decrease of surface loading with increasing temperature is observed. If surface water is present, surface adsorbed molecules hydrolyze and condense with other silane molecules. Thus, a multilayer coating is obtained.

At higher pretreatment temperatures, a constant loading is observed. While the degree of hydroxylation decreases in this temperature region, the specific surface area remains constant. Therefore, the total coverage is controlled by the specific surface area of the silica, rather than by the hydroxyl group content. Silane molecules are deposited on the silica surface with each molecule covering 0.5 nm^2. The previously mentioned course of APTS deposition, may be interpreted as a silanol group specific initial deposition, reaching equilibrium, followed by a filling of the free space on the silica surface. Non-specifically adsorbed molecules will desorb quickly in the curing phase.

For silica pretreated at 1073 °K, an increased surface coverage is observed. This may be due either to the structure of the coating layer, involving multilayer formation or to a change in the molecular orientation at the surface, or to the different porous structure of the 1073 °K pretreated silica. None of these hypotheses can be excluded on the basis of these data. The participation of strained siloxane groups[51] is another possible explanation. It has been previously reported that those siloxanes may enter into physical and chemical interactions with silanes[52,53] and ammonia.[54,55] Here it appears that aminosilanes are also able to react with strained siloxane bridges.[56] It has been generally accepted that the majority of the silane-to-surface siloxane bonds are formed in the curing phase. Above, we have demonstrated that already in the reaction phase 68% of the APTS molecules have formed at least one chemical bond with the surface. The formation of covalent bonds in the curing phase has been probed by a similar ethanol leaching test.

In Figure 13 the stability towards ethanol leaching is plotted as a function of curing time. Curves for both APTS and APDMS (γ-aminopropyl-diethoxymethylsilane; $(CH_3CH_2O)_2CH_3SICH_2CH_2CH_2NH_2$) are displayed. It can be seen that the APTS reaches its maximal stability within 3h of curing. Only 2% of the coating remains merely physisorbed. For the APDMS, maximal stability is reached after a much longer time. APDMS needs 20h of curing before maximal stability is reached. The difference in condensation behaviour is clearly due to the different number of ethoxy groups in the silane molecule. The higher number of ethoxy groups of the APTS molecule causes a much faster stabilization.
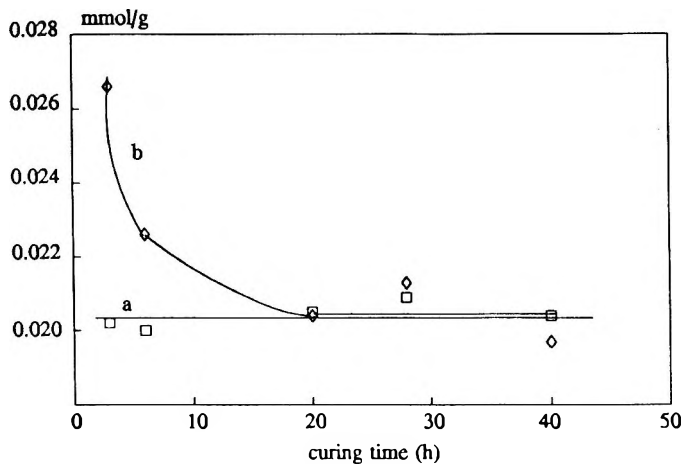
Figure 13. Amount of physisorbed silane molecules per g of modified silica as a function of curing time in vacuum.
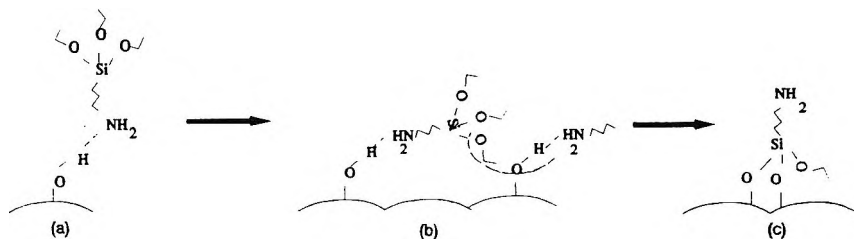
Figure 14. Flip mechanism for APTS reaction in dry conditions, (a) physisorption, (b) condensation, (c) main structure after curing.

Concerning the amine side of the molecule, valuable information can be drawn from ^{13}C solid state NMR spectra. The results have been reported elsewhere,[56] but it is worthwhile to recapitulate the conclusions. From the position of the peak due to the β-C atom of the propyl chain, information on the mobility of the aminopropyl chain may be obtained. It appeared that upon curing, the amine group relinquishes its interaction with the silica surface.

Therefore, the aminosilane molecule turns from the original amine-down position in the reaction phase towards an amine-up position after condensation. This is called the flip-mechanism (Figure 14).

SUMMARY

In this review, we have discussed the silylation of silica with various silanes, including chlorosilanes, organosilanes and aminosilanes, both in the liquid phase and in the gas phase. In every case, the reaction mechanism involved is more complex than is often believed. Many reactions can occur simultaneously and the resulting surface layer depends largely on the synthesis conditions.

Special attention should be given to the role of water in the synthesis procedure. Water can occur as physisorbed molecules on the substrate prior to modification, but it may be involved in the reaction mixture itself or even as humidity during the post-reaction curing step. In every case, the water molecules have an enormous impact on the modification reactions, causing a polymerization of the silane molecules, resulting in a thick but irreproducible and irregular surface layer.

Since in these modification reactions, there are often more unknowns than independently measurable values, the parameters that facilitate the optimization of a modification, such as effectiveness, surface coverage and stoichiometry, have been introduced and exemplified.

REFERENCES

1. E. F. Vansant, P. Van Der Voort, K. C. Vrancken, **Characterization and Chemical Modification of the Silica Surface**, Studies in Surface Science and Catalysis, Vol. 93, Elsevier Science Publishers, Amsterdam, The Netherlands.

2. A. V. Kiselev, V. I. Lygin, **Infrared Spectra of Surface Compounds**, John Wiley & Sons, New York, 1975.

3. B. Arkles, Chemtech, 7, 766 (1977).

4. J. P. Blitz, R. S. S. Murthy, D. E. Leyden, J. Colloid Interface Sci., 121, 63 (1988).

5. J. P. Blitz, R. S. S. Murthy, D. E. Leyden, J. Am. Chem. Soc., 109, 7141 (1987).

6. J. P. Blitz, R. S. S. Murthy, D. E. Leyden, J. Colloid Interface Sci., 126, 387 (1988).

7. R. Maoz, J. Sagiv, J. Colloid Interface Sci., **100**, 465 (1984).

8. D. A. Offord, J. H. Griffin, Langnuir, **9**, 3015 (1993).

9. J. D. Le Grange, J. L. Markham, C. R. Kurkjian, Langmuir, **9**, 1746 (1993).

10. S. R. Wasserman, G. M. Whitesides, I. M. Tidswell, B. M. Ocko, P. S. Pershan, J. D. Axe, J. Am. Chem. Soc., **111**, 5852 (1989).

11. M. J. Wirth, H. O. Fatunmbi, in **Chemically Modified Surfaces**, J. J. Pesek, I. E. Leigh, eds., Royal Soc. of Chem., Cambridge, UK, 1994, p. 253.

12. M. J. Wirth, H. O. Fatunmbi, Anal. Chem., **65**, 822 (1993).

13. Y. Yongan, PhD. dissertation, University of Antwerpen, University Press, 1987.

14. K. M. R. Kallury, P. M. MacDonald, M. Thompson, Langmuir, **10**, 492 (1994).

15. D. G. Kurth, T. Bein, J. Phys. Chem., **96**, 6707 (1992).

16. A. A. Chuiko, V. A. Turtykh, V. A. Khranovskii, Y. P. Egorov, L. M. Roev, Teoreticheskaya I Eksperimental'naya Khimiya, **2**, 247 (1966); Engl. transl., p. 189.

17. M. J. D. Low, A. G. Severdia, J. Chan, J. Colloid Interface Sci., **86**, 111 (1982).

18. M. L. Hair, W. Hertl, J. Phys. Chem., **73**, 2372 (1969).

19. M. L. Hair, W. Hertl, J. Phys. Chem., **77**, 2070 (1973).

20. M. L. Hair, W. Hertl, J. Phys. Chem., **77**, 1965 (1973).

21. M. L. Hair, J. Colloid Interface Sci., **60**, 154 (1977).

22. M. L. Hair, "Silica Surfaces," in **Surfaces and Interfaces,**, D. E. Leyden, ed., Gordon & Breach Science Publ., 1985.

23. P. Van Der Voort, K. C. Vranken, E. F. Vansant, J. Chem. Soc. Faraday Trans., **91**, 353 (1995).

24. P. Van Der Voort, I. Gillis-D'Hamers, E. F. Vansant, J. Chem. Soc. Faraday Trans., **86**, 3751 (1990).

25. P. Van Der Voort, I. Gillis-Hamers, K. C. Vranken, E. F. Vansant, J. Chem. Soc. Faraday Trans., **87**, 3899 (1991).

26. B. A. Morrow, I. A. Cody, L. S. M. Lee, J. Phys. Chem., **80**, 2692 (1976).

27. R. Maoz, J. Sagiv, J. Colloid Interface Sci., **100**, 465 (1984).

28. N. Tillman, A. Ulman, T. L. Penner, Langmuir, **5**, 101 (1989).

29. S. R. Wasserman, G. M. Whitesides, I. M. Tidswell, B. M. Ocko, P. S. Pershan, J. D. Axe, J. Am. Chem. Soc., **111**, 5852 (1989).

30. G. A. Carson, S. Granick, J./ Appl. Polym. Sci., **37**, 2767 (1989).

31. M. D. Porter, T. B. Bright, D. L. Allara, C. E. D. Chirdsy, J. Am. Chem. Soc., **109**, 3559 (1987).

32. C. D. Bain, G. M. Whitesides, Science, **240**, 62 (1988).

33. P. Silberzan, L. Leger, D. Ausserre, J. J. Benattar, Langmuir, 7, 1647 (1991).

34. D. L. Angst, G. W. Simmons, Langmuir, 7, 2236 (1991).

35. C. R. Kessel, S. Granick, Langmuir, 7, 532 (1991).

36. J. Nawrocki, B. J. Buzewski, J. Chromatogr. Rev., **449**, 1 (1988).

37. J. Sagiv, J. Am. Chem. Soc., **102**, 92 (1980).

38. C. P. Tripp, M. L. Hair, Langmuir, **8**, 1120 (1992).

39. H. Ishida, J. L. Koenig, Appl. Spectros., **32**, 462 (1978).

40. H. Ishida, J. L. Koenig, Appl. Spectros., **32**, 469 (1978).

41. C. P. Tripp, M. L. Hair, Langmuir, **8**, 1961 (1992).

42. C. P. Tripp, M. L. Hair, Langmuir, **8**, 1961 (1992).

43. C. P. Tripp, M. L. Hair, J. Phys. Chem., **97**, 5693 (1993).

44. J. M. Kinkel, K. K. Unger, J. Chromatogr., **316**, 193 (1984).

45. J. P. Blitz, R. S. Murthy, D. E. Leyden, J. Colloid Interface Sci., **126**, 387 (1988).

46. G. S. Caravajal, D. E. Leyden, G. R. Quinting, G. E. Maciel, Anal. Chem., **60**, 1776 (1988).

47. D. J. Kelly, D. E. Leyden, J. Colloid Interface Sci., **147**, 213 (1991).

48. T. G. Waddell, D. E. Leyden, M. T. DeBello, J. Am. Chem. Soc., **103**, 5303 (1981).

49. K. C. Vrancken, P. Van Der Voort, K. Possemiers, P. Grobet, E. F. Vansant, in **Chemically Modified Surfaces**, J. J. Pesek, I. E. Leigh, eds., The Royal Soc. of Chem., Cambridge, UK, 1994, p. 46.

50. K. C. Vrancken, K. Possemiers, P. Van Der Voort, E. F. Vansant, Colloids Surfaces A: Physicochem. Eng. Aspects, **98**, 235 (1995).

51. B. A. Morrow, I. A. Cody, J. Phys. Chem., **80**, 1998 (1995).

52. P. Van Der Voort, I. Gillis-D'Hamers, K. C. Vrancken, E. FR. Vansant, J. Chem. Soc. Faraday Trans., **87**, 3899 (1991).

53. L. H. Dubois, B. R. Zegarsky, J. Phys. Chem., **97**, 1665 (1993).

54. P. Van Der Voort, K. C. Vrancken, E. F. Vansant, J. Riga, J. Chem. Soc. Faraday Trans., **74**, 2509 (1993).

55. P. Fink, I. Plotski, G. Rudakoff, Wiss. Z. Friedrich Schiller Univ., Jena, Math. Naturwiss., **39**, 217 (1990).

56. K. C. Vrancken, P. Van Der Voort, K. Possemiers, E. F. Vansant, J. Colloid Interface Sci., **174**, 86 (1995).

REACTIONS OF ETHOXYSILANES WITH SILICA: A SOLID-STATE NMR STUDY

Klaus D. Behringer, Janet Blümel*

Anorganisch-chemisches Institut der TU München
85747 Garching, Germany

ABSTRACT

Ethoxysilanes are of growing interest in the fields of immobilized catalysts and chromatography. In spite of this, the reactions of ethoxysilanes with silica surfaces are still not fully explored. This contribution demonstrates that besides the reaction temperature and the degree of dryness of the silica surface, the solvent plays a crucial role during the silanization step: Optimal surface coverage can, for example, be obtained either without solvent or with hydrocarbons like *iso*-octane or pentane under mild reaction conditions. Hereby, ^{13}C and ^{29}Si solid-state NMR spectroscopy serves as a powerful analytical method. The modified silica can be successfully applied for the purification of bifunctional phosphines and their carbonylnickel complexes.

INTRODUCTION

Alkoxysilane reagents are important for a variety of chemical applications: In the form of bifunctional phosphine linkers they can be used in order to immobilize catalysts on inorganic supports,[1-7] most often on silica.[8] The other application lies in the field of silanized silica for chromatography.[9-24]

2753

The most powerful method in order to characterize silane modified silica is solid-state NMR spectroscopy.[3-7,11-29] Using Magic Angle Spinning (MAS,[25-29]) and Cross Polarization (CP,[25-29]) the surface species can be detected without any difficulties arising from the bulk material.

The advantages of alkoxysilanes as compared to chlorosilanes, are that no acidic byproducts are formed upon reaction with silica, which could destroy sensitive transition metal complexes when they are immobilized on silica or chromatographed. Furthermore, due to addition reactions of alkoxysilanes to surface siloxane groups, there is no need for "endcapping" in a further step.[31]

However, in contrast to the reactions of chlorosilanes, comparatively few studies deal with the reactions of ethoxysilanes with silica surfaces.[4,5,11,13,15,22,24,31] Triethoxysilanes are most interesting, because they should provide a strong bonding to the support via up to three siloxane bonds.

Up to now, the dependence of the number of siloxane bonds formed on the reaction temperature and the degree of dryness of the silica used has been primarily studied. In the following, we want to shed some light on the influence of the solvent used for the silanization procedure.

EXPERIMENTAL SECTION

a) Solid-State NMR Spectroscopy

All the spectra were recorded on a BRUKER MSL 300 NMR spectrometer, equipped with a 7 mm broadband double bearing MAS probehead and ZrO_2 rotors. The modified silica was loosely filled into the rotors under air. Cross polarization (CP) and Magic Angle Spinning (MAS) with a rotational speed of 4 kHz was applied for all the spectra shown. The contact times were 5 ms (^{13}C), 1 ms (^{31}P) or 6 ms (^{29}Si), if not stated otherwise, and the relaxation delays 4 s (^{13}C, ^{31}P), and 10 s (^{29}Si).

For all measurements, 500 to 1000 transients gave satisfactory signal to noise ratios. All spectra were recorded at room temperature (298 K). The ^{13}C, ^{29}Si, and ^{31}P NMR spectra were referenced with respect to external solid adamantane, [(CH$_3$)$_3$Si]$_4$Si, and $NH_4H_2PO_4$, respectively. For the exponential multiplication, line broadening factors of 40 Hz (^{13}C) and 60 Hz (^{29}Si, ^{31}P) were applied.

b) Preparation of the Silica

The silica was dried in a vacuum of about 10^{-2} Pa for 12 h either at 600 °C ($SiO_2(600)$) or 25 °C ($SiO_2(25)$) prior to use. All the experiments were carried out with Merck silica 40 (specific surface area: 750 m^2/g; average pore size: 40 Å; particle size 0.063 - 0.2 mm). All solvents used were rigorously dried by standard procedures.

c) Silanization Procedures

All the silanization reactions were carried out following this scheme: 1 g of silica was suspended in about 50 mL of the indicated solvent. Then 1 mL of the ethoxysilane was added and the reaction mixture stirred for 12 h at the temperature given in the text. Finally the supernatant solution was decanted and the silica was washed three times with pentane, before it was dried in vacuo for about 4 h.

RESULTS

1. ^{13}C CP/MAS Spectra

All the studies presented here were carried out with trimethylethoxysilane (**1**), vinyltriethoxysilane (**2**), and 3-chloropropyltriethoxysilane (**3**). The silica was dried in vacuo at 600 °C ($SiO_2(600)$) or at 25 °C ($SiO_2(25)$), in order to condense surface silanol groups or to remove adsorbed water.[8] When pure $(CH_2{=}CH)Si(OEt)_3$ (**2**) is reacted with both types of silica, the ^{13}C CP/MAS spectra of the materials shown in Fig. 1 result.

The ^{13}C NMR signals at 16.6 ppm and 58.4 ppm stem from the methyl and methylene groups of residual silane- or surface-bound ethoxy groups.[31] The resonances at 129.7 and 135.1 ppm, with their rotational sidebands and, therefore, larger CSA (Chemical Shift Anisotropy,[25-29]) can be attributed to the CH_2 and CH carbon atoms, respectively.[32] This assignment is in accord with the halfwidths of the vinyl carbon signals. The CH group gives a broader ^{13}C resonance, because it is less mobile than the CH_2 group, which can rotate about the Si-CH axis.

While, in the case of rigorously dried silica (Fig. 1 B), a large amount of ethoxy groups is retained on the surface, silicas containing more Si-OH groups lead to a lower ratio of EtO groups to vinyl groups (Fig. 1 A). The analogous observation is made, when $Cl(CH_2)_3Si(OEt)_3$ (**3**) is reacted with silica. Again,
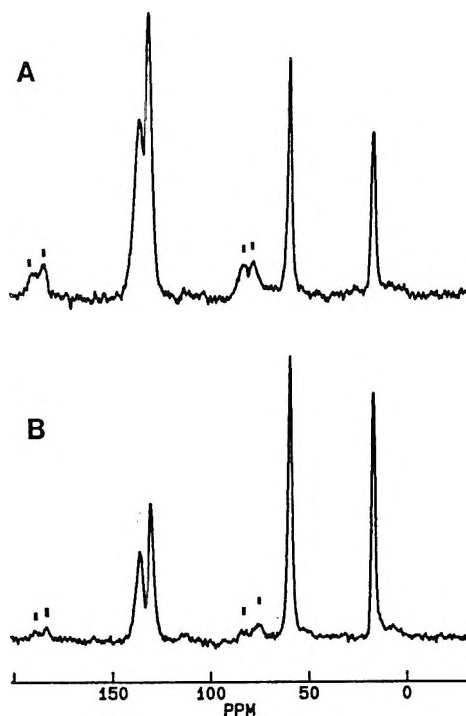
Figure 1. 75.5 MHz ^{13}C CP/MAS spectra of vinyltriethoxysilane **(2)** after reaction with $SiO_2(25)$ (A) and $SiO_2(600)$ (B). Details see text and Experimental Section.

the resonances of ethoxy groups (17.0 and 58.3 ppm) are visible besides those of the $ClCH_2$ (45.8 ppm), CH_2Si (8.8 ppm), and $CH_2CH_2CH_2$ (25.8 ppm) signals.

2. The Influence of Reaction Time

When $SiO_2(600)$ is treated with an excess of pure **2** for 12 h at 60 °C, after washing and drying, a material results, whose ^{29}Si CP/MAS spectrum is displayed in Fig. 2 A. Adding again an excess of **2** and stirring the slurry for three more days at 60 °C, leads to the ^{29}Si CP/MAS spectrum shown in Fig. 2 B. While the signal intensities of the $HO-SiO_3$ and SiO_4 ^{29}Si resonances at -102 and -110 ppm are somewhat sensitive to changes of the contact time, as described in ref.,[13] the signal intensities within the silane region were not
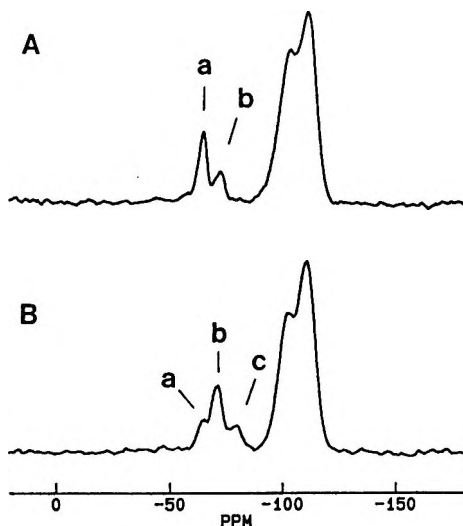
Figure 2. 59.6 MHz ^{29}Si CP/MAS spectra of SiO$_2$(600) after reaction with vinyltriethoxysilane (2) for 12 h (A) and for 3 days (B). a, b, and c denote silane species with 1, 2, and 3 siloxane bonds. Details see text and Experimental Section.

altered within the range of contact times from 5 to 12 ms. Both spectra of Fig. 2 are recorded with a contact time of 6 ms and the same batch of silica is employed. Therefore, a rough estimate of quantities should be feasible. While the silanol signal is shrinking somewhat with prolonged heating of the material, the overall signal intensity in the silane region remains roughly unchanged. The assignment of the resonances a, b, and c (Fig. 2) at -65.7, -71.6, and -79.8 ppm is made in analogy for example to refs.:[12,13,22,25] The more siloxane bridges to the support are formed, the lower is the resonance frequency. The resonance at -65.7 ppm corresponds to (CH$_2$=CH)Si(OEt)$_2$-O-{SiO$_2$} exclusively, while cross-linking might take place in the case of the other two resonances with more than one siloxane group.

When silica SiO$_2$(25) is applied for the same reactions, the intensities of the silane signals b and c are greater, while the sum of the silane signal intensities is somewhat lower than in the case of SiO$_2$(600). The analogous trends are observed in all the above reactions, when the chloropropylsilane **3** is used instead of **2**. The silane signals corresponding to a, b, and c have the chemical shifts -51.5, -58.7, and -65.7 ppm. When all the materials described in this paragraph are treated with an excess of Me$_3$Si(OEt) at 80 °C in toluene for 12 h, the ^{29}Si CP/MAS spectra do not even show traces of surface bound **1**.
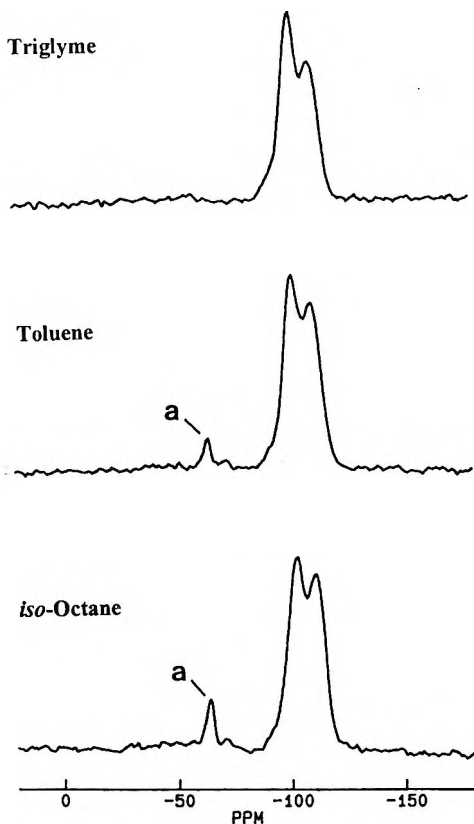
Figure 3. 59.6 MHz ^{29}Si CP/MAS spectra of $SiO_2(600)$ after reaction with vinyltriethoxysilane (2) in the solvents indicated. Details see text and Experimental Section.

3. The Influence of the Solvent

In order to study the influence of the solvent, silica $SiO_2(600)$ can be reacted with **2** and **3** under identical reaction conditions (80 °C, 12 h) but using different solvents, namely CCl_4, *iso*-octane, toluene, and triglyme. In analogous runs at 25 °C, ether, acetone, and pentane is applied.

Three representative ^{29}Si CP/MAS spectra of the materials are displayed in Fig. 3. Since the silane signal intensities are not very sensitive to the CP parameters used, a rough quantitative judgment might be allowed. In the case

of the solvents ether, acetone, and triglyme, no silane signals could be detected in the ^{29}Si CP/MAS spectra (Fig. 3, top trace). CCl_4 gave a spectrum analogous to the one when toluene was applied (Fig. 3, middle spectrum), while pentane resulted in comparable silane signal intensity, but with a ratio of about 1 : 1 of species a and b. *iso*-Octane leads to maximal silane signal intensity and the nearly exclusive presence of species a bound by one siloxane bridge to the support. The surface coverage, however, does not reach the one found when silica is treated with **2** without any solvent (Fig. 2). The results of the reactions of **3** with $SiO_2(600)$ parallel closely the ones found for **2**. When the materials described in this and the previous paragraph are treated with triglyme at 80 °C or with acetone at 25 °C for 12 h, the overall surface coverage with silanes does not change.

4. Chromatographic Purification of Phosphines and their Nickel Complexes

Bifunctional phosphines, like $Ph_2P(C_6H_4)SiMe_2SiOEt$ (**4**) and $Ph_2P(C_6H_4)Si(OEt)_3$ (**5**) and their carbonylnickel complexes,[33] are difficult to purify. Most often they do not crystallize and due to their weight, they cannot be sublimed. Ordinary chromatography does not help here, because **4** and **5** are immobilized on silica. Silane modified silica, however, is suitable for the purification of these species. While commercial Me_2SiCl_2- modified silica leads to major loss of phosphines, optimal results have been obtained with the silica modified with **1** and described in Ref. 31.

For example, when **4** is applied to a column packed with Me_3Si-O-{SiO_2}/pentane, all pentane-soluble impurities can be removed by elution with this solvent. Due to strong adsorption of **4** on the stationary phase, it does not migrate with pentane. The adsorption can be seen in the ^{31}P CP/MAS spectrum after drying the column material.

The narrow linewidth and the NMR behavior are indicative of merely adsorbed phosphine.[3,34] The phosphines and nickel complexes can be eluted as a narrow band by applying a solvent mixture of pentane and THF in the ratio 8 : 2. The purity of the nickel complexes can, for example, be checked by ^{61}Ni NMR spectroscopy.[35] Strongly colored orange-brown impurities stay on the column, while the phosphines and their complexes are eluted as colorless oils. There is usually only minimal loss of the substrates and the absence of phosphine species on the stationary phase can again be checked by ^{31}P CP/MAS spectroscopy.

DISCUSSION

1. Addition or Condensation Reactions?

Figure 1 shows that in the case of rigorously dried silica $SiO_2(600)$, more ethoxy groups are retained than with $SiO_2(25)$. This rough quantitative interpretation should be allowed regarding the high mobility of all the groups present[20,21,24] and, keeping in mind, that both spectra have been recorded under identical conditions and they display the same species. Therefore, these results with the triethoxysilanes **2** and **3** follow the trend already observed for the monoethoxysilane **1**.[31] However, the results for **2** and **3** are not that clearcut. For example, the ratio of vinyl to ethoxy groups as found in spectrum 1 B is about 1 : 2 which means that on average one ethoxy group of originally three is lost during the immobilization. Therefore, the addition reaction of the triethoxysilane group to surface siloxane groups[31,33] is not the only reaction taking place here. There must be either a condensation reaction with residual surface silanol groups or some cross-linking between adjacent surface bound silanes.

On the other hand, in the case of $SiO_2(25)$, there are more OEt- groups present than there should be, according to the corresponding ^{29}Si CP/MAS spectrum. This again, corroborates the assumption of addition reactions taking place.[31,36]

These results, however, mean that there is always a variable amount of ethoxy groups present and, that determinations of surface coverages by elemental analysis are not very reliable without the knowledge of the ethoxy group ratio, as determined by ^{13}C CP/MAS spectroscopy.

2. The Reaction Time and Temperature

When silane modified silica is heated for a prolonged period of time with additional ethoxysilane present, the surface coverage with silane does not increase substantially, which can be seen in Fig. 2. This means that the ethoxysilanes already cover the silica surface with maximal density, even if they are bound by only one siloxane bond to silica. The already surface-bound vinylsilane groups, due to sterical reasons, prevent the attack of further silane reagent. This assumption is further corroborated by the finding, that no traces of Me_3Si groups can be found on the surface, when the material of spectrum 2 A is treated with **1**. This means that a) no endcapping is necessary or possible when alkoxysilane reagents are used to modify silica and b) that

monoethoxysilanes should lead to the same dense surface coverage as triethoxysilanes. However, prolonged heating in the case of the latter leads to the formation of additional siloxane bonds, which might make the bonding to the support stronger and enhance the lifetime of chromatographic materials or immobilized catalysts.

The formation of more than one siloxane bond to the support is facilitated when the amount of surface silanol groups is increased. This means that in contrast to the formation of the first siloxane bond, where the addition reaction to surface siloxane groups seems to be preferred,[31,33] the formation of one or two more siloxane bridges needs - probably due to steric reasons - adjacent silanol groups. This assumption is corroborated, for example, by the signal intensity of the surface silanol signals, which diminishes on going from spectrum 2A to 2B.

3. Which solvent should be chosen?

The above results and Fig. 3 show, that given one type of silica, the solvent applied plays a crucial role regarding the surface coverage with silanes and the number of siloxane bonds formed. While polar solvents lead to minimal coverages, if at all, the unpolar solvents pentane and *iso*-octane give large signals in the silane regions of the ^{29}Si CP/MAS spectra (Fig. 3). However, maximal signal intensities are obtained without any solvent (Fig. 2). We interpret these findings as being the results of strong adsorption of the solvents on the silica surface.[37] The stronger the adsorption on the surface, the denser is the shielding towards attacking ethoxysilane reagents. However, once siloxane bridges are formed, they are not broken by polar solvents, since the surface coverage stays the same after treatment with polar solvents (results, 3.).

This assumption of strong adsorption of polar solvents on the silica surface is corroborated by the linewidth reduction of suspension NMR signals, when phosphine moieties are detached from the support by polar solvents.[38]

The above results also demonstrate, that regarding the surface coverages, aromatic solvents like toluene, which are commonly used for the silanization procedures, are not optimal. The surface coverages are greater when hydrocarbons like *iso*-octane or pentane are used. These two solvents are indicative of an influence of solvent viscosity on the number of siloxane bridges formed. The less viscous pentane probably allows greater mobility of the surface-bound silane and, therefore, sterically facilitates the formation of further siloxane bonds.

4. Chromatography of Bifunctional Phosphines

Chapter 4 of the Results section shows, that silica modified with alkoxysilane reagents can be applied for the successful chromatographic purification of bifunctional phosphines and their complexes. Although the procedure described is not a real reverse phase chromatography, it is still very useful, simple and effective.

As in the case of **1**, the ethoxysilane groups of **4** and **5** do not remove the silanes already bound to the support via siloxane bonds. Since no acidic byproducts are formed during the silanization step with ethoxysilane reagents, no phosphonium salts are formed on the stationary phase.

CONCLUSIONS

In this contribution, it is demonstrated by solid-state NMR spectroscopy, that during the silanization of silica with ethoxysilanes a) the solvent applied determines the surface coverage and number of siloxane bonds formed, and b) that the number of siloxane bonds formed is further dependent on the reaction time and temperature, and of the degree of dryness of the silica. Silica modified with trimethylethoxysilane can be applied for the purification of bifunctional phosphines and their nickel complexes.

ACKNOWLEGDEMENTS

REFERENCES

1. F. R. Hartley, **Supported Metal Complexes**, D. Reidel Publishing Company, Dordrecht, Holland, 1985, and literature cited therein.

2. U. Deschler, P. Kleinschmit, P. Panster, Angew. Chem., Int. Ed. Engl., **25**, 236 (1986).

3. J. Blümel, Inorg. Chem., **33**, 5050 (1994).

4. L. Bemi, H. C. Clark, J. A. Davies, C. A. Fyfe, R. E. Wasylishen, J. Am. Chem. Soc., **104**, 438 (1982).

5. L. Bemi, H. C. Clark, J. A. Davies, D. Drexler, C. A. Fyfe, R. E. Wasylishen, J. Organomet. Chem., **224**, C5 (1982).

6. E. Lindner, R. Schreiber, M. Kemmler, T. Schneller, H. A. Mayer, Chem. Mater., **7**, 951 (1995).

7. E. Lindner, M. Kemmler, H. A. Mayer, P. Wegner, J. Am. Chem. Soc., **116**, 348 (1994).

8. R. K. Iler, **The Chemistry of Silica**, John Wiley, New York, 1979.

9. R. P. W. Scott, **Silica and Bonded Phases**, John Wiley & Sons, New York, 1993.

10. H. Colin, G. Guiochon, J. Chromatogr., **141**, 289 (1977).

11. E. Bayer, A. Paulus, B. Peters, G. Laupp, J. Reiners, K. Albert, J. Chromatogr., **364**, 25 (1986).

12. B. Pfleiderer, K. Albert, E. Bayer, J. Chromatogr., **506**, 343 (1990).

13. K. Albert, E. Bayer, J. Chromatogr., **544**, 345 (1991).

14. E. Bayer, K. Albert, J. Reiners, M. Nieder, D. Müller, J. Chromatogr., **264**, 197 (1983).

15. K. Albert, B. Evers, E. Bayer, J. Magn. Reson., **62**, 428 (1985).

16. B. Pfleiderer, K. Albert, K. D. Lork, K. K. Unger, H. Brückner, E. Bayer, Angew. Chem., **101**, 336 (1989).

17. R. K. Gilpin, M. E. Gangoda, J. Chromatogr. Sci., **21**, 352 (1983).

18. R. K. Gilpin, M. E. Gangoda, Anal. Chem., **56**, 1470 (1984).

19. R. K. Gilpin, Anal. Chem., **57**, 1465A (1985).

20. R. C. Zeigler, G. E. Maciel, J. Phys. Chem., **95**, 7345 (1991).

21. R. C. Zeigler, G. E. Maciel. J. Am. Chem. Soc., **113**, 6349 (1991).

22. D. W. Sindorf. G. E. Maciel, J. Am. Chem. Soc., **105**, 3767 (1983).

23. D. W. Sindorf. G. E. Maciel, J. Phys. Chem., **86**, 5208 (1982).

24. G. E. Maciel, D. W. Sindorf, V. J. Bartuska, J. Chromatogr., **205**, 438 (1981).

25. C. A. Fyfe, Y. Zhang, P. Aroca, J. Am. Chem. Soc., **114**, 3252 (1992).

26. C. A. Fyfe, **Solid-State NMR for Chemists**, C. F. C. Press, Guelph, Canada, 1983, and literature cited therein.

27. G. Engelhardt, D. Michel, **High-Resolution Solid-State NMR of Silicates and Zeolites**, John Wiley, Chichester, U. K. 1987.

28. A. T. Bell, A. Pines, Eds., **NMR Techniques in Catalysis**, Marcel Dekker, New York, 1994, and literature cited therein.

29. R. K. Harris, **Nuclear Magnetic Resonance Spectroscopy**, Longman, Harlow (1986).

30. E. O. Stejskal, J. D. Memory, **High Resolution NMR in the Solid State**, Oxford University Press, New York, 1994.

31. J. Blümel. J. Am. Chem. Soc., **117**, 2112 (1995).

32. Assignment judged from increment calculations according to H.-O. Kalinowski, S. Berger, S. Braun, **^{13}C-NMR-Spektroskopie**, Georg Thieme Verlag, New York, 1984, p. 264.

33. K. D. Behringer, J. Blümel. Inorg. Chem., in press.

34. L. Baltusis, J. S. Frye, G. E. Maciel, J. Am. Chem. Soc., **108**, 7119 (1986).

35. K. D. Behringer, J. Blümel, Magn. Reson. Chem., **33**, 729 (1995).

36. L. H. Dubois, B. R. Zegarski, J. Am. Chem. Soc., **115**, 1190 (1993).

37. H. Pfeifer, W. Meiler, D. Deininger, "NMR of Organic Compounds Adsorbed on Porous Solids", in **Annual Reports on NMR Spectroscopy**, Vol. 15, Ed.: G. A. Webb, Academic Press, New York, 1983.

38. K. D. Behringer, J. Blümel, Z. Naturforsch., **50b**, 1723 (1995).

ADSORPTION CHARACTERIZATION OF OCTYL BONDED PHASES FOR HIGH PERFORMANCE LIQUID CHROMATOGRAPHY

Y. Bereznitski, M. Jaroniec, M. Kruk

Separation and Surface Science Center
Department of Chemistry
Kent State University
Kent, Ohio 44242, USA

B. Buszewski
Department of Environmental Chemistry
Copernicus University
87-100 Torun, Poland

ABSTRACT

Adsorption-desorption isotherms were measured for selected chromatographic silica gels with chemically bonded octyl groups. The standard sorption characterization of these packings provided the BET specific surface area, the total pore volume and the pore size distribution. Advanced numerical methods based on the density functional theory and the regularization method were used to calculate the pore volume and the adsorption energy distributions. The surface and structural properties of the silicas with chemically bonded octyl phases were compared to those of the original silica gels. The surface coverage of octyl groups occurred to be similar for all samples studied. After the octyl groups were bonded, the porous structure of the silica gels was not altered significantly, resulting in similar adsorption behavior of both unmodified and modified silica gels at pressures close to

the saturation pressure. However, the adsorption properties in low pressure region were changed significantly. Namely, all modified silicas exhibited very low adsorption and similar shape of adsorption isotherms at low pressures. Therefore, their adsorption energy distributions resembled each other and did not feature the higher energy sites present on the surface of unmodified silicas. The low pressure adsorption behavior indicates that essentially all higher energy sites on the silica surface reacted in the course of the chemical modification.

INTRODUCTION

Porous silicas are widely applied in liquid chromatography due to their remarkable surface properties and high mechanical, thermal and chemical stability.[1-3] The surface of unmodified silica is polar and therefore bare silica is suitable for normal phase (NP) liquid chromatography (LC) separations. However, the presence of surface silanol groups allows us to chemically bond organic ligands, which change the polarity of the surface. Chemically bonded stationary phases (CBP) found wide application in reverse phase (RP) liquid chromatography.[2-4] The introduction of specific interaction sites in hydrophobic ligands allows us to obtain CBP useful in separations of polar compounds, such as drugs, antibiotics and peptides.[5-8] Chirally selective CBPs, for example immobilized cyclodextrines, proteins or Pirkle-type phases,[2, 9-11] were also applied. However, many RP LC separations can be performed using standard C_8 or C_{18} alkyl bonded stationary phases, which are much easier to synthesize and usually more thermally and chemically stable.

The chromatographic properties of CBPs depend not only on the type of ligands attached to the surface, but also on the properties of the silica used for their synthesis.[2] Hence, the surface and structural properties of the silica need to be known in order to obtain well-defined CBPs in a reproducible way. Our recent paper[12] reported extensive sorption studies of several commercially available chromatographic silica gels. Adsorption-desorption measurements in a wide pressure range were used to evaluate the specific surface area, the pore size distribution and the adsorption energy distribution for the silicas under study. The specific surface area is required to meaningfully compare different stationary phases with the same bonded groups on the basis of the surface coverage of the ligands.[4] The knowledge of the pore width and the pore size distribution for silica gels allows one to choose a brand of silica best suited for a given application as CBP support for chemically bonded phases.

Table 1

Surface Coverage of Octyl Groups

Silica	Manufacturer	Percentage of Carbon	Surface Coverage ($\mu mol/m^2$)
Hypersil	Alltech, IL, USA	2.52	3.9
LiChrospher	EM Science, NJ, USA	2.68	4.1
Partisphere	Whatman, Inc., NJ, USA	3.21	3.5
SG-7/G	Polymer Institute Bratislava, Slovakia	14.84	3.4
Silasorb	Lachema, Brno, Czech Republic	8.76	3.6
Vydac	Supelco, PA, USA	3.98	4.1

The current paper is a continuation of the previous work.[12] Several commercially available silica gels were modified by the chemical bonding of octyl (C_8) ligands. Subsequently, the properties of the octyl CBPs and the original silica gels were studied by means of nitrogen adsorption, elemental analysis and high resolution thermal gravimetry.

The obtained data were used to compare the surface and structural properties of the synthesized CBPs with one another and with the original silica gels.

MATERIALS

The silica gels used in the current study are listed in Table 1. The octyl phases were synthesized according to the following procedure. The silica gel was dried in a glass reactor for 12 hours under vacuum (0.01 Pa) at 458 K. Then, octyldimethylchlorosilane and dry morpholine were added and the reaction mixture was kept at 388 K for 12 hours.

Subsequently, the silica with bonded stationary phases was washed with toluene, methanol and hexane , and dried under vacuum at ambient temperature. The octyldimethylchlorosilane was purchased from Pertrach System (Levitton, PA, USA) and morpholine was obtained from E. Merck.

METHODS

Sorption and Thermogravimetric Measurements

Nitrogen adsorption-desorption isotherms were measured on an ASAP 2010 volumetric sorption instrument from Micromeritics (Norcross, GA, USA). The purity of nitrogen was 99.99 %. Before the measurements, samples were degassed for 2 hours in the degas port of the adsorption apparatus at 473 K under the vacuum of about 10^{-1} Torr. The measurements were performed for a wide range of relative pressures, usually from 10^{-5} in the case of bare silicas and 10^{-3} for octyl stationary phases.

Thermogravimetric measurements were performed under quasi-isothermal conditions in a nitrogen atmosphere on a high resolution thermogravimetric analyzer TGA 2950 from TA Instruments, Inc. (New Castle, DE, USA). The elemental analysis was carried out by Huffman Laboratories (Golden, CO, USA).

Characterization Methods

Most of the characterization methods used in the study were described in details elsewhere.[12] Several standard methods[13,14] were employed in order to calculate the specific surface area, the total pore volume and the pore size distribution for the samples studied. The specific surface area of the samples was evaluated from the standard BET method. The micropore volume was calculated from the t-plot method. The Barrett-Joynder-Halendra (BJH) method was employed to obtain the pore size distributions, total pore volumes and average pore sizes from adsorption and desorption data. Advanced numerical procedures based on the regularization method[15] were used to calculate the adsorption energy and the pore volume distributions. The local isotherms for pores of different sizes were obtained on the basis of the density functional theory.[16,17] In order to evaluate the adsorption energy distributions, the Fowler-Guggenheim adsorption isotherm was used as a local isotherm in the integral equation for the total amount adsorbed. The number of nearest neighbors and their interaction energy (divided by the Boltzmann constant) were set to 4 and 95 K, respectively. In most of our calculations, the regularization parameter γ was set to 0.1 for silicas and 0.01 for bonded stationary phases. Further details of the methods employed in the study can be found in our previous paper[12] and references therein.
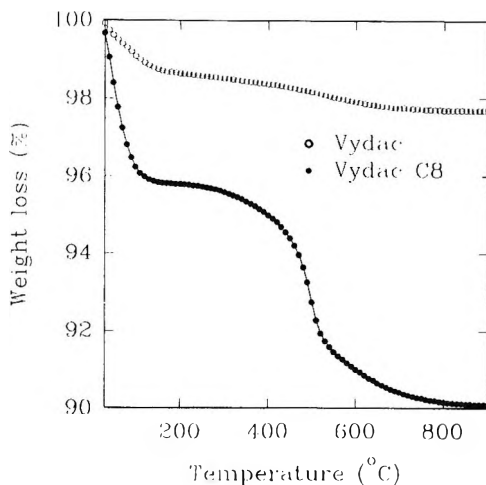
Figure 1. Thermogravimetric weight loss curves for unmodified Vydac and Vydac with chemically bonded octyl phase.

RESULTS AND DISCUSSION

Shown in Table 1, are percentages of carbon in octyl CBPs and the surface coverages of octyl groups. The latter were calculated on the basis of the BET specific surface area and the percentage of carbon in the samples[18] The octyl group surface coverage for the samples was in the range from 3.4 to 4.1 mmol/m^2 and tended to be higher for the samples of low surface areas. The above values of the surface coverage indicate that an appreciable amount of unreacted silanol groups is still present on the surface.[19]

In order to obtain information about thermal stability of the synthesized CBPs, high resolution thermoanalytical measurements were carried out. The samples were heated up to 1273 K in nitrogen atmosphere and the weight loss was recorded. As it is shown in Figure 1, after physically sorbed water was removed, there was a small step on the weight loss curves for unmodified silicas related to decomposition of surface silanols. In the case of silicas with bonded octyl groups, the physically adsorbed water and solvents left from the synthetic procedure were removed at the temperature below 373 K and the weight loss curve leveled. Then, in the temperature interval from 573 to 1023 K, there appeared a considerable weight loss, which can be attributed to the degradation of the chemically bonded stationary phase. The percentage of the weight loss for this step is in a good agreement with a weight percentage of the
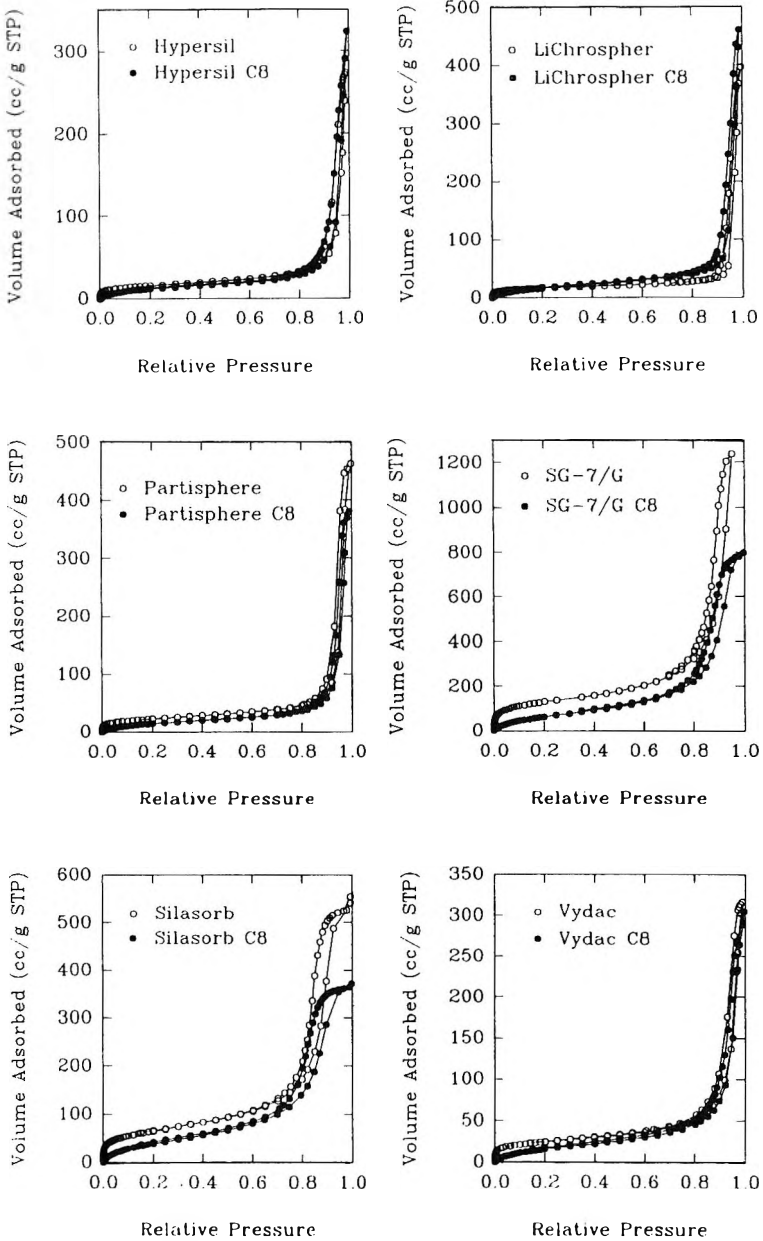
Figure 2. Adsorption-desorption isotherms for the chemically bonded phases and unmodified silicas.
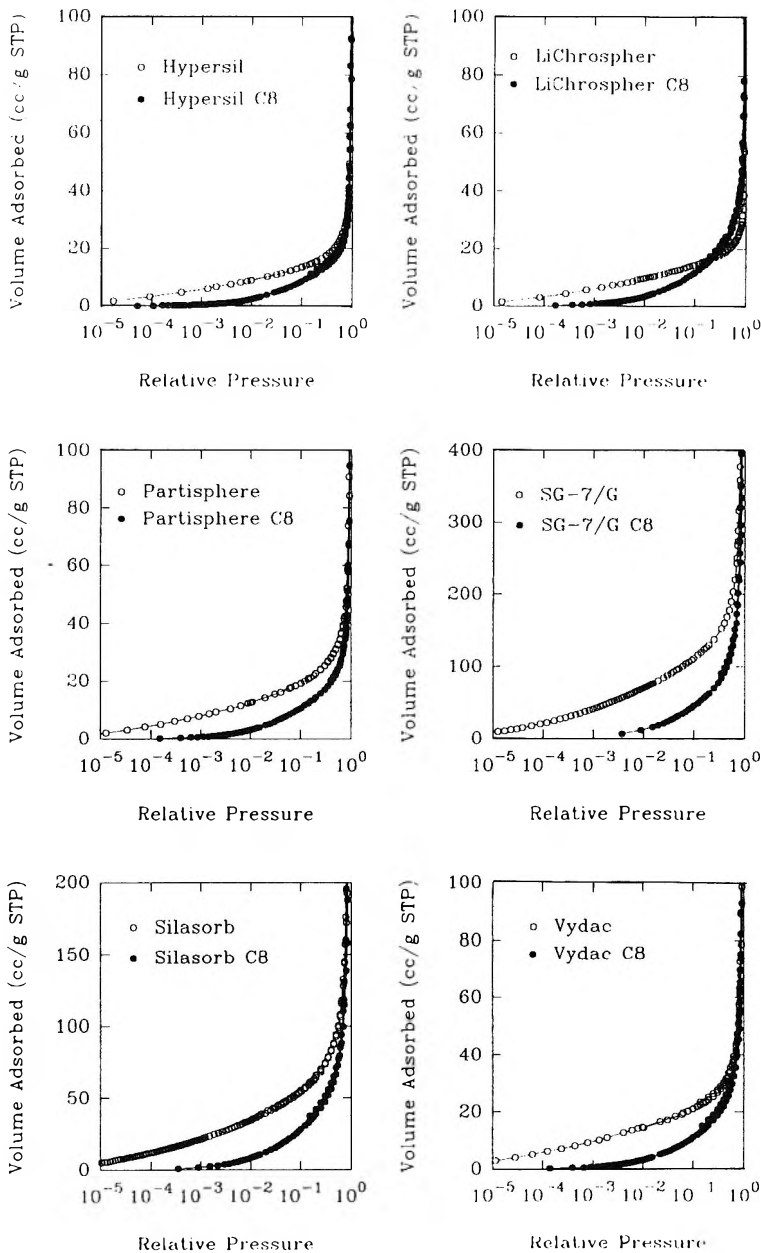
Figure 3. Low pressure parts of adsorption isotherms for the chemically bonded phases and unmodified silicas.

Table 2

BET Specific Surface Area and BJH Desorption Total Pore Volume
(1.7 to 300 nm)

Silica	BET Surface Area (m^2/g)		BJH Total Pore Volume (cc/g)	
	Original	C_8 Phase	Original	C_8 Phase
Hypersil	56	47	0.42	0.50
LiChrospher	57	67	0.61	0.71
Partisphere	81	58	0.72	0.59
SG-7/G	464	268	1.86	1.24
Silasorb	234	162	0.86	0.57
Vydac	86	64	0.49	0.47

bonded octyl groups in the samples. It can be seen in Figure 1, that the temperature of 473 K is suitable for the outgassing procedure before adsorption measurements, since it is high enough to remove physically adsorbed species, but yet below the temperature of the degradation of the CBP.

Shown in Figures 2 and 3, are adsorption isotherms for the silicas with CBP and the unmodified silicas. It can be noticed that the adsorption behavior at high relative pressure (in the range from about 0.5 to 1 p/p_0) does not change significantly after the octyl groups were introduced, which indicates that the porous structures of the samples were not altered appreciably in the course of the modification. All isotherms are of the type IV (or intermediate between II and IV) according to the IUPAC classification[20,21] and exhibit adsorption-desorption hysteresis loops . In the case of Hypersil, LiChrospher, Partisphere and Vydac (both modified and unmodified), the hysteresis loop occurs at relative pressures from about 0.85 to 0.95 and most closely resembles type H1 according to the IUPAC classification.[20, 21] SG-7/G and Silasorb exhibit hysteresis loops intermediate between type H1 and H2 for pressures from 0.75 to 0.95. The low pressure parts of the adsorption isotherms are shown in Figure 3. For all C_8 bonded phases, the adsorption at relative pressures up to about 0.002 was very small, which was not the case for the original silica samples. Moreover, the shape of low pressure parts of the isotherms for CBPs was almost identical, which indicates, that their surface properties are similar. The values of the BET specific surface area and the BJH pore volume (calculated from the desorption data) are listed in Table 2. The average pore size data obtained from the BJH method (adsorption and desorption) are shown

Table 3

BJH Adsorption and Desorption Pore Diameter

Silica	BJH Adsorption Average Pore Diameter (nm)		BJH Desorption Average Pore Diameter (nm)	
	Original	C_8 Phase	Original	C_8 Phase
Hypersil	33	38	29	32
LiChrospher	57	36	39	32
Partisphere	37	34	30	31
SG-7/G	16	14	16	13
Silasorb	14	11	12	9
Vydac	26	23	23	21

in Table 3. It needs to be remarked, that the samples of the CBPs used for the sorption measurements were very small and one might expect an error in weighing the samples. Moreover, in the range of pressures very close to the saturation pressure (above 0.95 relative pressure), the adsorption on the walls of the glass tube with adsorbent may noticeably increase the gas uptake, which introduces some error, especially for very small samples. However, the errors are not expected to influence the shape of the isotherms (except for pressures very close to the saturation pressure), the pore size distribution functions and the adsorption energy distribution functions.

It can be expected, that the introduction of the octyl groups on the silica surface would decrease the total pore volume, the average pore diameter and the specific surface area of the samples, provided the only process in the course of the modification is just chemical bonding between the surface silanol groups and ligands. The reason is that the bonded groups would occupy some space in the porous structure, decreasing the pore diameter and hence the volume of pores, or maybe even block some of them and make them inaccessible to nitrogen adsorption. Moreover, the presence of CBP increases the mass of the sample, so even if the surface area or the pore volume are not altered, the specific surface area and the specific pore volume will decrease. Our measurements show that indeed such trends can be observed, especially for samples of higher surface area (SG-7/G, Silasorb), where the decrease in the specific surface area and the pore volume was quite pronounced. However, in the case of the samples of the lowest surface area, the opposite tendency could be noticed. The specific surface, the average pore diameter, the pore volume of Hypersil and the pore volume of LiChrospher increased after the octyl groups
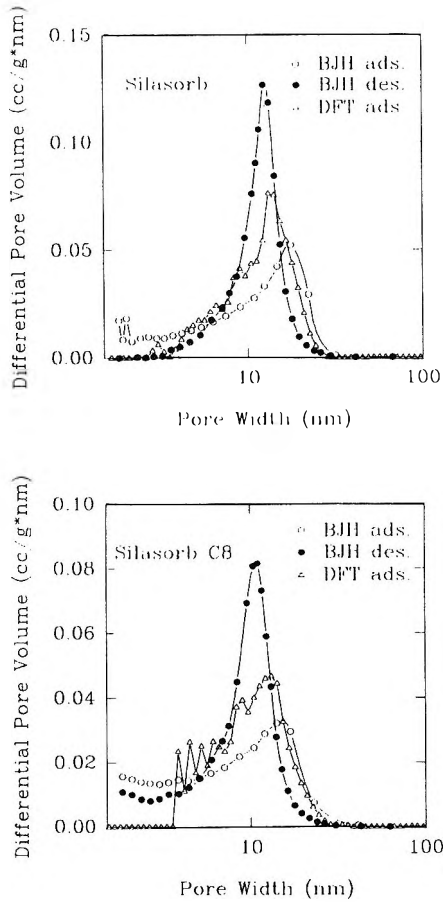
Figure 4. Comparison of the differential pore volume distributions obtained by means of the BJH method (from adsorption and desorption data) and the DFT software.

were bonded. It is not clear if these results arise from the experimental error or they are caused by minor structural changes of the silica samples in the course of their modification. Further studies are required in order to find out the reason of these unexpected findings.

The pore size distributions (PSD) for the samples under study were calculated by using BJH method (adsorption and desorption) and the DFT software supplied by Micromeritics, Inc. Shown in Figure 4, are differential PSD for Silasorb and Silasorb-based octyl stationary phase obtained by means of these methods. The overall shape of the PSD functions for a given sample

is similar, but there is a difference in the location of the peak corresponding to the maximum on PSDs. Namely, the peaks from the DFT calculations lie between these from the BJH adsorption and the BJH desorption. However, all three methods consistently show no considerable differences between PSDs for the original silica gel and the octyl CBP. It can be seen that in order to trace the changes of porous structures of the samples, the results from one of these methods need to be compared between one another.

In the current paper, the DFT software was used to provide the PSDs for the samples under study. The DFT program is best suited to slitlike pores with graphite type surfaces. The pores in silica gels are rather irregular in shape and their surface has different properties than the surface of graphite. However, PSDs are calculated from high pressure parts of isotherms, for which the surface is covered by at least a monolayer of the adsorbate and the surface properties are not that important, as in the submonolayer region. Secondly, the studied silicas have fairly wide pores, for which the effect of the geometry should be somewhat smaller. Finally, the comparative analysis of the unmodified and the modified samples is performed. Therefore, the DFT software was used to carry out the required PSD calculations, since it is numerically the most advanced method available now.

The incremental pore size distribution functions are shown in Figure 5. The PSDs for both octyl CBPs and the corresponding original silicas are of the same shape and lie in the same pore size range, which indicates that the porous structures of the samples were essentially unchanged in the course of the modification. All samples are mostly mesoporous (mesopores are pores with the widths between 2 and 50 nm according to the IUPAC recommendations[20,21]), but some of them (Hypersil, LiChrospher, Partisphere and Vydac) also possess appreciable fractions of small macropores (the widths above 50 nm). The PSDs show little or no evidence of the presence of micropores, which is in agreement with the micropore volumes obtained from the t-plot method.

The bonding of octyl groups to the silica surface is likely to decrease the pore size diameter. However, taking into account the size of the bonded ligand, the decrease is not expected to exceed 1 nm. The sizes of most pores present in the samples are above 10 nm, which is much higher than the expected decrease. Therefore, the latter decrease may be difficult to infer from the pore size distribution functions. This actually seems to be the case, since the distributions for some of the CBPs (Hypersil, LiChrospher, Silasorb) are slightly shifted towards small pore sizes with respect to the distributions for the unmodified silica gels, but this tendency is not well pronounced.
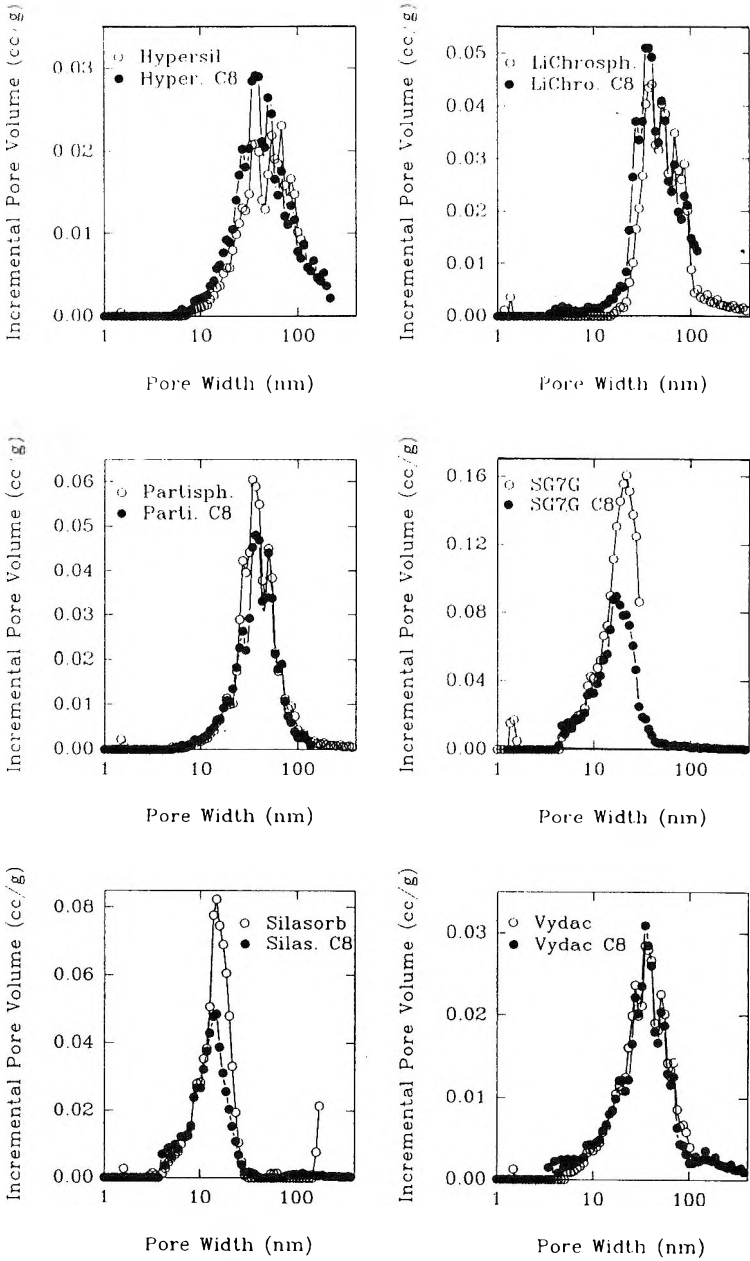
Figure 5. Incremental pore volume distributions for the chemically bonded phases and unmodified silicas.
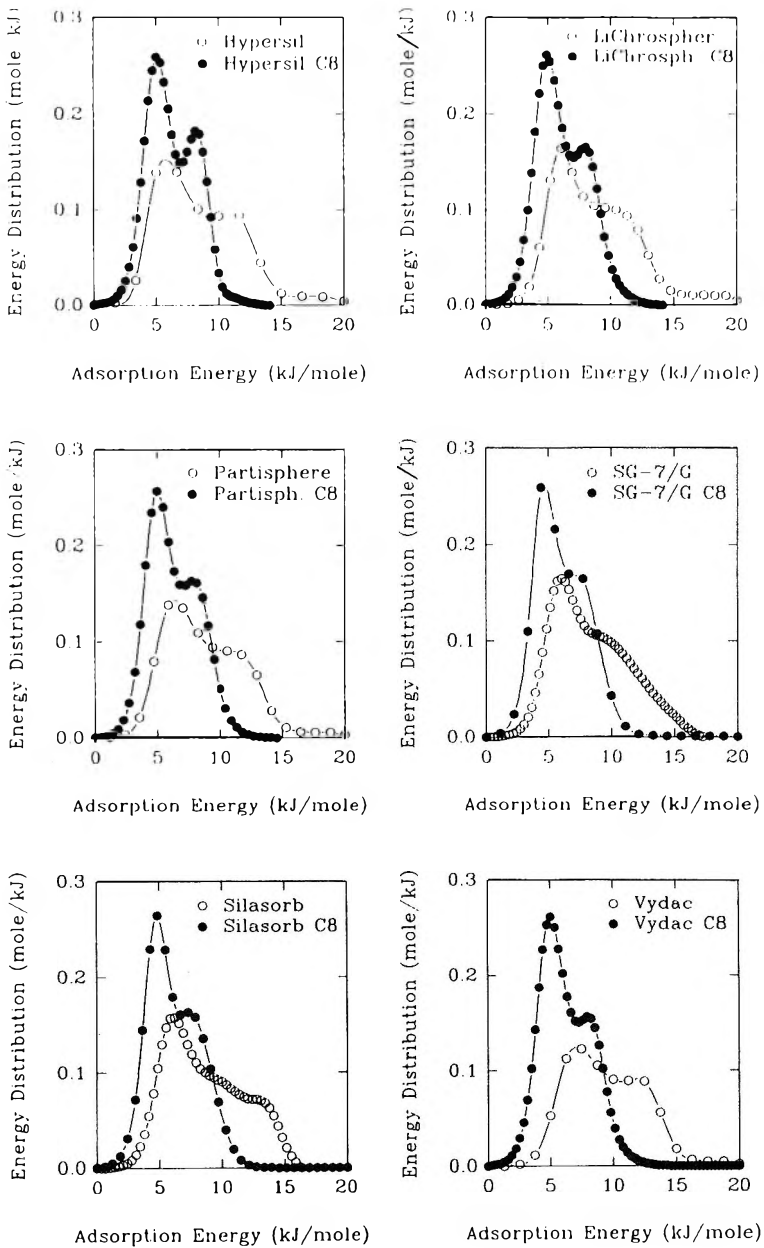
Figure 6. Adsorption energy distributions for the chemically bonded phases and unmodified silicas.

The adsorption energy distributions (AEDs) for both the CBPs and the unmodified silicas are shown in Figure 6. In order to obtain the AED functions, the inversion of the integral equation for the total amount adsorbed needs to be performed.[12] In the case of the CBPs, the inversion procedure occurred to be stable even for small values of the regularization parameter (γ). The latter parameter indicates the degree of smoothing of the input data, which is introduced in order to obtain numerically stable solution for the AED. In Figure 7, shown are adsorption energy distributions for Silasorb and Silasorb-based CBP, calculated for different values of γ. The distribution for the CBP does not exhibit negative (nonphysical) solutions for γ as low as 10^{-4}. In the case of the silica gel, the negative solutions are present to some extent even for the regularization parameter equal to 10^{-1}. The numerical stability of the solutions for the octyl CBPs allows obtaining physically meaningful adsorption energy distribution functions, with several (two to four; three in case of the Silasorb-based CBP) coalesced but yet distinct peaks, appearing for similar adsorption energy values for most CBP under study. However, their presence or absence seems to be dependent on the number of points on the isotherms in the submonolayer range of pressures. Further studies are needed to assess, if these peaks correspond to some adsorption sites on the surface of CBPs or are just the computational artefact. Because of the reasons mentioned above, the values of the regularization parameter used in the current study were chosen to be rather high and equal to 0.1 for the unmodified silicas and 0.01 for the octyl CBPs. For some unmodified silicas, their AEDs exhibit small negative parts (see Figure 7), which are nonphysical and therefore not shown in Figure 6.

The AED functions for unmodified silica gels cover the range from about 4 to 15 kJ/mol. The presence of small populations of higher energy sites (15-20 kJ/mol) is evidenced for Hypersil and LiChrospher. Previous thermogravimetric studies[22] showed that these gels contain relatively high amount of physically adsorbed water. The latter finding can be caused by the presence of these higher adsorption energy sites. However, these high energy tails may just be artefacts arising from the fact that too few isotherm data points were available for the calculations. Hence, the definite solution of that problem requires further studies. The distributions for bare silicas show the presence of two or more broad peaks. One of them is well pronounced and appears for about 6 kJ/mol, whereas the other peak, which corresponds to the adsorption energy of about 11-13 kJ/mol, is broader and maybe coalesced with other peaks. Because of that, the distributions show no considerable decrease in the range of 10-12 kJ/mol and then decline rapidly in the energy interval of about 13 to 15 kJ/mol. The adsorption energy distribution for SG-7/G is somewhat distinct from the others, as it exhibits a rather steep decrease in population of the adsorption energy sites in the range from 10 to 16 kJ/ mol.
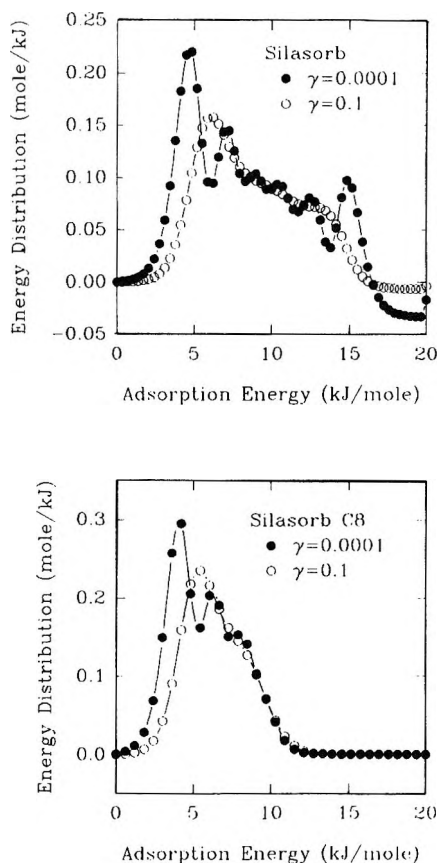
Figure 7. Comparison of the adsorption energy distributions calculated for different values of the regularization parameter.

The adsorption energy distributions for the octyl CBPs differ significantly from those for the unmodified silicas. The former are essentially the same for all CBPs samples studied and lie in the adsorption energy range from 3 to 10 kJ/mol. They exhibit two more or less distinct peaks corresponding to energies of 5 and about 8 kJ/mol. There is no evidence of the high energy sites (10-15 kJ/mol), which are present on the surface of the unmodified silicas. The distributions for both unmodified and modified samples show low energy peaks for very similar values of adsorption energies, that is 5-6 kJ/mol. It can be best seen in Figure 7, where the same regularization parameters were applied for both compared samples.

In Figure 6, the lowest energy peaks for silicas and the corresponding CBPs are somewhat shifted with respect to one another, most likely because of the different values of the regularization parameter used in the calculations.

As it was mentioned before, the surface coverages of octyl groups indicate that a considerable amount of unreacted silanol groups is still present on the surface of the CBPs. It is not likely that the octyl groups are able to shield the remaining silanols so effectively that the latter are not exposed to the nitrogen adsorption. Moreover, the similar shape of the low energy parts of the AEDs for both modified and unmodified silicas suggests that the low energy peaks may correspond to the adsorption sites on the unshielded silica surface. Therefore, the absence of the high energy sites on the surface of the CBPs arises presumably from the fact that these sites reacted in the course of the derivatization. The high energy sites can probably be identified with isolated silanols, as other silanols can be involved with hydrogen bonding between one another or with water molecules, which is likely to lower their accessibility and/or their interaction energy with nitrogen molecules used for the adsorption study. Other groups present on the surface of silica , such as siloxanes, are not expected to interact strongly with the adsorbate.

Since low energy peaks on the adsorption energy distributions for the CBPs seem to correspond to the peaks present on the AEDs for the unmodified silicas, the same groups on the silica surface may be responsible for their presence. But, adsorption energies of interactions of nitrogen molecules with octyl ligands are still unidentified. However, they may just be similar to the energy of one or even both of the low energy peaks, which seem to have their counterparts in the distribution functions for unmodified silicas. This is another problem, which would need to be addressed in further studies.

CONCLUSIONS

Samples of silicas with octyl bonded phases were analyzed by sorption measurements, high resolution thermogravimetry and elemental analysis. The latter technique allowed us to obtain the percentage of carbon in octyl bonded phases. High resolution thermogravimetry was employed to assess the thermal stability of the silicas and the CBPs studied. Nitrogen adsorption measurements provided the specific surface area, the pore volume distribution and the adsorption energy distribution for the samples. The surface and structural properties of octyl CBPs were compared with each other and with properties of corresponding unmodified silica gels. It was shown that although the coverage of C_8 groups varied by about 15% from one sample to another, the surface properties of the octyl CBPs were quite similar, which can be seen

from the low pressure adsorption behavior and the adsorption energy distributions. Unmodified silicas possess considerable fraction of adsorption sites of the adsorption energy between 10 and 15 kJ/mol. After octyl groups were bonded, these sites were no longer evidenced, which can be explained by assuming that most of them reacted in the course of the octyl group bonding. Owing to the absence of high energy adsorption sites, the adsorbed amount for octyl CBPs in low pressure region is much lower than in the case of unmodified silicas. However, the high pressure behavior of both modified and unmodified gels of the same type is similar, which indicates, that the porous structure of gels is not altered significantly in the course of the chemical bonding of octyl ligands.

REFERENCES

1. **Characterization and Modification of the Silica Surface**, E. F. Vansant, P. Van der Voort, K. C. Vrancken, eds., Elsevier, Amsterdam, 1995.

2. **Packings and Stationary Phases in Chromatographic Techniques**, K. K. Unger, ed., Marcel Dekker, New York, 1990.

3. R. P. W. Scott, **Silica Gel and Bonded Phases**, John Wiley & Sons, Inc., Chichester, 1993.

4. J. G. Dorsey, J. P. Foley, W. T. Cooper, R. A. Barford, H. G. Barth, Anal. Chem., **64**, 353R (1992).

5. B. Buszewski, J. Schmid, K. Albert, E. Bayer, J. Chromatogr., **552**, 415-427 (1991).

6. B. Feibush, C. T. Santasania, J. Chromatogr., **544**, 41-49 (1991).

7. C. T. Pinkerton, J. Chromatogr., **544**, 13-23 (1991).

8. K. K. Unger, Chromatographia, **31**, 507-511 (1991).

9. S. G. Allenmark, **Chiral Separations by HPLC**, Ellis Horwood, Chichester, 1989.

10. V. Tittelbach, R. K. Gilpin, Anal. Chem. **67**, 44-47 (1995).

11. W. H. Pirkle, R. S. Readnour, Chromatographia, **31**, 129-132 (1991).

12. Y. Bereznitski, M. Jaroniec, M. Kruk, accepted to J. Liquid Chromatogr.

13. M. Jaroniec, in **Access in Nanoporous Materials**, T. J. Pinnavaia, M. F. Thorpe, eds., Plenum Publ. Co., New York, 1996, pp. 255-272.

14. S. J. Gregg, K. S. W. Sing, **Adsorption, Surface Area and Porosity**, Academic Press, London, 1982, 2nd Edition.

15. M. v. Szombathely, P. Brauer, M. Jaroniec, J. Comput. Chem., **13**, 17-32 (1992).

16. J. P. Olivier. J. Porous Mater. **2**, 9-17 (1995).

17. J. P. Olivier, W. B. Conklin, M. v. Szombathely, Stud. Surf. Sci. Catal., **87**, 81-89 (1994).

18. B. Buszewski, M. Jaroniec, R. K. Gilpin, J. Chromatogr. A, **673**, 11-19 (1994).

19. H. Engelhardt, H. Low, W. Gotzinger, J. Chromatogr., **544**, 371-379 (1991).

20. K. S.W. Sing et al., Pure Appl. Chem., **57**, 603-619 (1985).

21. J. Rouquerol et al., Pure Appl. Chem., **66**, 1739 -1758 (1994).

22. W. Bhagwat, M.S. Thesis, Kent State University, 1995.

GAS AND LIQUID CHROMATOGRAPHIC INVESTIGATIONS INTO ALKYLNITRILE COMPOUNDS CONTAINING AMINE IMPURITIES

S. D. McCrossen, C. F. Simpson*

SmithKline Beecham Pharmaceuticals
Tonbridge, Kent TN11 9AN, UK.

*Department of Chemistry
Birkbeck College,
Gordon House, 29 Gordon Square
London WC1H 0PP, UK.

ABSTRACT

The purity of alkylnitrile compounds has been investigated using gas chromatography (GC), gas chromatography-mass spectrometry (GC-MS) and high performance liquid chromatography (HPLC). The investigation was carried out to supplement earlier reported work using the alkylnitrile compounds, hexanenitrile and valeronitrile, as mobile phase additives in HPLC. GC impurity profiling and GC-MS experiments showed the presence of low level nitrogenous impurities in the alkylnitrile compounds. Analytical interrogation and chemical isolation were employed to identify the impurities as alkylamines. Tri-n-butylamine (TBA) and di-n-pentylamine (DPA) impurities were found in batches of hexanenitrile and valeronitrile respectively and it was found that it was the amine impurities, at very low levels, which caused the observed chromatographic improvements for basic solutes when

using the alkylnitrile compounds as mobile phase additives in reversed-phase HPLC. The amines themselves were subsequently used at extremely low levels (ppm) in the mobile phase and were found to be very effective in their action.

INTRODUCTION

The chromatography of basic solutes has always presented problems on silica-based reverse phase columns because of the residual silanol groups resident on the silica substrate.[1-5] It is well known that silanol groups cause undesired secondary retention processes and distorted peak shapes.[2,6-8] Many techniques are employed to overcome these problems e.g. use of specialised base-deactivated column packings and polymer coated phases,[9-11] amine additives[12-14] and ion suppression.[2]

In an earlier investigation using aliphatic compounds as mobile phase additives to influence the retention characteristics of solutes on reverse phase media, we reported the successful use of alkylnitrile compounds to improve the chromatography of basic solutes.[15,16] Our recent studies have shed further light on this area and the results are reported here. Di-n-pentylamine (DPA) impurities were found in batches of valeronitrile at very low levels using a chemical isolation procedure and GC-MS analysis. Similarly, tri-n-butylamine (TBA) was found in batches of hexanenitrile. Both DPA and TBA were shown to be effective mobile phase additives in that only very low quantities (ppm) were required to bring about good chromatography for some basic solutes.

This paper describes these recent findings which show that our initial explanation for the observed chromatographic effects needs to be revised.

EXPERIMENTAL

Materials

HPLC

A Hewlett-Packard 1090M HPLC system (Stockport, UK) was used. Data were collected and reduced using the Waters 860 Expert Ease data system (Millipore, Watford, UK). HPLC grade solvents (Romil Chemicals, Loughborough, UK) and purified water were used for the investigations. All
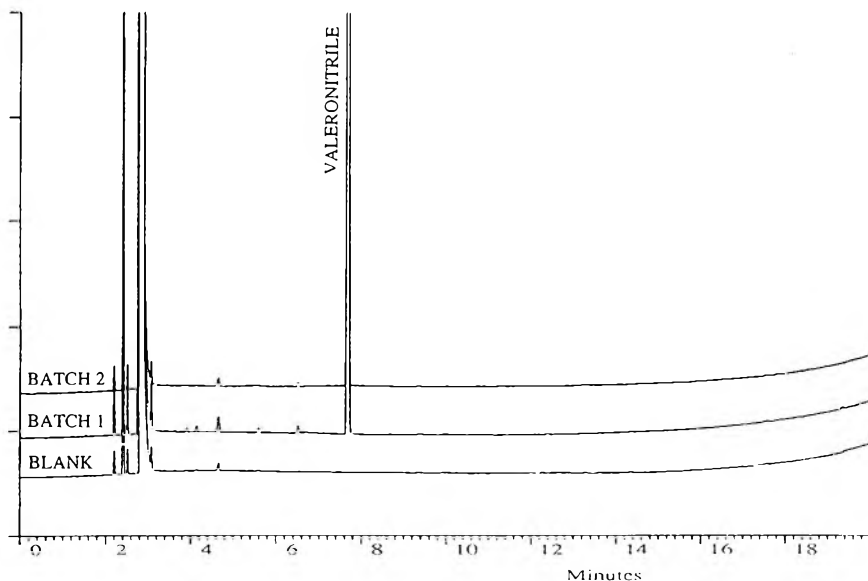
Figure 1. GC Impurity profile chromatograms of two valeronitrile batches. [Column DB 624, 30mx0.32mm, carrier gas:helium at 2.5 mLmin^{-1}, split flow 50mLmin^{-1}; Program: 10°Cmin^{-1} from 40° to 240°C, injection: 1.0 μL at 200°C, Detection: FID at 250°C].

chemicals were of analytical grade (Aldrich, Gillingham, UK). Chromatographic separations were performed on Spherisorb C8, 3 μm, 3 cm x 4.6 mm I.D. columns (Phase Separations, Deeside, UK) thermostatted at 40°C. The flow-rate was 1.0 mLmin^{-1} and UV detection set at 254 nm. The injection volume was 1.0 μL.

Mobile phases were prepared from methanol-water (50:50 w/w) and the additive and degassed with helium before use. The test solutes aniline, N-methylaniline, and N, N-dimethylaniline were prepared in methanol at 0.5 mgcm^{-3} concentration. All separations were carried out in isocratic mode.

GC and GC-MS

A Hewlett-Packard 5890 gas chromatograph (Stockport, UK) was used for the GC experiments. A DB-624, 30m x 0.32mm, 1.8 μm film capillary column (J&W Scientific, Folsom, USA) was used. Dichloromethane was used as the
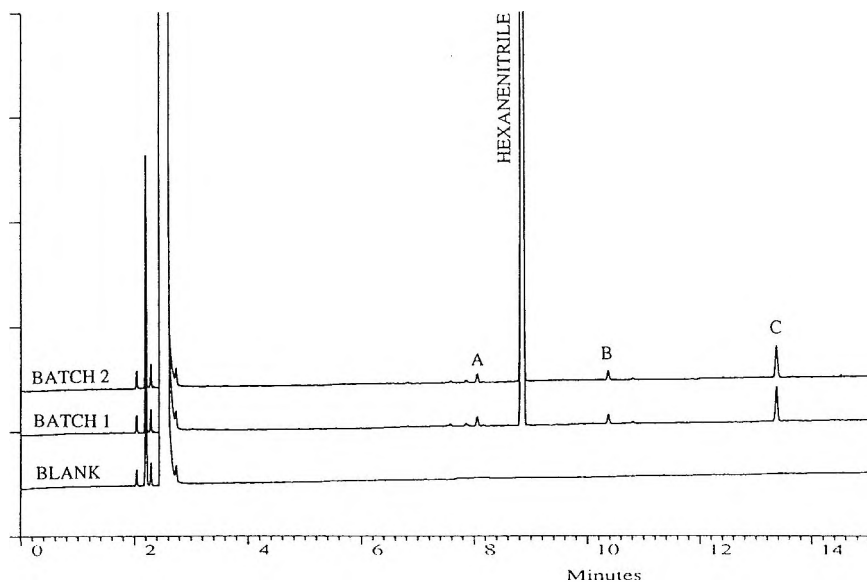
Figure 2.   GC Impurity profile chromatograms of two hexanenitrile batches. Conditions as in Figure 1, except program:10°Cmin^{-1} from 50° to 200°C]

sample diluent.   GC-MS was performed using a Hewlett-Packard 5890 GC coupled to a VG Trio-2 single quadrupole mass spectrometer (Altringham, UK).

METHODS

Isolation of Impurities from and Purification of Alkylnitrile Compounds

Hexanenitrile and valeronitrile were purified individually by washing the compound with 2M HCl three times. The organic phase was then washed with aq. NaHCO$_3$ three times to neutralise residual acid followed by three washings of aq. NaCl until neutral. The organic phase was dried over anhydrous MgSO$_4$ and filtered to give the purified compound. The acidic aqueous washings from the purification procedure were then adjusted to pH 12 with aq. NaOH and then another extraction with dichloromethane performed.   This dichloromethane extract was analysed by GC.
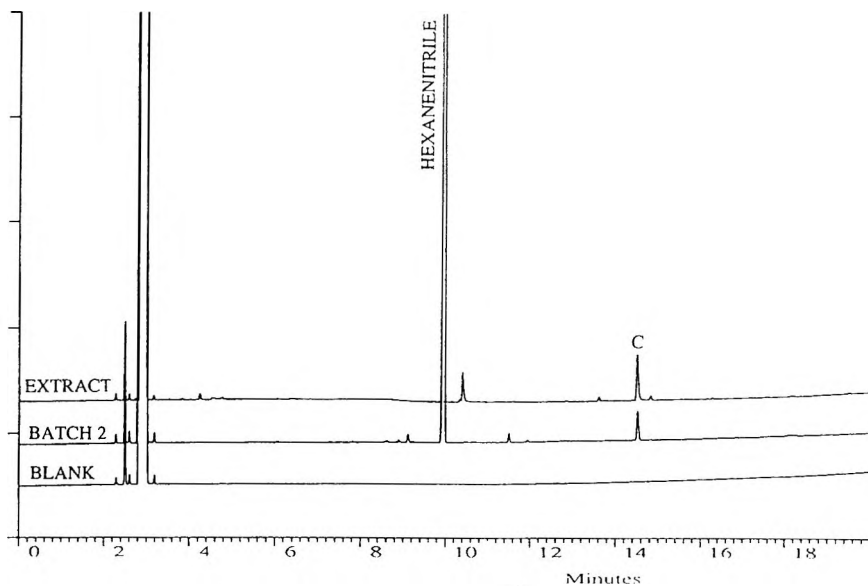
Figure 3. GC Chromatograms showing the presence of Impurity C in hexanenitrile and its dichloromethane extract. [Conditions as in Figure 1].

RESULTS AND DISCUSSION

The chromatography of basic solutes has always been problematical on silica-based reverse phase columns because of the residual silanol groups resident on the silica substrate.[1-5] It is well known that silanol groups cause undesired secondary retention processes and give rise to distorted peak shapes.[2,6-8]

Many techniques are employed to overcome these problems e.g. use of specialised base-deactivated column packings and polymer coated phases,[9-11] amine additives[12-14] and ion suppression.[2] In our earlier work we suggested the use of the alkylnitrile additives, hexanenitrile and valeronitrile, for use as mobile phase additives as an additional approach for the reverse phase chromatography of basic solutes.[15,16]

Our subsequent investigations have revealed that the chemical purity of the alkylnitrile additives employed is in question. Impurities, in some cases at trace levels, in the additives have been found to be responsible for our initial findings as described in the following sections.
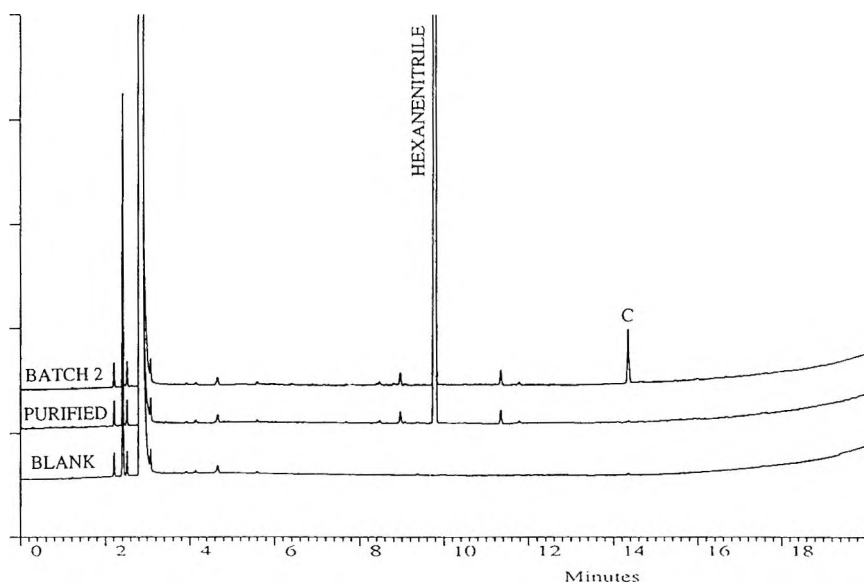
Figure 4. GC Chromatograms comparing parent and purified hexanenitrile. [Conditions as in Figure 1].

GC and GC-MS Investigation of Alkylnitrile Compounds

In the course of our earlier investigations into the use of valeronitrile as a mobile phase additive the chemical purity of the valeronitrile was determined to supplement the study. Valeronitrile was found to have high chemical purity (> 99.8% by area) using GC impurity profiling. Figure 1 shows the impurity profiles of two valeronitrile batches.

In our subsequent investigations into the use of hexanenitrile, its purity was determined similarly by GC impurity profiling. Hexanenitrile was found to be considerably less pure (98.0% by area for two batches) than valeronitrile as shown by the GC chromatograms in Figure 2. Some impurities (**A, B** and **C**) in hexanenitrile were deemed significant. To identify the impurities GC-MS was employed. Results showed that Impurities A and B had molecular masses of 114 and 128 respectively but were not identified. More importantly, MS data for Impurity C showed that its molecular mass was 185 and its molecular formula to be $C_{12}H_{27}N$. It was likely that Impurity C could be an amine, possibly di-n-hexylamine (DHA) or more probably tri-n-butylamine (TBA). Impurity **C** was found in both batches (1.2% by area). The presence of a
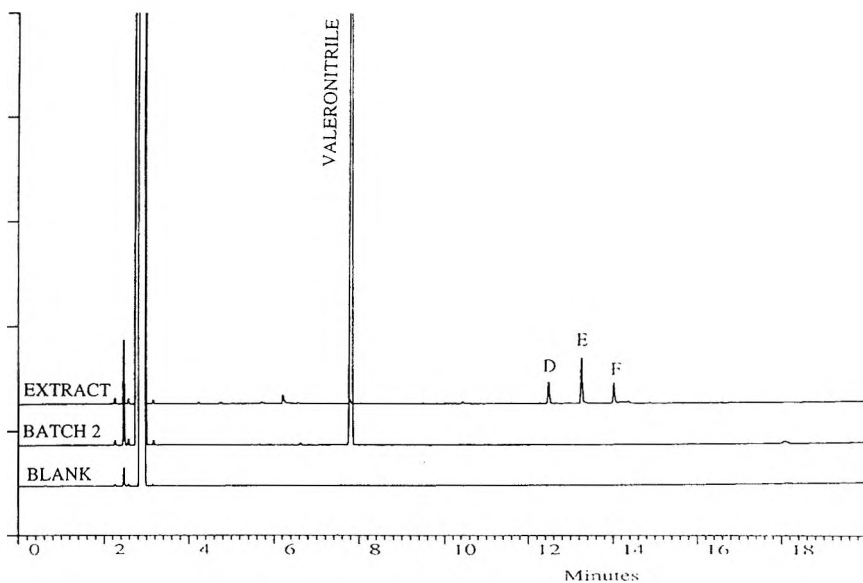
Figure 5. GC Chromatograms comparing valeronitrile with its dichloromethane extract. [conditions as in Figure 1].

nitrogen containing compound prompted further investigation. Work was performed to isolate any possible nitrogen impurities from the hexanenitrile and to purify it using an acid washing and extraction procedure (see Methods). Using the acid washing procedure any nitrogen containing impurities were converted to their respective HCl salts and could be removed from the hexanenitrile. The acid washings were neutralised, rendered basic and extracted with dichloromethane. The nitrogenous impurities (in their non-protonated form) were isolated in the dichloromethane extract. The extract was subsequently analysed by GC and GC-MS. The GC chromatogram of the extract was compared with the hexanenitrile impurity profile (Figure 3). The main component of the extract was found to correspond to Impurity **C**. Impurity **C** was confirmed as tri-n-butylamine from its mass spectrum and by use of an authentic specimen as a GC retention marker. No other significant impurities found in the extract were identified as amines. Figure 4 shows a comparison of the parent and the purified hexanenitrile. The level of TBA was found to be 0.03% (by area) in the purified material thus showing that the purity of the hexanenitrile had been upgraded significantly.
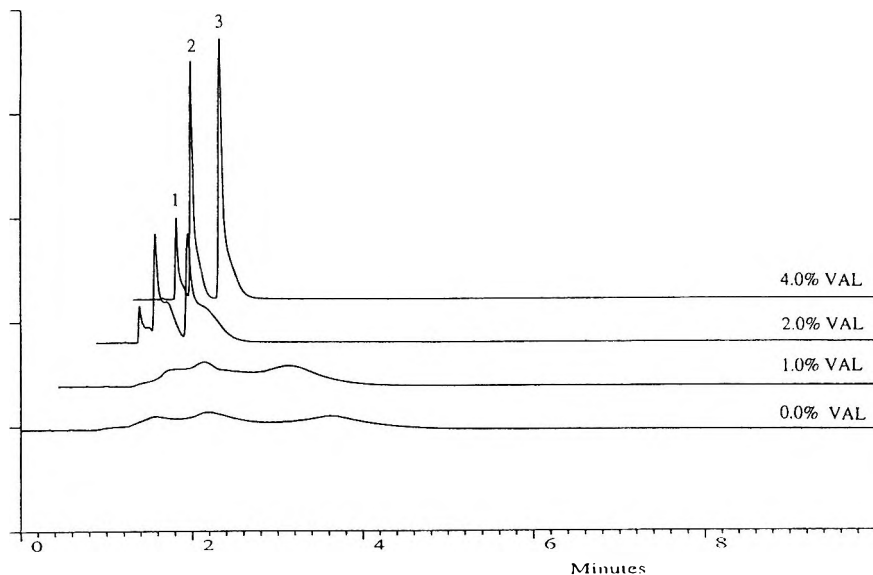
Figure 6. HPLC Chromatograms showing the effect of purified valeronitrile in the
chromatography of aniline solutes in a methanol-water mobile phase.
1 = Aniline, 2 = N-methylaniline, 3 = N, N-dimethylaniline [conditions: Column: 3μ
Spherisorb C8, 30mm x 4.6mm ID, thermostatted at 40°C, Flow rate: 1cm^3 min^{-1}
methanol-water (50:50 w/w) plus additive].

The presence of amine in hexanenitrile was a cause for concern in light of
the HPLC mobile phase additive investigations so the purity of valeronitrile was
re-examined.   Valeronitrile was subjected to the same acid washing and
extraction procedure as hexanenitrile. The extract was analysed using GC and
GC-MS with chemical ionization (ammonia gas) employed to maximise
detection of nitrogen compounds. Three significant components (**D, E** and **F**)
were identified in the extract using GC analysis (Figure 5).   Using GC-MS
components **D, E** and **F** were found to have the same molecular mass (157) and
molecular formula, $C_{10} H_{23} N$. The components were isomers and had identical
fragmentation patterns. MS could not distinguish the isomers but they were
tentatively assigned as di-n-pentylamine isomers. Using an authentic mixture
of di-n-pentylamines the components (impurities) **D, E** and **F** were identified as
bis-2-methylbutylamine, pentyl-2-methylbutylamine and di-N-n-pentylamine
respectively. The retention of these compounds was compared with the GC
chromatogram of the parent valeronitrile from which the extract was derived.
The presence of di-n-pentylamines could   not   be detected in the parent
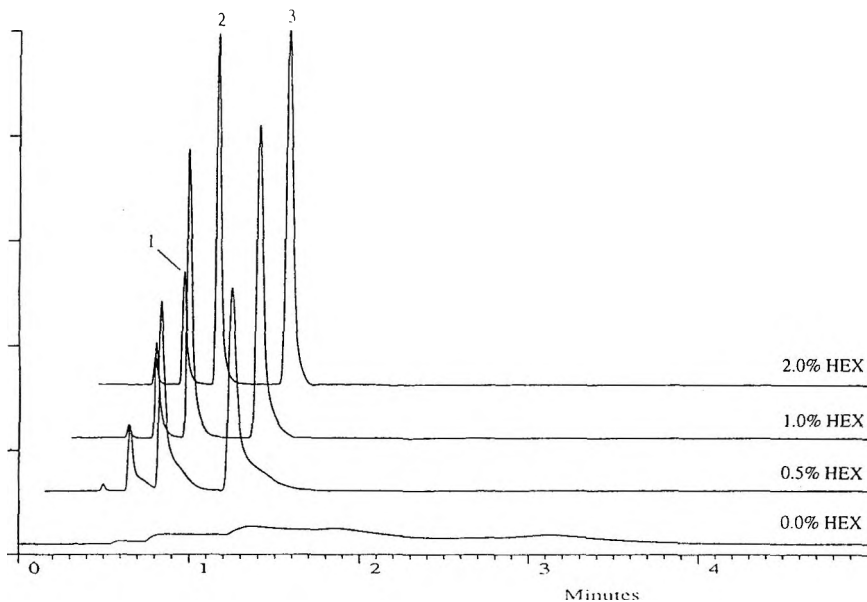
Figure 7.. HPLC Chromatograms showing the effect of purified hexanenitrile on the chromatography of aniline solutes in a methanol-water mobile phase. [Peak identification and conditions as in Figure 6].

valeronitrile under the method conditions used. The levels of di-n-pentylamines in the parent valeronitrile were thus exceedingly small (limit of detection (0.02% by area), however, a trace of impurity D (0.04% by area) could be determined in one valeronitrile batch.

HPLC - Use of Purified Valeronitrile and Hexanenitrile

HPLC chromatograms were obtained using purified and untreated valeronitrile and hexanenitrile as mobile phase additives and the results compared. It was found that substantial quantities of the valeronitrile (> 4% w/w) and hexanenitrile (2.0% w/w) were required to bring about the chromatographic improvements (Figures 6 and 7 respectively). Previous work[15,16] had indicated that only small quantities of valeronitrile (ca. 0.2% w/w) and hexanenitrile (ca. 0.05% w/w) were needed to improve the peak shapes of basic materials. It is clear that the purified additives are very much less effective at reducing peak tailing and that the previously observed chromatographic improvements should be attributed to the presence of amines
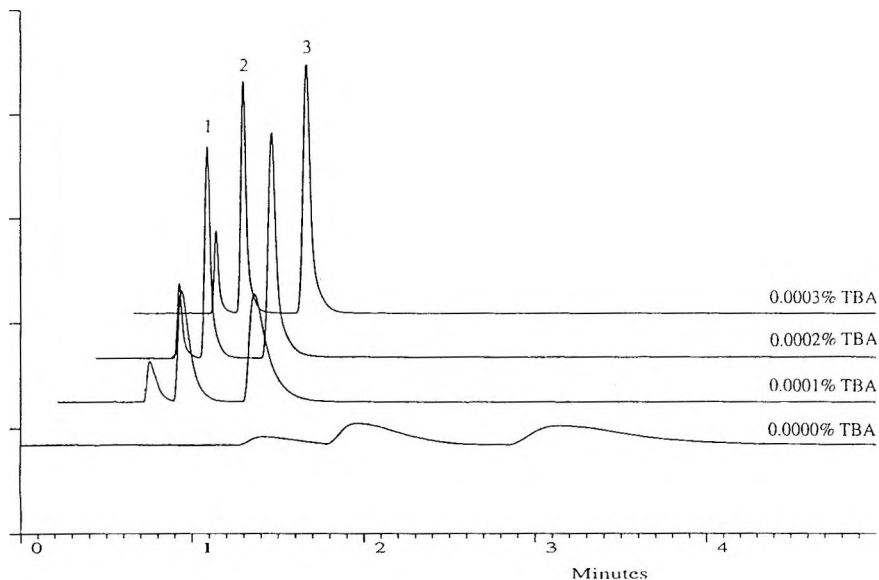
Figure 8. HPLC Chromatograms showing the use of tri-n-butylamine (TBA) as an additive in a methanol-water mobile phase.[Peak identification and condiitons as in Figure 6].

in the mobile phase.   In our previous work, the action of the alkylnitrile compounds was attributed to the possible adsorption of the alkylnitrile molecules effectively covering the surface of the reverse phase preventing solute-silanol interactions.[16]   Since it was not possible to totally eliminate TBA from hexanenitrile the observed chromatographic improvements in Figure 7 are probably due to the presence of this small quantity of amine in hexanenitrile rather than from the effect of hexanenitrile itself.

HPLC - Use of Amines as Additives

TBA and DPA were used separately as mobile phase additives for the reverse phase chromatography of the aniline test solutes. DPA was used as a mixture of three isomeric di-pentylamines (available commercially).   It was found that only very low levels (ppm) of TBA and DPA in the mobile phase were required to bring about good peak shapes for aniline solutes (Figures 8 and 9 respectively). Removal of the amine from the mobile phase returned the chromatography to its previous state.
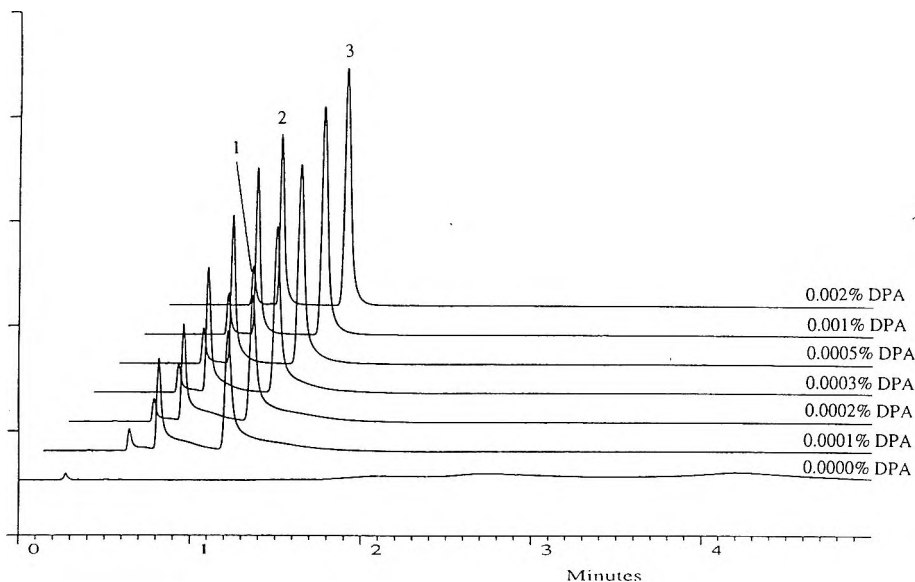
Figure 9. HPLC Chromatograms showing the use of di-n-pentylamines (DPA) as additives in a methanol-water mobile phase.[Peak identification and conditions as in Figure 6]

The efficacy of both DPA and TBA is high because of the properties of the compounds i.e. high basicity and low aqueous solubility. Literature pK_a values for DPA (water) and TBA (in aqueous ethanol) are 11.2 and 9.9 respectively.[17] These values are in reasonable agreement with calculated pKa data of 12.0 for DPA and 10.1 for TBA (programme: PALLAS v.1.1, Compudrug Chem. Ltd). Both amines are strongly basic and depending on the apparent pH of the mobile phase (approximate neutrality) could be ionized i.e. will have a high affinity for silanol groups on the silica substrate. Owing to the lipophilicity of the compounds, molecules of DPA and TBA will also have a strong affinity for the reverse phase which will augment their retention and contribute to their efficacy as additives. Wehrli et al. showed in a study on the effect of amines on the dissolution of silica that there was an order of "aggressivity" of the amine toward silica.[18] It was shown that the type of alkyl substituent on the amine affected the rate of column deterioration i.e. propyl substitution was found to be less aggressive than ethyl substitution and so forth. It follows that TBA and DPA should be even less severe towards silica-based packings and because of the low concentration required may offer an advantage over other commonly employed amines.

Origin of Impurities

The origin of the impurities is not clear, but it is possible that the impurities could be formed from large-scale production of nitrile compounds from an ammoxidation reaction using ammonia in the presence of an alkyl reagent such as an alcohol.[19,20] Proprietary information regarding the synthesis for both valeronitrile or hexanenitrile could not be obtained. Information on potential impurities in valeronitrile was obtained but no details were given for expected amine contamination. No information could be obtained regarding potential impurities in hexanenitrile. The work reported here and previously reported work, was undertaken using the highest quality chemicals that could be commercially purchased and accepted in good faith. This work has shown that for some studies it may be necessary to further purify chemicals in-house or consider the effect of impurities (if known) on study results.

CONCLUSION

It has been shown that the observed chromatographic improvements in the peak shapes for aniline solutes, when using valeronitrile and hexanenitrile as mobile phase additives, can be attributed to the presence of low level amine impurities in the additives and not to the adsorption of the alkylnitrile compounds on to the reverse phase. DPA impurities were found in batches of valeronitrile at very low levels using a chemical isolation procedure and GC-MS analysis. TBA was found in batches of hexanenitrile using GC-MS analysis. Both DPA and TBA were shown to be effective mobile phase additives in that very low quantities were required to bring about good chromatography for some basic solutes.

REFERENCES

1. G. B. Cox, J. Chromatogr., **656**, 353 (1993).

2. M. A. Stadalius, J. S. Berus, L. R. Snyder, LC-GC, **6**, 494 (1989).

3. R. J. M. Vervoort, F. A. Maris, H. Hindriks, J. Chromatogr., **623**, 207 (1992).

4. J. G. Dorsey, W. T. Cooper, Anal. Chem., **66**, 857 (1994).

5. D. V. McCalley, J. Chromatogr., **664**, 139 (1994).

6. J. W. Dolan, LC GC Int., **2**, 18 (1989).

7. A. Nahum, C. Horvath, J. Chromatogr., **203**, 53 (1981).

8. K. E. Bij, C. Horvath, W. E. Melander, A. Nahum, J. Chromatogr., **203**, 65 (1981).

9. J. Paesen, P. Claeys., E. Roets, J. Hoogmartens, J.Chromatogr., **630**, 117 (1993).

10. D. V. McCalley,   J.Chromatogr., **636**, 213 (1993).

11. Y. Ohtsu, Y. Shiojima, T. Okumura, J. Koyama, K. Nakamura, O. Nakata, K. Kimata, N. Tanaka, J.Chromatogr., **481**, 147 (1989).

12. J. S. Kiel, S. L. Morgan, R. K. Abramson, J.Chromatogr., **320**, 313 (1985).

13 T. Hamoir, Y. Verlinden, D. L. Massart, J.Chromatogr.Sci., **32**, 14 (1994).

14. R. W. Roos, C. A. Lau-Cam, J.Chromatogr., **370**, 403 (1986).

15. S. D. McCrossen, C. F. Simpson, Anal. Proc. including Anal. Comms, **31**, 9 (1994).

16. S. D. McCrossen, C. F. Simpson, J. Chromatogr., **697**, 53 (1995).

17. N. Hall, M. Sprinkle, J.Am.Chem.Soc., **54**, 3469 (1932).

18. A. Wehrli, J. C. Hildenbrand, H. P. Keller, R. Stampfli, R. W. Frei, J.Chromatogr., **149**, 199 (1978).

19. R. E. Kirk, D. F. Othmer, **Encyclopedia of Chemical Technology**, Wiley, New York, 1978, pp. 892.

20. **Ullmann's Encyclopedia of the Chemical Industry**, VCH, Meinheim, 1991, pp. 363.

PREPARATION OF MIXED C_{18}/C_1 HORIZONTALLY POLYMERIZED CHROMATOGRAPHIC PHASES

Mary J. Wirth,* R. W. Peter Fairbank

Department of Chemistry & Biochemistry
University of Delaware
Newark, DE 19716

ABSTRACT

The horizontal polymerization of trichlorosilanes on silica is discussed with regard to its use in chromatographic separations to reduce silanol activity and improve hydrolytic stability. It is shown that the use of C_1 spacers, which were previously demonstrated to provide very low silanol activity, are resistant to a pH 10 solution for at least 36 hr. It is also shown that the adsorptivity of water by silica gel is an important factor in achieving dense horizontal polymerization.

INTRODUCTION

Two imposing problems exist for presently available silica-based reversed phase chromatographic columns. First, unreacted surface silanols can deprotonate to form a negatively charged surface, causing strong adsorption of organic cations. This strong adsorption gives rise to peak tailing. Mobile phase additives, such as trifluoroacetic acid, amines, or phosphate ions, can reduce adsorption to these negatively charged sites on the surface.[1]

2799

A better way to minimize such adsorption has been to use silica gel that has a high initial concentration of hydroxyl groups because the resulting hydrogen bonding among the silanols reduces their acidity.[2,3] Peak tailing is especially a problem in pharmaceutical applications because the pervasive amine functionality is positively charged at neutral pH. The second problem with available columns is that organosilane monolayers hydrolyze at pH extremes. Low pH, often needed to achieve efficient separations, causes degradation of commercial columns, which leads to added costs and down-time. The stability of silica-based columns is even worse at high pH, limiting typical applications to pH 8 and below.[4] At high pH, the silica substrate is attacked rather than the organosilane monolayer, ultimately resulting in bed collapse. Peak tailing is exacerbated by hydrolytic instability because hydrolysis exposes more surface silanols. There is a great demand for hydrolytically stable stationary phases having minimal silanol activity.

The majority of bonded chromatographic phases are "monomeric" phases, where a chlorodimethylorganosilane is covalently bonded to silica with 1:1 attachment of reagent to surface silanol. The straightforwardness of the reaction makes for a reproducible phase. However, most of the surface silanols remain unreacted, and some of these deprotonate to cause tailing. A technique called end-capping is often used to react some of the remaining silanols with a sterically smaller reagent, such as chlorotrimethylsilane. Endcapping reduces tailing of organic cations, but the improvement is temporary because the trimethylsiloxane groups hydrolyze readily. One variation has been devised to improve hydrolytic stability: larger sidegroups, such as isopropyl and isobutyl, replace the two methyl groups in the chlorodimethyloctadecylsilane reagent.[5,6]

Two factors might contribute to the higher stability. First, the bulky groups could sterically hinder attack at the siloxane bond. Second, the bulky groups could impede diffusion of the silicon moiety away from the site, allowing the siloxane bond to form again. These "sterically protected" phases are commercially available and are bonded to Zorbax-RX-sil, providing not only high stability but inherently lower silanol activity due to the lower acidity of Zorbax-RX-sil. As with any silica-based stationary phase, these cannot be used at excessively high pH.

If the use of silica could be avoided, high pH could be used routinely in liquid chromatography. This would allow separation of species that are only soluble or only separable at high pH, and would also open up a new area for HPLC: biotechnology. Presently, polymeric resins are used for purification in biotechnology because a base wash is required to remove irreversibly adsorbed proteins or cellular materials from the column. Copolymers of polystyrene and divinylbenzene provide hydrophobicity comparable to that of C_{18} monolayers, but offer virtually unlimited stability at high pH. However, polymeric resins are quite compressible, degrading

analytical separation efficiency and compromising resolution. A much less compressible stationary phase for use at high pH employs zirconia in place of silica.[7] Unlike silica, zirconia is not attacked by strong base. A thin polymer film, such as butadiene, provides a stable stationary phase covering the stable substrate. The one difficulty with zirconia is that its high surface charge gives rise to strong peak tailing of charged analytes such as proteins.[8]

There is not yet another substrate that satisfactorily replaces silica gel, and many research efforts are underway, using a variety of bonding schemes, to improve the performance of silica-based stationary phases. One alternative approach is the "polymeric" phase, where trichlorosilanes are mixed with a small amount of water and allowed to bond to the silica gel.[9] These polymeric phases are made of pure C_{18}, and have a bonding density of typically 5 $\mu mol/m^2$.

Analysis of a polymeric C_{18} phase using quantitative ^{29}Si NMR dispelled the notion of "vertical polymerization": there is an average 1:1 attachment between reagent and surface silanol.[10] These still differ from the monomeric phases, despite their common 1:1 attachment, because there is frequent covalent bonding to nearest neighbors. The resulting nearest neighbor spacing is much closer than that for monomeric phases, offering unique shape selectivity that can be especially valuable for PAH analysis, distinguishing species based on nonplanarity.[11]

Polymeric phases have improved hydrolytic stability, presumably owing to the multiple bonding. The procedure for synthesis is likely to cause significant oligomerization before attachment to the surface, making the organization on the molecular scale unknown. These phases have been commercially available for years but are believed to be less reproducible than monomeric phases, possibly a consequence of oligomerization before bonding.

A newer innovation that also uses trifunctional reagents is made by reacting a trifunctional hydrosilane, such as $HSi(OCH_2CH_3)_3$, with silica gel to form a hydrosilane surface. The desired functional group is subsequently linked to theSi-H surface through a reagent having a terminal carbon-carbon double bond.[12] The functional group is attached by a direct Si-C bond, which is much more hydrolytically stable than the Si-O-Si bond formed in the conventional monomeric phases. The initial layer of Si-H groups forms a dense monolayer, thus protecting the silica substrate and lowering the silanol activity.[13]

The absence of sidegroups on the ligand allows the same denser bonding that is believed to give the polymeric phases their unique selectivity. One would expect these hydrosilane phases to be more reproducible than the polymeric phases because the olefin reaction involves no danger of oligomerization before bonding.
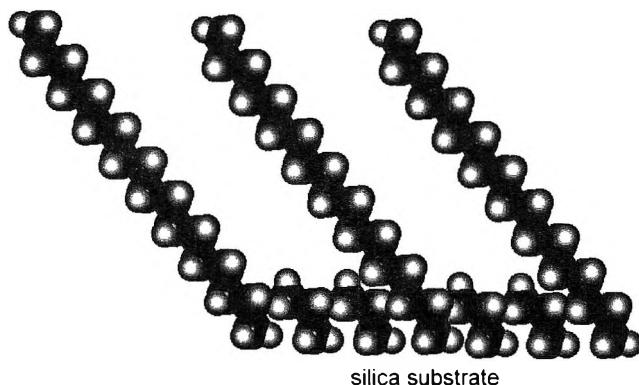
silica substrate

Figure 1. Space-filling model of a cross-section of the horizontally polymerized C_{18}/C_3 monolayer. The dense polymerization of trifunctional silanes in two-dimensions is designed to form a solid barrier immediately above the silica substrate, with little covalent attachment to the silica substrate. The mixing of C_{18} groups and short spacers gives a liquid-like density of functional groups to perform chromatographically as monomeric phases. The C_{18} chains are drawn in their all-trans conformations only for artistic convenience.

We have devised a bonding scheme for organosilanes on silica that also uses trifunctional silanes.[10,14,15] The bonding scheme is illustrated in Figure 1, where the process of "horizontal polymerization", or "self-assembly" is used to make mixed monolayers. ^{29}Si NMR spectroscopy has revealed that the trifunctional reagents are bonded to one another, with only an occasional covalent bond to the surface.[10] The oriented copolymer covering the surface is intended to provide a steric barrier between the mobile phase and the silica substrate. This dense barrier would reduce surface charge by impeding the exchange of protons between the unreacted silanols and the mobile phase. The surface concentration of octadecyl (C_{18}) or other functional groups is adjustable by varying the reagent ratio.

There are two features that distinguish horizontally polymerized phases from the polymeric phase described earlier. First, the synthesis of the horizontally polymerized phase uses the water intrinsically adsorbed to silica gel, as illustrated in Figure 2. Consequently, no oligomerization occurs until the reagents have reached the surface. The use of a reproducible amount of adsorbed water provides a reproducible stationary phase. Second, a mixture of trifunctional silanes is used, providing a steric barrier with controllable coverage of the functional group.
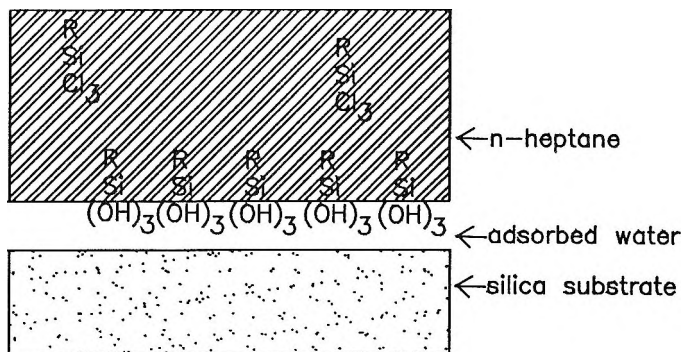
Figure 2. The oriented polymerization reaction. A monolayer of water adsorbed to the silica gel rapidly hydrolyzes the trichlorosilanes. The resulting trisilanols are adsorbed and oriented at the heptane/silica interface, and subsequently polymerize to form the dense monolayer.

The self-assembly of pure trichlorosilanes on silica surfaces has been studied by other groups with the goals of controlling the wetting properties of surfaces,[16,17] enhancing resolution in lithography,[18,19] electrochemical sensing,[20-22] molecular electronics,[23,24] preparing membrane mimetics[25] and biocompatible surfaces.[26] Our work represents the first use of the concept of applying the solid bonding density of self-assembly to make chromatographic stationary phases.

Previous Studies

Trifunctional silanes tend to be more susceptible to base hydrolysis than are monomeric silanes. This is because the silicon atom is a better electrophile when bonded to three oxygens compared to one, accelerating reaction with the bases, which are nucleophilic. This is the same reason that silica gel itself dissolves at high pH. Analogously, at low pH, trifunctional silanes are expected to be less susceptible to hydrolysis (per Si-O bond) because acids are electrophilic.

In stability studies of the C_{18}/C_3 horizontally polymerized phase, the retention time of benzo(a)pyrene was found to be constant at pH 2 over an observation period of one week.[15] This was not surprising given that the functional groups are the inherently acid-stable trifunctional silanes. However, the phase was also stable to a mobile phase at pH 10 over the observation period of 36 hours, again using benzo(a)pyrene as the probe.[15] The hydrolytic stability of a monomeric C_{18}, made on the same silica gel, Whatman Partisil, was poorer at both pH extremes.
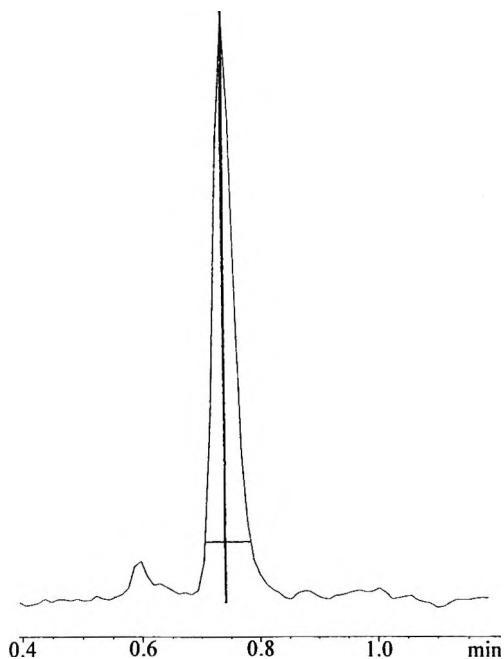
Figure 3. Chromatogram of aniline after 36 hr. exposure of stationary phase to pH 10 solution. The retention time is 0.75 min. and the asymmetry factor is only 1.2. A column length of 15 cm and flow rate of 2 mL/min. were used.

Separation Performance

The horizontally polymerized C_{18}/C_3 phase gave a chromatogram similar to that of a conventional C_{18} phase for a mixture of benzo(a)pyrene, hexanophenone and uracil; however, aniline was retained inordinately long.[15] The phase thus improved the hydrolytic stability but increased the silanol activity. This behavior indicates that the C_3 spacers did not form an adequately dense barrier over the silica substrate. A careful consideration of the steric interactions involved in creating an oriented, two-dimensional polymerization reveal that the C_3 spacers cannot be accommodated by the short Si-O-Si distances linking the reagents together. However, a network of C_1 groups is capable of forming a dense, two-dimensional methylsiloxane polymer.[27] Experimental measurements confirm this expectation. ^{29}Si NMR spectra revealed that a C_{18}/C_1 monolayer is comprised primarily of the alkylsiloxane groups covalently bonded to other reagent groups through all three oxygen atoms, with little attachment to the silica surface, while the C_{18}/C_3 monolayer is
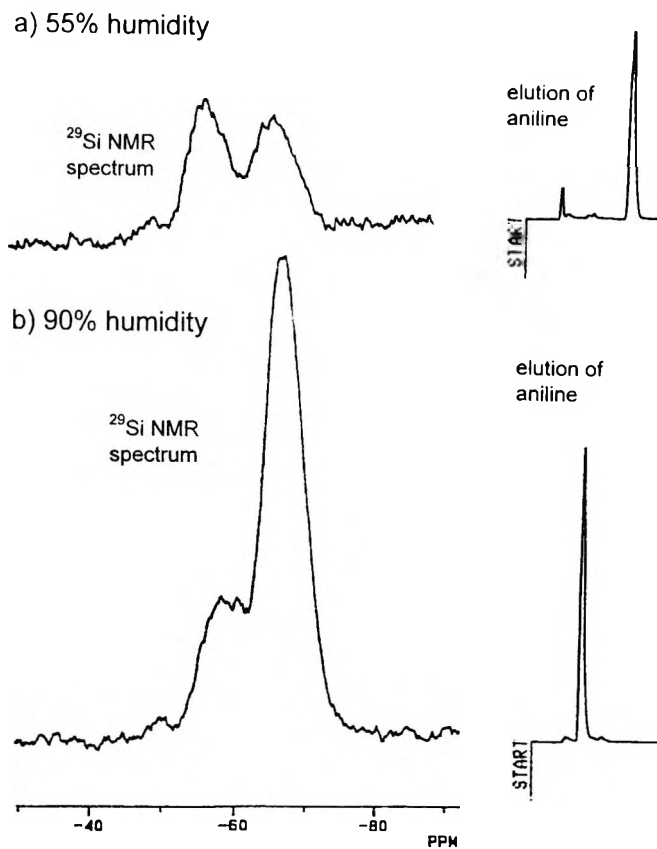
Figure 4 ^{29}Si NMR spectra and chromatograms of aniline for horizontally polymerized C_{18}/C_1 phase obtained upon pretreatment with a) 55% humidity and b) 90% humidity.

comprised primarily of the alkylsiloxane groups covalently bonded through only two oxygen atoms, with occasional attachment to the silica surface.[27] The NMR spectra thus reveal that the C_{18}/C_1 monolayer is a two-dimensional network while the C_{18}/C_3 monolayer is comprised of long chains packed close to one another. Since the reagents are bonded to one another, it would be possible for the small methyl groups to be oriented toward the surface.

Contact angle studies of C_1 monolayers on flat plates indicate that the methyl groups are oriented away from the surface: the contact angle is 78° for both the methylsiloxane monolayer on silica[27] and the methylthiol monolayer

on gold,[25] where the latter is known to have the methyl groups point away from the surface. The research thus shows that C_1 is a significantly better spacer group than C_3 for achieving maximum bonding density.

Finally, for the chromatographic test, aniline elutes early with little tailing, and a baseline separation of a mixture of cytochrome c genetic variants (bovine, equine, canine), was demonstrated using the C_{18}/C_1 phase.[27] These studies indicate exceptionally low silanol activity for the C_{18}/C_1 phase.

Stability Of The C_{18}/C_1 Phase

While the hydrolytic stability of the C_{18}/C_3 phase is excellent, the hydrolytic stability of the C_{18}/C_1 phase has not previously been tested. Hydrolytic stability of the C_{18}/C_1 phase is a concern because the shorter spacer group might be more prone to hydrolysis, particularly at defects, due to less steric hindrance. On the other hand, one might argue that the C_{18}/C_1 phase should be more stable due to its denser bonding. Over the course of our studies, we have not observed any unusual degradation of the C_{18}/C_1 phases.

For a freshly prepared C_{18}/C_1 phase, we reported a short retention time and a low asymmetry value for the zone profile of aniline at neutral pH.[27] If this phase degraded, the exposed silica would partially deprotonate, retaining aniline more strongly and giving rise to tailing. We exposed this stationary phase to a solution of triethylamine in 85% acetonitrile/water at 30°C for 36 hours, the same harsh conditions and exposure time applied to the C_{18}/C_3 horizontally polymerized phase.

Figure 3 shows the chromatogram for aniline, where its zone maintains its short retention time and low asymmetry. These data alleviate concerns about the stability of methyl spacers.

Applicability to other Silica Gels

While impressively low silanol activity was demonstrated for the C_{18}/C_1 horizontally polymerized phase, this phase was made on Zorbax-300RX-sil, and it is not been established that horizontal polymerization works well with other silica gels. Initial experiments with a variety of other silica gels did not yield acceptable stationary phases. It is possible that these early problems were caused by different water adsorptivities of different silica gels.

The Zorbax-RX-sil had been exposed to 55% humidity for depositing the reagent water on the surface because this was the humidity reported to work well for self-assembled monolayers of C_{18} on silicon wafers.[29]

Recently it is has been shown that the density of self-assembled C_{18} monolayers on flat silica surfaces varies with the amount of reagent water available for the trichlorosilanes.[30,31] For chromatographic surfaces, we varied the amount of adsorbed water by varying the relative humidity to which the bare silica was exposed, then measured the ^{29}Si NMR spectra and the chromatographic behavior. The same conditions for cross-polarization were used as previously reported.[10]

The spectral intensities for the resonances due to the reagent silicon atoms can be compared to one another because their relaxation times are comparable.[10] Figure 4 shows the ^{29}Si NMR spectra of a C_{18}/C_1 phase on SMR22, a silica gel available from Davison, Inc., where a) 55% humidity was used, and b) 90% humidity was used.

The NMR spectrum in part a) shows weak cross-linking for the lower humidity: the predominant peak, at -58 ppm, owes to reagent silicon atoms having a terminal OH group. The spectrum in part b) reveals extensive cross-linking for the higher humidity: the predominant peak, at -68 ppm, owes to reagent silicon atoms bonded through all three oxygens to other silicon atoms. A fully cross-linked network would have a peak only at -68 ppm, so room still remains for improvement in the synthesis of horizontally polymerized monolayers. The stronger overall signal in the silicon NMR spectrum for case b also indicates a higher coverage of reagent silicon atoms, consistent with the denser monolayer.

The chromatograms, shown to the right of the NMR spectra, reflect these structural differences: for case b, aniline elutes earlier and with a much narrower peak. The humidity required for good horizontal polymerization on SMR22 thus differs markedly from that for Zorbax-RX: 55% vs. 90%. The likely reason Zorbax-RX is so adsorptive toward water is that it has a very high concentration of surface hydroxyl groups.[2]

The ability to vary surface water concentration to control the quality of horizontal polymerization suggests that horizontal polymerization can be used with virtually any silica gel, provided that the humidity is appropriately adjusted to obtain the appropriate water coverage. We are currently investigating the quantitative amount of water needed for different silicas to determine whether or not there is a requisite amount of water that is a constant.

Application to Capillary Electrophoresis

Strong adsorption due to surface silanol activity is also a major problem in capillary electrophoresis, particularly for proteins that are strongly positively charged. Horizontal polymerization has been shown to provide a surface coating that has virtually no charge, as indicated by the absence of detectable electro-osmotic flow and the elution of very surface-active proteins.[32] A mixture of allyl groups and C_1 groups were used in the horizontal polymerization, followed by copolymerization of the allyl groups with polyacrylamide to make the surface hydrophilic. This demonstrates the use of functional groups other than C_{18} in horizontal polymerization, as well as applicability of horizontal polymerization to another area of separation science.

Future Studies

Horizontal polymerization has thus far been demonstrated for C_{18} and allyl functional groups. The bonding scheme may find valuable application for separations requiring shorter alkyl chains, such as C_4, to minimize the denaturing of proteins. Other reactions of allyl groups for controlling the chemical functionality of the monolayer are also attractive, such as amino and other ion exchanging groups. Also, hydrophilic groups such as diols can be dispersed among the spacers to moderate the hydrophobicity of the surface. Finally, there is much more to be learn about the process of two-dimensional polymerization, and physical studies of this process may ultimately lead to chromatographic stationary phases stable toward very high pH.

ACKNOWLEDGMENTS

REFERENCES

1. J. Paesen, P. Claeys, E. Roets, J. Hoogmartens, J.Chromatogr., **630**, 117 (1993).

2. J. Köhler, D. B. Chase, R. D. Farlee, A. J. Vega, J. J. Kirkland, J. Chromatogr., **352** 275 (1986).

3. J. Köhler, J. J. Kirkland, J. Chromatogr., **385**, 125 (1987).

4. J. J. Kirkland, M. A. van Straten, H. A. Claessens, J. Chromatogr., **691**, 3-19 (1995).

5. J. J. Kirkland, J. L. Glajch, R. D. Farlee, Anal. Chem., **69,** 2 (1989).

6. J. J. Kirkland, C. H. Dilts, J. E. Henderson, LC•GC, **11**, 290 (1993).

7. J. Nawrocki, C. J. Dunlap, P. W. Carr, J. A. Blackwell, Biotech. Prog. ,**10**, 561-573 (1994).

8. L. F. Sun, P. W. Carr, Anal. Chem., **67**, 3717-3721 (1995).

9. L. C. Sander, S. A. Wise, Anal. Chem., **56**, 504 (1984).

10. H .O. Fatunmbi, M. D. Bruch, M. J. Wirth, Anal. Chem., **65**, 2048 (1993).

11. L. C. Sander, S. A. Wise, J. Chromatogr. **316**, 163 (1984).

12. J. E. Sandoval, J. J. Pesek, Anal. Chem., **63**, 2634-2642 (1991).

13. C. -H. Chu, E. Jonsson, M. Auvinen, J. J. Pesek, J. E. Sandoval, Anal. Chem., **65**, 808-818 (1993).

14. H. O. Fatunmbi, M. J. Wirth, Anal.Chem., **64**, 2783 (1992).

15. H. O. Fatunmbi, M. J. Wirth, Anal.Chem., **65**, 822 (1993).

16. N. L. Abbott, C. B. Gorman, G. M. Whitesides, Langmuir, **11**, 16 (1995).

17. P. E. Laibinis, G. W. Whitesides, D. L. Allara, Y.-T. Tao. A. N. Parikh, R. G. Nuzzo, J. Am. Chem. Soc., **113**, 7152 (1991).

18. C. R. K. Marrian, F. K. Perkins, S. L. Brandow, T. S.Koloski, E. A. Dobisz, Appl. Phys. Lett., **64**, 390 (1994).

19. C. B. Ross, L. Sun, R. M. Crooks, Langmuir, **9**, 632 (1993).

20. F. Malem, D. Mandler, Anal. Chem., **65**, 37 (1993).

21. D. E. Weisshaar, B. D. Lamp, M. D. Porter, J. Am.Chem. Soc., **114**, 5860 (1992).

22. R. J. Willicut, R. L. McCarley, Langmuir, **11**, 296 (1995).

23. C. B. Gorman, H. A. Biebuyck, G. W. Whitesides, Chem. Mat., **7**, 526 (1995).

24. X. O. Zhang, X. -Z. You, S. -H. Ma, Y. Wei, J. Mat. Chem., **5**, 643 (1995).

25. Y. Maeda, H. Yamamotot, H. Kitano, J. Phys. Chem., **99**, 4837 (1995).

26. R. S. Petember, M. Matsuzawa, P. Liesi, Syn. Met., **71**, 1997 (1995).

27. R. W. P. Fairbank, Y. Xiang, M. J. Wirth, Anal. Chem. **67**, 3879 (1995).

28. C. D. Bain, E. B. Troughton, Y -T. Tao, J. Evall, G. M. Whitesides, R. G. Nuzzo, J. Am. Chem. Soc., **111**, 321 (1989).

29. S. R. Wasserman, Y -T. Tao, G. M. Whitesides, Langmuir, **5**, 1074 (1989).

30. J. G. Terlingen, J. Feijen, A. S. Hoffman, J. Colloid Int. Sci., **155**, 55-65 (1993).

31. D. H. Flinn, D. A. Guzonas, R. -H. Yoon, Colloids Surf., **87**, 163-176 (1994).

32. M. Huang, E. Dubrovcakova, M. Novotny, H. O. Fatunmbi, M. J. Wirth, J. Micro. Sep., **6**, 571 (1994).

COMPETITIVE INTERACTIONS OF PHENOL DERIVATIVES AND ALIPHATIC ALCOHOLS FOR ALKENYL AND DIOL SILICA SURFACES

R. K. Gilpin, M. Asif, M. Jaroniec,* S. Lin

Separation and Surface Science Center
Department of Chemistry
Kent State University
Kent, Ohio 44242

ABSTRACT

A thermodynamic equation is used to analyze the retention behavior of phenolic solutes at low modifier concentrations on alkenyl and diol chemically modified silica packings. These materials were prepared by attaching alkenyl and diol ligands with four, six, eight and ten carbon atoms to the surface of LiChrosorb Si-60 silica. The thermodynamic analysis of the capacity ratios of various phenolic solutes measured at different concentrations of simple aliphatic alcohols (used as modifiers) in n-hexane have provided information about solute and solvent interactions with the alkenyl and diol modified silicas. This analysis shows that the solute-alcohol competitive interaction for the alkenyl bonded phases changes significantly with chain length, whereas this effect is not observed for the diol phases. Also, the influence of polarity and geometric structure of functional groups on solute retention have been examined.

2811

INTRODUCTION

For many years chromatography has been used successfully to study molecular interactions at both gas-solid and liquid-solid interfaces. Knowledge of these interactions is necessary not only for developing retention theory but first of all it is needed for understanding the mechanisms of chromatographic separations and for designing and optimizing these separations. Fundamental studies of the role of molecular interactions in tsolute retention accelerated considerably development of optimization methods for chromatographic separations (e.g., see works[1-3] and references therein).

While retention mechanisms at the gas-solid interfaces are relatively simple because they are controlled almost solely by solute-solid interactions, they are much more complex at liquid-solid interfaces.[4,5] Even in the simplest case of liquid chromatography, where a single component mobile phase is used, a solute's retention is controlled by at least four different types of interactions, i.e., solute-solvent, solvent-solvent, solute-solid and solvent-solid interactions. The molecular picture is even more complex for binary solvent mixtures, which are frequently used in carrying out liquid chromatography separations.[6,7] In this latter case, the number of types of interactions controlling a solute retention increases at least up to eight. This number is higher for LC with chemically bonded phases, where the solute and solvent molecules can interact with bonded ligands and with unreacted surface groups of the solid support. In addition, one should consider that solute-solvent and solvent-solvent interactions in the stationary phase differ from those in the mobile phase because they are under the influence of the forces acting between solid and surface molecules.[8] Although the unified statistico-thermodynamical description of LC with mixed-mobile phases[9,10] automatically incorporates all types of molecular interactions, the final expressions resulting from this description are complicated and their practical utility is limited. Therefore, simple models are frequently used to represent solute retention in LSC systems (see papers[11-16] and references therein). Usually, solute retention in normal-phase systems is represented by the displacement (competitive sorption) models,[11,12] whereas for reversed phase systems, it is represented by the partition models.[8,13,14,17,18]

In the current paper, a simple thermodynamic equation, which is based on a displacement model, is employed to analyze the dependencies of the capacity ratios of phenolic derivatives on the modifier concentration. These dependencies were measured at low concentrations of simple aliphatic alcohols (used as modifier's) on alkenyl and diol modified silica surfaces and, at present, they are unique in the chromatographic literature. Up to now, these types of measurements have been reported only for selected alcohol-hydrocarbon mobile

phases on unmodified silicas.[19,20] Analysis of the measured capacity ratios by means of the above mentioned thermodynamic equation provides information about solute-alcohol competitive interactions for alkenyl and diol bonded phases and permits comparison of chromatographic properties of these phases.

EXPERIMENTAL

Reagents

The HPLC grade solvents were obtained from the Fisher Scientific Company (Fairlawn, N.J.) and the reagent grade compounds used as test substances were from the Aldrich Chemical Company (Milwaukee,WI). Water used for preparation of chromatographic packings was purified using a Milli-Q reagent water system from Millipore Model Continental Water Systems (El Paso, TX). The 1,3-butadiene, 1,5-hexadiene, 1,7-octadiene, 1,9-decadiene and triethoxysilane, also purchased from Aldrich, were used without further purification. The synthesis of alkenyltriethoxysilane was carried out as follows: about 20 mL of a given diene was placed in a 52cm x 11mm i.d. stainless steel reactor tube which was flushed with a stream of dry nitrogen gas and placed in a dewar containing dry ice and acetone. Next, 10 mL of triethoxysilane were added to the reactor, followed by 10 drops of a 1% solution of H_2PtCl_6 in 2-propanol. The reactor was sealed, removed from the dry ice-acetone,and allowed to warm. The reactor was placed in an oven and heated for 12 hours at 383K. After the reaction was completed, the tube was again placed in dry ice-acetone and allowed to cool for 1 hr. The reactor was opened and its contents were transferred to a 50mL round bottom flask and vacuum distilled. The identity of the silane product was verified by FTIR.

Chromatographic Packings

The chromatographic packings were prepared in-house by the following procedures. Four grams of LiChrosorb Si-60 silica (E. Merck, Cherry Hill, N.J.; specific surface area 550 m^2/g) were preconditioned with dionized water and dried overnight in an oven at 383K. The dry silica was placed in a reaction vessel with 100 mL of 1-propanol and allowed to stand for 6 hours. Half of the 1-propanol was removed and 10 mL of a given alkenyltriethoxysilane and 10 drops of n-butylamine were added to the reaction vessel. The mixture was refluxed for 24 hr using a stream of dry nitrogen for stirring. Excess solvent was removed using a sintered glass filter under vacuum.

The modified silica was washed several times with methanol and diethylether, and dried overnight in an oven at 383K. This procedure was used to attach 3-butenyl, 5-hexenyl, 7-octenyl and 9-decenyl ligands to silica.

Two grams of a given alkenyl modified silica were stirred with 75 mL of persuccinic acid for 24 hr at 323K; this acid was prepared by reacting succinic anhydride with hydrogen peroxide according to literature procedures.[21,22] The modified silica was washed several times with methanol and then diethylether and dried overnight in an oven at 383K. By stirring alkenyl modified silica with persuccinic acid, the terminal double bond in the alkenyl ligand was converted to a diol group; this conversion was confirmed using diffusive reflectance FTIR and CP/MAS[13]C solid state NMR.[21] By this procedure, the alkenyl bonded phases were converted to suitable phases with dihydroxyalkyl (diol) ligands, i.e., the 3-butenyl, 5-hexenyl, 7-octenyl and 9-decenyl ligands on the silica surface gave, respectively, 3,4-dihydroxybutyl, 5,6-dihydroxyhexyl, 7,8-dihydroxyoctyl and 9,10-dihydroxydecyl bonded ligands.

The alkenyl and diol modified silicas were packed into 25cm x 1.8mm i.d. stainless steel columns by using a dynamic packing procedure. One gram of each packing material was stirred with 30mL of isopropanol in the solvent reservoir and was pressurized into the empty column using methanol as the delivery solvent. The packing procedure was continued for an hour using a Haskel (Burbank, CA) Model DSTV-52C air-driven fluid pump.

Characterization of Modified Silicas

Summmarized in Table 1 are the surface coverages (i.e., % carbon) for the alkenyl and diol bonded phases determined by combustion analysis using a Leco Corporation (St. Joseph, MI) Model CS-244 Carbon Analyzer. The levels of coverage for the alkenyl bonded phases are greater than those for the corresponding diol phases. In addition, the alkenyl and diol phases were characterized by diffuse reflectance infrared spectroscopy and solid state CP/MAS[13]C NMR spectrometry.[21] The diffusive reflectance infrared spectra for the modified silicas with alkenyl bonded ligands had the 3080 cm^{-1} band (also present in the IR spectra for synthesized alkenyltriethoxysilanes), which results from the =C-H stretch. When the double bond in alkenyl bonded ligands was converted to the diol group, this band disappeared. However, the -OH stretch band was not observed because of the background interferences. The unreacted surface silanol groups gave a broad -OH stretch band, which obscured the band for the ligand hydroxyls.

Table 1

Surface Coverages of Chemically Modified Lichrosorb Si-60 Silicas

Bonded Ligand	Code	Total % C
3-butenyl	A4C	4.99
3,4-dihydroxybutyl	D4C	1.89
5-hexenyl	A6C	6.07
5,6-dihydroxyhexyl	D6C	4.39
7-octenyl	A8C	8.39
7,8-dihydroxyoctyl	D8C	6.60
9-decenyl	A10C	9.59
9,10-dihydroxydecyl	D10C	8.06

The solid state CP/MAS ^{13}C NMR spectra for alkenyl modified silicas had resonances at 112 PPM and 138 PPM, which are characteristic for =C-H and =CH$_2$ groups. Two additional resonances at 125 and 132 PPM were observed because of migration of the double bond from the terminal to the 2nd and 3rd positions. A similar effect has been observed during isomerization of 1-pentene adsorbed on silica.[23] After conversion of the alkenyl ligands to dihydroxyalkyl (diol) bonded ligands the above mentioned resonances either disappeared completely or their intensities were reduced significantly. Appearance of two new resonances between 68 and 78 PPM confirmed the presence of -C-OH groups[24] and showed that hydrolysis of the epoxy groups to diols took place during the chemical conversion of the alkenyl ligands. Other experimental details including the IR and NMR spectra with band assignments for alkenyl and diol modified silicas are reported elsewhere.[21]

Chromatographic Measurements

All retention data were recorded and processed on an IBM Instruments Model 9000 data system. Column temperature was maintained at 298K in a water bath using a Fisher Model 730 controller (Pittsburgh, PA). All columns were preconditioned using the procedure reported by Gilpin and Sisco.[25] Before each change in the mobile phase composition, each chromatographic column was conditioned with 500mL of n-hexane and 200mL of the weakest mobile phase and, before the first solute injection, it was additionally equilibrated with at least 100mL of the mobile phase of a selected composition. The retention measurements were performed for the mobile phase compositions changing from low to higher concentrations of the polar modifier. Simple

aliphatic alcohols. i.e., methanol, ethanol, 1-propanol, 2-propanol, 2-butanol and t-butanol, were used as modifiers. The capacity factors of phenol and its o-, m- and p-derivatives with fluoro, chloro, bromo. iodo. hydroxy, nitro and cyano groups were measured at different concentrations of a given aliphatic alcohol in n-hexane. i.e., 0.8, 1.2, 1.6, 2.0, 2.5 and 3.0 v/v% of the modifier in n-hexane. In the case of the methanol-hexane mobile phase the highest concentration was equal to 2.0% modifier because of the low solubility of methanol in n-hexane. The flow rate of the mobile phase was equal 1mL/min. The void volume for each column was evaluated using n-pentane. Each solute was injected separately. The reported values of the capacity ratio, k'_s, are averages from at least duplicate injections.

RESULTS AND DISCUSSION

The chromatographic systems studied in this paper can be considered to be normal-phase because the modified silica surfaces contained polar groups (unreacted silanols and alkenyl or diol ligands) and the hexane-based mobile phases contained only small amounts of aliphatic alcohols used as modifiers. In these systems. the competitive interactions between solute and modifier molecules for active surface groups should dominate over the non-specific interactions characteristic for solute retention on alkyl bonded phases.[8] The competitive interactions of solute (s) and alcohol (a) molecules with the specific surface groups can be represented by a displacement mechanism,[11,12] which is described quantitatively by the following equilibrium constant, K_{sa} :[26]

$$K_{sa} = (a_s^\sigma/a_s^l)\ (a_a^l/a_a^\sigma)^r \qquad (1)$$

where a_s^α and $a_a^\alpha (\alpha = \sigma.l)$ are respectively activities of solute and alcohol (modifier) in the α-phase. the superscripts σ and l refer, respectively, to the stationary (surface) and mobile (bulk) phases, and r is the ratio of molecular areas occupied by the solute and alcohol molecules in the surface phase. Since the solute concentrations in both phases are infinitely dilute and the modifier concentrations are low, the activity coefficients can be approximated by concentration-independent constants and included in the K_{sa}-constant; then equation (1) can be rewritten as follows:

$$K_{sa}^* = (x_s^\sigma/x_s^l)\ (x_a^l/x_a^\sigma)^r \qquad (2)$$

Here K_{sa}^* is the modified constant K_{sa}, which includes the solute and modifier activity coefficients, x_s^α and x_a^α ($\alpha = \sigma$, l) are, respectively, the solute and modifier mole fractions in the α-phase. The solute capacity factor can be defined as follows:[6]

$$k_s' = \phi \ (x_s^\sigma/x_s^l) \quad for \ x_s^l \longrightarrow O \tag{3}$$

where ϕ is the phase ratio. Combination of equations (2) and (3) allows to express k_s' by means of the mole fractions of modifier in both phases:

$$k_s' = \phi \ K_{sa}^* \ (x_a^\sigma/x_a^l)^r \tag{4}$$

Since, in the systems studied here, the specific interactions of solute and modifier molecules with the active surface groups are similar, the solute-modifier ratio r of molecular areas can be approximated by unity. Then equation (4) simplifies as follows:

$$k_s' = \phi \ K_{sa}^* \ (x_a^\sigma/x_a^l) \tag{5}$$

While the mole fraction of modifier (in the current case, alcohol) in the mobile phase, x_a^l, is known, its mole fraction in the surface phase is unknown. If chromatographic measurements are carried out at sufficiently high concentrations of the polar solvent (e.g., $x_a^l > 0.1$-0.2), its mole fraction in the surface phase can be approximated by unity and then equation (4) reduces to the well-known Snyder-Soczewinski relationship:[11,12,27]

$$\log k_s' = \log \left(\phi K_{sa}^* \right) \ -r \log x_a^l \tag{6}$$

Since the retention measurements presented in the experimental section were carried out at low concentrations of modifier, equation (6) cannot be used for analyzing these data. In this region the surface composition x_a^σ changes with the mobile phase composition. Low concentrations of modifier in the mobile phase permit the modifier-solvent composition in the surface phase to be represented by an ideal displacement model;[12,28] then

$$x_a^\sigma = K_{ah}^* \ x_a^l/(x_h^l + K_{ah}^* \ x_a^l) \tag{7}$$

where K_{ah}^* is the modifier-solvent equilibrium constant (K_{ah}^* denotes the constant for the alcohol-hexane liquid mixture). Replacing x_a^σ in equation (5) by equation (7), one can obtain:

$$1/k_s' = (\phi \, K_{sa}^* K_{ah}^*)^{-1} \, (x_h^l + K_{ah}^* \, x_a^l) \tag{8}$$

Since x_a^l is small (below 0.03), the mole fraction x_h^l can be replaced by unity because $x_a^l + x_h^l = 1$ for $x_s^l \to 0$. Then, equation (8) simplifies as follows:

$$1/k_s' = (\phi \, K_{sh}^*)^{-1} + (\phi \, K_{sa}^*)^{-1} \, x_a^l \tag{9}$$

where $K_{sh}^* = K_{sa}^* K_{ah}^*$. Equation (9) shows that, in the region of low concentrations of modifier, the reciprocal of the capacity ratio is linearly dependent on the modifier's concentration.

It is noteworthy that the same type of dependence of the capacity ratio on the modifier concentration has been predicted by Scott and Kucera,[19] who defined k_s' as the ratio of total forces acting on the solute in the stationary phase to the total forces acting on the solute in the mobile phase. In contrast to their probabilistic description, equation (9) is based on a displacement model, which assumes competitive interactions between solute, modifier and solvent molecules for active sites on the solid surface. This model is commonly accepted for describing the physical adsorption of multicomponent non-electrolytic liquid mixtures on solid surfaces.[5] In the current paper equation (9) will be used to analyze the measured dependences of the capacity ratio on the modifier concentration.

Capacity ratios were measured for 22 phenolic solutes (i.e., phenol, o-, m- and p-fluorophenols, o-, m- and p-chlorophenols, o-, m- and p-bromophenols, o-, m- and p-iodophenols, o-, m- and p-cresols, o-, m- and p-nitrophenols, and o- m- and p-cyanophenols), in six alcohol/n-hexane mobile phases (i.e., methanol, ethanol, 1-propanol, 2-propanol, 2-butanol and t-butanol) and nine silicas (i.e., unmodified Lichrosorb Si-60, four modified silicas with C4, C6, and C8 and C10 alkenyl ligands and four modified silicas with C4, C6, C8, C10 dihydroxyalkyl ligands). For each chromatographic system, the capacity ratio was measured as a function of the modifier's concentration up to 3 v/v% in the mobile phase. These data were plotted according to equation (9) (i.e., the reciprocal of the capacity factor against the mole fraction of modifier in the mobile phase) giving 1188 linear plots. Analysis of these plots showed that equation (9) is a good representation for the capacity ratios measured at the
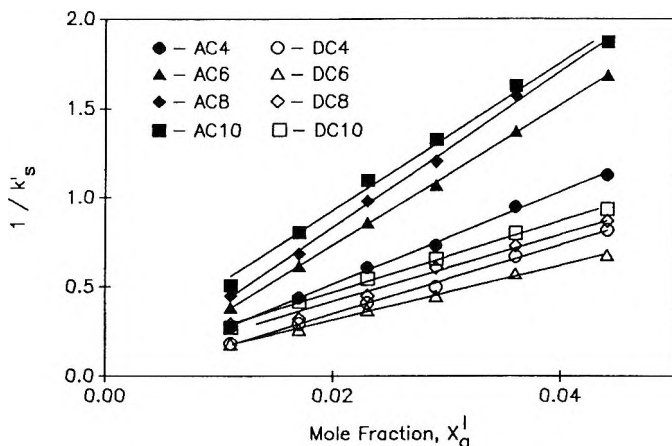
Figure 1. Reciprocal of the capacity ratio plotted as a function of the mole fraction of modifier in the mobile phase for phenol chromatographed in 2-butanol/n-hexane on various alkenyl and diol bonded phases.

low modifier concentrations. For the majority of the systems studied the values of the correlation coefficient were at least 0.99 or better. For the purpose of illustration Figure 1 contains the linear plots of $1/k_{s'}$ vs. x_a^l for phenol chromatographed in the 2-butanol/n-hexane mobile phase on the columns packed with modified silicas.

According to Snyder[6] the phase ratio ϕ, to a first approximation, is a fundamental property of the solid phase and is independent of the nature of the solvent. Thus, the intercept and the slope of the linear relationship given by equation (9) are respectively proportional to the equilibrium constants $K_{hs}^* = 1/K_{sh}^*$ and $K_{as}^* = 1/K_{sa}^*$. These constants are proportional to the differences in the sorption energies of solute, solvent and modifier as follows:

$$K_{hs}^* \sim \exp\left(\frac{\epsilon_h - \epsilon_s}{RT}\right) \qquad (10)$$

and

$$K_{as}^* \sim \exp\left(\frac{\epsilon_a - \epsilon_s}{RT}\right) \qquad (11)$$

Here ε_h, ε_s and ε_a denote, respectively, the sorption energies of n-hexane, solute and modifier molecules, R and T have their usual meaning. Since ε_s is considerably greater than ε_h, the difference $\varepsilon_h - \varepsilon_s$ is a relatively large negative number and the constant K_{hs}^* is very small. Thus, the quantity $1/\phi K_{sh}^*$ [cf., equation (9)] is succeptable to a large error; in some cases even a negative value of $1/\phi K_{sh}^*$ is obtained, which has no physical meaning according to equation (9). It is noteworthy that negative values of the intercept also have been reported by Scott and Kucera,[19] who tried to interpret them in terms of their retention model. The constant K_{hs}^* characterizes competitive interactions between molecules of solute and nonpolar solvent (in the current case, n-hexane) for active surface groups but the solvent plays a less significant role in the retention mechanism in comparison to the modifier, which influences strongly the solute-surface interactions. Therefore, the values of $1/\phi K_{sh}^*$ are not discussed in this paper, whereas the analysis of the values of $1/\phi K_{sa}^*$, which characterize the competitive interactions between solute and modifier molecules for active surface groups, is emphasized. These interactions control the solute retention in the chromatographic systems studied. As mentioned above, the slope, $1/\phi K_{sa}^*$, is proportional to the equilibrium constant K_{as}^* which, through equation (11), is associated with the solute and modifier sorption energies. While the difference between the sorption energies of n-hexane and solute is a large negative number, the difference between the sorption energies of alcohol and solute is considerably smaller but still negative. If $\varepsilon_a - \varepsilon_s$ tends to zero, the exponential energy term (<1) tends to unity. The observed values of K_{as}^*/ϕ are greater than unity because ϕ is a small number and the pre-exponential entropy factor in the K_{as}^*/ϕ - constant can be greater than unity.

The quantity K_{as}^*/ϕ characterizes the competitive interactions of solute and modifier molecules with the active surface groups and ligands. Analysis of the values of K_{as}^*/ϕ obtained for all systems studied has provided information about the influence of the solute, modifier and ligand on the retention process. Based on these values it was possible to distinguish two groups of solutes: the first group contains halophenols and cresols, the other one contains nitro- and cyanophenols. The values of K_{as}^*/ϕ for halophenols and cresols chromatographed in the same system usually varied up to 10%; higher
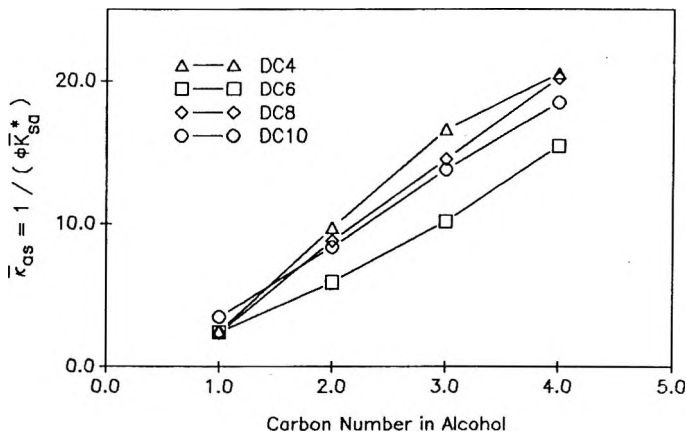
Figure 2. Dependencies of $\overline{\kappa}_{as}$ on the number of carbon atoms in the modifier for halophenols chromatographed in various alcohol/n-hexane mobile phases on the diol bonded phases. Modifiers: methanol, ethanol, 1-propanol and 2-butanol.

variations were observed for the ortho-derivatives of phenol phases chromatographed in the methanol/n-hexane and ethanol/n-hexane mobile phases. These variations show a regular tendency and can be associated with the size and position of the halogen atom in phenol (this problem will be discussed later).

In order to study the effect of the mobile phase on solute retention, the average value $\overline{\kappa}_{as} = \overline{K}_{as}/\phi$ was calculated by taking into account the values of K_{as}^{*}/ϕ for halophenols and cresols. Figures 2 and 3 show, respectively, the dependencies of $\overline{\kappa}_{as}$ on the number of carbon atoms in the modifier (alcohol) for the dihydroxyalkyl and alkenyl bonded phases. In both cases an increase in the $\overline{\kappa}_{as}$ -value denotes an increase in the adsorption energy of the alcohol since the solute is fixed. Thus, for all bonded phases, the interaction energy between modifier and surface groups and ligands increased in direction from methanol to butanol. In the case of the alkenyl bonded phases this energy increase was about 2.5 times stronger than that observed for the dihydroxyalkyl phases. For the alkenyl phases, the increase in the $\overline{\kappa}_{as}$ -values associated with addition of the methylene group to the alcohol molecule are not additive and decrease with increasing number of carbon atoms. However, these increases are more regular for the dihydroxyalkyl phases. The increasing dependencies of $\overline{\kappa}_{as}$ vs. n_C shown in Figures 2 and 3 are expected because the adsorption energies of
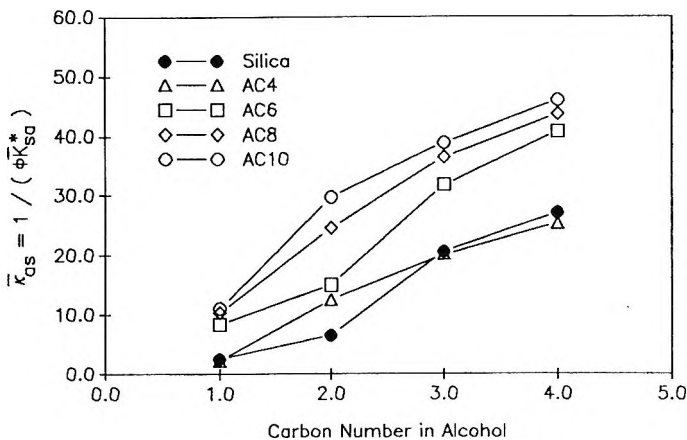
Figure 3. Dependencies as in Figure 2 for the alkenyl bonded phases

organics usually increase with their molecular weights. It is more difficult to explain the differences in these dependencies for alkenyl and dihydroxyalkyl bonded phases. For example, the difference in $\overline{K}_{as}$ for methanol and 2-butanol on the decenyl phase is about 35, whereas this difference for the dihydroxydecyl phase is about 15. The higher values of $\overline{K}_{as}$ for alcohols on the alkenyl phases in comparison to those on the dihydroxyalkyl phases may be due to additional interactions from polar and nonpolar parts of the alcohol molecule with the bonded phase, i.e., specific interaction of the hydroxyl group of an alcohol with the unreacted silanol group and additional nonspecific interactions of the alcohol nonpolar chain with the alkenyl ligand.

In the case of the dihydroxyalkyl bonded phases, these additional interactions are small because of the polar terminal diol groups. Thus, the alcohol chain effect for diol phases is smaller in comparison to that for alkenyl phases and therefore the differences between the $\overline{K}_{as}$ vs. n_C -curves for the DC4, DC8 and DC10 phases are not significant. These curves can be approximated by one line because the $\overline{K}_{as}$ -values representing averages for various halophenols and cresols contain about 10% error. Because the $\overline{K}_{as}$ - values for alkenyl phases are considerably greater than those for diol phases, the $\overline{K}_{as}$ -curves shown in Figure 3 for these phases change systematically from the AC4 to AC10 columns.
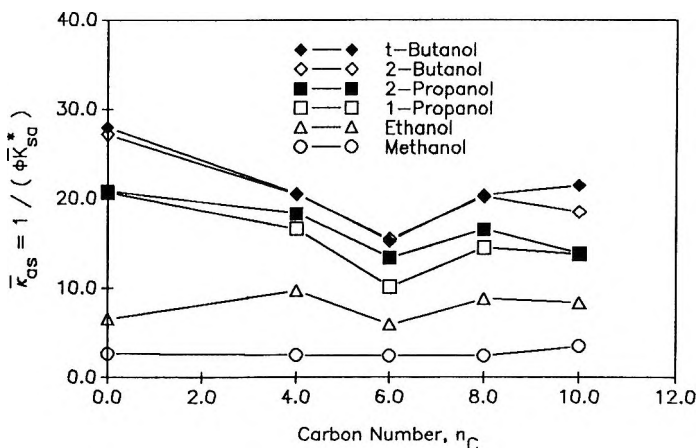
Figure 4. Dependencies of $\overline{\kappa}_{as}$ on the number of carbon atoms in the dihydroxyalkyl (diol) bonded ligands for halophenols chromatographed in various alcohol/n-hexane mobile phases. Points at $n_C = 0$ denote the $\overline{\kappa}_{as}$ -values for unmodified silica

Figures 4 and 5 are interesting because they illustrate the effect of the surface ligand length on the $\overline{\kappa}_{as}$ -value. These figures show distinctly different behavior of the alkenyl and diol phases. For all modifiers the values of $\overline{\kappa}_{as}$ did not change significantly with increasing length of the diol ligands (see Figure 4). Generally, the values of $\overline{\kappa}_{as}$ on unmodified silica were greater than those on the diol phases. A comparison of the $\overline{\kappa}_{as}$ -values for the diol phases shows that they are similar for all phases studied except for the DC6 phase, where a small minimum was observed. The similar values of $\overline{\kappa}_{as}$ indicate that the differences between the modifier and solute adsorption energies were similar for the diol bonded phases, which is not surprising if one considers that, for these systems, the hydrogen bonding between the hydroxyls of the modifier and solute, and the diol groups is relatively strong. It is more difficult to explain why the DC6 phase was significantly different compared to the other diol phases. In contrast to the effect shown in Figure 4, the $\overline{\kappa}_{as}$ vs. n_C -curves presented in Figure 5 for the alkenyl phases increases with increasing length of the alkenyl ligands. The values of $\overline{\kappa}_{as}$ for unmodified silica and the AC4 phase are analogous and a rapid increase in $\overline{\kappa}_{as}$ was observed for the AC6 phase. For the AC8 and AC10 phases, an increase in $\overline{\kappa}_{as}$ was observed, but it was significantly smaller than that for the AC6 phase. An increase in the $\overline{\kappa}_{as}$ -
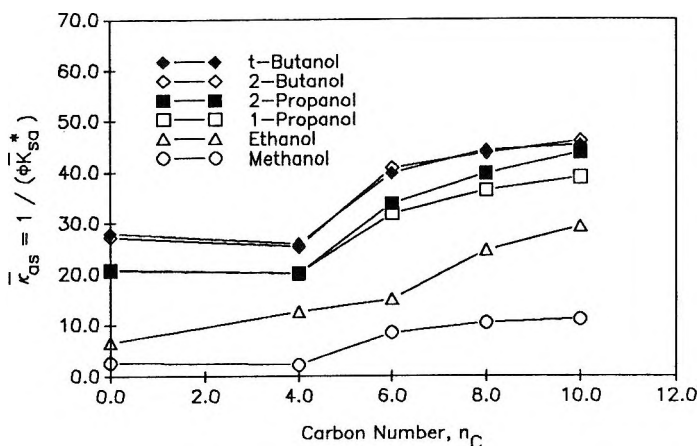
Figure 5. Dependencies as in Figure 4 for the alkenyl bonded ligands

value with increasing length of the alkenyl ligand shows that the absolute difference in the modifier and solute adsorption energies decrease. For longer ligands, the solute-ligand interaction can be weakened by the presence of other groups in the solute (e.g., halogen atom) which create an unfavorable steric situation. This weakening of solute-ligand interactions can explain a decrease of the absolute difference in the modifier and solute adsorption energies with increasing length of alkenyl ligands.

For both types of bonded phases, the C6-ligands showed a special behavior. The interactions of modifier molecules with the C6-diol ligands were weakest in comparison to the other diol phases, whereas these interactions with the hexenyl ligands were greater and comparable to those with octenyl and decenyl ligands. Perhaps the steric and orientational effects for solute and modifier molecules in the C6 phases are optimal.

In the case of the nitro- and cyanophenols, the retention was more complex because physicochemical properties of nitro and cyano groups differ considerably from those for halogens.[6] These groups are composed, respectively, from three and two atoms, and are capable of strong interactions with the surface groups and ligands. According to Snyder,[6] the solute localization on silica surfaces is considerably stronger for solutes with a cyano group than for solutes with a nitro group. Also, for these solutes, the isomeric effects associated with the o-, m- and p- positions of functional groups are strong. Thus, for nitro- and cyanophenols, the values of κ_{as} cannot be averaged because they show a strong dependence on chemical nature of the

functional group and dependence on its position in the solute. Generally, the values of κ_{as} for cyano- and nitrophenols were up to twice time smaller than the corresponding values for halophenols. For a given chromatographic system, the adsorption energies of nitro- and cyanophenols are higher than those for halophenols. However, their κ_{as} -dependencies on the number of carbon atoms in the modifiers and the surface ligands are analogous to those observed for halophenols.

It is noteworthy that the values of κ_{as} for p-cyanophenol on various modified silicas were lower than the corresponding values of κ_{as} for m- and o-derivatives. This result means that, for these systems, the adsorption energies of p-cyanophenol are greater than those for o- and m- cyanophenols. This is not surprising because the para-position of hydroxy and cyano groups in a solute facilitates interactions of both these groups with the modified silica surface. The para-effect seems to be characteristic for bi-functional solutes with relatively polar groups. However, the isomeric effect for halophenols is smaller because the difference is the κ_{as} -values for o-, m- and p- derivatives do not exceed 10-15%. For these solutes this effect seems to be controlled by steric factors.

CONCLUSIONS

Analysis of the retention data for phenolic solutes which contain halo, hydroxy, nitro and cyano groups chromatographed at low concentrations of an aliphatic alcohol (methanol, ethanol, propanol or butanol) in n-hexane on the alkenyl and dihydroxyalkyl (diol) bonded phases have shown that the molecular interactions in these phases are different. This analysis, performed on the basis of a displacement model for solute retention, which takes additionally into account the alcohol composition in the stationary phase, has shown that the differences in the alcohol and solute adsorption energies are analogous betweem the unmodified silica and diol bonded phases. However, for alkenyl phases the difference decreases with increasing length of the bonded ligands. Although. for both types of bonded phases, the adsorption energies of alcohols increase with the number of carbon atoms in their chain. this effect is stronger for alkenyl ligands. The structure and polarity of functional groups in the solute mainly affect the magnitude of the interaction energies of solute and modifier with the bonded phase. For example, these energies are greater for phenol solutes with cyano and nitro groups than for halophenols. For cyano and nitrophenols, the positional isomeric effect is stronger than for halophenols.

REFERENCES

1. P. J. Schoenmakers, **Optimization of Chromatographic Selectivity**, Elsevier, Amsterdam, 1986.

2. D. Nurok, Chem. Rev., **89**, 363 (1989).

3. J. L. Glajch, L. R. Snyder, **Computer-Assisted Method Development for High Performance Liquid Chromatography**, Elsevier, Amsterdam, 1990.

4. J. Oscik, **Adsorption**, Harwood Ltd., Chichester, 1982.

5. M. Jaroniec, R. Madey, **Physical Adsorption on Heterogeneous Solids**, Elsevier, Amsterdam, 1988.

6. L. R. Snyder, **Principles of Adsorption Chromatography**, M. Dekker, New York, 1968.

7. L. R. Snyder, J. J. Kirkland, **Introduction to Modern Liquid Chromatography**, Wiley, New York, 2nd Edition, 1979.

8. M. Jaroniec, D. E. Martire, J. Chromatogr., **351**, 1 (1986).

9. D. E. Martire, R. E. Boehm, J. Phys. Chem., **87**, 1045 (1983); **91**, 2433 (1987).

10. R. E. Boehm, D. E. Martire, J. Phys. Chem., **84**, 3620 (1980).

11. L. R. Snyder, H. Poppe, J. Chromatogr., **184**, 363 (1980).

12. M. Jaroniec, D. E. Martire, M. Borowko, Adv. Colloid Interface Sci., **22**, 177 (1985).

13. W. R. Melander, Cs. Horvath, Chromatographia, **18**, 353 (1984).

14. M. Jaroniec, D. E. Martire, J. Chromatogr., **387**, 55 (1987).

15. E. D. Katz, K. Ogan, R. P. W. Scott, J. Chromatogr., **352**, 67 (1986).

16. S. N. Lanin, Y. S. Nikitin, J. Chromatogr., **537**, 33 (1991).

17. R. K. Gilpin, M. Jaroniec, S. Lin, Anal. Chem., **62**, 2092 (1990).

18. R. K. Gilpin, M. Jaroniec, S. Lin, Chromatographia, **30**, 393 (1990).

19. R. P. W. Scott, P. Kucera, J. Chromatogr., **112**, 425 (1975).

20. E. H. Slaats, J. C. Kraak, W. J. T. Brugman, H. Poppe, J. Chromatogr., **149**, 255 (1978).

21. M. Asif, **Synthesis and Characterization of Linear and Cyclic Diol Bonded Silica Surfaces for Liquid Chromatography and the Corresponding ω-Alkenyl Precursors**, Ph.D. Dissertation, Kent State University, Kent, Ohio, 1991.

22. L. F. Fieser, M. Fieser, **Reagents in Organic Synthesis**, Wiley, New York, 1967, p. 820.

23. M. Takasugi, N. Wantanabe, Y. Ujihira, Fresenius Z. Anal. Chem., **315**, 502 (1983).

24. L. F. Johnson, W. C. Jankowski, **Carbon-13 NMR Spectra,** Wiley, New York, 1972.

25. R. K. Gilpin, W. R. Sisco, Anal. Chem., **50**, 1337 (1978).

26. M. Jaroniec, J. K. Rozylo, B. Oscik-Mendyk, J. Chromatogr., **179**, 237 (1979).

27. E. Soczewinski, J. Chromatogr., **112**, 425 (1975).

28. M. Jaroniec, J. Chromatogr. A, **656**, 37 (1993); **772**, 19 (1996).

APPLICATION OF ALKYLAMIDE PHASES TO SEPARATE COMPOUNDS OF DIFFERENT POLARITY UNDER REVERSED PHASE CONDITIONS

T. Czajkowska

American Cyanamid Company
Agricultural Products Research Division
Princeton, New Jersey 08543

M. Jaroniec*

Separation and Surface Science Center
Department of Chemistry
Kent State University
Kent, Ohio 44242

ABSTRACT

The effects of pH and ionic strength of the mobile phase, as well as the concentration of organic modifiers, on the retention and elution order of zwitterionic and neutral compounds related to imidazolinone herbicides was studied by using polymeric alkylamide stationary phases. It is shown that retention of these compounds on alkylamide phases is governed by a mixed ion-exchange and partition-displacement mechanism. After adjusting pH, ionic strength and composition of the eluent, these phases allow a simultaneous separation of nonpolar and ionic compounds.

5-Methylpyridinedicarboxylic Acid
(MPDC)

5-Methylpyridinedicarboxylic Acid
Dimethyl Ester (MPDC.DME)

5-Ethylpyridinedicarboxylic Acid
(EPDC)

5-Ethyl-2-(4-isopropyl-4-methyl-5-oxo-2-
imidazolin-2-yl) nicotinic acid
(Imazetaphyr)
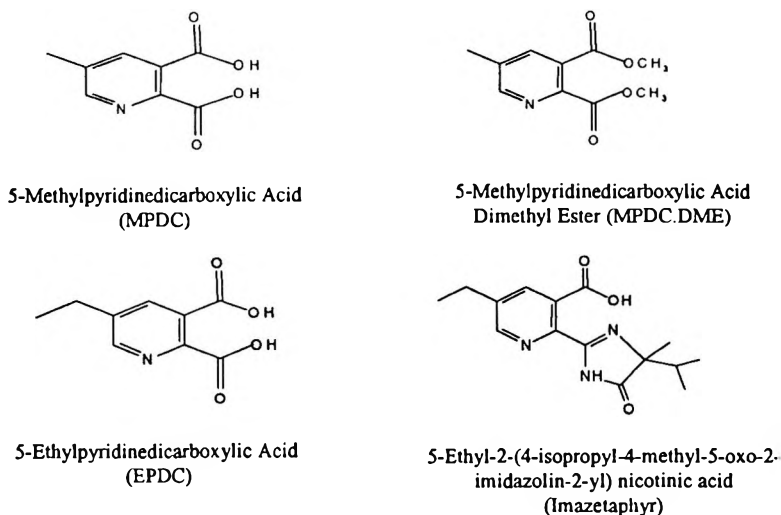
Figure 1. Structures of the solutes studied.

INTRODUCTION

Chemically bonded phases, containing a ligand with an internal polar group, appeared to be promising for separation of basic compounds under reversed phase conditions.[1,2] Among this type of packing materials the alkylamide phases, which contain an internal amide functional group, become very popular because they exhibit a combination of specific and non-specific interactions with respect to the solutes of various polarities.[3,4]

These phases are usually synthesized by a two-step process, in which initial aminopropyl phase is prepared and subsequently reacted with a suitable alkanoyl chloride.[2-10] This synthesis pathway gives phases which, in addition to alkylamide ligands and residual silanols, contain unreacted aminopropyl ligands. It is suspected that unreacted aminopropyl ligands increase the structural stability of the stationary phase and change significantly its sorption affinity to solvent molecules.[5,6]

O'Gara et al.[11] synthesized an octylcarbamate phase by using monofunctional bonding chemistry. The carbamate functional group was incorporated into an octyldimethylchlorosilane compound and than the entire ligand was directly attached to the silica surface. This synthesis pathway gives bonded phases without residual aminogroups. A comparative study of

Monomer Type:

Polymer Type:
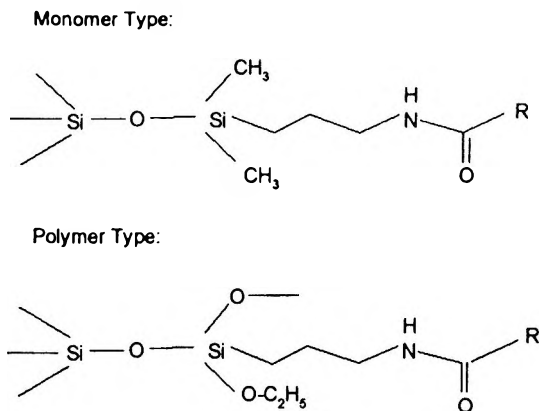
Figure 2. Schematic representation of alkylamide ligands in monomeric and polymeric bonded phases.

alkylamide phases prepared, according to both pathways, would allow the estimation of the effect of residual aminopropyl groups on the retention mechanism of basic solutes.

The current work is focused on the effects of pH and ionic strength of the mobile phase, as well as the role of organic modifiers, on the retention of zwitterionic and neutral compounds related to imidazolinone herbicides. This work is a continuation of the studies reported previously.[3,4]

EXPERIMENTAL

The retention measurements at different pH, ionic strength (concentration of phosphate buffer) and various compositions of the hydro-organic eluent were carried out at 35°C by using flow rate of 1 mL/min. Acetonitrile and methanol were used as organic modifiers. Chromatographic measurements were performed by using the 15 cm, 4.6 mm I.D. column packed with polymeric dodecylamide phase bonded to 5 µ Eka Nobel Kromasil silica. This column denoted as AA-PC-12 was described previously.[4] For the comparative purposes, the following 15 cm x 4.6 mm columns packed with the conventional alkyl phase were also used: Kromasil C-8 from Eka Nobel and Inertsil C-8 prepared at Kent State University.[3,4] Organic solvents were obtained from Baxter.
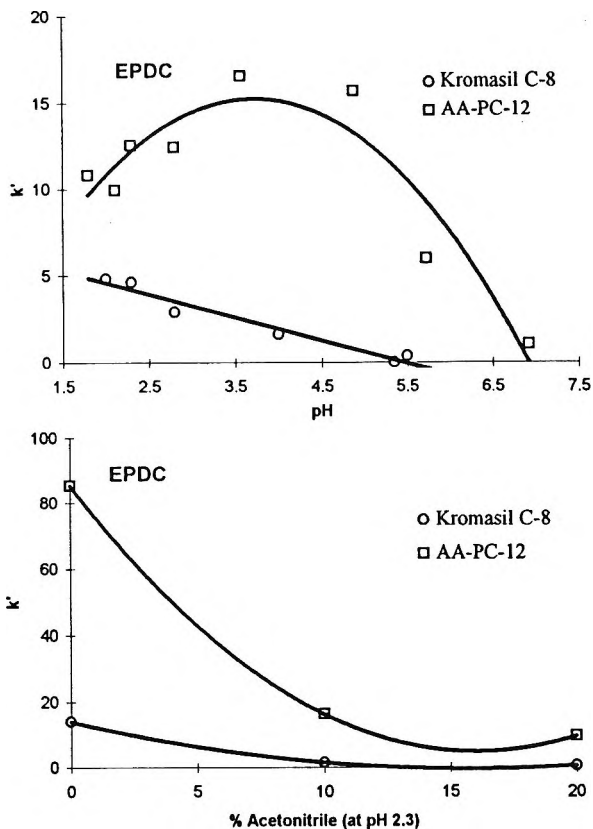
Figure 3. A comparison of the capacity factor k' vs pH and % acetonitrile for 5-ethylpyridinedicarboxylic acid on conventional alkyl and alkylamide columns.

Deionized water was purified using a Millipore Milli-Q system. Aldrich and American Cyanamid were sources of the chromatographic solutes (see Figure 1).

The Hewlett-Packard HP 1050 and a modular liquid chromatograph with a Spectra Physics SP8800 pump, a LKB Model 2125 column oven, a variable wavelength UV detector (ABI 785A) and a Hewlett-Packard 1050 autosampler were used in the current study. Data were acquired and processed using a Hewlett Packard 3350 Laboratory Data System.
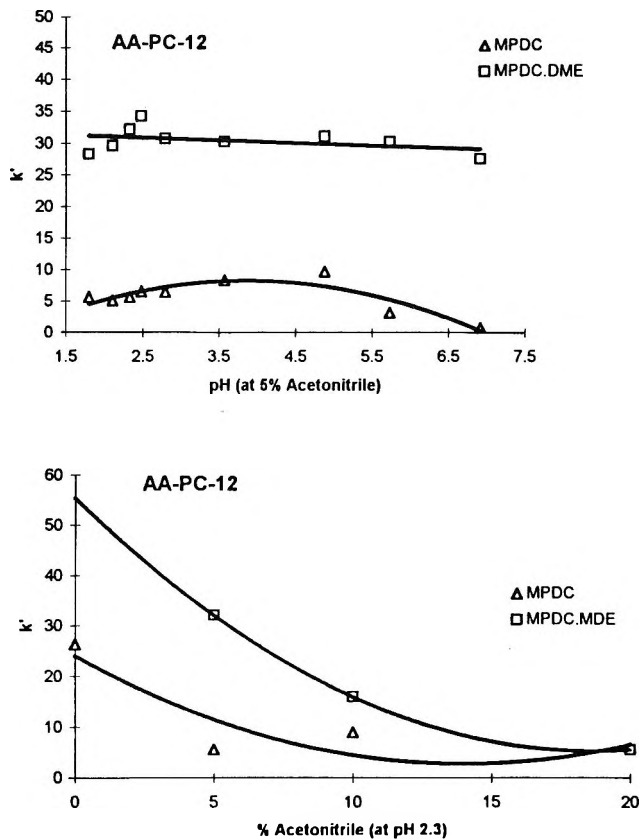
Figure 4. A comparison of the capacity factor k' vs pH and % acetonitrile for 5-methylpyridinedicarboxylic acid and its dimethyl ester on the AA-PC-12 column.

RESULTS AND DISCUSSION

Separation of the imidazolinones and their very polar impurities, such as pyridine based acids under reversed phase conditions, is difficult since these zwitterionic compounds tend to interact strongly with the uncovered surface of silica. Organic acids, especially those with the carboxylic group in the α position to the ring nitrogen, are substances difficult to analyze due to their poor peak shape, irreversible adsorption or complete lack of retention. Even when an ion pairing reagent is added, in order to improve their peak shape and to modify the retention mechanism, the pyridine diacids are practically unretained under conditions suitable for separation of imidazolinones (~20%
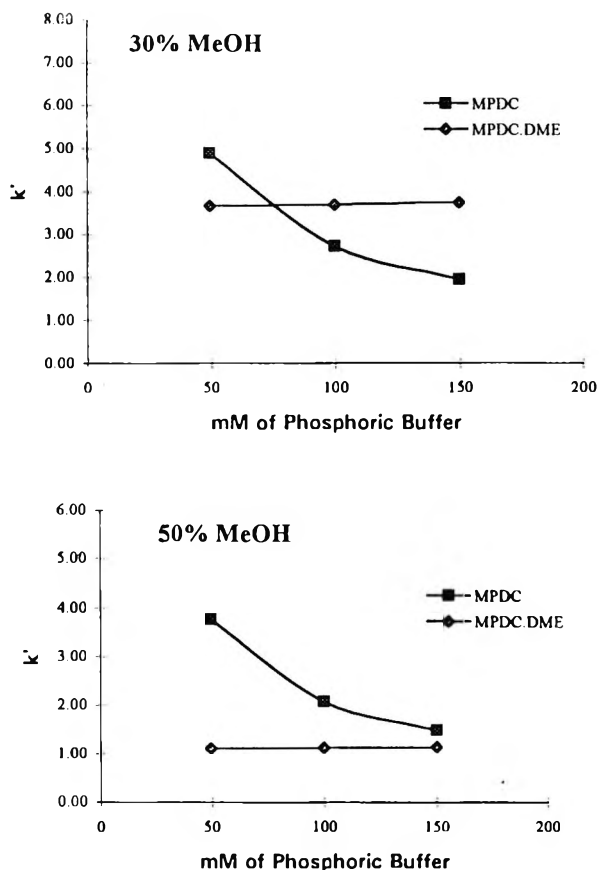
Figure 5. Dependence of k' *versus* phosphate buffer concentration (pH = 2.8) for MPDC and MPDC.DME at two different concentrations of methanol on the AA-PC-12 column.

of organic modifier). The monomeric and polymeric alkylamide packings are chemically bonded phases in which alkyl chains contain an internal amide group (see Figure 2). The retention of polar, ionic and zwitterionic compounds on alkylamide phases occurs according to a mixed ion-exchange and partition-displacement mechanism.[3,4] The dependencies of the capacity ratio on pH and the acetonitrile concentration for a very polar compound EPDC on the conventional alkyl bonded columns and a polymeric dodecylamide column are compared in Figure 3. As can be seen in this figure, the ionic type of interactions plays a substantial role in the retention mechanism.
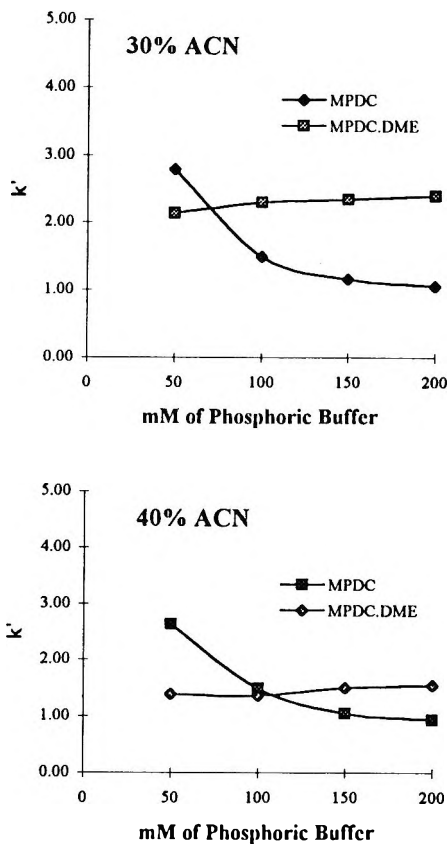
Figure 6. Dependence of k' *versus* phosphate buffer concentration (pH = 2.8) for MPDC and MPDC.DME at two different concentrations of acetonitrile on the AA-PC-12 column.

In the case of the alkyl column, the retention of EPDC decreases with the degree of acid ionization, while on the polymeric alkylamide column EPDC is retained longer at higher pH values. Also, the effect of the acetonitrile concentration on the retention of EPDC on alkyl and alkylamide columns is different. Over the entrie region of acetonitrile concentrations, EPDC is retained longer on the alkylamide column and after an initial significant decrease, the retention volume remains practically unchanged up to 20% acetonitrile.
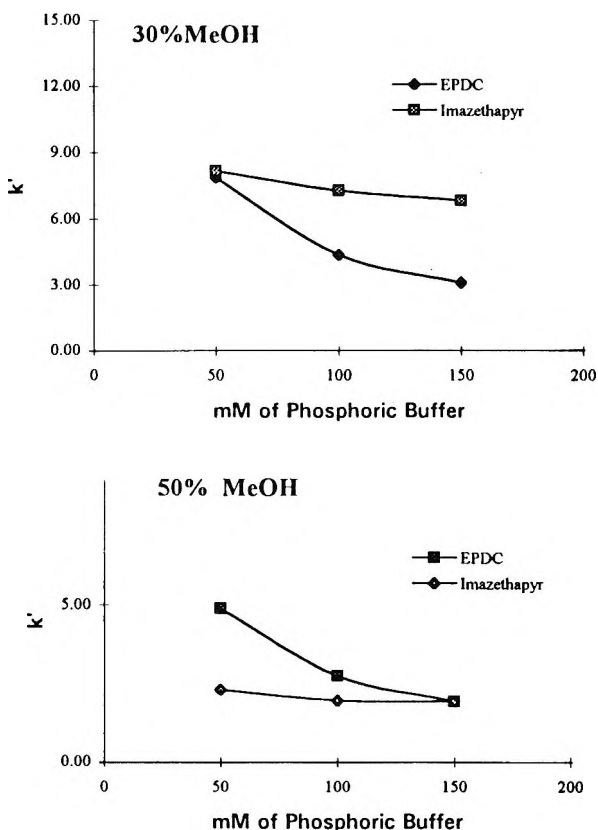
Figure 7. Dependence of k' *versus* phosphate buffer concentration (pH = 2.8) for EPDC and Imazethapyr at two different concentrations of methanol on the AA-PC-12 column.

Retention behavior of two compounds of different polarity on   the polymeric dodecylamide phase AA-PC-12 is compared in Figure 4.   The capacity factors of ionic 5-methylpyridine dicarboxylic acid (MPDC) and its analogue, i.e., neutral dimethyl ester (MPDC.DME), are plotted versus pH of the mobile phase and acetonitrile content.   As can be seen, the retention of a neutral compound does not depend on pH and decreases faster with increasing acetonitrile concentration than the retention of the ionic component.

In Figures 5-8 the capacity factors of MPDC-MPDC.DME and EPDC-Imazethapyr pairs on the AA-PC-12 column are plotted against the concentration of phosphate buffer for different kinds and levels of organic
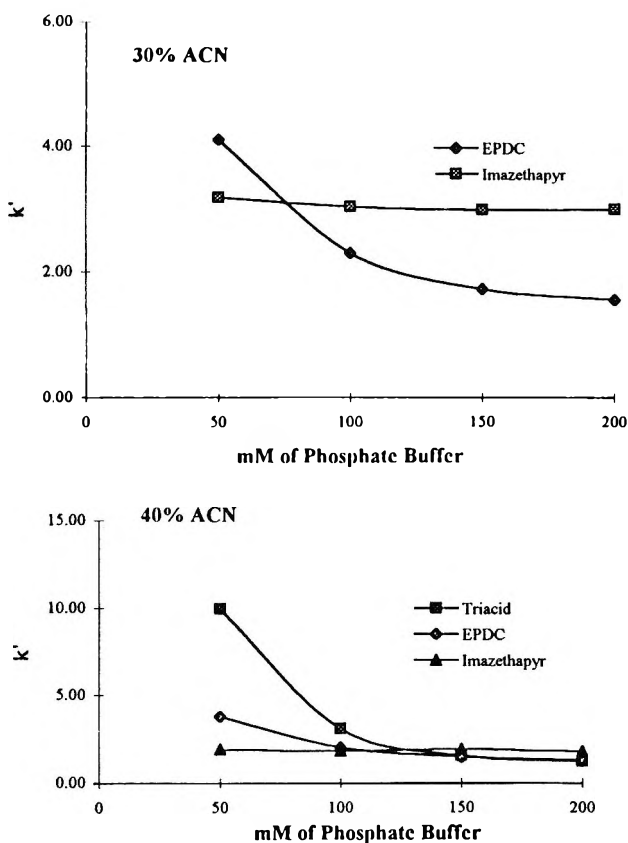
Figure 8. Dependence of k' *versus* phosphate buffer concentration (pH = 2.8) for EPDC, Triacid and Imazethapyr at two different concentrations of acetonitrile on the AA-PC-12 column.

modifiers in the mobile phase. These plots demonstrate that the retention of diacids is controlled by the ionic strength of the mobile phase, whereas the retention of neutral (MPDC.DME) or a less polar (Imazethapyr) compound is controlled by the nature and level of the organic solvent. For both solvents (acetonitrile and methanol) used, each combination of solvent and phosphoric acid concentrations may lead to an inverted elution order of polar and non-polar compounds. In addition, shown in Figure 8 is the dependence of the capacity factor k' on the concentration of phosphoric acid for 2,3,5-pyridine-tricarboxylic acid.

50 mM   100 mM   200 mM

EPDC- small peak   Imazethapyr - big peak
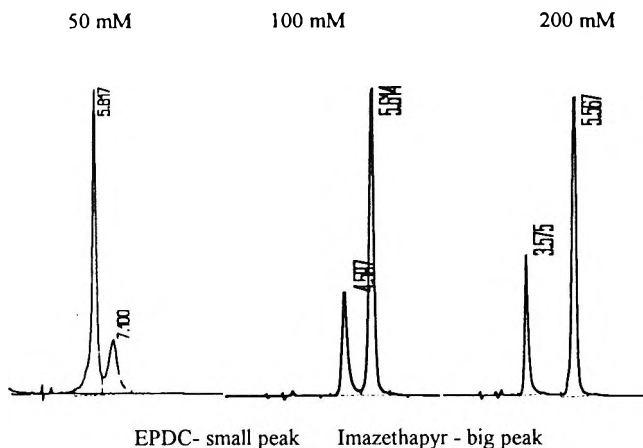
Figure 9. A comparison of the elution order and peak shape for 5-ethyl-pyridinedicarboxylic acid (EPDC) and Imazethapyr at different concentrations of phosphate buffer (pH = 2.8) and 30% acetonitrile on the AA-PC-12 column. Conditions: 35 °C, 1 mL/min, 254 nm. Small peak in each panel refers to EPDC.

Methanol   Acetonitrile   2-Propanol

EPDC- small peak   Imazethapyr - big peak
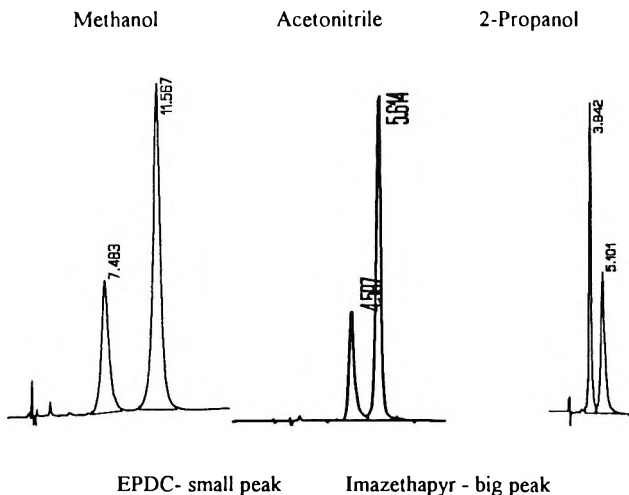
Figure 10. A comparison of the elution order and peak shape for 5-ethyl-pyridinedicarboxylic acid (EPDC) and Imazethapyr chromatographed in the mobile phase containing 100 mM of phosphate buffer (pH = 2.8) and 30% organic modifier on the AA-PC-12 column. Conditions: 35 °C, 1 mL/min, 254 nm. Small peak in each panel refers to EPDC.

Kromasil C-8

AA-PC-12

A - MPDC, B - MPDC.DME, C - EPDC, D - Imazethapyr
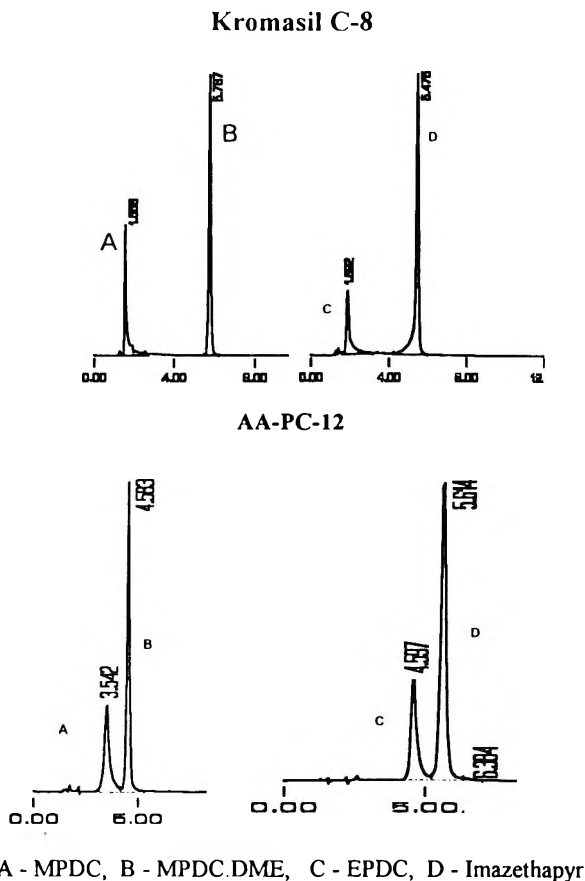
Figure 11. A comparison of separation of the MPDC (A) - MPDC.DME (B) and EPDC (C) - Imazethapyr (D) pairs on the 15 cm Kromasil C-8 and AA-PC-12 columns with 30% acetonitrile and 70% 100 mM phosphate buffer at pH = 2.8. Conditions: 35 °C, 1 mL/min, 254 nm.

As can be seen, this very polar compound shows the highest retention on the AA-PC-12 column. However, it was eluted at the dead time on the conventional alkyl column with 40% acetonitrile. Exemplary chromatograms, shown in Figures 9 and 10, illustrate the reversed elution order where pyridine diacids elute after their nonpolar derivatives (methyl esters and/or pyridine imidazolinones). A comparison of selected chromatograms obtained on the AA-PC-12 column with those on the conventional RP Kromasil C-8 column is presented in Figure 11.

For 30% of acetonitrile in the mobile phase both diacids are virtually unretained, whereas their retention on the AA-PC-12 column is comparable to that of neutral components.

CONCLUSIONS

Comparative studies of retention of ionic and neutral compounds on the polymeric dodecylamide phase have shown that the specific interactions sites in this phase have a significant influence on the solute retention and selectivity. Since the retention of multifunctional organic acids is governed by a mixed ion-exchange and partition-displacement mechanism, while the retention of neutral compounds is governed by the latter mechanism only, the effective optimization of chromatographic conditions for simultaneous separation of ionic and non-polar compounds is possible.

REFERENCES

1. T. L. Ascah. B. Feibush, J. Chromatogr., **506**, 357-369 (1990).

2. B. Buszewski. J. Schmid, K. Albert, E. Bayer, J. Chromatogr., **552**, 415-427 (1991).

3. T. Czajkowska, I. Hrabowsky, B. Buszewski, R. K. Gilpin. M. Jaroniec. J. Chromatogr. A, **691**, 217-224 (1995).

4. T. Czajkowska. M. Jaroniec, B. Buszewski, J. Chromatogr. A, in press.

5. B. Buszewski. R. K. Gilpin, M. Jaroniec, Chem. Anal. (Warsaw), **39**, 673-679 (1994).

6. B. Buszewski, M. Jaroniec, R. K. Gilpin, J. Chromatogr. A, **668**, 293-299 (1994).

7. B. Buszewski, M. Jaroniec. R. K. Gilpin, J. Chromatogr. A. **673**, 11-19 (1994).

8. P. Kasturi, B. Buszewski, M. Jaroniec, R. K. Gilpin, J. Chromatogr. A, **659**, 261-265 (1994).

9. B. Buszewski, R. K. Gilpin. M. Jaroniec, Chem. Anal. (Warsaw), **39**, 653-661 (1994).

10. B. Buszewski. P. Kasturi, R. K. Gilpin, M. E. Gangoda , M. Jaroniec, Chromatographia, **39**, 155-161 (1994).

11. J. E. O'Gara, B. A. Alden, T. H. Walter, J. S. Petersen, C. L. Niederlander, U. D. Neue, Anal. Chem., **67**, 3809-3813 (1995).

SYNTHESIS, CHARACTERIZATION AND APPLICATIONS OF HYDRIDE-BASED SURFACE MATERIALS FOR HPLC, HPCE AND ELECTROCHROMATOGRAPHY

J. J. Pesek, M. T. Matyska, J. E. Sandoval,
E. J. Williamsen

Department of Chemistry
San Jose State University
One Washington Square
San Jose, CA 95192

ABSTRACT

The chemical modification method based on the silanization of an oxide surface to a hydride intermediate followed by hydrosilation with an organic molecule containing a terminal olefin is reviewed. The resulting bonded organic moiety is attached to the surface via a direct Si-C bond which leads to high stability. The method has been more extensively applied to silica surfaces for the production of stationary phases in HPLC but it can also be used on other oxides such as alumina, zirconia, titania and thoria. More recent applications have been in the modification of the inner wall of fused silica capillaries for HPCE. The bonded moieties possess high stability and useful applications have been developed for the separation of proteins and peptides under a variety of buffer conditions. The same procedure for modifying the inner wall of a fused silica capillary

has also been extended to etched surfaces for use in electrochromatography (CEC). This type of CEC has been shown to be applicable to the separation of macromolecules as well as small solutes.

INTRODUCTION

Chemically bonded stationary phases for high performance liquid chromatography have been an essential component of this method for nearly twenty-five years. Since the majority of phases for HPLC consist of silica as the support material, the bonding of various organic moieties to the substrate is based on the chemistry of the silanols at the surface.[1] A number of possible reactions can and have been used for the attachment of organic ligands to silica, which ultimately lead to a range of surface properties varying from hydrophobic to hydrophilic and ionic. A summary of these reaction schemes is given in Figure 1.

The first reaction, generally referred to as esterification, involves bonding of an alcohol to the silanol. Because of its simplicity, it was the first method used for making chemically bonded stationary phases for HPLC.[2] However, the Si-O-C linkage which is formed in this reaction is hydrolytically unstable and therefore not suitable for any aqueous mobile phases. This bonding method was quickly supplanted by the second reaction type usually referred to as organosilanization. It is still today the method of choice for producing a wide variety of silica-based chemically bonded stationary phases for HPLC.

As shown in Figure 1 there are two general approaches to organosilanization. The first (a) involves the use of an organosilane reagent with a single reactive group (X). X is usually chlorine, methoxy or ethoxy. This process results in a monomeric stationary phase, i.e. one where each organic moiety is bonded to a single silanol on the surface. The second approach (b) involves the use of an organosilane with three reactive groups. In this case, bonding not only occurs to the surface of silica but there is extensive cross-linking between adjacent organosilane moieties resulting in what is usually referred to as a polymeric phase. It should be noted that the so-called "self-assembled monolayer phases" also are based on the principle of organosilanization.[3]

The third approach is a two-step process which involves chlorination of the silica surface with thionyl chloride followed by attachment of the organic moiety through either a Grignard reagent or organolithium compound.[4] The main advantage to this method is that the product is bonded to the surface

REACTION TYPE	REACTION	SURFACE LINKAGES
ESTERIFICATION	Si - OH + R - OH → Si - OR + H₂O	Si - O - C
ORGANO-SILANIZATION	a).Si - OH + X - SiR'₂R → Si - O - SiR'₂R + HX b).Si - OH + X₃ - Si - R → Si - O - Si - R + 3HX Y = Si or H	Si - O - Si - C
CHLORINATION FOLLOWED BY REACTION OF GRIGNARD REAGENTS AND ORGANOLITHIUM COMPOUNDS	Toluene Si - OH + SOCl₂ → Si - Cl + SO₂ + HCl a). Si - Cl + BrMgR → Si - R + MgClBr or b). Si - Cl + Li - R → Si - R + LiCl	Si - C
a). TES SILANIZATION	a). (structure diagram of silanol surface converting to Si-O-Si-H network)	a). Si - H monolayer
b). HYDROSILATION	Catalyst b).Si - H + CH₂ = CH - R → Si - CH₂ - CH₂ - R	b). Si - C

Figure 1. Chemical reactions used to modify silica surfaces

through a direct silicon-carbon linkage which is hydrolytically more stable than the Si-O-Si-C structure which is formed during organosilanization. The principal drawback to this approach is the scrupulously dry conditions which must be maintained during the synthesis. The chlorinated surface can be easily hydrolyzed back to silanols.

An alternative procedure for achieving the same or similar material to that produced by the chlorination/organometallic process is shown by the last reaction type cited in Figure 1. In this method, the silanols on the surface are

Figure 2. Relative loss of retention for C_8 columns as a function of column volumes of mobile phase. A = hydrosilation product; B = high coverage conventional organosilanization product; C = low coverage conventional organosilanization product. (Reprinted with permission from ref. 9)

first converted to hydrides and these sites are then reacted with a terminal olefin in the presence of a suitable catalyst to produce the final bonded material. There are two ways in which the silanols can be replaced by hydrides. One approach involves reducing the silanols with lithium aluminum hydride.[5] This process can be visualized as a direct replacement for surface silanols since each hydride that is formed requires an Si-OH group. The second approach involves silanization of the surface[6] with an appropriate reagent such as triethoxysilane (TES) as shown in Figure 1.

Under carefully controlled conditions a monolayer is formed on the surface so that the final result should be complete replacement of hydroxide groups by hydrides. This appears to be the case since the physical properties such as pore size and surface area of the hydride intermediate are the same as the starting silica.[6]   After the hydride surface is formed, the organic moiety is
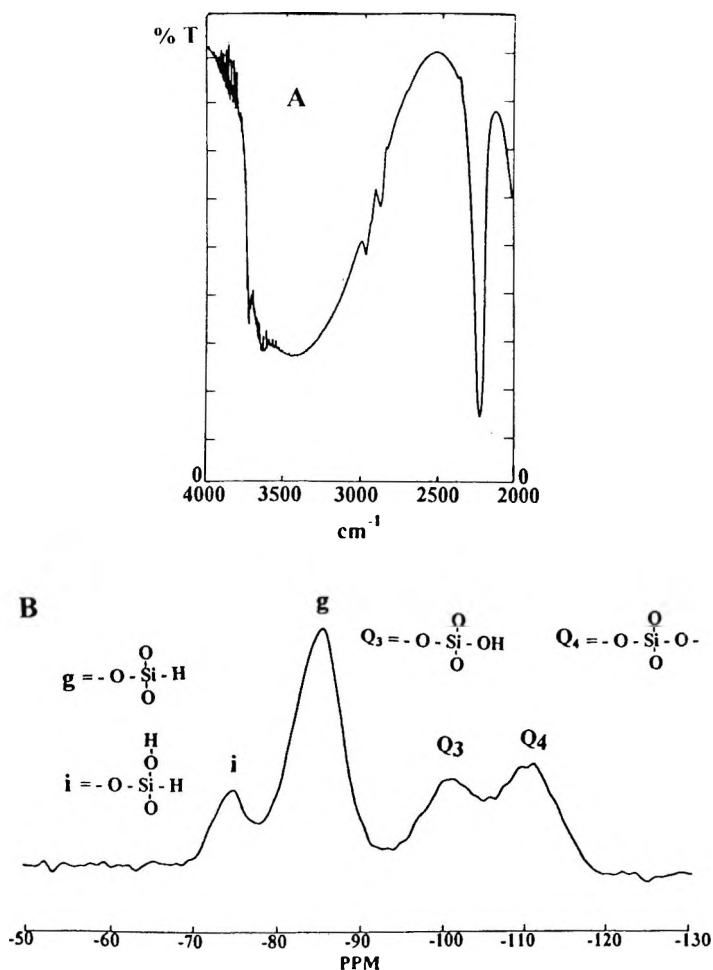
Figure 3. Spectral characterization of hydride intermediate on silica. A = DRIFT spectrum; B = ^{29}Si CP-MAS NMR spectrum.

attached via hydrosilation[7,8] as shown in the second step of this sequence in Figure 1. Because there is a single point of attachment for the organic moiety, it should more closely resemble the monomeric phases produced in organosilanization reaction "a)", or those produced by the two-step chlorination/organometallic reaction sequence. In fact, chromatographic tests with a standard polycyclic aromatic hydrocarbon mixture show that these phases behave like densely coated monomeric materials.[9] The stability of the material produced by this process is significantly greater than similar phases

% T

A

cm^{-1}

B

$$h = -O - \underset{\underset{O}{|}}{\overset{\overset{O}{\|}}{Si}} - CH_2 - _{(1)}$$

g

Q$_3$

Q$_4$

i

h

PPM

C

X = H or X = Si

i = =CH$_2$

k = HĊ=

j   k

C$_{(7)}$

C$_{(8)}$

C + C$_{(5)\ (6)}$

C$_{(4)}$ C$_{(3)}$ C$_{(2)}$

C$_{(1)}$

PPM
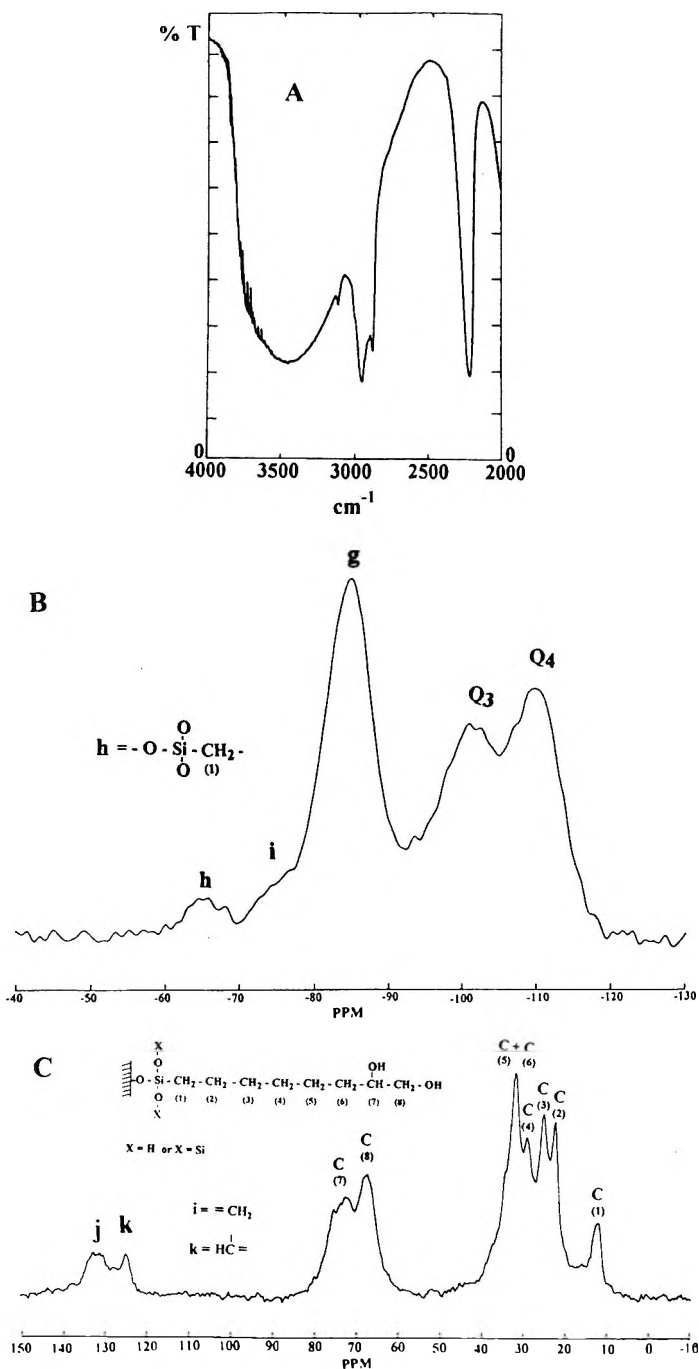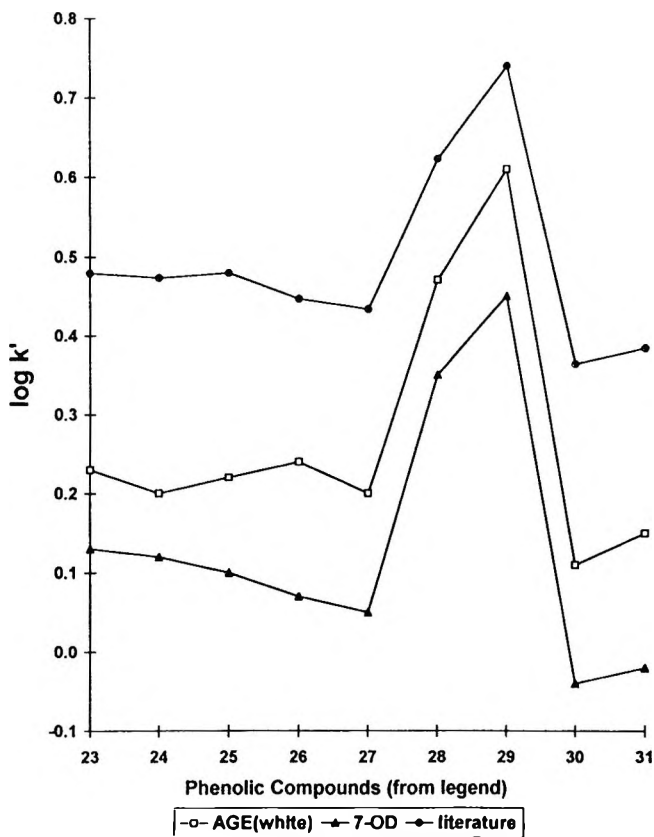
Figure 5. Comparison of retention data for phenols on various diol columns. AGE = diol from hydrosilation of allyl glycidyl ether on hydride intermediate; 7-OD = diol from hydrosilation of 7-octene-1,2-diol on hydride intermediate; literature = Merck diol. Solutes: **23**; 4-bromophenol, **24**; 3-chlorophenol, **25**; 4-chlorophenol, **26**; 4-fluorophenol, **27**; 2-napthol, **28**; 3-nitrophenol, **29**; 4-nitrophenol, **30**; phenol, **31**; 4-phenylphenol. (Reprinted with permission from ref. 19)

which are made by conventional organosilanization.[9] Figure 2 shows the log k' value of a test probe as a function of columns volumes of an aggressive mobile phase containing trifluoroacetic acid for the hydride-based material (A) and

Figure 4 (left). Spectral characterization of diol product made by hydrosilation of 7-octene-1,2-diol on hydride intermediate. A = DRIFT spectrum; B = ^{29}Si CP-MAS NMR spectrum; C = ^{13}C CP-MAS NMR spectrum.
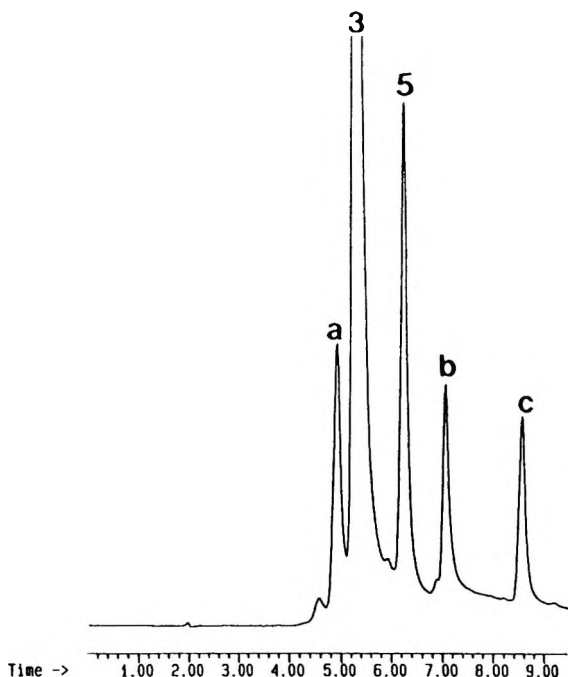
Figure 6. Gradient separation of typical commercial tetracycline mixture on mono-ol column made from hydrosilation of 1-octene-8-ol on hydride intermediate. Solvent A - 10:90 MeCN/0.02M NaClO$_4$ (pH=2.5) and solvent B 50:50 MeCN/0.02M NaClO$_4$ (pH=2.5). Gradient: 0-1 min, 100% A; 1-5 min, linear increase to 100% B. Solutes: a) 4-epitetracycline; b) 4-epianhydrotetracycline; c) anhydrotetracycline; 3) tetracycline; 5) chlorotetracycline.

conventional phases with high (B) and low (C) surface coverage. Clearly, the hydride-based material exhibits less of a decrease in k' than either of the conventional phases. Similar results are obtained at high pH so that it can be concluded the silicon-carbon linkage leads to the higher stability observed.

POROUS OXIDE MATERIALS

Silica

The synthetic scheme for the silanization/hydrosilation process described in Figure 1 can be readily monitored by spectroscopic means. Two of the most useful methods for the evaluation of chemically bonded stationary phases have
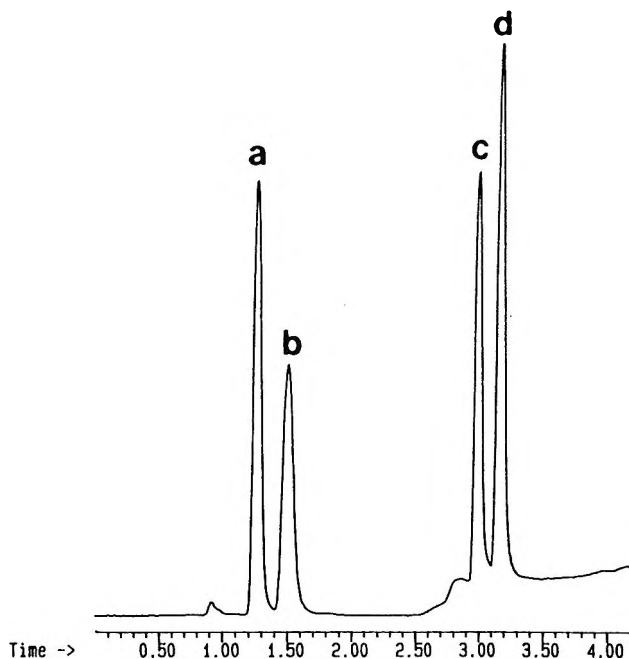
Figure 7. Gradient separation of steroid mixture on diol column made from hydrosilation of allyl glycidyl ether on hydride intermediate. Gradient: 2-propanol in methylene chloride from 2.5% to 15% between 1 and 2.5 min in the chromatographic run. Solutes: a) 4-androstene-3,17-dione; b) adrenosterone; c) corticosterone; d) prednisone. (Reprinted with permission from ref. 19)

been diffuse reflectance infrared Fourier transform (DRIFT) and solid-state cross-polarization magic-angle spinning (CP-MAS) NMR spectroscopy.[10] Their utility in the silanization step with TES is documented in Figure 3. The partial DRIFT spectrum for a typical hydride intermediate is shown in Figure 3A. The most essential feature is the strong Si-H stretching frequency which is observed near 2250 cm^{-1}. The appearance of this band is accompanied by a significant decrease in the free silanol stretching near 3750 cm^{-1}. In addition, the ^{29}Si CP-MAS NMR spectrum (Figure 3B) confirms the presence of the Si-H moiety on the surface. Two peaks in the spectrum (Q_3 and Q_4) are the result of the base silica material, with Q_4 representing the silicon atoms in the siloxane backbone and Q_3 representing silicon atoms that have a surface silanol attached to them. The other two peaks are the result of the silanization process. Peak g at -85 ppm is due to silicon atoms with three siloxane linkages and a hydride, while Peak i at -75 ppm represents silicon atoms with two siloxane linkages, a hydroxide and a hydride. These observations which confirm the formation of
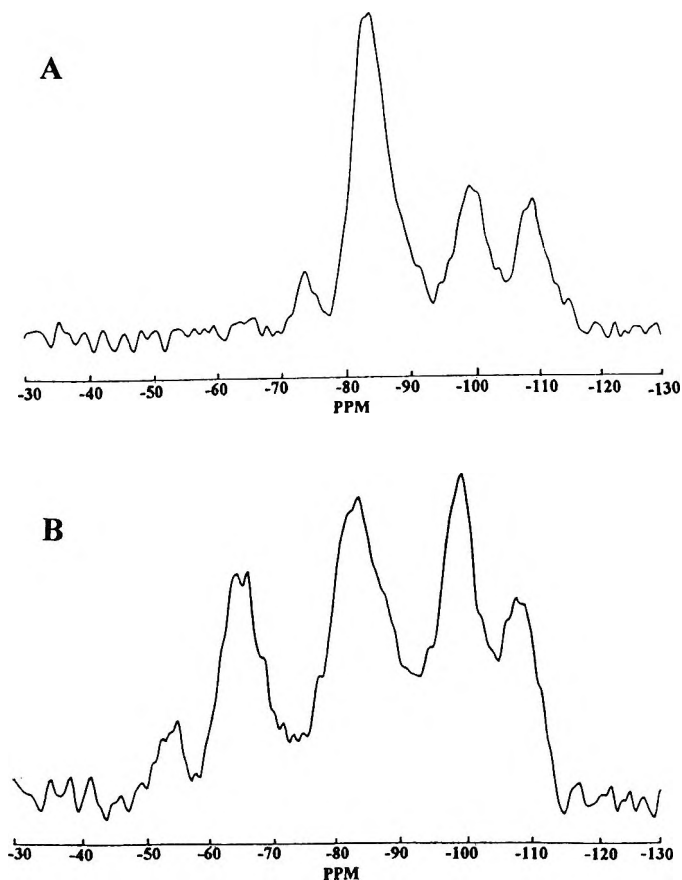
Figure 8. ^{29}Si CP-MAS NMR spectra of zirconia support material. A. Zirconia after reaction with TES. B. Zirconia after material in A is reacted with 1-octene by hydrosilation. (Reprinted with permission from ref. 25)

the hydride intermediate are independent of the commercial source (Vydac, Partisil, Kromasil, Nucleosil, YMC, Porasil) of the silica. In addition, ^{29}Si CP-MAS NMR data indicate that greater than 90% efficiency is achieved in the silanization reaction.[6]

Similar spectroscopic characterization of the final product can be done after the hydrosilation step as shown in Figure 4. In this step any compound containing a terminal olefin should react with the hydride intermediate in the presence of a suitable catalyst such as hexachloroplatinic acid.[11] The specific
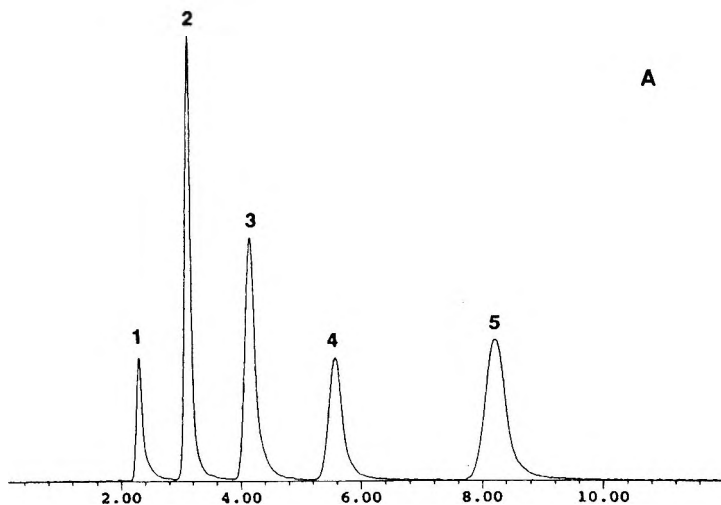
Figure 9. Chromatogram of test mixture for reversed-phase behavior on alumina modified by hydrosilation of 1-octadecene on a hydride intermediate. Mobile phase: MeCN-water (50:50). Solutes: 1) theophylline; 2) *p*-nitroaniline; 3) methylbenzoate; 4) phenetol; 5) *o*-xylene. (Reprinted with permission from ref. 24)

olefin used for the material which is spectroscopically characterized in Figure 4 is 7-octene-1,2-diol (7-OD). The partial DRIFT spectrum (A) reveals two important features of the surface. First, the presence of the organic moiety is confirmed by the strong C-H stretching bands between 2800 and 3000 cm^{-1}. Second, the surface below the bonded organic ligand consist mainly of hydride groups as seen by the strong Si-H band at 2250 cm^{-1} and the absence of any isolated silanol groups with no evidence of a peak at 3750 cm^{-1}. A more definitive answer concerning bonding can be obtained from the ^{29}Si CP-MAS NMR spectrum (B). In addition to the peaks observed for the hydride intermediate described in Figure 3B, a new peak is observed near -65 ppm. This is due to a silicon atom with three siloxane linkages and a carbon atom. This spectrum is used to prove the success of the hydrosilation reaction since the presence of the peak at -65 ppm confirms reaction of the hydride to form an Si-C bond at the surface. The presence of the Q_3 peak indicates that there are still silanols as part of the overall composition of the material. However, the absence of the 3750 cm^{-1} peak in the DRIFT suggests that most of the silanols are associated and not isolated. Because of the mesopores that exist in all particulate silica material, it is not surprising that some silanols remain since they are probably inaccessible to the TES silanization reagent. Further confirmation of the surface structure can be obtained from the ^{13}C CP-MAS
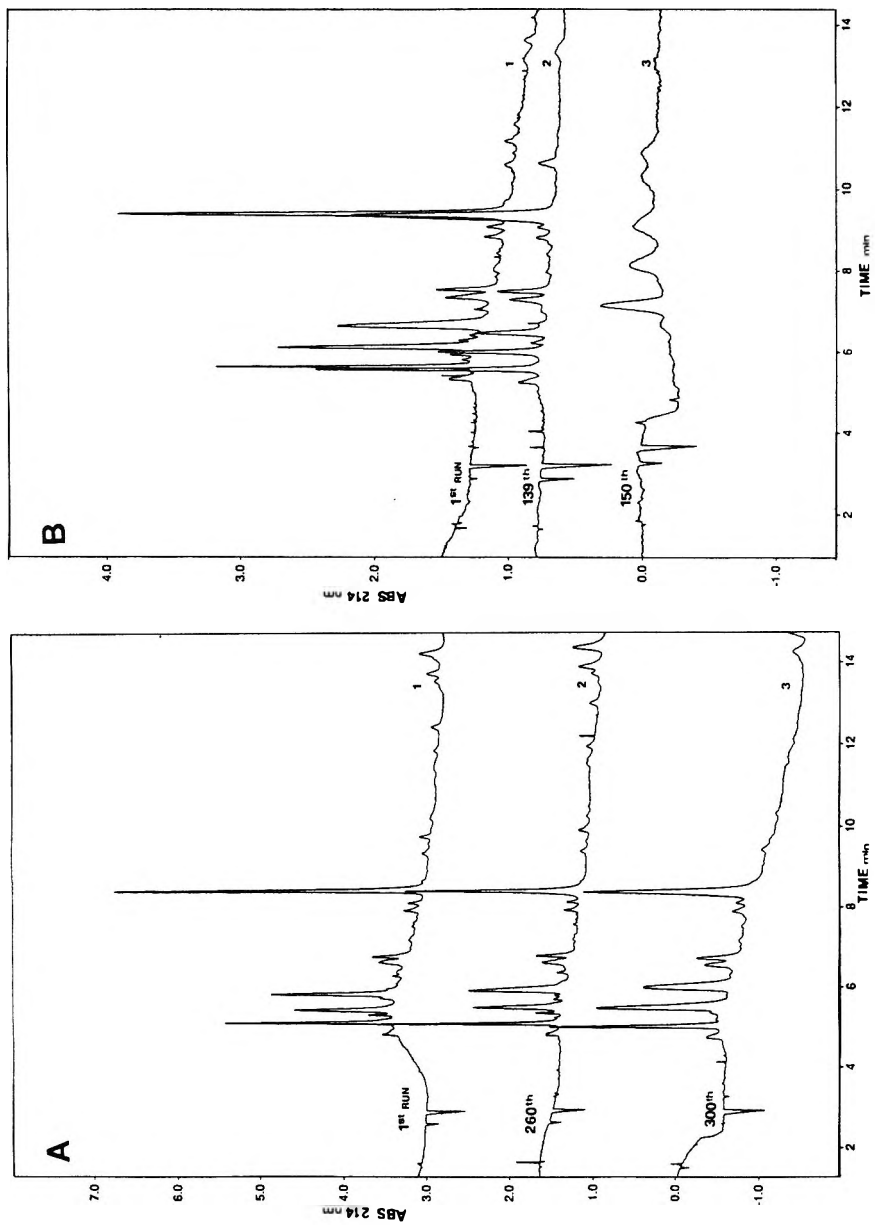
NMR spectrum which is shown in Figure 4C. Peaks for each of the carbons in the bonded moiety can be easily assigned according to the expected structure. Of particular interest is the peak at 12 ppm, which is due to the methylene carbon attached to the silica surface. In addition, for this molecule with two hydroxide groups, it appears that some bonding of 7-OD has occurred through one of the OH groups because two peaks in the olefinic portion of the spectrum can be seen between 120 and 140 ppm. In combination, the three spectra shown in Figure 4 give a relatively complete picture of the surface and the bonded moiety.

One of the advantages of the silanization/hydrosilation bonding scheme is the lack of interferences in the reaction from other functional groups which might be present on the organic ligand being attached to the hydride.[11] It would be expected that normal hydrocarbons with a terminal olefin should present the fewest problems in bonding. This has been observed for the bonding of 1-octene and 1-octadecene with surface coverages that are comparable to or better than those obtained by conventional organosilanization to form monomeric phases.[7,9] Since the majority of separations done by HPLC are done in the reverse phase mode, this result along with the high stability cited earlier[9] make this process a viable alternative for producing bonded phases suitable to a wide range of applications.

However the versatility advantages of this method facilitate the synthesis of a wide variety of specialty phases including some that might be difficult or impossible to make by other reaction schemes. One such possibility has been cited above which is a diol phase based on the bonding of 7-OD.[12] This material is different than the usual diol phases which are based on a propyl glycidyl ether moiety. The 7-OD phase has an alkyl chain of six methylene groups in addition to the diol functionality, while the current commercial phases consist of two methylene groups, an ether linkage ($-CH_2-O-CH_2-$) and the diol group. However, a phase identical to those now available can be made by bonding allyl glycidyl ether (AGE) to the hydride intermediate.[12] These two phases, as well as others that might be synthesized with different alkyl chain lengths and the diol group, lead to a range of hydrophobic/hydrophilic

---

Figure 10 (left). Protein separations on chemically modified capillaries. A) poly(AAEE) capillary modified by silanization/hydrosilation method after 1st, 260th and 300th runs and B) polyacrylamide capillary modified by organosilanization after 1st, 139th and 150th runs. Conditions: V = 20kV, buffer is 25 mM bicine-Tris (pH=8.5). Four largest peaks in order of increasing migration time: trypsin inhibitor, β-lactoglobulin A, β-lactoglobulin B, and α-lactalbumin. (Reprinted with permission from ref. 26)

properties which can be utilized in either reverse phase or normal phase chromatography. Some other examples of bonded materials synthesized by the silanization/ hydrosilation method with a terminal olefin, include a mono-ol phase based on a C_8 moiety, a butyl phenyl phase and a perfluorinated C_8 phase.[13] Current testing of these bonded materials involve normal phase, hydrophobic mode and reverse phase applications.

Perhaps one of the more unique moieties bonded to the hydride surface for use in HPLC are two liquid crystals, which also contain terminal olefins. Their structures are shown below. Bonded liquid crystals have been shown to possess properties which are different from other organic groups attached to silica surfaces and in particular, they exhibit a high selectivity based on molecular shape.[14-16] It appears that there is a high degree of association between adjacent ligands. This has been shown through variable temperature solid-state NMR studies. The spin-spin relaxation time measured from the line width (T_2^*) can be used to determine the molecular motion of the bonded moiety.[17] In a typical C_{18} bonded phase, T_2^* decreases regularly as the temperature is lowered indicating a restriction of the molecular motion.[17] However, for liquid crystal phases an increase in T_2^* over a restricted range is observed as the temperature is lowered.[18] This observation has been attributed to

A.

CH$_2$ = CH - CH$_2$ - O - ⬡ - C(=O) - O - ⬡ - O - CH$_3$
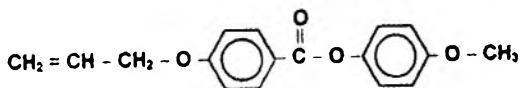
4-Methoxyphenyl-4-allyloxy benzoate

B.

CH$_2$ = CH - CH$_2$ - (CH$_2$)$_6$ - CH$_2$ - C(=O) - O
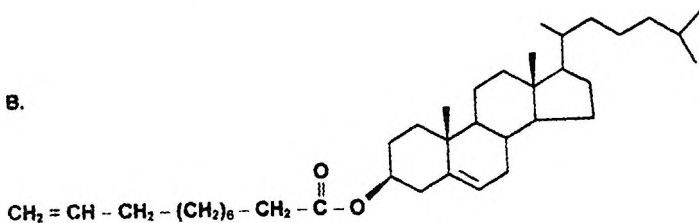
Cholesteryl 10-undecenoate
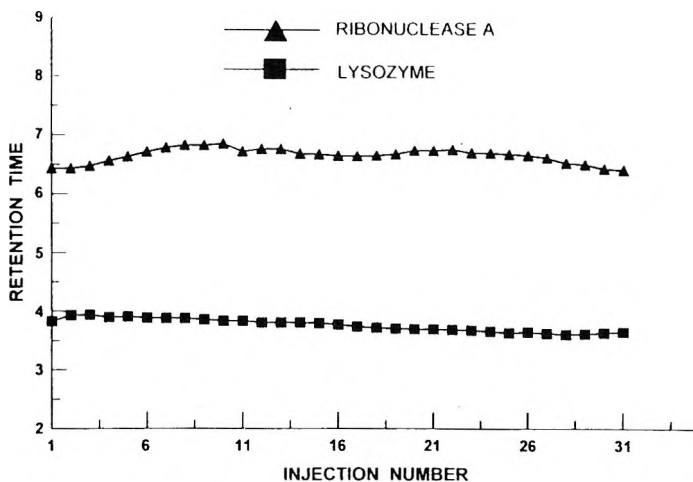
Figure 11. Retention time as a function of injection number for two proteins on an etched C_{18} modified capillary.

phase transitions where the bonded moieties change their degree of association similar to the molecular reorientations which occur for pure liquid crystalline materials.   In the pure state, liquid crystals exhibit physical properties intermediate between those of a solid and an isotropic liquid over a well-defined temperature range. A similar phenomena in the bonded state could be responsible for the high shape selectivity exhibited in the chromatographic data.

Chromatographic characterization and testing potential applications provides further information about the nature of the hydride-based materials. For example, the effects of the hydride surface and the differences in diol phases have been tested in the normal phase with a heptane-chloroform mobile phase using a series of substituted phenols as solutes.[19] The results are shown in Figure 5 where the log k' values are plotted for each compound. The relative order of retention is the same for the three columns: commercial diol > diol from AGE > diol from 7-OD. In this case, the degree of retention changes as a function of the hydrophilic nature of the bonded material.   The highest retention is for the commercial phase since it has a shorter alkyl chain, an ether linkage and residual silanols on the surface. When the residual silanols are mostly removed in the hydride material, retention decreases for the same bonded organic moiety as shown by the AGE phase. Retention decreases further as the alkyl chain length increases, the ether linkage is removed and the hydride surface is present in the case of the 7-OD phase.

With respect to practical applications, the hydride-based material has been tested in both normal and reverse phase. An example in reverse phase involves the separation of various tetracycline mixtures at low pH on the mono-ol column.[20] The analysis of a typical commercial tetracycline sample is shown in Figure 6. The separation shown here is considerably better than previous reports involving polymeric stationary phases, which cannot separate the first two components well (a & 3) and retention of the last two components (b & c) is too long to be practical. In addition, the low pH conditions (2.0-2.5) did not result in any deterioration of the column after long exposure to the mobile phase. An example in normal phase is the separation of a steroid mixture shown in Figure 7.[19] The diol column with the hydride surface, is well-suited to the broad range of polarities present in this mixture. The use of a gradient is still necessary to resolve the low polarity components which elute first, as well as the more polar species which are more strongly retained. However, the excellent selectivity observed in these examples and for other hydride-based bonded materials in both normal and reverse phase modes, as well as their stability, indicates their potential for a wide variety of practical applications.

While terminal olefins have been almost exclusively used for the attachment of organic moieties to hydride-based supports, hydrosilation is also possible for double bonds at other points on an alkyl chain.[11] An interesting example is the attachment of squalene to a silica hydride intermediate.[21] Squalene contains six double bonds, none being in a terminal position. The ^{13}C CP-MAS NMR spectrum of the bonded materials contains olefinic peaks indicating that not every double bond has reacted.

However, the ^{29}Si CP-MAS NMR spectrum has a peak at -65 ppm which confirms the formation of an Si-C bond, proving that at least one olefin per squalene molecule has reacted with the hydride surface to provide attachment of the organic moiety. This result opens up the possibility of synthesizing other useful bonded phases from molecules with a double bond in other than the terminal position. The squalene phase was prepared for use in gas chromatographic analysis of low molecular weight hydrocarbons.

Another example of a gas chromatographic phase[22,23] utilized a hydride intermediate prepared from a cyclic siloxane (pent-amethylcyclopentasiloxane). Subsequent attachment of 1-octadecene or 1-octene indicates that this approach can also provide a hydride surface suitable for hydrosilation. HPLC testing of bonded phases, based on the cyclic siloxane and TES intermediates, would be useful in determining whether one of the approaches produces a material with any specific chromatographic advantages.

Other Oxides

In principle, the silanization/hydrosilation reaction scheme can apply to any oxide surface where hydroxides are present. While silica is the most common support material due to its availability with a wide range of physical properties such as particle size, pore size and surface area, it is limited mainly by its hydrolytic stability, generally from pH 2-8. Other oxides which have the necessary hydroxide groups and are stable over a broader pH range include alumina, zirconia, titania and thoria. It has already been demonstrated that formation of hydride surfaces on each of these four oxides is possible.[24,25]

Once the hydride intermediate is formed, then hydrosilation should proceed in the same manner as on silica. These processes can be readily monitored spectroscopically by DRIFT and solid-state CP-MAS NMR. An example of the spectroscopic evaluation by ^{29}Si CP-MAS NMR of a modified zirconia material is shown in Figure 8. The spectrum of the hydride intermediate (A) has a large peak at -85 ppm which represents the Si-H moiety on the surface. In addition, there also is a peak near -75 ppm indicating there are some silicon atoms with both a hydride and a hydroxide.

An interesting feature are the peaks at -110 and -100 ppm. These peaks indicate that some polymerization of the TES has occurred during formation of the hydride layer. This is the only explanation for the presence of a silicon with four siloxane bonds. The spectrum of the octyl bonded phase (B) contains the same four peaks which are found in the hydride intermediate (the peak at -75 ppm is not resolved) as well as two additional peaks which are characteristic of attached organic moiety. The peak at -65 ppm represents a silicon atom with a carbon attached to it, while the peak at -55 ppm is due to a silicon atom with a carbon and a hydroxyl group. The presence of these two peaks are confirmation that bonding of the 1-octene to the hydride intermediate was successful. Similar spectroscopic evidence has been used to confirm both the formation of the hydride intermediate and the bonded product on alumina, titania and thoria.

For other supports to be competitive with silica, they must also possess good chromatographic properties in addition to their potential for use under conditions which are not compatible with current stationary phases. Figure 9 shows the separation of a reverse phase test mixture run on a column with an octadecyl moiety bonded via a hydride intermediate on an alumina support.[24] The chromatogram has good peak shape with the most polar component eluting first and the least polar component eluting last.

FUSED SILICA CAPILLARIES

The same reactions which are used to modify porous silica surfaces can be applied to the modification of fused silica capillary walls. As a consequence, organosilanization has been the most popular method for modifying capillaries in high performance capillary electrophoresis (HPCE). However, the same advantages that the silanization/hydrosilation reaction scheme has for porous silica should be present for fused silica capillaries because the reactive site is the same, i.e. silanols.

The first reported application of this method to HPCE involved the attachment of a linear polymer, poly(acryloylaminoethoxyethanol), to a capillary wall for the separation of proteins.[26] This particular polymer, poly(AAEE), was selected because it is hydrolytically more stable than polyacrylamide. Therefore, the combined effect of having a more stable attachment of the organic moiety to the capillary wall via an Si-C linkage, and the resistance to hydrolysis of the substituted amide, results in a separation media that can function under buffer conditions which cause the rapid deterioration of conventionally bonded polymers such as polyacrylamide. This improvement in performance is documented in a series of electropherograms shown in Figure 10. The comparison was run on a series of acidic proteins so that a basic pH buffer was selected with the separation taking place using reverse polarity and cathodic injection. Panel A shows selected runs of these four proteins on the poly(AAEE) capillary. It is clear that no significant change in the electropherogram has occurred between the 1st and the 300th injection. However, for polyacrylamide (Panel B), little if any analytical information is available from the electropherogram by the 150th injection. Similar high efficiencies and stability were achieved when basic proteins were separated under acidic or neutral conditions. Electroosmosis was low and stable with the poly(AAEE) capillary at pH 8.5, while the polyacrylamide capillary showed a rapid increase in a relatively short time under identical buffer conditions. Since the stability observed in HPCE parallels that obtained in HPLC, the attachment of other organic moieties to capillary surfaces should also result in continued high performance after many injections.

While additional examples of capillaries modified by the silanization/hydrosilation reaction method for HPCE are not yet available, there is further confirmation of the utility of this bonding scheme in capillary electro-chromatography (CEC). However, the approach to CEC is somewhat different than the normal one where the capillary is packed with particulate silica identical to material used in HPLC. In this method the capillary is first extensively etched with an aggressive reagent, ammonium hydrogen difluoride,[27] which increases the surface area by up to a factor of 1000. Then

Table 1

Separation Factors for Various Pairs of Proteins and Peptides

Solute Pair	Bare Capillary	Etched C_{18} Capillary
Angiotensin III/lysozyme	1.12	1.15
Bradykinin/angiotensin III	1.02	1.28
Ribonuclease A/bradykinin	0.97	1.16
Angiotensin I/ribonuclease A	1.11	1.15
Angiotensin I/lysozyme	1.22	1.97

the surface is modified by the silanization/hydrosilation method in a manner similar to that reported for HPCE.[26] The increase in surface area and the presence of radial extensions from the inner capillary wall leads to an increase in solute/bonded phase interactions (k'). Therefore, electromigration and/or electroosmosis is the driving force which moves the solute through the column, while separation is achieved by differences in electrophoretic mobility and/or k' interactions, depending on whether the solute is charged or neutral. The presence of solute/bonded phase interactions can be verified in several ways. For several charged solutes, the peak width in a bare, etched or hydride-modified capillary is narrow, with efficiencies between 300,000 and 500,000. For a C-18 modified etched capillary, peaks become noticeably broader leading to efficiencies between 30,000 and 70,000[27] due to resistance to mass transfer effects. This result is certainly a strong indication of solute/bonded phase interactions. Measurable differences in retention are also found for small neutral molecules such as 1- and 2-napthol. Finally, a comparison of migration times for various proteins and polypeptides leads to significant differences in separation factors between bare and etched C-18 modified capillaries, as shown in Table 1. These results indicate that k' interactions are present in the etched modified capillary since the separation factors clearly change from the bare capillary where migration is determined only by electrophoretic mobility. There are increases in separation factors, a reversal of the order of migration for one pair and a much greater range in the difference of migration times, which can be seen by comparing the α values for the first and last eluted compounds on both columns. This system requires no packing or frits and there is no bubble formation as a consequence of these two factors.

The question of stability is also important in CEC just as it is in HPLC and HPCE. Because the modification is based on the silanization/hydrosilation reaction scheme, the bronded moiety should possess the same high stability that was demonstrated for porous silica and ordinary modified capillaries for CE.

Table 2

Separation Factors for Component Pairs in Commercial Tetracycline*

Solute Pair	α
4-epi-anjydrotetracycline/4-epitetracycline	1.08
Tetracycline/4-epi-anhydrotetracycline	1.05
Chlorotetracycline/tetracycline	1.20
anhydroetracycline/chlorotetracycline	1.10

*Conditions: electrolyte, 30mM citric acid + 24.5 mM β-alanine (pH=3.0), V=30 kV. 1=25 cm.

Table 3

Separation Factors for Component Pairs in Commercial Oxytetracyline*

Solute Pair	α
Oxytetracycline/tetracycline	1.10
4-epioxytetracycline/oxytetracycline	1.08
α-apo-oxytetracycline/4-epioxytetracycline	1.25

* Conditions: electrolyte, 30 mM phosphate and 19 mM Tris (pH=2.14). 60:40 buffer/MeOH, V=30 kV, 1=35 cm.

Figure 11 shows the results of 31 consecutive injections of lysozyme followed by 31 consecutive injections of ribonuclease A. No discernible increase or decrease in retention times is observed for either protein. The reproducibility for each series of 31 injections was ±1.5%. The test was not conducted on a new capillary, but one that had been mounted and demounted several times. washed several times with methanol followed by dry storage and had more than 100 injections of other samples under a variety of buffer conditions.

A more practical example of the usefulness that this mode of CEC might develop involves the separation of various tetracycline mixtures.[28] Table 2 shows the separation factors obtained for a typical commercial tetracycline

mixture with the etched C_{18} modified capillary. Resolution of the various components and analysis time are comparable to the best separations reported in HPLC.[20] An even better result can be obtained for the analysis of commercial oxytetracycline as shown in Table 3. In particular, oxytetracycline and 4-epioxytetracycline were easily separated on the etched C_{18} modified capillary but are not resolved on a polymeric column and only partially resolved on the mono-ol column cited above.[20] In addition, the analysis time for the CEC method is less than 6 min.

CONCLUSIONS

The silanization/hydrosilation method has proven to be a viable method for the modification of oxide supports for HPLC and capillary surfaces for HPLC and CEC. Further development to expand the range of applications in each of these techniques is still necessary. It is likely that other functional groups and other modes of catalysis can be used to attach the organic moiety to the hydride surface during the hydrosilation reaction. Further improvement in the formation of the hydride intermediate and the final bonded product will lead to a wide variety of bonded surfaces and increased stability.

ACKNOWLEDGEMENTS

REFERENCES

1. E. F. Vansant, P. Van Der Voort, K. C. Vrancken, **Characterization and Chemical Modification of the Silica Surface**, Elsevier, Amsterdam, 1995.

2. J. F. K. Huber, F. F. M. Kolder, J. M. Miller, Anal. Chem., **44**, 105-110 (1972).

3. M. J. Wirth, H. O. Fatunmbi, Anal. Chem., **65**, 822-826 (1993).

4. J. J. Pesek, S. A. Swedberg, J. Chromatogr., **361**, 83-92 (1986).

5. J. E. Sandoval, J. J. Pesek, Anal. Chem., **61**, 2067-2075 (1989).

6. M. C. Montes, C. -H. Chu, E. Jonsson, M. Auvinen, J. J. Pesek, J. E. Sandoval, Anal. Chem., **65**, 808-818 (1993).

7. J. E. Sandoval, J. J. Pesek, Anal. Chem., **63**, 2634-2641 (1991).

8. O. V. Simurov, L. A. Belyakova, V. A. Tertykh, Functional Materials **2**, 51-57 (1995).

9. M. C. Montes, C. van Amen, J. J. Pesek, J. E. Sandoval, J. Chromatogr. A, **688**, 31-45 (1994).

10. J. J. Pesek, J. E. Sandoval, E. J. Williamsen, Trends in Appl. Spectroscopy, **1**, 41-50 (1993).

11. B. Marciniec, **Comprehensive Handbook on Hydrosilylation**, Pergamon Press, Oxford, 1992.

12. J. J. Pesek, M. T. Matyska, J. Chromatogr., **687**, 33-44 (1994).

13. J. J. Pesek, M. T. Matyska, E. Soczewinski, P. Christensen, Chromatographia, **39**, 520-528 (1994).

14. J. J. Pesek, Y. Lu, A. M. Siouffi, F. Grandperrin, Chromatographia, **31**, 147-151 (1991).

15. Y. Saito, K. Jinno, J. J. Pesek, Y. L. Chen, G. Luehr, J. Archer, J.C. Fetzer, W. R. Biggs, Chromatographia, **38**, 295-303 (1994).

16. Y. Saito, H. Ohta, H. Nagashima, K. Itoh, K. Jinno, J. J. Pesek, J. Microcol. Sep., **7**, 41-49 (1995).

17. H. Ohta, Y. Saito, K. Jinno, J. J. Pesek, M. T. Matyska, Y. L. Chen, J. Archer, J.C. Fetzer, W.R. Biggs, Chromatographia, **40**, 507-512 (1995).

18. J. J. Pesek, M. T. Matyska, E. J. Williamsen, R. Tam, Chromatographia, **41**, 301-310 (1995).

19. J. J. Pesek, M. T. Matyska, H. Hemphala, P. Christensen, J. Liq. Chromatogr., **18**, 2507-2526 (1995).

20. M. T. Matyska, J. J. Pesek, A. M. Siouffi, Chem. Anal., **40**, 517-530 (1995).

21. S. O. Akapo, J. -M.D. Dimandja, M. T. Matyska, J. J. Pesek, Chromatographia, **42**, 141-146 (1996).

22. S. O. Akapo, J. -M. D. Dimandja, M. T. Matyska, J. J. Pesek, J. Microcol. Sep., **8**, 189-200 (1996).

23. S. O. Akapo, J. -M. D. Dimandja, M. T. Matyska, J. J. Pesek, Anal. Chem., in press.

24. J. J. Pesek, J. E. Sandoval, M. Su, J. Chromatogr., **630**, 95-103 (1993).

25. J. J. Pesek, V. H. Tang, Chromatographia, **39**, 649-654 (1994).

26. M. Chiari, M. Nesi, J. E. Sandoval, J. J. Pesek, J. Chromatogr., **717**, 1-13 (1995).

27. J. J. Pesek, M. T. Matyska, J. Chromatogr., in press.

28. J.J. Pesek, M.T. Matyska, J. Chromatogr., in press.

APPLICATION OF 3-(1,8-NAPHTHALIMIDO) PROPYL-MODIFIED SILYL SILICA GEL AS A STATIONARY PHASE IN HIGH PERFORMANCE LIQUID CHROMATOGRAPHY OF BARBITURATES AND DIASTEREOMERIC COMPOUNDS

Naotaka Kuroda, Keiko Inoue, Kumiko Mayahara, Kenichiro Nakashima, Shuzo Akiyama

School of Pharmaceutical Sciences
Nagasaki University
1-14 Bunkyo-machi
Nagasaki 852, Japan

ABSTRACT

The application of a column packing material, 3-(1,8-naphthalimido)propyl-modified silyl silica gel (NAIP) developed by us, for high performance liquid chromatography (HPLC) of barbiturates and diastereomeric compounds is described. The separation of barbiturates by using an NAIP column as a stationary phase was at first investigated. Six commercially available barbiturates (Barbital, Phenobarbital, Amobarbital, Pentobarbital, Secobarbital and Thiopental) were well separated on an NAIP column by an isocratic elution with borate buffer (pH 7.0)-acetonitrile (9:1, v/v). Further, the applicability of the HPLC system including an NAIP column to the determination of barbiturates in human blood plasma was examined. Barbiturates extracted from plasma sample using a solvent extraction (hexane-diethyl ether, 3:7, v/v) were subjected to the HPLC system and

determined by an internal standard method with UV detection at 220 nm. The recoveries of barbiturates spiked to human plasma were obtained in the range of 88.6 to 100.0%. The lower detection limits of barbiturates spiked ranged from 0.05 to 0.33 μg/mL, and the within-day and day-to-day precisions for plasma sample (n=5) gave relative standard deviations of less than 9.07% and 18.68%, respectively.

Next, the applicability of an NAIP column to the separation of diastereomeric derivatives was studied. Epinephrine (EP), norephedrine (NE) and α-phenylethylamine (PA) carrying an aromatic ring were used as representative targets for derivatization with three kinds of chiral reagents. Resolution behavior on NAIP was compared with that on a conventional reverse phase ODS column. Diastereomeric derivatives of targets were satisfactorily separated by an NAIP column as well as an ODS column. The best separation of S(+)-1-(1-naphthyl)ethyl isocyanate derivatives with PA was obtained on an NAIP column and the calibration curves showed good linearity in the concentration range examined.

INTRODUCTION

In recent years, we synthesized a series of 3-(N-substituted)aminopropyl-modified silyl silica gels immobilizing organic dyes or aromatic dicarboxylic anhydrides as new column packing materials with an expectation of a π-π interaction. Their ability to separate biologically important compounds related to nucleic acids, i.e., adenine derivatives,[1-3] was examined in HPLC. Among them, 3-(1,8-naphthalimido)propyl-modified silyl silica gel (NAIP, Figure 1) was found to be useful for the separation of purine derivatives. i.e., xanthine, hypoxanthine, uric acid, theobromine, theophylline and caffeine. The resolution behavior obtained with the gel suggested that an NAIP column had a reverse phase-like mode with some π-π interaction. By using this column, caffeine concentrations in commercially available medicinal drinks and pharmaceutical preparations were successfully determined. Furthermore, time curves of plasma caffeine and its demethylated metabolite, 1,7-dimethylxanthine, concentrations after an oral ingestion of caffeine could be also determined.[4]

In this work, we at first examined the separation of barbiturates carrying a pyrimidine skeleton with a view to extend the applicability of the NAIP column. Barbiturates are widely used as sedative, hypnotic and anticonvulsant
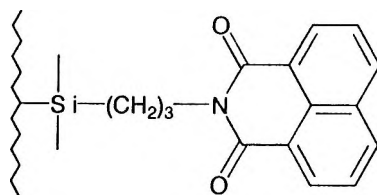
Figure 1. Proposed structure of NAIP.

drugs. Therefore, accurate, simple and rapid method for determining of these is important in pharmaceutical, clinical and toxicological studies. For this purpose, several methods including gas-liquid chromatography (GLC),[5,6] gas chromatography/mass spectrometry (GC/MS)[7] and HPLC[8-10] have been reported. In HPLC methods, a reverse phase ODS column is exclusively employed as a separation column. This paper describes an HPLC separation of barbiturates using an NAIP column and its preliminary application to the determination of these in human blood plasma. Furthermore, to evaluate the scope and limitations of an NAIP column, we examined the separation of diastereomeric compounds carrying an aromatic ring and compared the resolution behavior on an NAIP column with that on an ODS column. Epinephrine (EP), norephedrine (NE) and α-phenylethylamine (PA) were chosen as tentative targets for the labelling with three kinds of chiral reagents.

EXPERIMENTAL

Chemicals

NAIP prepared from 3-aminopropylsilyl silica gel (particle size, 5 μm; pore diameter, 1.2 μm) and 1,8-naphthalic anhydride was packed by a slurry method in a stainless-steel column (150x6 mm I.D.) as described previously.[2]

The sources of barbiturates employed were as follows: Barbital and Phenobarbital from Astra Japan (Osaka, Japan), Amobarbital from Nippon Sinyaku (Kyoto, Japan), Pentobarbital calcium and Thiopental sodium from Tanabe Seiyaku (Osaka, Japan) and Secobarbital sodium from Yoshitomi Pharmaceutical Industries (Osaka, Japan). 5-(2-Cyclohexen-1-yl)-1-phenyl barbituric acid and 5-(2-cyclohexen-1-yl)-5-propenyl barbituric acid as candidates for internal standards (I.S.) were prepared in our laboratory.

D-(+)-Norephedrine, L-(-)-norephedrine, 2,3,4-tri-*O*-acetyl-α-D-arabino-pyranosyl isothiocyanate (AITC) and 2,3,4,6-tetra-*O*-acetyl-β-D-glucopyranosyl isothiocyanate (GITC) were purchased from Aldrich (Milwaukee, WI, USA). D-(+)-α-Phenylethylamine and L-(-)-α-phenylethylamine were obtained from Nacalai Tesque (Kyoto, Japan). D-(+)-Epinephrine from Sigma (St. Louis, MO, USA), L-(-)-epinephrine from Merck (Darmstadt, Germany), and S(+)-1-(1-naphthyl)ethyl isocyanate (NEIC) from Fluka (Buchs, Switzerland) were employed. An ODS column used was Hibar LiChrosorb 100 RP-18 (7 μm, 250x4.0 mm I.D., Kanto Chemical, Tokyo, Japan).

Borate buffer (Palitzsch buffer) was prepared as follows: H_3BO_4 (6.183 g) and NaCl (1.461 g) were dissolved in 500 mL water. The solution was brought to the appropriate pH by adding of $Na_2B_4O_7/10\ H_2O$ (4.767 g) in 250 mL water.

Water was deionized and passed through a water purification system (Pure Line WL21P, Yamato Kagaku, Tokyo, Japan). Other reagents and solvents used were of analytical reagent grade.

HPLC Apparatus and Conditions

The HPLC system for the separation of barbiturates consisted of a Tosoh CCPD pump (Tokyo, Japan), a Tosoh UV-8011 UV monitor (220 nm), a Rheodyne 7125 injector (Cotati, CA, USA) with a 20-μL sample loop, an NAIP column (5 μm, 150x6 mm I.D.) in a Tosoh CO 8010 column oven, and a Rikadenki R-01 recorder (Tokyo, Japan).

The column temperature was maintained at 30 °C. The elution was performed with borate buffer (pH 7.0)-acetonitrile (9:1, v/v) at a flow rate of 1.0 mL/min.

The HPLC system for the separation of diastereomeric compounds was consisted of two HPLC pumps (LC-9A) with a system controller (SCL-6B, Shimadzu, Kyoto, Japan), a 7125 injector with a 20-μL loop (Rheodyne, Cotati, CA, USA) and a Shimadzu SPD-6A UV-VIS detector (290 nm) for absorbance measurement.

The mobile phases for HPLC separation were as follows: acetonitrile-water for NEIC derivatives, and acetonitrile-10 mM phosphate buffer (pH 3.0) for AITC and GITC derivatives. The flow rate was set at 1 mL/min at an ambient temperature.

Extraction of Barbiturates from Human Plasma

To 100 μL of plasma were added 500 μL of 0.1 M phosphate buffer (pH 7.0) and 10 μL of ethanolic solution of barbiturates.   After addition of 5.0 mL of hexane-diethyl ether (3:7, v/v), the mixture was vortex-mixed for 10 s and allowed to stand for 3 min. The organic layer (4.5 mL) was evaporated to dryness under a stream of nitrogen gas, and the resultant residue was dissolved in 100 μL of methanol. The solution was passed through a membrane filter (0.45 μm) and injected onto the HPLC system.

Procedure for Diastereomeric Derivatization

NEIC derivatives: to 200 μL of 5 mM PA or NE in chloroform, or EP in N,N-dimethylformamide (DMF) was added 200 μL of 5 mM NEIC in chloroform. After mixing, the mixture was evaporated to dryness under a stream of nitrogen gas and the resultant residue was dissolved in 2 mL of methanol. The solution was passed through a membrane filter (0.45 μm) and injected onto the HPLC system.   For the preparation of calibration curves, 25 mM NEIC was used.

AITC and GITC derivatives were prepared according to the previously reported method[11] with minor modifications: 500 μL of 0.2 mM PA, NE or EP in 0.25 M acetic acid was evaporated by a centrifugal evaporator (Yamato Kagaku) and to the resultant residue was added 500 μL of 1 mM AITC or GITC in DMF. After standing at room temperature for 30 min, the solution was passed through a membrane filter and injected onto the HPLC system.

RESULTS AND DISCUSSION

HPLC Separation of Barbiturates by an NAIP Column

In this study, six commercially available barbiturates (Barbital, Phenobarbital, Amobarbital, Pentobarbital, Secobarbital and Thiopental) and two barbiturates as candidates for I.S., 5-(2-cyclohexen-1-yl)-1-phenyl and 5-(2-cyclohexen-1-yl)-5-propenyl barbituric acids, were tested.

Separation of barbiturates by an NAIP column was examined using the borate buffer and 10 mM phosphate buffer with various pHs as mobile phases, and the former providing better results was selected for further experiments.
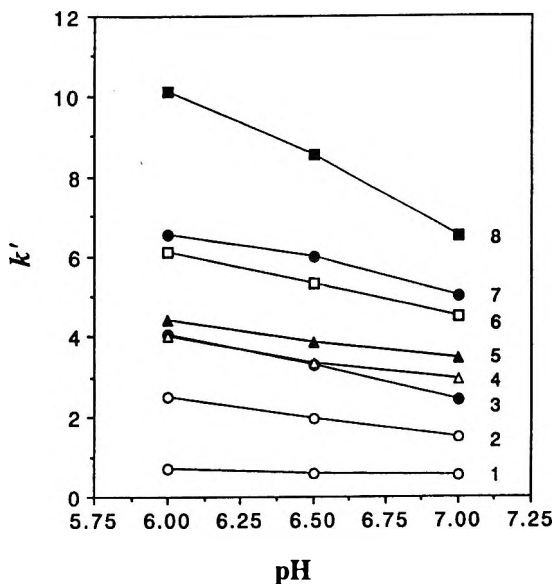
Figure 2.   Effect of pH of borate buffer used in a mobile phase on separation of barbiturates by an NAIP column.

Sample (0.1 mM):   1 = Barbital,   2 = 5-(2-cyclohexen-1-yl)-1-phenyl barbituric acid, 3 = Phenobarbital,   4 = Amobarbital,   5 = Pentobarbital,   6 = Secobarbital,   7 = 5-(2-cyclohexen-1-yl)-5-propenyl barbituric acid,   8 = Thiopental.

As shown in Figure 2, the best separation was observed at pH 7.0 of the borate buffer, and thus was selected in this study. The content of acetonitrile in the mobile phase also affected the separation of barbiturates.

The capacity factor (k') for each barbiturate decreased with an increase in acetonitrile contents from 5 to 10%. The best peak separation with a proper retention time was obtained with 10 % acetonitrile.

Figure 3 shows a typical chromatogram of eight barbiturates. Under the experimental conditions, all barbiturates were separated from each other within 30 min.
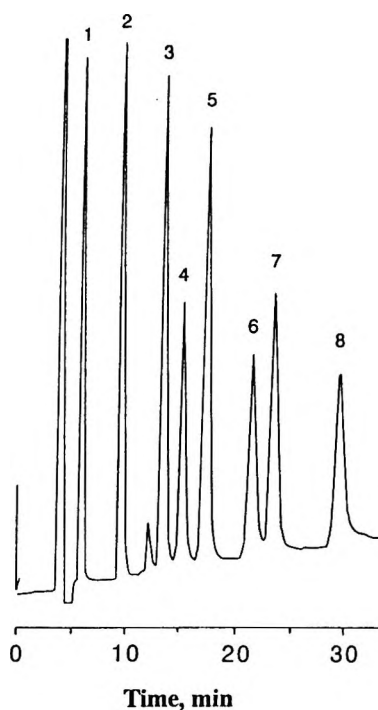
Figure 3 A typical chromatogram of barbiturates by an NAIP column.
Sample (0.1 mM): 1 = Barbital, 2 = 5-(2-cyclohexene-1-yl)-1-phenyl barbituric acid, 3 = Phenobarbital, 4 = Amobarbital, 5 = Pentobarbital, 6 = Secobarbital, 7 = 5-(2-cyclohexen-1-yl)-5-propenyl barbituric acid, 8 = Thiopental.

Preliminary Study on the HPLC Analysis of Barbiturates in Human Plasma

A solvent extraction method was examined for the sample pretreatment using plasma spiked with six commercially available barbiturates. Recoveries of barbiturates spiked to plasma were affected by the pH of 0.1 M phosphate buffer added to the plasma sample before extraction. The ratio of hexane and diethyl ether in a solvent for extraction of barbiturates also affected the recoveries. As shown in Figure 4, the combination of the buffer of pH 7.0 and the extraction with hexane-diethyl ether (3:7, v/v) gave the best results; the recoveries obtained for six barbiturates were in the ranged of 88.6 to 100.0 %.
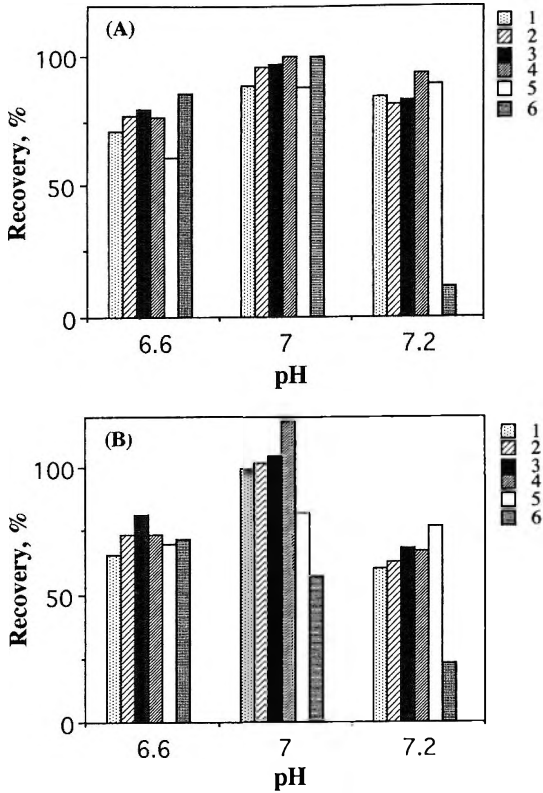
Figure 4. Recoveries of barbiturates spiked to human plasma by extraction with solvent (A) hexane-diethyl ether (3:7, v/v) and (B) hexane-diethyl ether (5:5, v/v). Spiked sample (μg/mL): 1 = Barbital (18.4), 2 =Phenobarbital (23.2), 3 = Amobarbital (22.6), 4 = Pentobarbital (22.5), 5 = Secobarbital (23.7), 6 = Thiopental (24.1).

The calibration curves, in which 5-(2-cyclohexen-1-yl)-5-propenyl barbituric acid was used as an I.S., were linear over the range of 1.11-27.63 μg/mL for Barbital, 1.39-34.84 μg/mL for Phenobarbital, 1.36-33.94 μg/mL for Amobarbital, 1.35-33.79 μg/mL for Pentobarbital, 1.42-35.59 μg/mL for Secobarbital and 1.45-36.20 μg/mL for Thiopental (r=0.982-1.000). The lower limits of detection obtained ranged from 0.05 to 0.33 μg/mL at a signal-to-noise ratio of 3, which are comparable with those of the HPLC method using an ODS column with UV detection[8] (Table 1). These values suggest that the proposed method can be applied to the blood monitoring of barbiturates, because the blood levels of most barbiturates after an oral ingestion of therapeutic doses are generally more than 1 μg/mL.[8]

Table 1

Precision Data and Detection Limits with the Proposed Method

Compound	Spiked (μg/mL)	Precision (R.S.D., %) Within-day	Day-to-day	Detection Limit (μg/mL)
Barbital	5.53	3.48	6.83	0.10
Phenobarbital	6.97	3.87	4.72	0.05
Amobarbital	6.97	4.82	4.68	0.12
Pentobarbital	6.76	4.60	4.99	0.05
Secobarbital	7.12	4.61	6.55	0.13
Thiopental	7.24	9.07	18.68	0.33

The precision of the proposed method was examined using plasma samples spiked with known concentrations of barbiturates (5.53-7.24 μg/mL). The within-day and day-to-day precision with five replicate determinations gave relative standard deviations (R.S.D.) of 3.48-9.07% and 4.72-18.68%, respectively (Table 1). A typical chromatogram of a plasma spiked with six commercially available barbiturates and I.S. is presented in Figure 5.

Resolution Behavior for Diastereomeric Derivatives

Since an NAIP column behaved like a reverse phase column with some π-π interaction as reported previously,[4] it was expected to separate diastereomeric compounds carrying an aromatic ring. Consequently, we examined a separation of these compounds. EP, NE and PA were selected as targets for the labelling with chiral reagents.

NEIC Derivatives

The separation properties of NEIC derivatives of PA, NE and EP on an NAIP packed column were examined using acetonitrile-water as a mobile phase. As shown in Figure 6, the capacity factor (k') and separation factor α) of NEIC derivatives of PA decreased with increasing acetonitrile contents in the mobile phase; it seemed to be a reverse phase-like separation. NE showed the similar tendency, but in the case of EP, diastereomeric derivatives could not be well separated by a peak tailing. This might be caused by a strong interaction between a catechol moiety of EP derivatives and the stationary phase under the conditions tested.
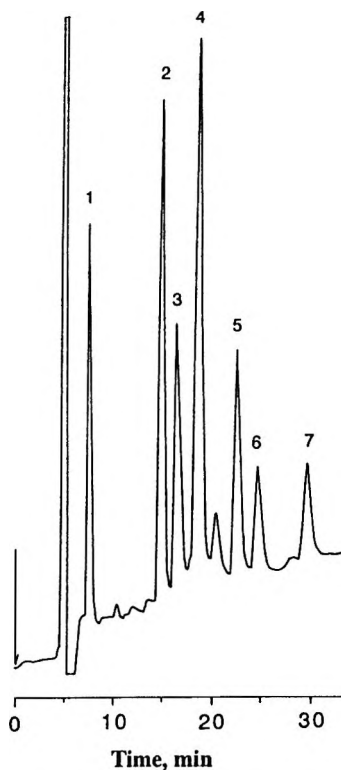
Figure 5. A typical chromatogram of plasma sample spiked with barbiturates by an NAIP column. Spiked sample (µg/mL): 1 = Barbital (5.53), 2 =Phenobarbital (6.97), 3 = Amobarbital (6.79), 4 = Pentobarbital (6.76), 5 = Secobarbital (7.12), 6 = 5-(2-cyclohexen-1-yl)-5-propenyl barbituric acid (7.41), 7 = Thiopental (7.24).

A comparison of diastereomeric separation data for NE and PA on NAIP and ODS columns are given in Table 2. The ratio of acetonitrile and water in the mobile phase was individually optimized for each derivative. The values for α and resolution *(Rs)* were calculated by the following equations:

$$\alpha = k'2 \: / \: k'1$$
$$Rs = 2 \: (t_{R2} - t_{R1}) \: / \: 1.70 \: (W1+W2)$$

where t_R = retention time and W = peak width.
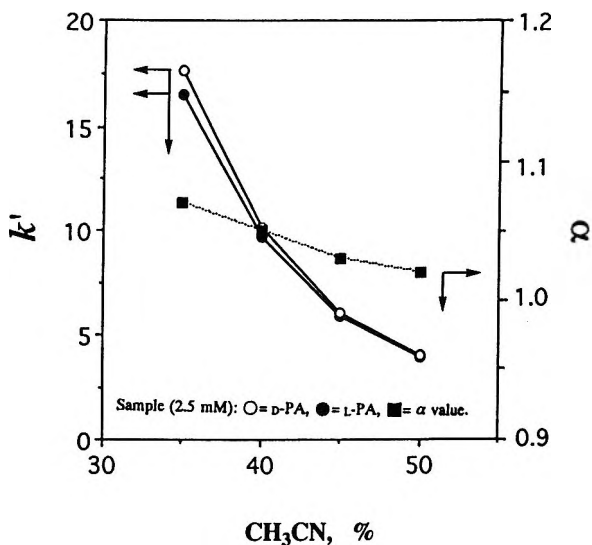
Figure 6. Effect of acetonitrile contents in the mobile phase on separation of NEIC derivatives of PA by an NAIP column.
Sample (2.5 mM): $\bigcirc$ = D-PA, $\bullet$ = L-PA, $\blacksquare$ = α value.

Table 2

**Comparison of Separation Properties of NAIP and ODS Column
for NEIC Diastereomers**

Compound	NE		PA	
Column	NAIP	ODS	NAIP	ODS
CH₃CN/Water*	30/70	33/67	35/65	40/60
First eluent	D	D	L	D
k′	17.99	22.55	16.51	20.30
α	1.05	1.06	1.07	1.05
Rs	1.14	0.94	1.59	1.06

* The ratio of acetonitrile and water in the mobile phase.

Table 3

**Comparison of Separation Properties of NAIP and ODS Column
for AITC Diastereomers**

Compound	NE		PA		EP	
Column	NAIP	ODS	NAIP	ODS	NAIP	ODS
CH$_3$CN/Buffer*	15/85	30/70	20/80	30/70	10/90	15/85
First eluent	D	D	L	L	D	D
k'	15.73	9.09	10.76	16.65	13.61	18.00
α	1.10	1.20	1.10	1.06	1.08	1.22
Rs	1.43	3.46	1.25	1.25	1.02	3.22

* The ratio of acetonitrile and 10 mM phosphate buffer (pH 3.0) in the mobile phase.

Table 4

**Comparison of Separation Properties of NAIP and ODS Column
for GITC Diastereomers**

Compound	NE		PA		EP	
Column	NAIP	ODS	NAIP	ODS	NAIP	ODS
CH$_3$CN/Buffer*	20/80	33/67	20/80	33/67	15/85	20/80
First Eluent	L	L	D	D	L	L
k'	10.10	18.68	12.08	18.46	17.20	17.98
α	1.05	1.19	1.10	1.07	1.09	1.22
Rs	0.74	3.85	1.38	1.39	1.40	3.46

* The ratio of acetonitrile and 10mM phosphate buffer (pH 3.0) in the mobile phase.

As shown in Table 2, the Rs values obtained from NE and PA derivatives on an NAIP column was found to be even or relatively better than those on an ODS column. The elution order for PA derivatives on an NAIP column was observed to be reversed on an ODS column.
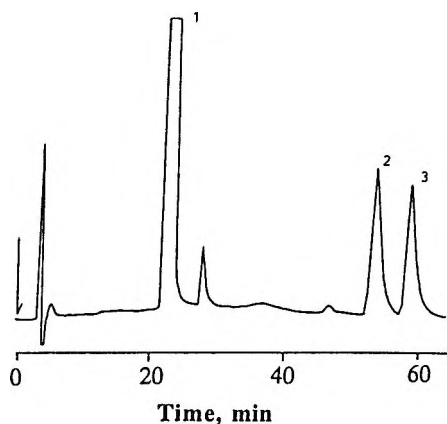
Figure 7. A typical chromatogram of NEIC derivatives of L- and D-PA by an NAIP column.
Sample (2.5 mM): 1 = Blank, 2 = L-PA, 3 = D-PA; mobile phase, CH_3CN-water (30:70, v/v).

AITC and GITC Derivatives

The separation data for AITC and GITC derivatives are given in Table 3 and 4, respectively. Acetonitrile-10 mM phosphate buffer (pH 3.0) system was used as a mobile phase. AITC and GITC derivatives of NE, PA and EP on an NAIP column behaved like those on a reverse phase column; the retention time for each derivative was shortened with an increase in acetonitrile contents in the mobile phase. AITC and GITC diastereomers were satisfactorily separated on both columns. However, the Rs values for NE and EP derivatives on an ODS column were better than those on an NAIP column for both AITC and GITC diastereomers.

As a preliminary study on the quantitation of the diastereomers, the linearity of the calibration curves obtained by an NAIP column was examined by using NEIC derivatives of L -and D-PA, which showed the best separation in the derivatives examined on this column (a typical chromatogram was shown in Figure 7). The linear relationships were obtained between the peak-heights and the concentrations of each derivative over the range of 3.14 μM to 0.25 mM (r=1.000 for both derivatives). The lower limits of detection were 0.83 μM for NEIC-L-PA and 1.07 μM for NEIC-D-PA at a signal-to-noise ratio of 3.

CONCLUSION

An NAIP column was found to be very useful for the separation of pyrimidine derivatives e.g., barbiturates as well as purine derivatives.[2,4] The sensitivity for barbiturates obtained by an NAIP column with UV detection was comparable with that by an ODS column. Thus, an NAIP column should be useful for the determination of barbiturates in human blood plasma.

In addition, it has become apparent that an NAIP column was also applicable to the separation of diastereomeric derivatives of NE, AP and EP like an ODS column. An NAIP column might be usable for the separation and determination of these compounds in pharmaceutical preparations and biological materials. It will be worthwhile to study further on the separation of other diastereomeric derivatives.

REFERENCES

1. S. Akiyama, K. Nakashima, K. Yamada, N. Kuroda, Biomed. Chromatogr., 7, 112-115 (1993).

2. S. Akiyama, K. Nakashima, K. Inoue, N. Kuroda, H. Nakazumi, Bunseki Kagaku, 42, 817-823 (1993).

3. S. Akiyama, K. Nakashima, K. Inoue, T. Mori, N. Kuroda, H. Nakazumi, Chemistry Express, 8, 565-568 (1993).

4. K. Nakashima, K. Inoue, K. Mayahara, N. Kuroda, Y. Hamachi, S. Akiyama, J. Chromatogr. A, 722, 107-113 (1996).

5. A. Turcant, A. Premel-Cabic, A. Cailleux, P. Allain, J. Chromatogr., 229, 222-226 (1982).

6. W. M. Chow, B. Caddy, J. Chromatogr., 354, 219-229 (1986).

7. Y. Benchekroun, B. Ribon, M. Desage, J. L. Brazier, J. Chromatogr., 420, 287-296 (1987).

8. R. Gill, A. A. T. Lopes, A. C. Moffat, J. Chromatogr., 226, 117-123 (1981).

9 . T. Y. Ryan, J. Liq. Chromatogr., 16, 315-329 (1993).

10. F. B. Ibrahim, J. Liq. Chromatogr., **16**, 2835-2851 (1993).

11. N. Nimura. Y. Kasahara, T. Kinoshita, J. Chromatogr., **213**, 327-330 (1981).

SHAPE SELECTIVITY OF POLYCYCLIC AROMATIC HYDROCARBONS AND FULLERENES WITH TRI-TERT-BUTYLPHENOXY BONDED SILICA PHASE IN MICROCOLUMN LIQUID CHROMATOGRAPHY

Kiyokatsu Jinno,* Chisa Okumura, Mitsuyo Harada,
Yoshihiro Saito

School of Materials Science
Toyohashi University of Technology
Toyohashi 441, Japan

Mitsuyoshi Okamoto

Gifu Prefectural Gero Onsen Hospital
Gero 509-22, Japan

ABSTRACT

Retention behaviors of various planar and non-planar polycyclic aromatic hydrocarbons (PAHs), and all carbon compounds so-called fullerenes with 2,4,6-(tri-tert-butylphenoxy)dimethyl (TBP) silica phase and benzyldimethyl (Benzyl) silica phase have been investigated using microcolumn liquid chromatography system. The results clearly indicate that these phases possess a "non-planarity" recognition capability of PAHs. Non-planar solutes were retained longer than planar ones with these phases under certain separation conditions, although the opposite trend where the planar solutes are retained longer than the non-planar ones was observed with typical octadecylsilica (ODS) phases. This unique behavior can be

2883

explained by the specific molecular-molecular interaction between non-planar solutes and the stationary phase moiety having a cavity like structure made by the three tert-butyls and phenyl ring of the moiety. The separation of C_{60} and C_{70} were also examined and the difference of the structural uniqueness between TBP phase and Benzyl phase showed interesting results for such bulky fullerenes separation.

INTRODUCTION

The analysis of PAHs based on molecular shape and planarity is very important because the molecular shape and planarity are directly related to its physicochemical properties and biological activities.[1,2] Therefore, it is important to separate PAHs based on the small difference of their molecular shapes and to accomplish this target the separation mechanism should be studied in detail.

As the most powerful method of separating PAHs reverse phase liquid chromatography (RPLC) has been known. The chemically bonded octadecyl silica (ODS) phases have been used as the stationary phase for the separation of PAHs. Generally, ODS phases can be devided into two types; i.e. polymeric and monomeric phases. Polymeric ODS phases have a higher molecular planarity recognition capability than monomeric ones. Non-planar molecules are eluted faster than planar ones with polymeric phases because these phases have a "slot-like" structure on the silica surface as proposed by Wise et al.[3-9] The development of new stationary phases which can accomplish more selective and unique separation has been necessary, because of difficulty to completely separate PAHs by the small difference of their molecular shapes and planarities using polymeric and monomeric ODS phases.

In our previous studies,[10,11] multidentate phenyl bonded phases were synthesized and evaluated for their molecular shape recognition power for various PAHs molecules. The planar solutes were eluted faster than non-planar ones with one of those, 1,3,5-tris(dimethyl phenyl) (TP) phase. The TP phase has a very unique structure of which moiety covers the silica surface horizontally, whereas common phenyl and ODS phases are attached vertically to silica surface by siloxane bonding. These results clearly have indicated that the retention behaviors of PAHs with these newly synthesized chemically bonded phases are very different from each other based on the steric structures of the bonded phase ligand on silica surfaces.[10,11]

Fullerenes are unique compounds made by all carbons in their structures and the purification of such compounds from carbon soot is the important task for separation chemistry because only LC can realize this goal. A number of works have been reported to use different types of stationary phases in LC to get better selectivity for fullerenes especially the most popular C_{60} and C_{70}.[12-18] The authors have also been investigating to find the most suitable stationary phase for such target and the latest conclusion we got from our basic investigations are that the phenyl group in the stationary phase structure is the first key and the shape of the bonded phase moiety is the second key to enhance the separation selectivity for C_{60} and C_{70}.

As an extension of these studies, we synthesized two new chemical bonded stationary phases which are a 2,4,6-(tri-tert-butylphenoxy)dimethyl (TBP) phase and benzyldimethyl (Benzyl) phase (Figure 1). The TBP phase has a specific structure formed by the phenyl ring and three bulky tert-butyl groups. The benzyl phase has a framework similar to the TBP phase, but no tert-butyl groups.

In this study, we examined the basic retention mechanism for PAHs and fullerenes with TBP and Benzyl phases and the influence of three bulky tert-butyl groups to the selectivity for PAHs and fullerenes.

EXPERIMENTAL

Reagent

Hexamethyldisilazane (HMDS), 2,4,6-(tri-tert-butylphenoxy)chlorosilane and benzyldimethylchlorosilane were purchased from Petrarch Systems (Bristol, PA, USA). Base silicas were obtained from Nomura Chemicals (Seto, Japan). The particle diameter is ca. 5 μm, the pore diameter is 150 Å and the specific surface area is ca. 280 m^2/g. Develosil ODS-5 packing (Nomura Chemicals) as a monomeric ODS phase was used as the reference. Other reagents and organic solvents were of analytical-reagent grade.

Bonded Phase Synthesis

As described previously,[19-21] 7 g of dried silica were added to 70 mL of 3.4 % solution of 2,4,6-(tri-tert-butylphenoxy)chlorosilane or benzyldimethylchlorosilane in dry toluene containing 3 mL triethylamine.

(a)
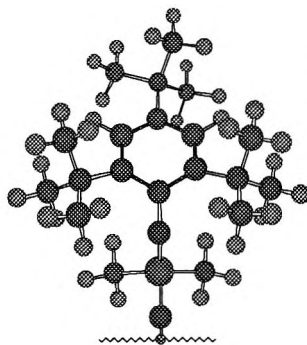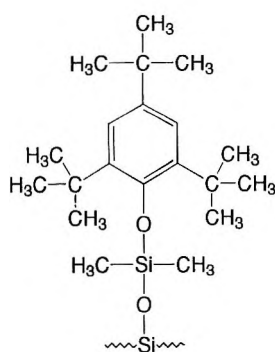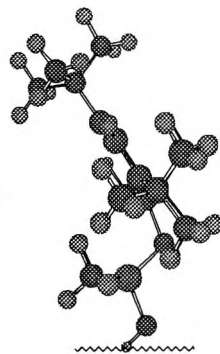
front view   side view

(b)
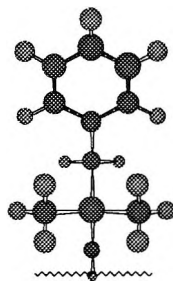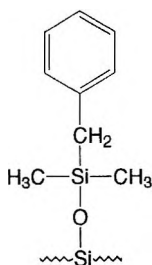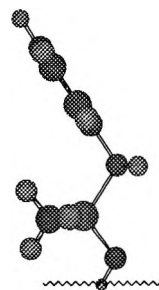
front view   side view

Figure 1. Two and three dimensional chemical structures of bonded phases investigated. (a) TBP phase and (b) Benzyl phase. The characteristics of these bonded phases are summarized in Table 1.

The silica suspension was refluxed for 5 h, filtered with a glass filter (1 μm), washed several times with toluene, chloroform, methanol, and acetone and then dried in vacuo at 70 °C for 2 days. Furthermore, in accordance with the Buszewski method.[22] a TBP phase or Benzyl phase was added to 70 mL of toluene and 4 mL of HMDS for end capping. The basic characteristics of these

Table 1

**Basic Characteristics of New Chemically Bonded Phases and
Commercially Available ODS Phase as the Reference**

Stationary Phase	Pore Size (Å)	Carbon Content (%)	Surface Coverage (μmol/m^2)
TBP	150	3.33	0.49
Benzyl	150	7.04	2.58
TP	120	7.46	2.27
Develosil ODS-5	100	20	3.31

phases are given in Table 1, and one of the commercially available ODS phase, Develosil ODS-5 is also listed in Table 1. The carbon contents of the treated silicas were determined by elemental analysis using an MT-3 CHN elemental analyzer (Yanagimoto, Kyoto, Japan). The specific surface areas and pore diameters of the silicas were determined with an MOD-220 porosimeter (Carlo Erba, Milan, Italy), SA-1000 surface area pore-volume analyzer (Shibata, Tokyo, Japan), and FT-IR 1640 (Perkin-Elmer, Yokohama, Japan) and then the surface coverages N (μmol/m^2) were calculated.

Chromatographic Measurements

The bonded phases were packed using a slurry method into a fused-silica capillary (Tokyo Kasei, Tokyo, Japan) of 0.53 mm i.d. x 150 mm length.

The microcolumn LC system consisted of a microfeeder MF-2 pump (Azuma Electric, Tokyo, Japan), a Rheodyne 7520 injector (Cotati, CA, USA) with a 0.2 μL injection volume and a Shodex M-315 UV detector (Showa Denko, Tokyo, Japan) set at 254, 275 or 300 nm.

The mobile phases were prepared from guaranteed reagent grade methanol (Kishida Chemical, Osaka, Japan) and deionized water purified by using Milli-Q water purification system (Millipore, Bedford, MA, USA). The typical flow-rate was 2 μL/min. The chromatographic measurements were done at least three times. For the column dead-volume measurements, Uracil was used.
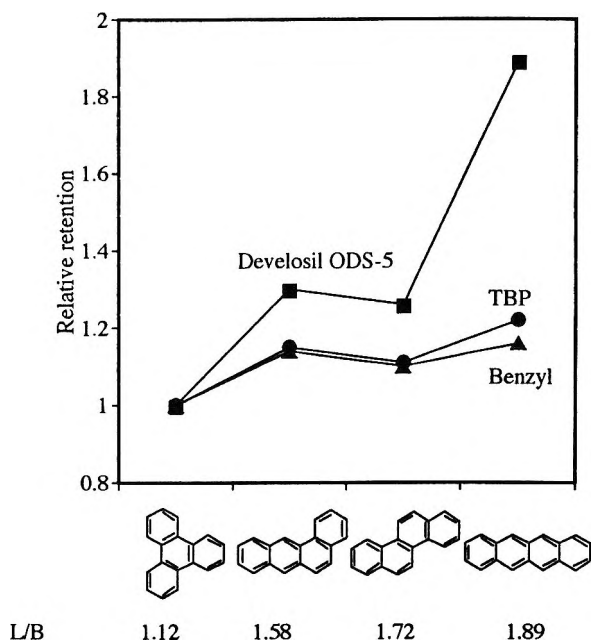
Figure 2. Relative retention plots of three PAHs to triphenylene with various phases.

Sample Solutes

PAHs used for evaluation in this study were commercially available (Tokyo Kasei, Tokyo, Japan) except phenanthro[3,4-c]phenanthrene (PhPh) which were obtained from Dr. W. Schmidt (Greifenberg am Ammersee, Germany) via. Dr. J.C.Fetzer (Chevron Research and Technology, Richmond, CA, USA) and Aldrich Chemical Co., Milwaukee, WI. Fullerenes of C_{60} and C_{70} were isolated from the carbon soot produced by using Ar-discharge in Toyohashi Science Core, Toyohashi, Japan and the mixture of C_{60} and C_{70} were obtained by toluene extraction from the soot.

Molecular Modeling

Molecular modeling was carried out using Chem 3D Plus software (Cambridge Scientific Computing Inc., MA, USA).

Table 2

Retention Factors of Various PAHs with Three Phases

F	Sample	Retention Factor(k')		
		TBP	Benzyl	Develosil ODS-5
3	benzene	0.12	0.20	0.77
5	naphthalene	0.17	0.32	1.64
6.5	fluorene	0.22	0.53	3.34
7	diphenylmethane	0.24	0.50	2.43
7	anthracene	0.23	0.58	4.25
7	phenanthrene	0.21	0.55	3.74
7	cis-stilbene	0.26	0.62	3.52
7	trans-stilbene	0.26	0.64	3.35
8	pyrene	0.25	0.68	5.48
8.5	benzo[ghi]fluoranthene	0.30	0.85	10.2
9	benzo[c]phenanthrene	0.31	0.92	9.49
9	triphenylene	0.27	0.80	6.99
9	o-terphenyl	0.33	0.88	4.50
9	m-terphenyl	0.33	0.99	6.82
9	p-terphenyl	0.36	1.02	8.10
9	benzo[a]anthracene	0.31	0.87	9.10
9	chrysene	0.30	0.88	9.78
9	naphthacene	0.33	0.93	13.2
10	bnezo[a]pyrene	0.35	1.11	17.2
10	benzo[e]pyrene	0.33	1.04	12.9
12	coronene	0.53	1.58	46.2
13	PhPh	0.40	1.53	12.6

Mobile phase; methanol/water = 80/20.

RESULTS AND DISCUSSION

Molecular Linearity Recognition for PAHs

To evaluate the chromatographic characteristics of the synthesized materials, the retention time of various PAHs samples were measured. The retention factors (k') were summarized in Table 2. The mobile phase was methanol/water = (80/20) for all stationary phases evaluation. In general, the
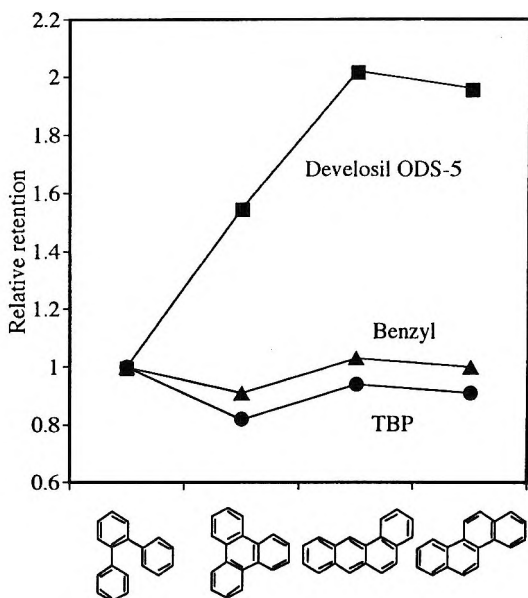
Figure 3. Relative retention plots of three PAHs to o-terphenyl with various phases.

retention values of PAHs in RPLC have a high correlation with the F number proposed by Schabron et al.,[23] where F is defined as the number of double bonds plus the number of primary or secondary carbons minus 0.5 times the number of non-aromatic rings.

As shown in Table 2, the elution orders of some planar and non-planar PAHs pairs with these synthesized bonded phases were different from that of ordinary ODS phases.[5-9] Figure 2 shows the plots of relative retention of benz[a]anthracene, chrysene and naphthacene compared to triphenylene. These PAHs have the same F number (F=9), but they have different L/B ratio.[24,25] L/B ratio is one of the molecular shape parameters which indicates molecular linearity of PAHs molecules. Therefore, more linear shape molecule has a larger L/B ratio.

Generally, it is known that in the case of isomeric PAHs which have the same F value the LC retention increases with increasing L/B ratio. The retention of linear molecule on these synthesized phases increases slightly
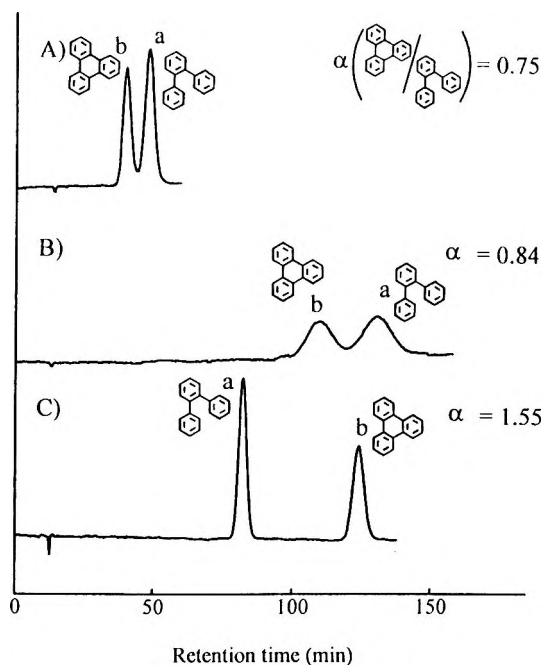
Figure 4. Typical chromatograms for the separation of o-terphenyl (a) and triphenylene (b). Mobile phase composition are as follows: (A) TBP phase, methanol/water=60/40; (B) Benzyl phase, methanol/water=60/40; and (C) ODS phase, methanol/water=80/20.

compared to that on the ODS phase. Therefore, it is found that these synthesized phases have a smaller linear molecular recognition power than the monomeric ODS.

Molecular Planarity Recognition for PAHs

Figure 3 shows the plots of relative retention of triphenylene, benz[a]anthracene and chrysene compared to o-terphenyl, where o-terphenyl is a non-planar molecule and others are planar molecules. The non-planar molecule was retained longer than planar ones with these synthesized phases although the opposite trend was observed with the ODS phase.

From these results, it was found that TBP and Benzyl phases have a non-planarity recognition capability. The chromatograms for the separation of triphenylene and o-terphenyl are shown in Figure 4. The mobile phases are

Table 3

Retention Factors (k') forTriphenylene and o-Terphenyl and the Separation Factors (α) with Three Stationary Phases Using Different Mobile Phase Compositions

Stationary Phase	k'						$\alpha = k'_{tri}/k'_{o-ter}$		
	Triphenylene			o-Terphenyl					
	80/20	70/30	60/40	80/20	70/30	60/40	80/20	70/30	60/40
TP	0.92	3.36	14.8	1.08	4.55	22.9	0.85	0.74	0.65
TBP	0.27	0.60	1.78	0.33	0.80	2.38	0.82	0.78	0.75
Benzyl	0.80	2.23	7.11	0.88	2.56	8.42	0.91	0.87	0.84

Mobile phase: methanol/water.

methanol/water=(60/40) for TBP (A) and Benzyl (B), and methanol/water=(80/20) for Develosil ODS phase (C). These separation factors are 0.75, 0.84 and 1.55 with TBP, Benzyl and Develosil ODS phase, respectively.

The experimental data obtained with TBP, Benzyl and TP phase are summarized in Table 3, where the retention factors of triphenylene and o-terphenyl and the separation factors with three different compositions of methanol/water mobile phase are shown. The elution order of triphenylene and o-terphenyl with TBP and Benzyl phase is the same as with TP phase. The reason for this trend with these phases can be explained by the similarity of these chemical structures on silica support.

Figure 5 shows three dimensional structures of PAHs pairs which have similar molecular size and different planarity, e.g., a pair of o-terphenyl and triphenylene. These separation factors are summarized in Table 4. As shown in Table 4, for these planar and non-planar PAHs pairs except the pair of coronene and PhPh, the two phases provided different elution order from the ODS phase, that means, that they provided different selectivity from the ODS phase, i.e., non-planar ones retained longer than planar ones. Due to the large molecular size of coronene and PhPh toward the phenyl-ring of TBP and Benzyl phase and to the relatively smaller distortion of PhPh molecule than other non-planar PAHs such as o-terphenyl, the pair of coronene and PhPh showed different retention behavior from other pairs with two new phases.
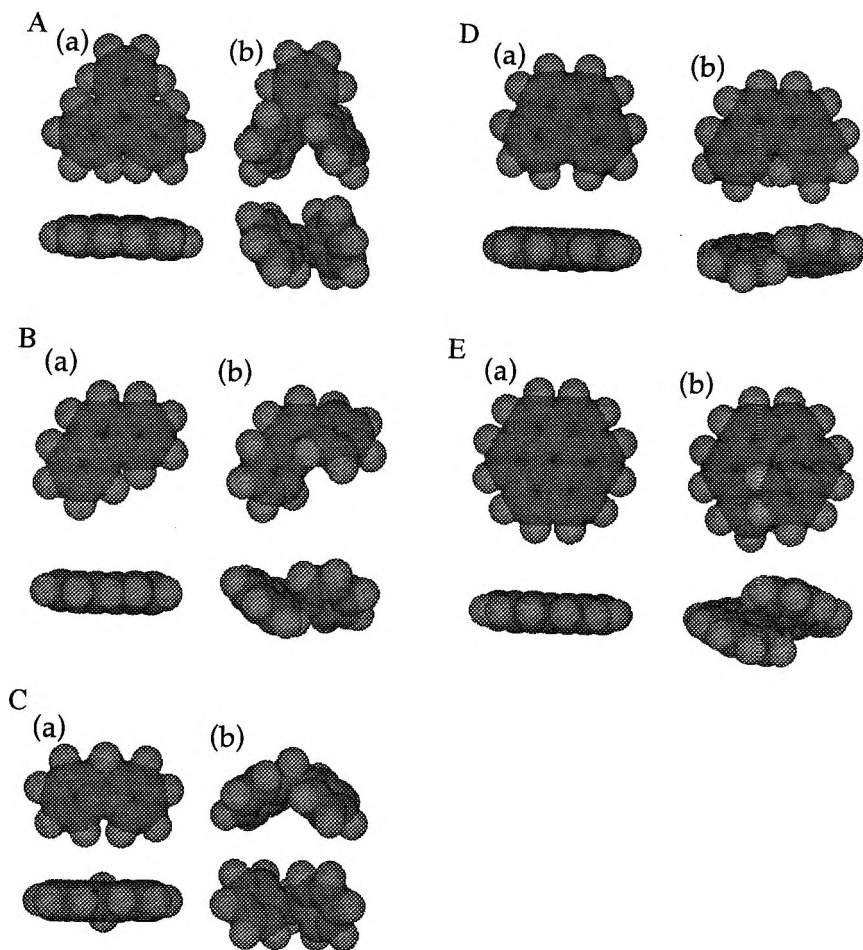
Figure 5. Three dimensional structures of planar and non-planar PAHs.
A: (a) triphenylene, (b) o-terphenyl; B: (a) phenanthrene, (b) cis-stilbene; C: (a) fluorene,   (b)   diphenylmethane;   D: (a)   benzo[c]phenanthrene,   (b) benzo[ghi]fluoranthene; and E: (a) coronene, (b) PhPh.

From the data obtained above and these PAHs structures, it can be concluded that TBP and Benzyl phases have the   non-planarity recognition capability for only small size PAHs.

Table 4

Separation Factors (α) for Planar and Non-planar Solute Pairs

Separation Factor α (k' Planar / k' Non-planar)
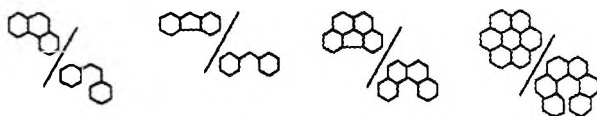
Stationary Phase				
TBP	0.71	0.89	0.87	1.33*
Benzyl	0.73	0.91	0.85	1.03*
Develosil ODS-5	1.06	1.37*	1.08*	3.67*

mobile phase: methanol/water = 60/40.
*mobile phase: methanol/water = 80/20.

Figure 6 shows the molecular-molecular interaction model between two solutes and TBP phase. Figure 6 (a) shows these three bulky tert-butyl groups disturb the interaction between TBP phase and planer solute such as triphenylene, because these tert-butyl groups covered the phenyl ring in the cavity-like structure and then the π-π interaction between planar PAHs and the phenyl ring in TBP moiety is prevented. However, as shown in Figure 6 (b), TBP phase having three bulky tert-butyl groups can produce more effective interaction between non-planar molecules such as o-terphenyl and the phenyl group than planar ones such as triphenylene. As the result, TBP phase retained non-planar solutes longer than planar ones.

Benzyl phase which has no tert-groups, can retain the solutes by π-π interaction without the interference caused from tert-butyl groups in TBP phase. For small size PAHs Benzyl phase has also a non-planarity recognition capability.

The phase retains the solutes by π-π interaction between the solute molecule and the stationary phase without the solute molecular planarity recognition. However if PAHs size is becoming larger, the moiety size is not enough to catch the solute molecules and therefore the non-planarity recognition power is decreased as in the case of coronene and PhPh.

(a)

(b)
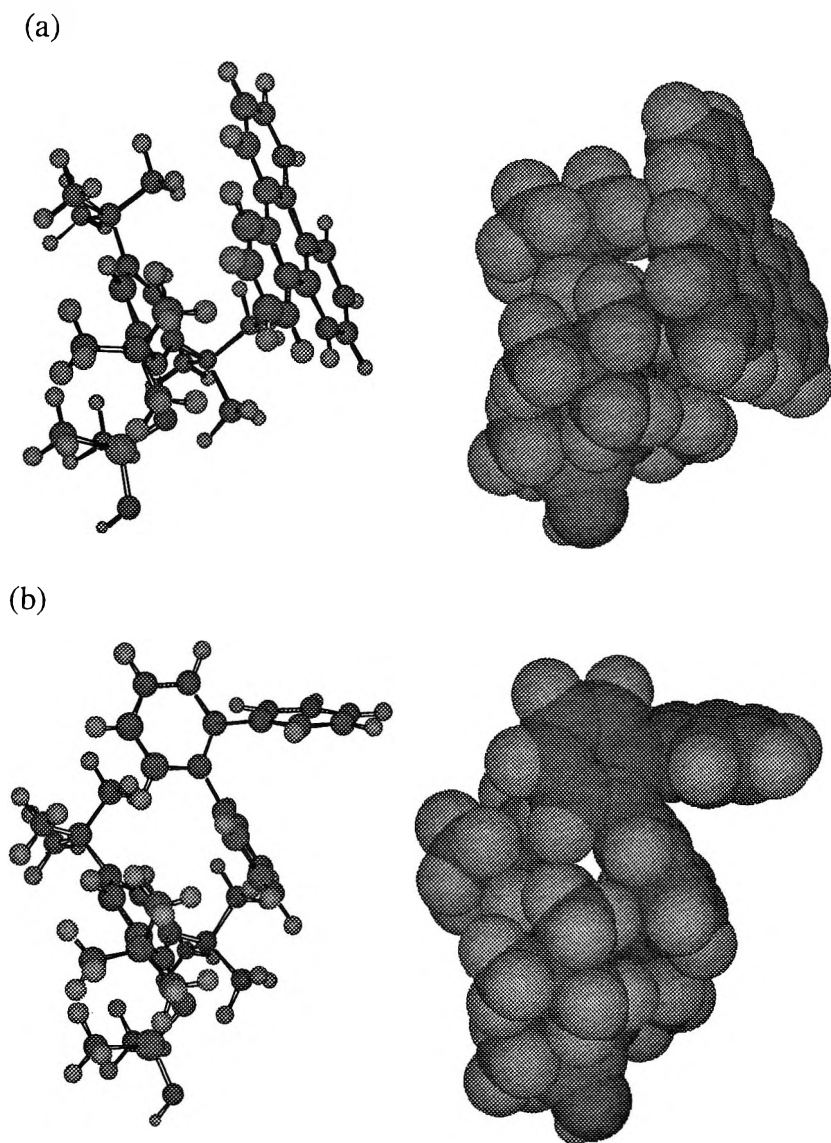
Figure 6. Three dimensional models of the interaction between solutes and TBP phase.
(a) triphenylene with TBP phase and (b) o-terphenyl with TBP phase.

Table 5

Retention Factors (k') for C_{60} and C_{70} and the Separation Factors (α) with three Stationary Phases

| | Retention Factor (k') | | Separation Factor (α) |
	C_{60}	C_{70}	$k'C_{70}/k'C_{60}$
TBP	0.37	0.69	1.86
Benzyl	0.90	1.37	1.50
Develosil ODS-5	47.8	170	3.55

Mobile phase: acetonitrile/toluene = 70/30.

Selectivity for C_{60} and C_{70}

In addition, we also examined the separation of fullerenes with these stationary phases. The retention factors (k') for C_{60} and C_{70} and these separation factors (a) with TBP and Benzyl phases are shown in Table 5.

As shown in Table 5, it seems that these stationary phases are less useful than ODS phase for the separation of fullerenes using acetonitrile/toluene mobile phase. The fullerenes provided small retention and separation factor on two new stationary phases, because of low surface coverage and selectivity comparing to ODS phase. The reason of low selectivity is that molecular sizes of fullerenes are too large for these stationary phases to be recognized the shape difference between C_{60} and C_{70}.

CONCLUSION

In this study, it is found that TBP phase has a non-planarity recognition for relatively small size PAHs. The planar-nonplanar selectivity on Benzyl phase is not so pronounced as obtained with TBP phase.

It is also apparent that tert-butyl groups of TBP phase contribute to the non-planarity recognition capability toward small PAH molecules. In view of the separation science, the results obtained are very useful to reveal the sight of the interactions between solutes and surface structures of the stationary phase in LC.

ACKNOWLEDGEMENTS

REFERENCES

1. I. A. Smith, G. D. Berger, P. G.Seybold, M. P.Serve, Cancer Res., **38**, 2968-2977 (1978).

2. G. H.Loew, J. Phillips, J. Wong, L. Hieldmeland, G. Pack, Cancer Biochem. Biophys., **2**, 113-122 (1978).

3. L. C. Sander, S. A. Wise, Anal. Chem., **56**, 504-510 (1984).

4. L. C.Sander, S. A. Wise, Anal. Chem., **59**, 2309-2313 (1987).

5. K. Jinno, T. Ibuki, N. Tanaka, M. Okamoto, J. C. Fetzer, W. R. Biggs, P. R. Griffiths, J. M. Olinger, J. Chromatogr., **461**, 209-(1989).

6. K. Jinno, T. Nagoshi, N. Tanaka, M. Okamoto, J. C. Fetzer, W. R. Biggs, J. Chromatogr., **392**, 75-82 (1987).

7. K. Jinno, S. Shimura, N. Tanaka, K. Kimata. J. C. Fetzer, W. R. Biggs, Chromatographia, **27**, 285-291 (1989).

8. L. C.Sander, S. A. Wise, LC.GC, **8**, 378-390 (1990).

9. L. C.Sander, S. A. Wise, HRC & CC, **8**, 248-255 (1985).

10. K. Jinno, K. Yamamoto, H. Nagashima, T. Ueda, K.Itoh, J. Chromatogr., **517**, 193-207 (1990).

11. K. Jinno, K. Yamamoto, T. Kuwamoto, H. Nagashima, T. Ueda, S. Tajima, E. Kimura, K.Itoh, J. C. Fetzer, W. R. Biggs, J. Chromatogr., **34**, 381-385 (1992).

12. K. Jinno, K. Yamamoto, T. Ueda, H. Nagashima and K. Itoh, J. Chromatogr., **594**, 105-109 (1992).

13. K. Jinno, K. Nakagawa, Y. Saito, H. Ohta, H. Nagashima, K. Itoh, J. Archer, Y. Chen, J. Chromatogr., **691**, 91-99 (1995).

14. Y. Saito, H. Ohta, H. Nagashima, K. Itoh, K. Jinno, M. Okamoto, Y. Chen, G. Luehr, J. Archer, J. Liq. Chromatogr., **18 (10)**, 1897-1908 (1995).

15. K. Jinno, Y. Saito, H. Nagashima, K. Itoh, Y. Chen, G. Luehr, J. Archer, J. C.Fetzer, W. R. Biggs, J. Microcol. Sep., **5**, 135-140 (1993).

16. Y. Saito, H. Ohta, H. Nagashima, K. Itoh, K. Jinno, J. J. Pesek, J. Microcol. Sep., **7**, 41-49 (1995).

17. K. Jinno, T. Uemura, H. Nagashima, K. Itoh, J. High Resolt. Chromatogr., **15**, 627-628 (1992).

18. H. Ohta, Y. Saito, K. Jinno, H. Nagashima, K. Itoh, Chromatographia, **39**, 453-459 (1994).

19. M. Okamoto, K. Nobuhara, K. Jinno, J. Chromatogr., **556**, 407-414 (1991).

20. M. Okamoto, F. Yamada, J. Chromatogr., **283**, 61-76 (1984).

21. M. Okamoto, K. Nobuhara, M. Masatani, K. Jinno, Chromatographia., **33**,203-207 (1992) .

22. B. Buszewski, Chromatographia, **28**, 574-578 (1989).

23. J. F. Schabron, R. J.Hurtubise, Anal.Chem., **49**, 2253-2260 (1977).

24. L. C.Sander, S. A. Wise, "Investigations of Selectivity in RPLC of Polycyclic Aromatic Hydrocarbons," in **Advances in Chromatography vol. 25**, J. C Giddings, E. Grushka, J. Cazes, P. R. Brown, eds., Marcel Dekker, Inc., New York, 1986, pp.139-218.

25. R. A. Hites, W. J. Simonsick Jr., **Physical Science Data 29, Calculated Molecular Properties of Polycyclic Aromatic Hydrocarbons**, Elsevier Science Publishers B. V., Amsterdam, 1987.

IMMOBILIZED PORPHYRINS AS VERSATILE STATIONARY PHASES IN LIQUID CHROMATOGRAPHY

J. Xiao, C. E. Kibbey,[2] D. E. Coutant,
G. B. Martin,[3] M. E. Meyerhoff[1]

[1]Department of Chemistry
University of Michigan
Ann Arbor, MI 41809

[2]Pharmaceutical Dept.
Warner Lambert-Parke Davis
Ann Arbor, MI

[3]Selective Technologies Inc.
Ann Arbor, MI

ABSTRACT

The preparation, characterization and potential liquid chromatographic applications of various porphyrin-silica stationary phases are reviewed. These new phases are synthesized by covalently linking unsymmetrical tetraphenylporphyrin (TPP) derivatives (monocarboxyl- or monohydroxyl-), as well as native protoporphyrin IX (ProP) to appropriately derivatized silica support matrices. The porphyrin-silicas may be further modified by metallation with a wide range of central metal ions (e.g., Cu^{2+}, Zn^{2+}, Ni^{2+}, Fe^{+3}, In^{3+}, Sn^{4+}, etc.) by refluxing in the presence of metal ion salts. Columns packed with either metallated or unmetallated materials exhibit exceptionally high shape selectivity in the separation of polycyclic aromatic hydrocarbons (PAHs) and fullerenes owing to

strong π-π interactions between such solutes and the immobilized porphyrin structures. Columns packed with metallated porphyrins, particularly In(III) and Sn(IV), may also be used for separation of anions, including aromatic carboxylates and sulfonates, via selective ligation reactions with the metal centers. Similar coordination chemistry can be exploited to achieve selective peptide separations through a combination of specific metal ion affinity reactions of certain amino acids (histidine, tryptophan) with given metal ion centers (i.e., Fe^{+3}, Cu^{+2}) and concomitant π-π interactions of aromatic amino acids with the immobilized conjugated macrocycle. In the area of peptide/protein separations, the metalloporphyrin-silicas may offer an attractive alternative to current immobilized metal ion affinity phases (IMAC), because of their exceptionally strong metal ion binding constants. This allows the columns to provide reproducible analytical and preparative separations without potential for metal ion contamination of the purified materials.

INTRODUCTION

The development of new stationary phases that offer unique selectivities above and beyond those afforded by conventional ODS, phenyl, ion-exchange and size-exclusion columns, represents a challenging yet very important avenue in liquid chromatography research. For example, significant effort has been placed on creating phases that can be used to preferentially retain planar polycyclic aromatic hydrocarbons (PAHs) over their less toxic non-planar homologues[1-6] so that greater resolution and hence better quantitation of these species can be achieved. In the area of anion-exchange chromatography, researchers have explored the use of different quaternary ammonium structures, varying lengths of spacer groups, and the principles of ligand exchange as a means of developing columns that offer greater selectivity.[7-11] The use of immobilized metal ions as stationary phases has also been examined with respect to selective separation of peptides and proteins, where the content of certain amino acids within the peptide/protein structure that interact strongly with the immobilized metal ion (e.g., histidine) dictates retention behavior. More recently, a number of researchers have synthesized novel stationary phases (e.g., pyrenyl(ethyl)-silica, tri(dinitrophenyl)-silica, etc.) for the specific purpose of purifying closely related fullerene structures, a rather difficult task, especially when attempting to purify large quantities of these species using mobile phases in which the fullerenes are most soluble.[12-30]

In the examples cited above, columns with radically different immobilized chemical structures have been required to achieve some level of selectivity (for the solutes mentioned) above and beyond that provided by conventional "off the shelf" stationary phases. Hence, packings designed for fullerene separations (e.g., tri(dinitrophenyl)-silica) are not likely to be useful for anion chromatography. Similarly, it is improbable that metal ion affinity columns previously reported for peptide and protein separations (metal ions tethered on immobilized iminodiacetate ligands)[31,32] could also be employed for PAH or fullerene separations. An interesting question then is whether specific chemical structures exist that when immobilized on LC supports (notably silica) could offer practical selectivities for a wide range of solute types simply by varying the operating mobile phase conditions.

One class of chemical structures that would appear to offer many possible modes of potential solute interaction for separation science is the porphyrins. Indeed, immobilized metalloporphyrins have been used previously in the development of gas and anion selective sensors, where selective coordination of the target gas/ion with a given central metal ion can result in changes in membrane potentials or optical properties of polymer films containing the immobilized porphyrin species.[33-35] The application of immobilized metalloporphyrins for batch separations has also been explored. Kokufuta *et al.* demonstrated that polystyrene particles possessing immobilized molybdenum porphyrins can be used for selective extraction of phosphate ions.[36] However, until recently, there have been no reports describing the use of immobilized porphyrins as stationary phases in HPLC systems. Herein, we summarize recently published,[37-42] as well as unpublished results regarding the preparation, characterization, and performance of various porphyrin and metalloporphyrin-silica phases. It will be shown that such phases offer unique versatility and selectivity for a wide range of liquid chromatography separations, ranging from highly shape selective separations of PAHs to reproducible separations of peptides via metal-affinity and π-π interactions.

EXPERIMENTAL

Equipment

The primary HPLC system used in these studies was composed of a Spectra Physics (San Jose, CA) SP 8700 solvent delivery system, a Spectra Physics SP 4290 computing integrator, a Kratos (Ramsey, NJ) Spectroflow 773 variable-wavelength UV-Vis detector, and a Rheodyne (Cotati, CA) Model 7010 sample valve equipped with a 20 μL sample loop. Columns were
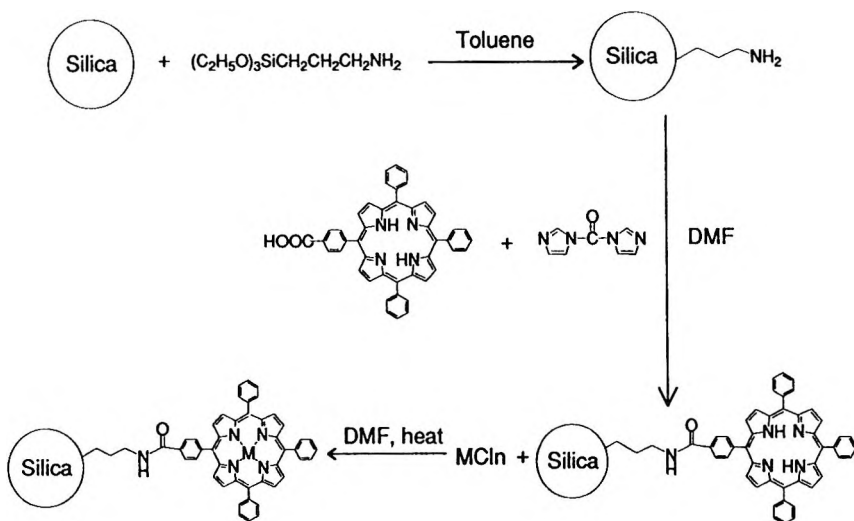
Figure 1. Synthetic scheme used to prepare metallated pCPTPP-silica.
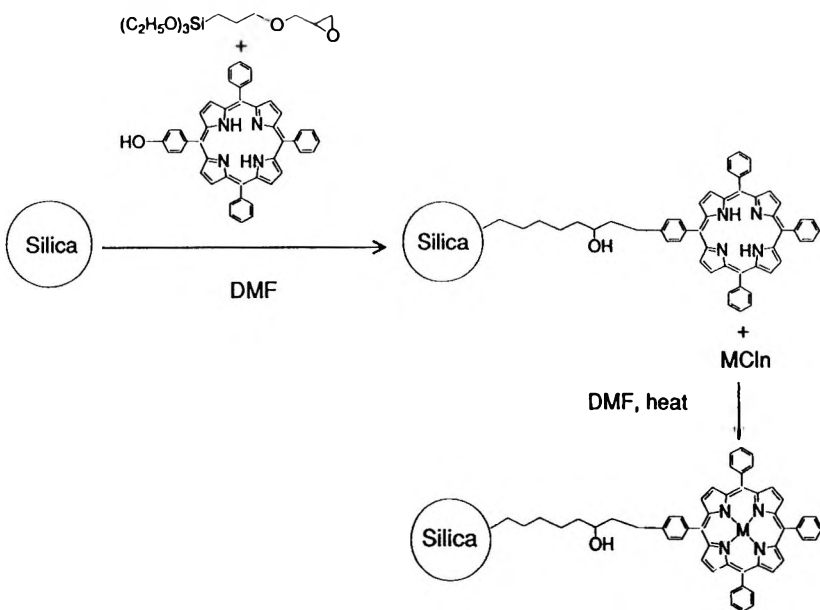
Figure 2. Synthetic scheme used to prepare metallated pHPTPP-silica.

thermostated using a Fisher Scientific water jacket (Pittsburgh, PA) connected to a Fisher Scientific Model 80 Isotemp constant temperature circulator. A second HPLC system consisting of a LKB Bromma (Piscataway, NJ) Model 2150 pump, a Hewlett Packard (Avondale, PA) 3396A computing integrator, a Rheodyne model 7125 injection valve with a 20 μL loop, and either a LKB Bromma Model 2238 Uvicord SII detector or an Anspec (Ann Arbor, MI) SM95 UV-Vis detector was also used for a portion of these studies.

Preparation of the Porphyrin-Silica Stationary Phases

Tetraphenylporphyrin (TPP) and protoporphyrin (ProP) structures were immobilized onto silica particles (10 μm) using the reaction schemes illustrated in Figures 1-3. The [5-(p-carboxyphenyl)-10,15,20-triphenyl] porphyrin (pCPTPP) based stationary phase (Figure 1) was prepared by first synthesizing the unsymmetrical monocarboxyltetraphenylporphyrin via a mixed aldehyde/pyrrole condensation reaction and then immobilizing this species covalently on aminopropyl silica gel using a carbonyldiimidazole reaction to yield a relatively stable amide linkage.[38] Briefly, the method consists of preparing amine derivatized silica gel by refluxing the silica in an aminopropyltriethoxysilane/toluene solution for 4h. The pCPTPP is then attached by activating the carboxylic acid with 1,1'-carbonyldiimidazole in dimethylformamide (DMF). The washed and dried aminated silica gel is then added with coupling being completed after 24 h. Residual amine sites on the silica gel are then acetylated by refluxing in acetic anhydride for 1.5 h.

A second route to preparation of a tetraphenylporphyrin-silica phase, and one still under study, is based on first reacting an unsymmetrical monohydroxy-TPP species (5-(p-hydroxyphenyl)-10,15,20-triphenyl] porphyrin (pHPTPP) with glycidoxypropyltrimethoxysilane (GPTS) to form a covalent ether linkage, followed by reaction of the trimethoxysilane terminal group with the surface silanols of the silica gel (Figure 2). Approximately 1.80 g of pHPTPP was added to 50 mL of anhydrous N,N-dimethylformamide (DMF). The phenol group of the porphyrin was reacted with 500 μL of GPTS in the presence of 50 μL of the catalyst[43] tri-n-butylamine by refluxing for 4 h. Porphyrin immobilization was carried out by the addition of 2 g of 10 μm, 100Å silica (Machery-Nagel, Düren, Germany) and refluxing for 4 h. followed by shaking for 16 h. The pHPTPP-silica solution was then filtered through a 10-15 ASTM sintered glass funnel and washed with subsequent aliquots of 50 mL dry chloroform, acetone, 10% acetic acid in acetone (v/v) and 50 additional mL of acetone.
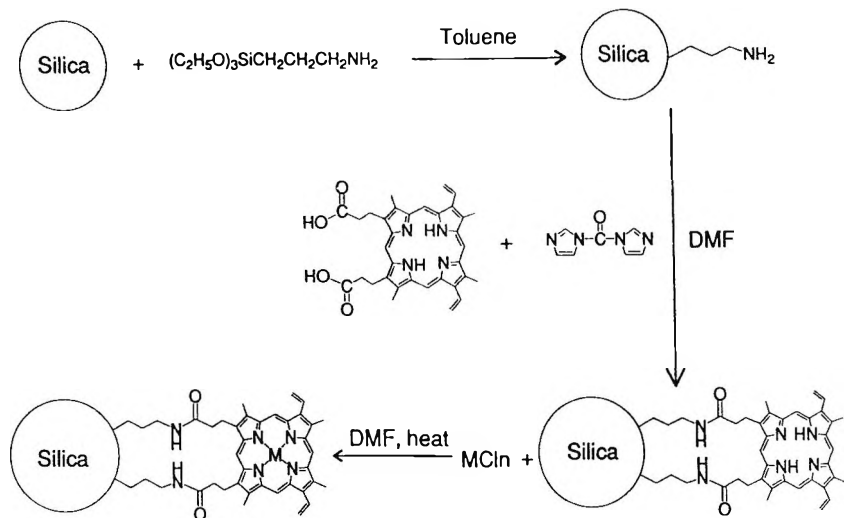
Figure 3.   Synthetic scheme used to prepare MProP-silica.

The ProP-silica phase was prepared by simply activating the native carboxyl groups of protoporphyrin IX with carbonyldiimidazole, and then allowing the activated species to react with aminopropyl silica to form amide bonds at either one or both original carboxyl groups of the porphyrin structure (Figure 3).   The specific conditions for this reaction are summarized in detail elsewhere.[44]

In general, metallation of all porphyrin-silicas structures can be accomplished by refluxing the porphyrin silica gel with the chloride salt of the metal in DMF for 4 h.   Metallation can be confirmed by taking the UV-Vis spectra of the silica phase after dissolution in concentrated NaOH.[38]

All porphyrin-silica phases were packed by the downfill slurry method[45] under a pressure of 6000 psi into either 100 mm x 4.6 mm or 250 mm x 4.6 mm stainless steel columns using 70% 2-propanol/ 30% methanol (v/v) as the packing solvent.

The dead volume (V_0) for all columns was measured by injection of a approximately 0.5% (v/v) carbon disulfide (CS_2) solution prepared in the mobile phase.

Materials

HPLC grade toluene, *p*-xylene, and carbon disulfide as well as analytical grade chlorobenzene were obtained from Aldrich (Milwaukee, WI). Various amino acids and peptides tested as solutes were products of Sigma Chemical (St. Louis, MO). The PAHs studied were reagent grade or better and purchased from Aldrich with the exception of α,α' -binapthyl which was obtained from ICN (Irvine, CA). The fullerene samples were produced via a carbon arc method as described elsewhere.[46,47]

RESULTS AND DISCUSSION

Preparation and Characterization of Porphyrin-Silica Phases

As illustrated in Figures 1-3, stationary phases consisting of covalently bound metalloporphyrins are prepared in essentially a two step process. The first step involves covalent attachment of the given porphyrin structure to a porous silica. The second step consists of inserting the metal ion of choice into the center of the immobilized porphyrin via refluxing in dimethylformamide containing high concentrations (e.g., 0.1 M) of metal ion salts. Immobilization of TPP structures based on either an amide (Figure 1) or ether (Figure 2) linkage have been developed. The ether linkage method, developed to simplify preparation and improve column stability, relies upon reaction of an epoxide with an monohydroxy-TPP derivative. The immobilization of ProP on silica (Figure 3) provides a means to readily assess the influence of the four phenyl groups orthogonal to the porphine ring of TPP on the observed retention behavior of given solutes (by comparison of retention on TPP- vs. ProP-silicas). At the same time, the ProP-silicas offer their own unique selectivities with respect to PAH and peptide retention (see below).

Preparation of all the porphyrin-silicas must be performed under rigorous anhydrous conditions in order to achieve reasonable yields of porphyrin surface coverage. Typically, elemental analysis (CHN) of resulting silica packings yields coverages for the TPP-silica stationary phases of around 0.4 μmol/m^2, which is approximately 10% of the total available amine sites. Preliminary experiments suggest that a significant increase in TPP coverage can be achieved   (to about 0.8 μmol/m^2) using the synthetic route (Figure 2) that involves coupling the monohydroxy-TPP directly to the silica support via the glycidoxypropyltrimethoxysilane reagent. In the case of less sterically hindered ProP, coverages are much higher, generally about 2 μmol/m^2, approximately 50% of the available amine sites.
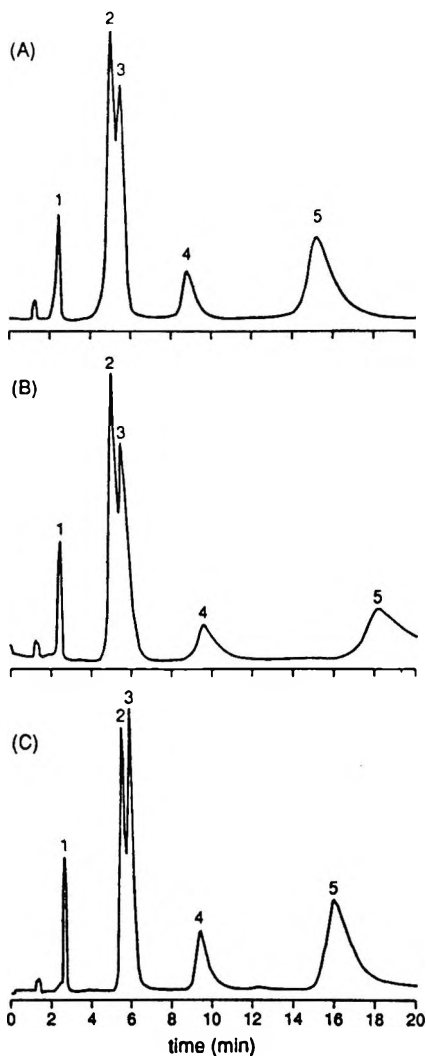
Figure 4. Typical separation of five PAHs on three different 100 mm x 4.6 mm columns packed with (A) H₂TPP-silica, (B) InTPP-silica, and (C) SnTPP-silica. Peak identity: (1) naphthalene, (2) phenanthrene, (3) anthracene, (4) pyrene, (5) chrysene. Conditions: mobile phase: 70% MeOH/30% H₂O; flow rate: 1.0 mL/min; column temperature: 25°C; detection: 254 nm (0.100 AUFS). (Adapted from Ref. 37 with permission)

Table 1

Selectivity Factors of PAH Pairs on Various Porphyrin Stationary Phases

Selectivity Factors	Stationary Phase			
	H_2TPP^a	$InTPP^a$	$SnTPP^a$	H_2ProP^b
α triphenylene/0-terphenyl	3.1	4.3	3.0	39.2
α perylene/α,α'-binapthyl	3.9	6.4	3.4	36.5
α chrysene/pyrene	1.6	1.8	1.6	2.1

[a] Conditions shown in Figure 5 legend.
[b] Conditions shown in Figure 6 legend.

Separation of Polycyclic Aromatic Hydrocarbons

The presence of a large planar aromatic system within the immobilized porphyrin structures (in the form of the porphine ring) suggests the potential application of such phases for the separation of PAHs. The ability to separate PAHs with shape selectivity for planar over non-planar forms has attracted considerable attention over recent years owing the obvious environmental significance of these compounds.[1-6] At present, polymeric ODS type phases offer a much higher degree of shape selectivity when compared to conventional monomeric ODS reversed phase columns.[1]

Figure 4 shows the typical separation of a mixture of PAHs on 10 cm columns packed with H$_2$TPP-, InTPP- and SnTPP-silica phases. Figure 5 summarizes the capacity factors (k') observed for a wide range of PAHs on the same three TPP-silica columns (H$_2$TPP-, InTPP- and SnTPP-silica). Several aromatic pairs, i.e. triphenylene/o-terphenyl, perylene/α,α'-binapthyl and chrysene/pyrene have been suggested previously as probes for assessing shape selectivity of new stationary phases.[4] Table 1 summarizes the selectivity factors for these pairs on the three TPP-silica columns. On a typical monomeric ODS stationary phase the selectivity factor ($\alpha_{triphenylene/o-terphenyl}$) ranges from 1.0 to 1.7,[6] while the value of a polymeric ODS phase lies between 2.0 and 2.7.[2] However, on the various TPP-silica phases, these values are all above 3.0. Furthermore, when the number of double bonds of the unsubstituted PAHs are plotted vs. log k' on the columns packed with TPP-silicas, a linear relationship

(not shown here) is observed suggesting that retention of the PAHs on these new columns is due primarily to a π-π interaction between immobilized TPP and the PAHs.

As shown in Figure 6 and Table 1, the retention behavior of various PAHs on columns packed with the ProP-silica phase reveals an even higher degree of shape selectivity. Indeed, the retention of PAHs on unmetallated ProP-silica columns is so strong that 100% acetonitrile must be used as the mobile phase to elute these solutes in a reasonable time frame (compared to 60% acetonitrile/40% water used for the TPP-silica work described above). There appears to be at least two factors responsible for this greatly enhanced interaction strength: first is the much greater surface coverage of porphyrin on the silica of the ProP-silicas $vs.$ TPP-silicas (2-3 $vs.$ 0.4 µmol/m^2); second is the potential for less steric hindrance for the interaction of PAHs with immobilized ProP compared to immobilized TPP. Indeed, for TPP, larger planar PAHs may be precluded from forming tight π-π complexes with the planar porphine ring due to the steric hindrance of the four phenyl rings perpendicular to the porphine plane. Preliminary fluorescence titration experiments (not shown here) do in fact reveal that ProP forms a charge transfer complex with perylene in acetone, while TPP does not.[48] As shown in Table 1, the much stronger interaction of the larger planar PAHs with immobilized ProP yields extraordinary shape selectivity for the three solute pairs examined.

It should be noted that retention behavior of PAHs on TPP- and ProP-silicas is not particularly sensitive to whether there is a metal ion in the center of the immobilized porphyrin or not (see Figure 4). Indeed, when the metal ion center is either in the +2 or +3 oxidation state, at least one side of the metal ion-porphine ring complex is accessible for direct interaction with neutral PAHs via π-π interaction. However, as shown in Figure 4, even when the metal ion is in the +4 oxidation state, such as Sn(IV), there is still significant interaction with the PAH solutes. Since the PAH separations are carried out under reversed phase conditions, it is likely that relatively small hydroxide anions serve as the ligands for the metal centers, and these are not large enough to block PAH π-π interactions with the planar portion of the porphyrin structure.

Separation of Fullerenes on TPP-Silicas

Since Krätschmer et al. published a method to produce fullerenes in macroscopic quantities in 1990,[49] there have been numerous reports describing new approaches to efficiently separate these novel allotropes of carbon via
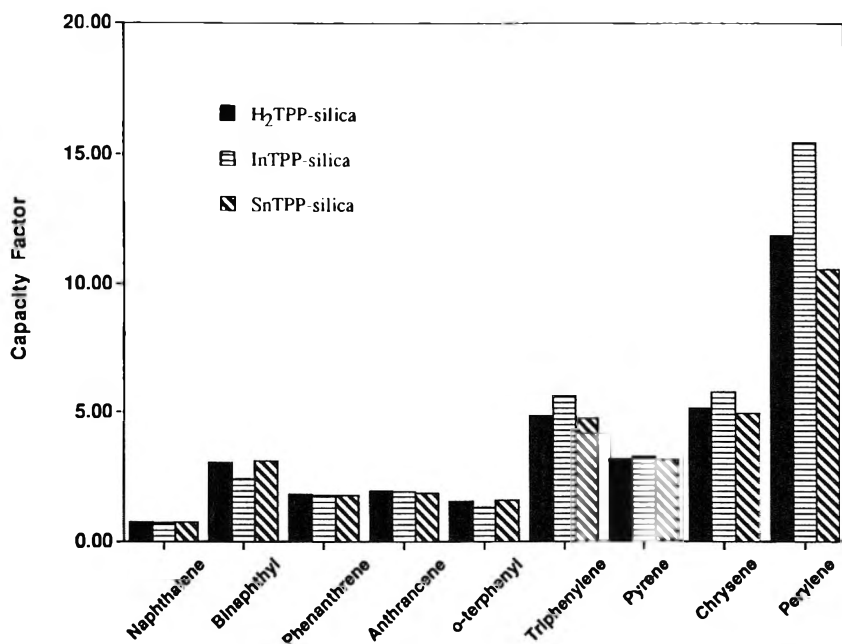
Figure 5. Capacity factors (k') of various PAHs on 100 mm x 4.6 mm columns packed with H_2TPP-silica, InTPP-silica, and SnTPP-silica columns. Conditions: mobile phase: 80% MeOH/20% H_2O; flow rate: 1.0 mL/min.; column temperature: 25°C; detection: 254 nm (0.100 AUFS).

HPLC methods. While separation of the various fullerenes using relatively weak mobile phases (e.g., hexane) is not particularly difficult on conventional columns, such as ODS phases, efforts to isolate much larger quantities of fullerenes for fundamental and applied studies requires purification with much stronger solvents. For example, the solubility of C_{60} is only 0.043 mg/mL in hexane, but 2.8 mg/mL in toluene, and 7.9 mg/mL in carbon disulfide.[28] Hence, columns that can operate using toluene or even CS_2 as mobile phases would provide the most efficient means of separating individual fullerenes on a preparative scale.

Supports with π-acidic character have shown to be well-suited for the separation of fullerenes. The tri(dinitrophenyl)-silica or "Buckyclutcher" phase developed by Welch and Pirkle,[13] in particular, was one of the first LC stationary phases to demonstrate reasonable selectivity for C_{60} and C_{70} separations ($\alpha_{C70/C60}$ = 1.5 in toluene). Kimata et al. have further demonstrated good selectivity in the separation of a variety of fullerene isomers with columns
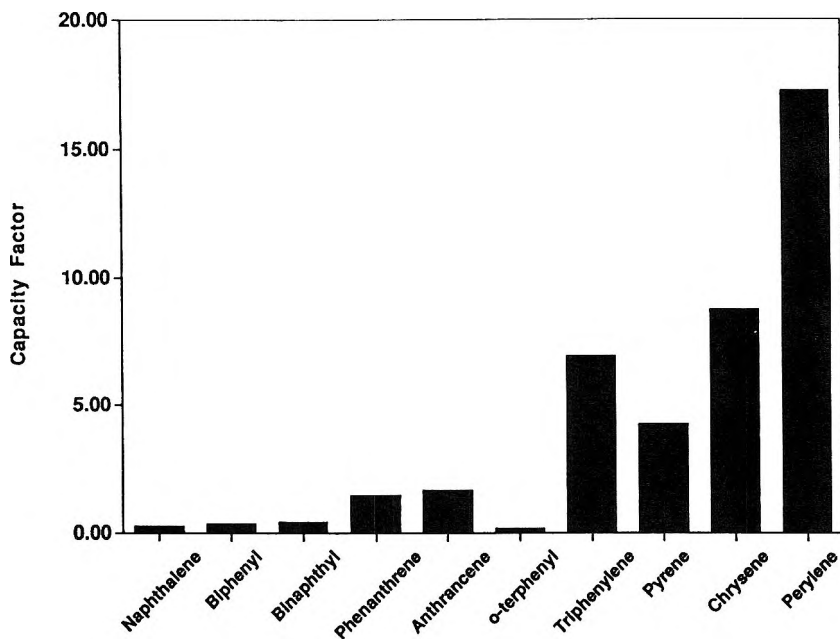
Figure 6. Capacity factors (k') of PAHs on a 100 mm x 4.6 mm column packed with H_2ProP-silica. Conditions: mobile phase: 100% acetonitrile; flow rate: 1.0 mL/min; column temperature: 25°C; detection: 254 nm (0.100 AUFS).

packed with 2-(1-pyrenyl)ethyl-silica (PYE)[21] and more recently with a 3-[(pentabrombenzyl)oxy]propylsilyl-silica (PBB) phase[50] ($\alpha_{C70/C60}$ = 1.8 and 2.5 in toluene, respectively). However, these and other stationary phases[51-63] exhibit only modest selectivity for the separation of C_{60} and C_{70} when using stronger solvents as the mobile phase.

The new TPP-silica phases described here have been shown to offer dramatically enhanced retention and selectivities for the separation of fullerenes.[39-41] As shown in Figure 7, C_{60} and C_{70} can be completely resolved using mobile phases ranging from 100% toluene to 100% CS_2 (with α values ranging from 4.3 to 1.8). Again, as in the case of PAHs, $\alpha_{C70/C60}$ values do not change appreciably whether or not the TPP structure is metallated (either with +3 or +2 metal ions). However, when Sn(IV) is the central metal ion, much poorer selectivity for the separation of C_{60} and C_{70} has been observed.[42] Since fullerene separations are performed in aprotic solvents, it is likely that the presence of larger anionic ligands (Cl⁻) on both axial sites of the central metal

ion partially block π-π interactions between the fullerenes and the immobilized TPP species (behavior that is significantly different from the case of PAH separations in methanol/water mobile phases, see above).

Beyond C_{60} and C_{70}, higher molecular weight fullerenes and endohedral metallofullerenes can also be separated on columns packed with TPP-silicas. Figure 8 shows the chromatogram obtained for the separation of a fullerene mixture obtained from the Soxhlet extraction of raw fullerenes with pyridine using soot that had been produced from graphite rods containing yttrium. As shown, a fairly clean separation of $Y@C_{82}$ can be achieved in one pass through a 25 cm column packed with ZnTPP-silica. Similar results have been published previously for the separation of $La@C_{82}$.[40] As with the separation of empty fullerenes, operation of the column with a mobile phase of 25% CS_2 and 75% toluene enables purification of much larger quantities of the endohedral metallofullerenes on the TPP-silica phases than on conventional columns.

The results presented above were obtained on columns packed with TPP-silicas prepared using the monocarboxyl-TPP derivative and aminopropyl silica as the starting materials (Figure 1). Very recent results obtained with packings prepared by coupling 5-(p-hydroxyphenyl)-10,15,20-triphenyl] porphyrin to glycidoxypropyltrimethoxysilane through an ether linkage, followed by immobilization on the silica surface (Figure 2) suggest that such phases exhibit both greater selectivities and efficiencies for the separation of fullerenes. Indeed $\alpha_{C70/C60}$ values of > 6.0 in 100% toluene and > 3.0 in 100% CS_2 have been observed on these new porphyrin-silica phases.[64] Moreover, the number of theoretical plates (N) is also considerably higher for columns packed with this new type of TPP-silica phase. Since the preparation of these materials does not require use of aminopropyl-silica, it is possible that much more homogeneous stationary phases may result (i.e., for TPP-silicas prepared with monocarboxyl-TPP, incomplete acetylation of the residual amine sites could yield rather heterogeneous phases).

Regardless of which method is used to prepare the TPP-silicas, it is clear that such phases interact very strongly with fullerenes. The strength of the fullerene-porphyrin interaction can be attributed to the similar diameter of the fullerene and the TPP cavity (see Figure 9), thereby providing the opportunity for π-π interactions to occur in three dimensions. Indeed, it is likely that the fullerene π-electrons enjoy not only face to face π-π interactions with the porphyrin macrocycle, but face to edge π-π interactions with the meso phenyl rings of the porphyrin. The importance of the meso phenyl groups on the immobilized porphyrin has been confirmed by efforts to separate C_{60} and C_{70} on ProP-silicas, where only minimal selectivity for C_{70}/C_{60} has been observed.[41]
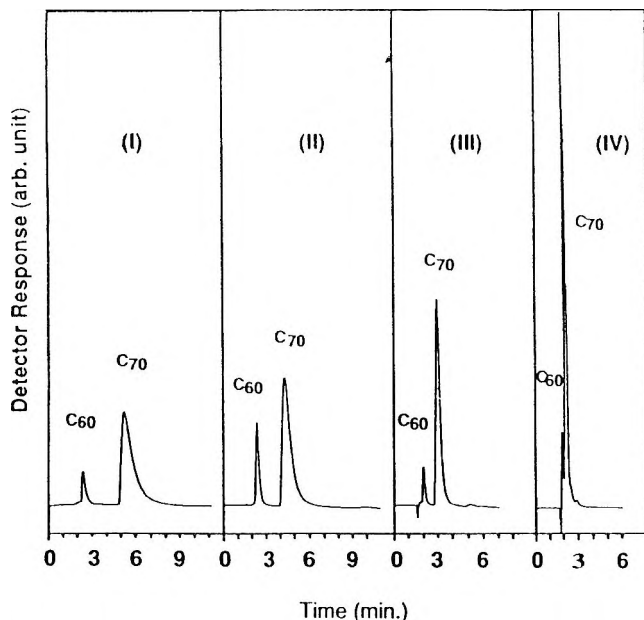
Figure 7. Typical separation of C_{60} and C_{70} on a 250 mm x 4.6 mm column packed with ZnTPP)-silica using four different mobile phases: (I) toluene, (II) p-xylene, (III) chlorobenzene and (IV) carbon disulfide. Conditions: flow rate: 2 mL/min; detection: UV@430 nm (0.100 AUFS); injection: 20 μL of fullerene solution in toluene; temperature: 30°C.

In general, fullerene retention on porphyrin-silica columns increases with increasing fullerene molecular weight, due to the fact that as fullerene size increases both the surface interaction area and the π-basicity of the fullerene increases. The importance of π-basicity in the retention mechanism is further supported by the evidence that La@C_{82} and Y@C_{82} are retained longer than C_{82} or C_{84}. Indeed, in such endohedral metallofullerenes, the central metal donates electrons to the fullerene π-orbitals, thereby making M@C_{82} species a stronger base than non-metallo C_{82}. Hence, although both species are exactly the same size, the metallofullerene is retained longer on the TPP-silica support.

One interesting aspect of fullerene separations on TPP-silica phases is the observed dependence of selectivity on the pore size of the silica.[42] For example, the selectivity factor for C_{60} and C_{70} was found to decrease from $\alpha = 5.6$ for a 60Å pore size silica to $\alpha = 2.6$ for a 300Å pore size silica using pure toluene as the mobile phase (with similar surface coverage of immobilized TPP).
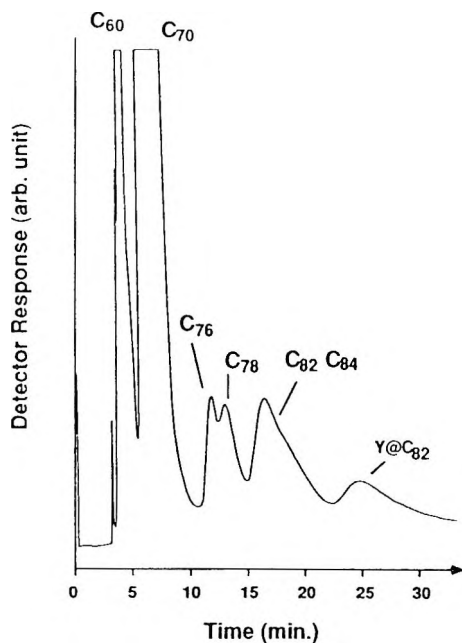
Figure 8. Chromatogram for sample of fullerene soot containing $Y@C_{82}$ on a 250 mm x 4.6 mm column packed with ZnTPP-silica. Conditions: flow rate: 2 mL/min; detection: UV@482 nm (0.100 AUFS); injection: 100 μL of fullerene solution in toluene; temperature: 25°C; mobile phase: 75% toluene/25% CS_2.

It is thought that the three dimensional size and shape of the fullerenes may allow a single fullerene solute to enjoy simultaneous interactions with more than one immobilized TPP species. Hence, the small diameter and high pore curvature of 60Å silica is likely to enhance the possibility for such simultaneous interactions compared to 300Å silica. Further studies to fully discern the role of pore size on fullerene separations are currently in progress in this laboratory.

Anion Separations on Metalloporphyrin-Based Stationary Phases

Metalloporphyrin-silica phases also exhibit unique properties as anion-exchange materials. The basis for the potential application of these phases in anion exchange chromatography can be found in previous literature reports regarding the technique termed ligand exchange chromatography.[10]

C_{60}

Zn(II) Tetraphenylporphyrin

Silica Support
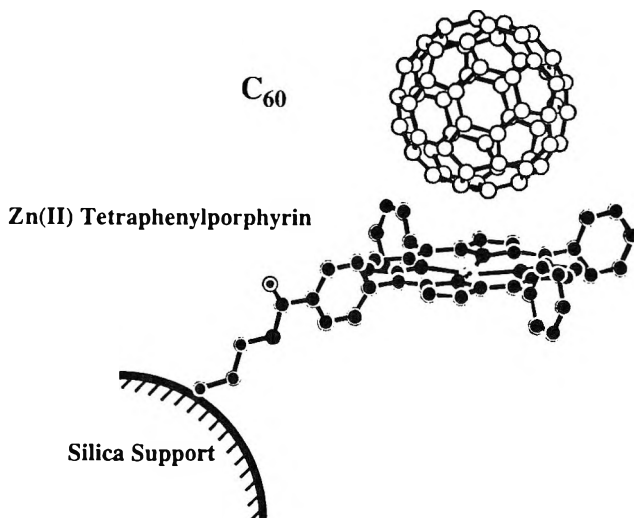
Figure 9. Molecular model of proposed π-π interaction between immobilized MTPP and C_{60}.

Ligand exchange chromatography has been defined by Davankov as a process in which complex-forming species are separated through the formation and breaking of labile coordinate bonds to a central metal ion. Anion retention in ligand exchange chromatography may occur by either an inner-sphere or outer-sphere coordination mechanism. Inner-sphere coordination involves direct interaction between the anionic ligand and the metal center of the exchanger while outer sphere mechanisms require initial tight inner sphere coordination of a solvent or other neutral ligand molecule and subsequent hydrogen bonding with anions not directly in contact with the metal center. Further, the metallic cations used in ligand exchange chromatography may be classified as "hard" or "soft."

Hard acid cations (e.g., Sn^{+4} and In^{+3}) have a large charge:radius ratio and preferentially associate with ligands containing oxygen, while soft acid cations (e.g., Zn^{+2} and Cu^{+2}) coordinate preferentially with ligands having sulfur or nitrogen electron donors. Hence, using the newly developed porphyrin-silicas with different metal ion centers that are in their +3 or +4 oxidation state, it should be possible to separate anions based on specific coordination reactions with a given metal center cation.
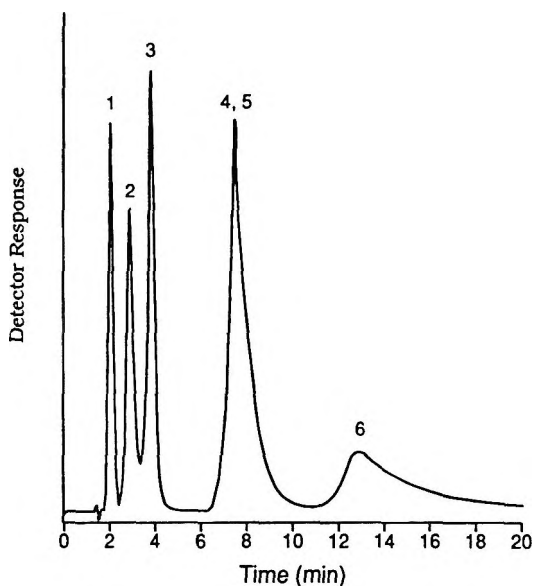
Figure 10. Typical separation of anions on 100 mm x 4.6 column packed with InTPP-silica. Peak identity: (1) iodide, (2) thiocyanate, (3) p-toluenesulfonate, (4) benzoate, (5) p-hydroxybenzoate, (6) salicylate. Conditions: mobile phase: 15% methanol/85% 10 mM acetate buffer, pH 4.5; column temperature: 25°C; detection: 220 nm (0.100 AUFS). (Adapted from Ref. 38 with permission).

Initial evaluation of the anion-exchange selectivities of columns packed with SnTPP- and InTPP-silica supports (Figure 10) was performed using inorganic (e.g., I^- and SCN^-) and organic anions (e.g., benzoate, p-hydroxybenzoate, salicylate and p-toluenesulfonate) as test solutes. Figure 10 shows the typical separation of these test anions achieved using a InTPP-silica column, and Figure 11 compares the capacity factors for these anions on both InTPP- and SnTPP-silica phases, as well as a conventional quaternary ammonium-based anion exchange column (Hamilton PRP X-100).

Figure 11 clearly illustrates that significant differences in selectivity among the three stationary phases are observed. The quaternary ammonium-based support shows little retention preference between the lipophilic inorganic anions and the aromatic anions. In contrast, the SnTPP- and InTPP-silica supports display markedly enhanced selectivity towards aromatic anions (e.g., salicylate) over the lipophilic inorganic anions, and this correlates well with the

potentiometric anion selectivities found when Sn(IV) or In(III)-based metallotetra- phenylporphyrins are incorporated in polymer membranes for the purpose of developing new anion selective electrodes.[65,66]

Differences in the chromatographic selectivity between SnTPP- and InTPP-silica phases towards aromatic carboxylates are also suggested by the data shown in Figure 11. The capacity factor of p-hydroxybenzoate on the SnTPP support is greater than that of salicylate or benzoate, while on the InTPP support, salicylate is the preferentially retained anion. The aromatic carboxylates elute as reasonably sharp symmetric peaks on the column packed with InTPP-silica, but on the SnTPP-silica column these solutes elute as broad tailing bands. The difference in peak shape on the two metalloporphyrin supports suggests slow kinetics for the dissociation of an inner sphere metal-carboxylate complex with the Sn(IV) metalloporphyrin stationary phase. Indeed, significant improvement in peak symmetry for salicylate on the SnTPP-silica support can be realized when separations are carried out at elevated temperatures (e.g., 60°C).

The InTPP-silica phase has been applied to separate a number of benzene- and naphthalene-based sulfonates.[38] While both solvophobic and/or π-π interactions between the aromatic anions and the immobilized metallo-TPP may play a role in solute retention, comparison of the capacity factors of aromatic carboxylates and sulfonates on metallated and non-metallated TPP-silica stationary phases clearly indicates that metal-ligand exchange is the primary retention mechanism for these aromatic anionic solutes on both the SnTPP- and InTPP-silica supports.[38]

Mobile phase pH has a significant impact on the retention of anionic compounds on the metalloporphyrin-silica supports. The capacity factors for a series of ten aromatic sulfonates on columns packed with SnTPP- and InTPP-silicas as a function of mobile phase pH (from pH 4.0-6.0) are tabulated in Table 2. Both metalloporphyrin supports exhibit decreased selectivity for the aromatic sulfonates with increasing pH of a 15% methanol/85% 10 mM succinate eluent. This decrease in retention occurs as a result of the very strong ligation reaction between hydroxide ions and the metal ion centers.[65] Thus, mobile phase pH, either using isocratic or gradients, can be used to optimize the separation of aromatic carboxylates and sulfonates, using higher pH values to decrease the retention of solutes that coordinate strongly with the metal ion centers.

The separation of anions on MProP-silica phases has not yet been explored, nor has there been any detailed examination of the anion exchange properties of TPP-silica phases containing metal ions other than In(III) and
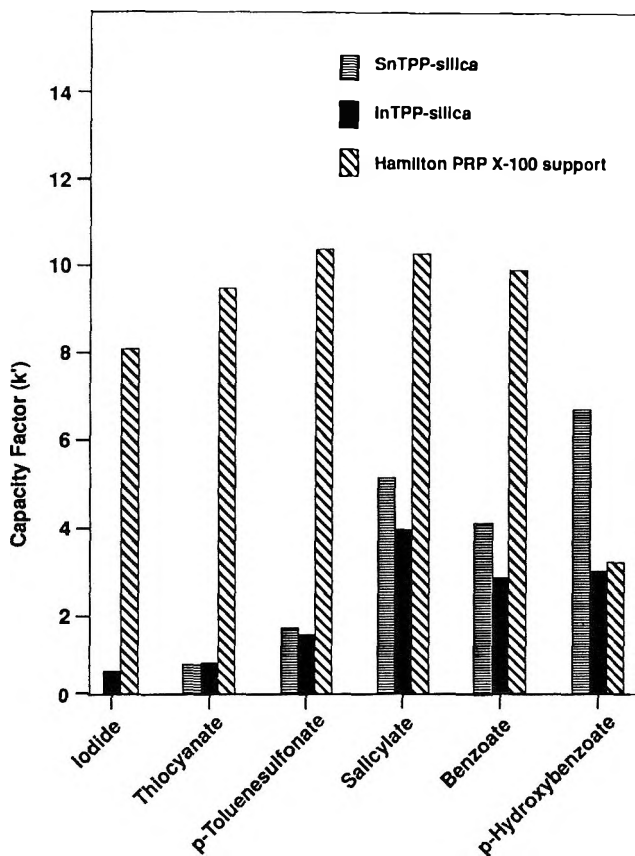
Figure 11. Capacity factors (k') of inorganic and organic anions on 100 mm x 4.6 mm columns packed with SnTPP-silica, InTPP-silica, and a Hamilton PRP X-100 support. Separations on the SnTPP and InTPP columns were carried out using a 10 mM sodium succinate, pH 5.5, eluent at a flow rate of 1.0 mL/min. These solutes were eluted from the Hamilton PRP X-100 column with 8 mM sodium carbonate, pH 11, containing 1 mM p-cyanophenol at a flow rate of 1.0 mL/min.

Sn(IV). In principle, it should be possible to use a wide range of other metal ions to achieve novel ligand exchange anion selectivities (e.g., Co(III) for selective nitrite retention[67]). Of course, only metal ions that form stable complexes with the porphyrin macrocycle in their +3 or +4 state can be used, since +2 metal centers will not require counter anions to satisfy electroneutrality conditions.

Table 2

Influence of Mobile Phase pH on the Capacity Factors of Aromatic Sulfonates on the In(III)TPP- and Sn(IV)TPP-silicas[a]

Capacity Factor (k')

Aromatic Sulfonate	pH 4.0 In(III)	Sn(IV)	pH 4.5 In(III)	Sn(IV)	pH 5.0 In(III)	Sn(IV)	pH 5.5 In(III)	Sn(IV)	pH 6.0 In(III)	Sn(IV)
Sulfanilic Acid	1.2	1.2	0.6	0.6	0.4	0.4	0.2	0.2	0.2	0.1
Benzenesulfonate	2.1	2.1	0.9	0.8	0.6	0.6	0.4	0.3	0.2	0.2
p-Toluenesulfonate	3.7	3.7	1.5	1.8	1.1	1.0	0.6	0.6	0.4	0.4
1-Naphthalenesulfonate	18.8	19.0	7.6	9.4	5.6	5.1	3.1	2.9	2.1	2.0
2-Naphthalenesulfonate	25.2	23.6	10.1	11.7	7.6	6.2	4.2	3.7	2.8	2.6
4-Amino-1-Naphthalenesulfonate	7.9	7.8	3.5	3.8	2.4	2.1	1.4	1.2	0.9	0.8
6-Amino-4-Hydroxy-2-Naphthalenesulfonate	11.5	>26.0	5.4	8.1	4.2	5.4	2.4	3.7	1.7	3.1
7-Amino-4-Hydroxy-2-Napthalenesulfonate	11.5	>26.0	5.6	12.5	4.3	8.2	2.4	8.0	1.7	5.6
1,5-Napthalenedisulfonate	9.8	10.0	2.1	2.0	0.8	0.7	0.2	0.2	0.1	>0.1
2,6-Naphthalenedisulfonate	13.1	12.4	2.7	2.5	1.2	0.9	0.4	0.3	0.2	0.1

[a] Column: 100 mm x 4.6 mm stainless steel column; mobile phase: 15% methanol/85% 10 mM succinate; flow rate: 1.0 mL/min; column temperature: 25°C; detection: 220 nm (0.100 AUFS).

Separation of Amino Acids/Peptides on Metalloporphyrin-Silicas

The concept of ligand exchange chromatography with immobilized metal ions has also been applied previously for the separation of amino acids, peptides and proteins, where given amino acid side chains (e.g., histidine, tyrosine, tryptophan)[31,32] can form coordination complexes with certain metal ions (e.g., Zn^{+2}, Ni^{+2}, Fe^{+3}). The technique, more often termed immobilized metal ion affinity chromatography (IMAC), normally utilizes supports composed of iminodiacetate ligands tethered to soft gels or silica supports.[31,32] Using the existing phases, however, IMAC has several shortcomings, particularly when it comes to performing reproducible analytical separations of peptides and proteins. Indeed, continuous metal ion leaching from current

support materials makes analytical IMAC virtually impossible (i.e., retention times change as metal is depleted from support). Since the affinity of metal ions to porphyrin structures is known to be on the order of 10^{30} M^{-1}, some 15 orders of magnitude greater than most metals bind diacetate type ligands,[68-74] it seems reasonable to expect that metalloporphyrin phases may be especially useful for reproducibly separating peptides and proteins by ligand exchange type reactions.

To examine this prospect in detail, preliminary experiments have been carried out using MProP-silicas rather than MTPP-silicas as stationary phases. The immobilized ProP structure is somewhat less hydrophobic than TPP and it also provides a phase that should have less steric hindrance for potential ligation reactions of larger peptides and protein structures. A test group of 9 amino acids was selected to be representative of the various classes of the 20 natural amino acids: i.e., L-glycine (Gly) and L-leucine (Leu) as hydrophobic amino acids; L-glutamate (Glu), L-lysine (Lys), L-serine (Ser) and L-cysteine (Cys) as charged/polar amino acids, and L-histidine (His), L-phenylalanine (Phe) and L-tryptophan (Trp) as aromatic amino acids. Table 3 summarizes the absolute capacity factors (k') measured on each of the six columns (10 cm) for each test amino acid using a 50 mM phosphate buffer, pH 7.0, as the mobile phase. As tabulated, Gly, Glu, Ser, Lys and Cys exhibit the least retention on any of the ProP-silica columns indicating that ionic interactions, in comparison to other retention mechanisms (see below), are minimal and make only a small contribution to the overall retention behavior of amino acids on the MProP-silica phases. Further, the more hydrophobic Leu and polar Ser amino acids are also not retained to any significant degree (relative to His and Trp) on any of the ProP-silica columns examined; these results suggest that the ProP-silica stationary phases do not exhibit substantial hydrophobic or hydrogen-binding character.

The retention behavior of His and Trp on the MProP columns *vs.* unmetallated ProP-silica clearly demonstrates the inherent amino acid ligand exchange selectivity of the new MProP-silica phases (see Table 3). Columns packed with FeProP-silica provide the greatest selectivity for retention of His, followed by the NiProP, CuProP, ZnProP and CdProP phases. The retention of His is due to coordination of the imidazole nitrogen with the central metal ion. It is interesting to note that Trp also exhibits extremely high affinity (much greater than His) on certain metalloporphyrin phases, e.g., CuProP, FeProP and NiProP, relative to that on the unmetallated H_2ProP-silica phase. The amino acid retention patterns shown in Table 3, however, also reveal that Trp is highly retained even on the unmetallated H_2ProP-silica phase (compared to all the other test amino acids). Further, MProP-silica phases that exhibit greatly enhanced retention of Trp also display the longest retention times for Phe,

Table 3

Capacity Factors of Selected Amino Acids on the Six Porphyrin Silical Columns[a]

| Amino Acids | Stationary Phase | | | | | |
	H_2ProP	FeProP	CuProP	ZnProP	NiProP	CdProP
Glycine	0.1	0.2	0.1	0.1	0.2	0.1
Histidine	1.0	14.6	4.1	2.1	7.3	1.3
Lysine	1.2	4.0	2.2	1.7	5.3	1.6
Cysteine	0.2	0.7	0.3	0.2	0.2	0.2
Serine	0.1	0.2	0.1	0.1	0.2	0.1
Phenylalanine	1.5	7.2	8.7	2.1	9.7	1.5
Tryptophan	10.5	70.7	109.0	13.9	63.2	11.2
Glutamine Acid	0	0	0	0	0	0

[a] Mobile phase: 100% 50 mM phosphate buffer, pH 7.0; flow rate: 1 mL/min; temperature: ambient; detection: 214 nm (0.100 AUFS).

although not nearly to the extent observed for Trp. These results suggest that there is a substantial contribution from π-π interactions between the immobilized porphyrin ring and the aromatic amino acids. Therefore, a combination of simultaneous metal ion ligation and π-π interactions are likely responsible for the exceptionally high selectivity toward Trp exhibited by several of the MProP-silica phases, especially CuProP-silica.

More detailed studies on the effect of organic modifier (acetonitrile) in the mobile phase (pH 7.0 phosphate buffer) on the retention of Trp, His, and Phe on the CuProP and FeProP silica phases demonstrates that increasing the acetonitrile content dramatically reduces the retention time of amino acids on both columns. In addition, lowering the pH of the mobile phase (from pH 7.0 to pH 2.5) also drastically reduces the retention of His on the FeProP-silica phase (from $k' = 14.3$ to $k' = 0.0$). At low pH, the imidazole nitrogen on His is protonated eliminating retention via a metal-ligation reaction with this nitrogen. Similar effects are observed for Trp and Lys. Since organic modifier dramatically decreases the π-π interaction and lowering pH weakens metal-ligation interactions, it is a simple matter to tune these two retention mechanisms, by choosing an appropriate pH and organic modifier content for the mobile phase (see below), to achieve the retention and selectivity desired.
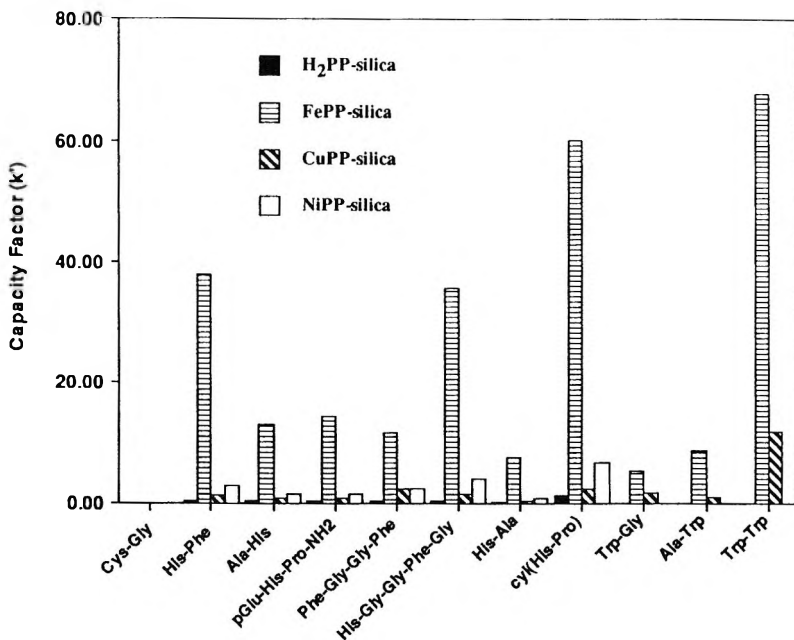
Figure 12. Capacity factors of model peptides on 100 mm x 4.6 mm columns packed with H₂ProP-silica, FeProP-silica, CuProP-silica and NiProP-silica. Conditions: mobile phase: 75% 50 mM phosphate buffer, pH 7.0 / 25% acetonitrile; flow rate: 1 mL/min; temperature: ambient; detection: UV@214 nm (0.100 AUFS).

Since the amino acids His, Trp, and Phe are all retained to varying but significant degrees on some MProP-silica phases, the retention behavior of small peptides containing these and other amino acids was also examined. Using a mobile phase of pH 7.0 phosphate modified with 25% acetonitrile (to elute all test peptides in a reasonable time while still allowing a practical evaluation of the different retention behaviors of the peptides) the capacity factors for a group of 10 test peptides on 10 cm H₂ProP-, CuProP-, ZnProP- and FeProP-silica columns are shown in Figure 12. For the most part, the results of these studies are consistent with the observed retention of individual amino acids on the same stationary phases (see above). For example, Cys-Gly elutes in the void volume on all the porphyrin columns while all peptides containing His and Trp are preferentially retained on the FeProP-silica column, presumably through metal ligation interactions. Other porphyrin columns exhibit only minimal retention of these peptides, except for Trp-Trp on the CuProP column. Even with 25% acetonitrile in the mobile phase, π-π interactions still contribute to some extent to the retention of the test peptides,

and this explains why peptides containing both His and Phe are retained longer than those with His alone. The Trp-Trp dipeptide is retained the longest on the FeProP- and CuProP-silica phases of any of the peptides tested. Overall, these results suggest that there is an enhanced cumulative interaction affinity for small peptides containing multiple amino acids that individually exhibit strong interactions with a given MProP-silica phase. This is analogous to what is observed on current IMAC phases. Indeed, polyhistidine sequences are now used routinely as N-terminus sequences of recombinant proteins so that such proteins can be retained strongly by IMAC supports, greatly simplifying the protein purification process.

Beyond unique chemical selectivities, the extremely tight binding of metal ions to the ProP-silicas represents a potentially significant advantage over conventional IMAC phases.[71-74] As stated previously, metal ion leaching from current IMAC phases is a major limitation to the use of such phases in routine HPLC peptide/protein separations. To demonstrate the inherent metal ion stability of the new MProP-silica stationary phases, the separation of two model peptides was conducted before and after extensive column washing (FeProP-silica) with 50 mM EDTA (pH 6.0) for about 30 min. As shown in Figures 13a,b, the chromatograms (using a gradient for elution; see the figure legend for exact conditions) for tryptophan-releasing hormone (TRH; pGlu-His-Pro-NH_2) and His-Phe are essentially the same before and after washing the column with EDTA. Any slight differences in retention times (see Figure 13 legend) are apparently due to small variations in the gradient profile from run to run. In another experiment, EDTA was deliberately added to the same peptide mixture at a concentration of 10 mM. Again, as shown in Figure 13c, there is no major change in the resulting chromatogram, indicating that no significant leaching of the Fe(III) within the ProP structure occurs even when a very strong chelator passes through the column (note: retention of TRH and His-Phe is largely due to retention of His via metal-ligation interaction). The reproducibility of the separation shown in Figure 13 exemplifies one of the potential advantage that metalloporphyrin-silica stationary phases may offer for peptide and protein separations via metal ion affinity.

Summary and Limitations of Current Porphyrin-Silica Phases

The initial HPLC studies with porphyrin-silica stationary phases summarized above demonstrate that very high chemical selectivities can be achieved in a variety of applications. It has been further shown that for fullerene, PAH and peptide separations, the observed retention relationship is highly dependent upon the specific structure (and metal cation) of the immobilized porphyrin. However, the superior selectivity exhibited by
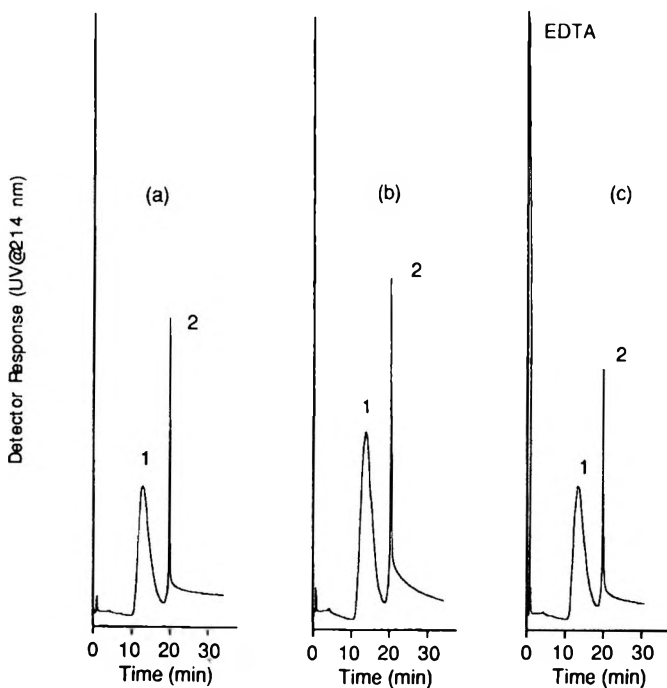
Figure 13. The effect of EDTA on the HPLC separation of TRH (1) and His-Phe (2) using a 100 mm x 4.6 mm column packed with FeProP-silica: (a) before 30 min washing with 50 mM EDTA (retention times of 1 and 2 were 12.72 min and 19.87 min); (b) after EDTA washing (retention times of 1 and 2 were 13.76 min and 20.56 min); (c) sample of peptides with 50 mM EDTA (retention times of 1 and 2 were 13.42 min and 20.24 min). Conditions: mobile phase: (A) 10% acetonitrile/90% pH 7.0 phosphate buffer and (B) 25% acetonitrile/75% pH 2.5 phosphate buffer; gradient: 0-100% B from 0-15 min and 100% B from 15-30 min; flow rate: 1 mL/min; temperature: ambient; detection: UV@214 nm (0.100 AUFS). (Adapted from Ref. 44 with permission).

porphyrin-silica stationary phases has not, as of yet, been matched with high efficiency. Peak shapes are routinely poor with a high degree of peak tailing. Experimental evidence appears to implicate a number of chemical sources for the low efficiencies observed, including: a) heterogeneity in the porphyrin structure and surface topology; b) incomplete silica surface deactivation; c) multiple modes of solute retention; d) and slow dissociation kinetics for solute interactions.

First, in the preparation of porphyrin derivatives, approximately 2-5% of the product is the corresponding chlorin (a reduced form of porphyrin with 2 additional hydrogens on one of the pyrrole rings). To date, no attempt has been made to synthesize stationary phases free of chlorin contamination. Although the porphyrin and chlorin are very similar in structure, even a slight deviation in stationary phase structure is likely to lead to different interaction energies with solutes.

Second, heterogeneity in the surface coverage has not been examined in detail. Because the surface coverage is much lower than a monolayer it is both conceivable and likely that large variations in porphyrin density occur over the silica surface. This is supported by the knowledge that porphyrins tend to aggregate into stacks[75] and this phenomenon is likely to occur during the immobilization procedure where high concentrations of the activated porphyrin derivatives are employed.

This stacking behavior would result in a highly varied surface structures with regions of densely stacked porphyrins as well as regions of highly spaced immobilized porphyrins. The resulting stationary phase can exhibit at least two, and likely more, distinct interaction behaviors.

Third, because of the comparatively low porphyrin coverages, compared to conventional columns such as ODS, there exist a large number of exposed silanols and amine sites. Thus, secondary solute interactions with the silica surface can be a significant source of solute retention.

A fourth contributor to band broadening in ligand exchange applications (peptide separations and anion exchange) relates to the high association constants for metal ion ligation reactions, which are generally much greater than those typically found in dynamic chromatographic systems (e.g. ODS, amine, phenyl). Hence, the slow kinetics of ligand dissociation can contribute significantly to band broadening in such systems. If dynamic chromatographic behavior is desired it appears that metal ligation interactions must be mitigated either through the addition of a competing complexation agents, judicious choice of mobile phase pH, or alteration of the porphyrin structure to sterically hinder solute ligation.

Further research into the relationship between each of these factors and peak tailing is in progress. As the contribution of each is understood, their adverse effect on solute efficiency can hopefully be reduced or eliminated, making the porphyrin-silica phases more useful as versatile supports for a variety of modern HPLC applications.

ACKNOWLEDGEMENTS

REFERENCES

1. S. A. Wise, L. C. Sander, W. E. May, J. Chromatogr., **642**, 329-349 (1993).

2. K. Jinno, T. Ibuki, N. Tanaka, M. Okamoto, J. C. Fetzer, W. R. Biggs, P. R. Griffiths, J. M. Olinger, J. Chromatogr., **461**, 209-227 (1989).

3. K. B. Sentell, J. G. Dorsey, J. Chromatogr., **461**, 193-207 (1989).

4. N. Tanaka, Y. Tokuda, K. Iwaguchi, M. Araki, J. Chromatogr., **239**, 761-772 (1982).

5. K. Jinno, T. Nagoshi, N. Tanaka, M. Okamoto, J. C. Fetzer, W. R. Biggs, J. Chromatogr., **386**, 123-135 (1987).

6. K. Jinno, K. Yamamoto, H. Nagashima, T. Ueda, K. Itoh, J. Chromatogr., **517**, 193-207 (1990).

7. R. E. Barron, J. Fritz, J. Chromatogr., **316**, 201-210 (1984).

8. R. E. Barron, J. Fritz, J. Chromatogr., **284**, 13-25 (1984).

9. M. C. Gennero, J. Chromatogr., **449**, 103-111 (1988).

10. V. A. Davankov, J. D. Navartil, H. F. Walton, **Ligand Exchange Chromatography**, CRC Press, Boca Raton, Florida, 1988.

11. M. Sinibaldi, V. Carunchio, A. Messina, C. Corradini, Annali di Chimica, **74**, 175-186 (1984).

12. J. M. Hawkins, T. A. Lewis, S. D. Loren, A. Meyer, J. R. Heath, Y. Shibato, R. J. Saykally, J. Org. Chem., **55**, 6250-6252 (1990).

13. C. J. Welch, W. H. Pirkle, J. Chromatogr., 609, 89-101 (1992).

14. H. Ajie, H. M. Alvarez, S. J. Anz, R. D. Beck, F. Diederich, K. Fostiropoulos, D. R. Huffman, W. Kratschmer, Y. Rubin, K. E. Schriver, D. Sensharma, R. L. Whetten, J. Phys. Chem., **94**, 8630- 8633 (1990).

15. F. Diederich, R. Ettl, Y. Rubin, R. L. Whetten, R. Beck, M. Alvarez, S. Anz, D. Sensharma, F. Wudl, K. C. Khemani, A. Koch, Science, **252**, 548-551 (1991).

16. K. Jinno, K. Yamamoto, T. Ueda, H. Nagashima, K. Itoh, J. Chromatogr., **594**, 105-109 (1992).

17. Y. Cui, S. T. Lee, S. V. Olesik, W. Flory, M. Mearini, J. Chromatogr., **625**, 131-140 (1992).

18. K. Cabrera, G. Wieland, M. Schafer, J. Chromatogr., **644**, 396-399 (1993).

19. A. Gügel, K. Müllen, J. Chromatogr., **628**, 23-29 (1993).

20. M. Diack, R. N. Compton, G. Guiochon, J. Chromatogr., **639**, 129-140 (1993).

21. K. Kimata, K. Hosoya, T. Araki, N. Tanaka, J. Org. Chem., **58**, 282-283 (1993).

22. A. D. Darwish, H. W. Kroto, R. Taylor, D. R. M. Walton, J. Chem. Soc., Chem. Commun., **115**, 5-16 (1994).

23. M. Diack, R. I. Hettich, R. N. Compton, G. Guiochon, Anal. Chem., **64**, 2143-2148 (1992).

24. K. Jinno, H. Ohta, Y. Saito, T. Uemura, H. Nagashima, Y. L. Chen, G. Luehr, J. Archer, J. C. Fetzer, W. R. Biggs, J. Chromatogr., **648**, 71-77 (1993).

25. K. Jinno, T. Uemura, H. Olhta, H. Nagashima, K. Itoh, Anal. Chem., **65**, 2650-2654 (1993).

26. J. Anacleto, M. Quilliam, Anal. Chem., **65**, 2236-2242 (1993).

27. K. Kikuchi, N. Nakahara, T. Wakabayashi, Chem. Phys. Lett., **188**, 177-180 (1992).

28. R. S. Ruoff, D. S. Tse, R. Malhotra, D. C. Lorents, J. Phys. Chem., 97, 3379-3383 (1993).

29. Y. Wu, Y. Z. Sun Gu, Q. Wang, X. Zhou, Y. Xiong, Z. Jin, J. Chromatogr., 648, 491-496 (1993).

30. W. H. Pirkle, C. J. Welch, J. Org. Chem., 56, 6973-6974 (1991).

31. M. Belew, T. T. Yip, L. Anderson, J. Porath, J. Chromatogr., 403, 197-206 (1987).

32. J. Porath, J. Carlsson, I. Olsson, G. Belfrage, Nature. 258, 598-599 (1975).

33. N. A. Chaniotakis, A. M. Chasser, M. E. Meyerhoff, J. T. Groves, Anal. Chem., 60, 185-188 (1988).

34. E. Wang, M. E. Meyerhoff, Anal. Chim. Acta, 283, 673-682 (1993).

35. M. Huser, W. E. Morf, K. Fluri, K. Seiler, P. Schulthess, W. Simon, Helv. Chim. Acta, 73, 1481-1496 (1990).

36. E. Kokufuta, T. Sodeyama, S. Takeda, Polymer Bulletin, 15, 479-484 (1986).

37. C. E. Kibbey, M. E. Meyerhoff, J. Chromatogr., 641, 49-55 (1993).

38. C. E. Kibbey, M. E. Meyerhoff, Anal. Chem., 65, 2189-2196 (1993).

39. C. E. Kibbey, M. R. Savina, B. K. Parseghian, A. H. Francis, M. E. Meyerhoff, Anal. Chem., 65, 3717-3719 (1993).

40. J. Xiao, M. R. Savina, G. B. Martin, A. H. Francis, M. E. Meyerhoff, J. Am. Chem. Soc., 116, 9341-9342 (1994).

41. J. Xiao, M. E. Meyerhoff, J. Chromatogr. A, 715, 19-29 (1995).

42. G. B. Martin, J. Xiao, M. R. Savina, M. Wilks, A. H. Francis, M. E. Meyerhoff, "Efficient Separation of Fullerenes on Porphyrin-Silica Stationary Phases Using Strong Mobile Phase Solvents," in Fullerenes, K. M. Kadish, R. S. Ruoff, eds., The Electrochemical Society, Pennington, 1994, pp. 178-190.

43. F. B. Alvey, J. Appl. Polymer Sci., **13**, 1473-1486 (1969).

44. J. Xiao, M. E. Meyerhoff, Anal. Chem., submitted for publication.

45. C. F. Poole, S. A. Schuette, **A Contemporary Practice of Chromatography**, Elsevier, New York, 1984, Chapter 4.

46. M. R. Savina, G. B. Martin, J. Xiao, N. Milanovich, M. E. Meyerhoff, A. H. Francis, "Chromatographic Isolation and EPR Characterization of La$@C_{82}$," in **Fullerenes**, K. M. Kadish, R. S. Ruoff, eds., The Electrochemical Society, Pennington, 1994, pp. 1309-1319.

47. D. H. Parker, et al., J. Am. Chem. Soc., **113**, 7499-7503 (1991).

48. J. Xiao, M. E. Meyerhoff, unpublished results.

49. W. Kratschmer, L. D. Lamb, K. Fostiropoulos, D. R. Huffman, Nature, **347**, 354-358 (1990).

50. K. Kimata, T. Hirose, K. Moriuchi, K. Hosoya, T. Araki, N. Tanaka, Anal. Chem., **67**, 2556-2561 (1995).

51. A. M. Vassallo, A. J. Palmisano, L. S. K. Pang, M. A. Wilson, J. Chem. Soc., Chem. Commun., 60-61 (1992).

52. D. M. Cox, S. Behal, M. Kisko, S. M. Gorun, M. Greaney, C. S. Hsu, E. B. Killin, J. Millar, J. Robbins, W. Robbins, R. D. Sherwood, P. J Tindall, J. Am. Chem. Soc., **113**, 2940-2944 (1992).

53. K. Jinno, Y. Saito, Y. Chen, G. Luehr, J. Archer, J. C. Fetzer, W. R. Biggs, J. Microcol. Sep., **5**, 135-140 (1993).

54. K. Kikuchi, et al., Chem. Phys. Letters, **216**, 67-71 (1993).

55. D. L. Stalling, K. C. Kuo, C. Y. Guo, S. Saim, J. Liq. Chromatogr., **16**, 694-722 (1993).

56. D. S. Tse, R. S. Ruoff, D. C. Lorents, R. Malhotra, "Preparative and Semipreparative HPLC of Fullerenes on Silica-Bonded Dinitro-anilinopropyl Phase," in **Fullerenes**, K. M. Kadish, R. S. Ruoff, eds., The Electrochemical Society, Pennington, 1994, pp. 191-199.

57. Y. Saito. H. Ohta, H. Nagashima, K. Itoh, K. Jinno, M. Okamoto, Y. Chen, G. Luehr, J. Archer, J. Liq. Chromatogr., **17(11)**, 2359-2372 (1994).

58. K. Yamamoto, H. Funasaka, T. Takahashi, J. Phys. Chem., **98**, 2008-2011 (1994).

59. S. Suzuki, Y. Kojima, Y. Nakao, T. Wakabayashi, S. Kawata, K. Kikuchi, Y. Achiba, T. Kato., Chem. Phys. Letters, **229**, 512-516 (1994).

60. S. Stevenson, H. C. Dorn, P. Burbank, K. Harich, J. Haynes, Jr., C. H. Klang, J. R. Salem, M. S. DeVries, P. H. M. van Loosdrecht, R. D. Johnson, C. S. Yannoni, D. S. Bethunre, Anal. Chem., **66**, 2675-2679 (1994).

61. Y. Saito, H. Ohta, H. Nagashima, K. Itoh, K. Jinno, M. Okamoto, Y. Chen, G. Luehr, J. Archer, J. Liq. Chromatogr., **18(10)**, 1897-1908 (1995).

62. K. Jinno. K. Nakagawa, Y. Saito, H. Ohta, H. Nagashima, K. Itoh, J. Archer, Y. Chen, J. Chromatogr. A, **691**, 91-99 (1995).

63. Y. Saito, H. Ohta, H. Nagashima, K. Itoh, K. Jinno, J. Microcol. Sep., **7**, 41-49 (1995).

64. D. E. Coutant, M. E. Meyerhoff, unpublished results.

65. N. Chaniotakis, S. Park, M. E. Meyerhoff, Anal. Chem., **61**, 566-570 (1989).

66. N. Chaniotakis, A. Chasser, M. E. Meyerhoff, J. Groves, Anal. Chem., **60**, 185-188 (1988).

67. E. Malinowska, M. E. Meyerhoff, Anal. Chem. Acta, **300**, 33-43 (1994).

68. L. G. Sillén, **Stability Constants of Metal-Ion Complexes**, Supplement No. 1. The Chemical Society, London, 1971, pp. 339-341, pp. 452-455.

69. J. E. Falk, **Porphyrins and Metalloporphyrins: Their General, Physical and Coordination Chemistry and Laboratory Methods**, Elsevier, Amsterdam, 1964, Chapter 2.

70. B. Dempsey, J. N. Phillips, Abstracts of I.U.P.A.C. Symposium on Natural Products, Australian Academy of Science, Canberra, 1960, p6.

71. M. Belew, J. Porath, J. Chromatogr., **516**, 333-354 (1990).

72. M. Belew, T. T. Yip, L. Andersson, R. Ehrnström, Anal. Biochem., **164**, 457-465 (1987).

73. G. Muszynska, Y. J. Zhao, J. Porath, J. Inorg. Biochem., **26**, 127-135 (1986).

74. L. Andersson, E. Sulkowski, J. Porath, J. Chromatogr., **421**, 141-146 (1987).

75. D. Dolphin, ed., **The Porphyrins**, Vol. 5, Academic Press, New York, 1978. Chapter 7.

CHIRAL RESOLUTION OF DIPEPTIDES BY LIGAND EXCHANGE CHROMATOGRAPHY ON CHEMICALLY BONDED CHIRAL PHASES

Gerald Gübitz,* Burkhard Vollmann, Giuseppe Cannazza, Martin G. Schmid

Institute of Pharmaceutical Chemistry
Karl-Franzens-University of Graz
Universitätsplatz 1
A-8010 Graz, Austria

ABSTRACT

This paper deals with studies on the optical resolution of glycyl-DL-amino acid dipeptides and diastereomeric dipeptides on three different chemically bonded chiral ligand exchange chromatography (LEC)-phases. The phases were prepared by binding L-proline or L-hydroxyproline to silica gel using different silanes as spacer. Using 10^{-5} M copper(II) sulfate as a mobile phase, eleven glycyl-dipeptides were resolved, nearly all of them with baseline separations. Several dipeptides containing two stereogenic centres were at least partially resolved into the four stereoisomers.

INTRODUCTION

Dipeptides are compounds of tremendous biological interest. Since the biological activity is mostly restricted to one of the enantiomers, the separation of the optical isomers has become increasingly important. Chiral separation of dipeptides is also of interest in protein research since certain peptide

2933

sequencing methods result in cleavage into dipeptide fragments. The optical purity control of the building blocks and the check for racemization processes in peptide synthesis are other important aspects.

Enantiomer separation of glycyl-DL-amino acid dipeptides (Gly-X-dipeptides) was done by LEC using chiral mobile phase additives[1] or chiral stationary phases[2] and by host-guest complexation using cyclodextrin-[3] or crown ether phases.[4,5] Furthermore, the use of TLC for the resolution of dipeptides has been described.[6] Several authors report the resolution of dipeptides containing two stereogenic centres into the two diastereomers; however, up to now only a few papers have described the chiral resolution of diastereomeric dipeptides into all four possible stereoisomers. Indirect separation of the stereoisomers of some dipeptides was carried out by Florence et al. using OPA and N-acetyl-L-cystein for chiral derivatization.[3] Oi et al. resolved some diastereomeric dipeptides by GC in the form of their N-TFA-isopropyl esters.[7] Hyun et al. resolved dipeptide methyl esters as their 3,5-dinitrobenzoyl derivatives using a chiral phase based on (S)-1-(6,7-dimethyl-1-naphthyl)isobutylamine.[8] The first direct resolution of an underivatized diastereomeric dipeptide into the 4 isomers has been reported by Gübitz,[2] using a chemically bonded chiral LEC-phase Crownpack columns have been employed successfully for the optical resolution of a series of diastereomeric dipeptides by Hilton[4] and Esquivel et al.[5]

Recently, we succeeded in obtaining baseline resolutions of the stereoisomers of several diastereomeric dipeptides using (+)-18-crown-6-tetracarboxylic acid in capillary electrophoresis.[9]

This paper deals with comparative studies on three chemically bonded chiral LEC phases for the optical resolution of dipeptides.

EXPERIMENTAL

Chemicals And Materials

All reagents were of analytical grade. L-proline , L-hydroxyproline and copper(II) sulfate were obtained from Fluka (Buchs, Switzerland). 3-Glycidoxypropyltrimethoxysilane and 2-(3,4-epoxycyclohexyl)ethyltrimethoxysilane were purchased from Petrach Systems (Bristol, PA, USA), LiChrosorb 100, 5μm was obtained from Merck (Darmstadt, Germany). Dipeptides were from Bachem (Bubendorf, Switzerland) and from Sigma (Deisenhofen, Germany).
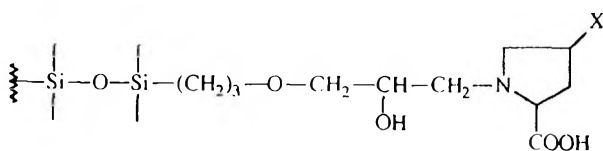
CSPIa: X=H
CSPIb: X=OH
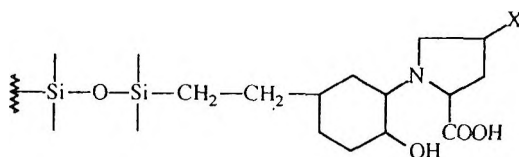
CSPIIa: X=H
CSPIIb: X=OH

Figure 1. Chemical structure of the CSPs investigated

Preparation of the CSPs:

CSP Ia and Ib (10): 4 g LiChrosorb 100, 5µm was suspended in 20 mL of toluene and after adding 2.4 mL of 3-glycidoxypropyltrimethoxysilane, the mixture was refluxed at 110°C with stirring for 6 h. The reflux condenser was kept at 65°C in order to remove the methanol formed in the reaction. The product was washed with toluene, methanol and acetone and dried at 50°C overnight. 4.4 g of either sodium prolinate (CSP Ia) or sodium hydroxy-prolinate (CSP Ib) dissolved in 40 mL of methanol were shaken with the product for 48 h at room temperature. The modified silica was washed with methanol and loaded with copper(II) ions by shaking with a 15% solution of copper(II) sulfate.

CSP IIa and IIb were prepared analogously, but 2-(3,4-epoxycyclohexyl) ethyltrimethoxysilane was used instead of 3-glycidoxypropyltrimethoxysilane.[11]

Elemental analysis: CSP Ib: C 9.2, H 1.4, N 0.7%
CSP IIa: C 9.0, H 1.4, N 0.6%
CSP IIb: C 9.5, H 1.6, N 0.6%
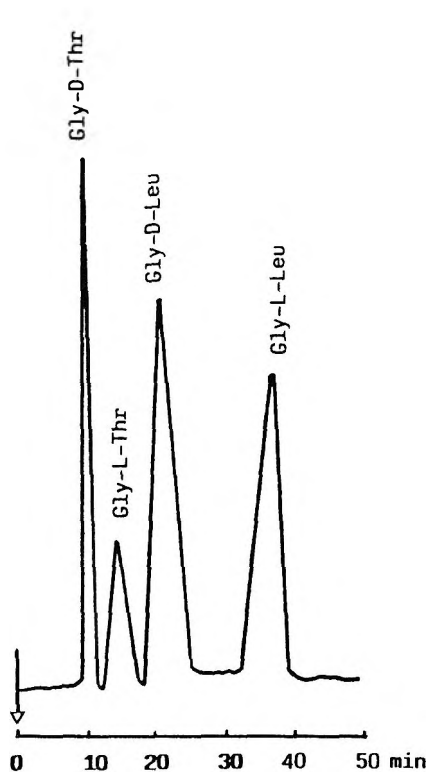
Figure 2. Chiral resolution of Gly-DL-Thr and Gly-DL-Leu on CSP IIb. Experimental conditions: Mobile phase: 10^{-5} M Cu(II), flow: 1 mL/min, Temp.: 50°C, detection: UV, 223 nm

HPLC Conditions

HPLC was performed using a Merck-Hitachi L-6200A intelligent pump and an L 4250 UV/VIS detector. Samples were injected by a Rheodyne Model 7161 six-port valve equipped with a 20 μl loop. The chiral phases were packed into stainless-steel columns (250 x 4.6 mm) by the descending slurry technique in methanol. As mobile phase a 10^{-5} M copper(II) sulfate solution was used in all cases.

Table 1

Chiral Resolution of Gly-X-Dipeptides on CSP Ib, IIa and CSP IIb

	Ib			IIa			IIb		
	k'_D	k'_L	α	k'_D	k'_L	α	k'_D	k'_L	α
Gly-DL-Ala	1.13	1.50	1.33	1.40	1.60	1.14	2.09	2.76	1.32
Gly-DL-Nval	1.94	3.00	1.55	n.d.	n.d.	n.d.	4.18	7.41	1.77
Gly-DL-Nleu	2.00	3.13	1.57	3.67	6.00	1.63	5.61	12.25	2.18
Gly-DL-Val	2.63	4.25	1.62	3.83	5.67	1.48	1.74	2.81	1.62
Gly-DL-Leu	3.00	5.00	1.67	5.30	8.17	1.54	5.19	10.32	1.99
Gly-DL-Phe	1.50	4.00	2.67	2.66	5.00	1.87	3.19	7.11	2.23
Gly-DL-Trp	2.19	8.13	3.71	n.d.	n.d.	n.d.	2.01	4.31	2.40
Gly-DL-Met	1.44	2.19	1.52	2.17	3.17	1.46	3.27	6.25	1.91
Gly-DL-Ser	0.75	1.00	1.33	1.50	1.96	1.31	0.71	0.71	1.00
Gly-DL-Thr	1.25	2.00	1.60	2.00	2.50	1.25	2.03	3.51	1.73
Gly-DL-Asn	0.94	1.25	1.33	1.10	1.10	1.00	1.53	2.12	1.39

Experimental conditions: Mobile phase: 10^{-5} M Cu(II), flow: 1mL/min, Temp.: 50°C, detection: UV, 223 nm, (n.d. = not determined).

RESULTS AND DISCUSSION

The surface coverage was comparable for all the three phases investigated. Based on the results of the elemental analysis the surface coverage was found to be about 2 μmol/m^2 on average for the different phases. Two different epoxyfunctional silanes, 3-glycidoxypropyltrimethoxysilane and 2-(3,4-epoxycyclohexyl)ethyltrimethoxysilane, were used as spacer (Fig.1). The cyclic moiety in the spacer of CSP II represents a more rigid structure element close to the chiral centre, which is expected to enhance stereoselectivity. CSP IIa containing L-proline as chiral selector ligand, has been shown to exhibit improved enantioselectivity for amino acids and hydroxy acids.[11] For the resolution of dipeptides, L-hydroxyproline as selector ligand was found to be superior to L-proline. The proline phase Ia showed almost no enantioselectivity for dipeptides. These results are in agreement with observations of Florence et al.,[3] who did not succeed in resolving dipeptides on Chirapack WH, which has identical structure with our CSP Ia. In the case of the phases containing the cyclic spacer, both the L-proline- (IIa) and L-hydroxyproline phase (IIb) resolved dipeptides; however, CSP IIb showed significantly higher α-values.
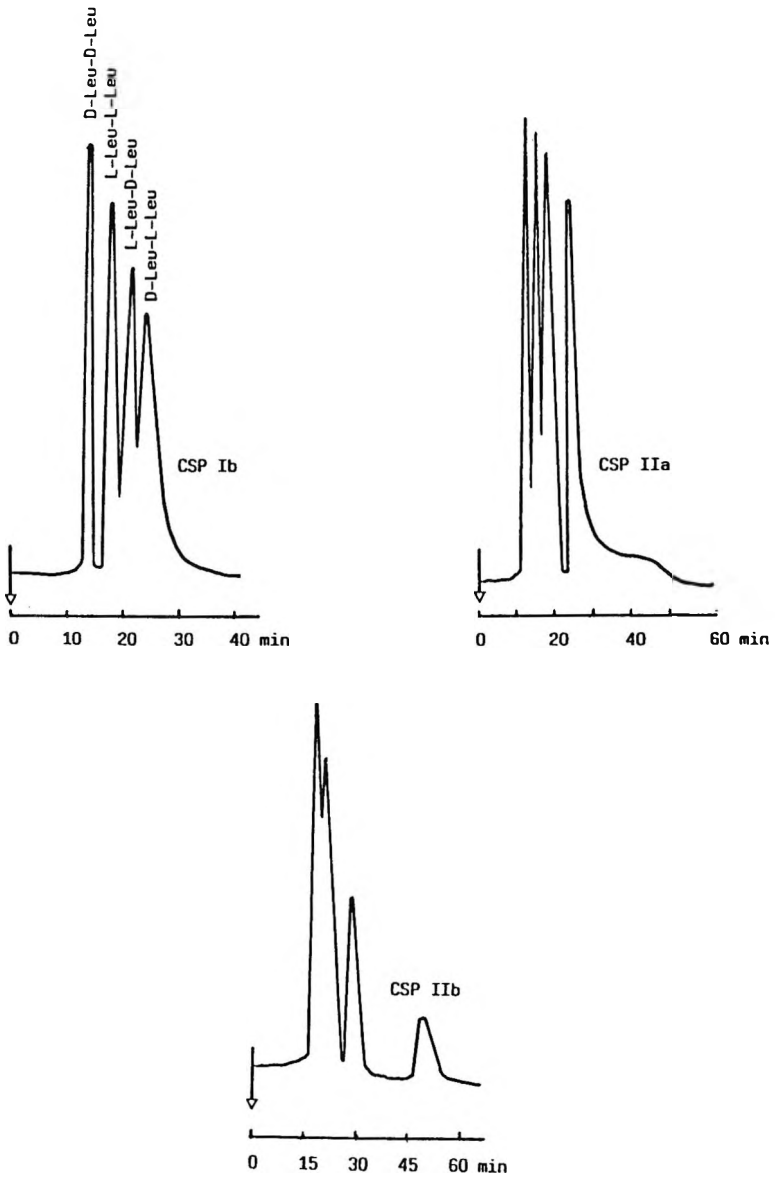
Figure 3 Chiral resolution of DL-Leu-DL-Leu on CSP Ib, IIa and IIb. Experimental conditions as in Fig.2
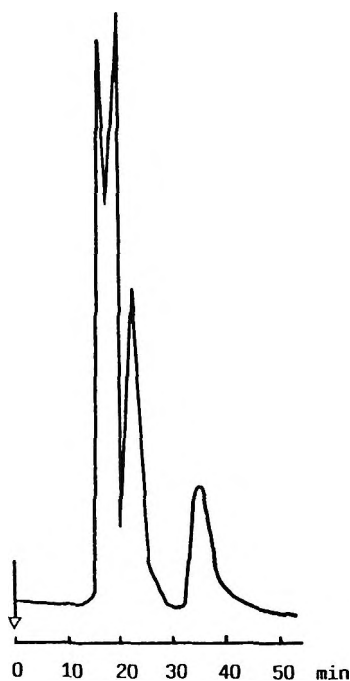
Figure 4. Chiral resolution of DL-Leu-DL-Val on CSP Ib. Experimental conditions as in Fig.2

While the pH optimum was found to be 4.5 for the resolution of amino acids,[10-12] resolution of dipeptides occurred only at pH 7. A 10^{-5} M copper(II) sulfate solution without any buffer turned out to be optimal. Raising the temperature to 50°C resulted in significant improvement in resolution.

Table 1 shows a comparison of the capacity factors and α-values for Gly-X-dipeptides on CSP Ib, IIa and IIb. CSP IIb showed the highest separation factors. Gly-X-dipeptides containing bulky and hydrophobic substituents were much better resolved than those with polar substituents. Nearly all Gly-X-dipeptides investigated showed baseline separation. The elution order was found to be D before L in all cases indicating a stronger complexation of the L-enantiomer with the chiral selector. The same elution order was observed for amino acids.[10-12] Fig.2 shows the resolution of Gly-DL-Thr and Gly-DL-Leu on CSP IIb.

GÜBITZ ET AL.

Table 2

Chiral Resolution of Diastereomeric Dipeptides on CSP Ib, CSP IIa and CSP IIb

	CSP Ib				CSP IIa				CSP IIb			
	k'_1	k'_2	k'_3	k'_4	k'_1	k'_2	k'_3	k'_4	k'_1	k'_2	k'_3	k'_4
DL-Leu-DL-Leu	0.78	1.00	1.39	3.22	5.0	5.7	9.7	16.7	2.56	3.67	4.62	5.54
DL-Leu-DL-Val	0.78	1.00	1.56	2.94	1.7	1.7	3.8	6.4	2.36	2.64	3.10	3.89
DL-Ala-DL-Ser	0.11	0.11	0.18	0.18	0.79	0.79	0.79	0.79	0.68	0.68	0.68	0.68
DL-Leu-DL-Ala	0.60	0|64	0.73	1.13	1.77	1.77	2.26	3.01	1.29	1.29	1.50	2.15
DL-Leu-DL-Phe	0.55	0.89	1.00	1.78	4.53	4.53	8.16	12.56	3.62	3.62	5.50	7.73
DL-Ala-DL-Val	0.55	0.69	0.82	1.78	2.84	2.84	3.33	6.60	1.62	1.62	2.07	3.01
DL-Leu-DL-Tyr	n.d.	n.d.	n.d.	n.d.	2.7	2.7	5.8	8.0	n.d.	n.d.	n.d.	n.d.

Experimental conditions as in Table 1, (n.d. = not determined).

Partial resolution was also obtained with dipeptides containing 2 stereo-genic centres. In this case CSP Ib showed the best results (Table 2). Six diastereomeric dipeptides were at least partially resolved into the four possible stereoisomers. Fig. 3 shows a comparison of the resolution of DL-Leu-DL-Leu on the three phases investigated. The elution order was DD, LL, LD and DL on all phases. Different elution profiles were observed on the different phases. While on CSP Ib the enantiomeric pairs DD and LL showed baseline resolution, on CSP IIa and IIb the enantiomeric pairs LD and DL were baseline resolved. The other peaks overlapped partially. The differing peak size of the isomers is due to abnormal isomer composition, which varies among different commercial products. Similar observations have been reported by Esquivel et al.[5] The elution order was determined for DL-Leu-DL-Leu only since in the case of the other diastereomeric dipeptides the individual stereoisomers were not available. Fig.4 shows the resolution of DL-Leu-DL-Val on CSP Ib.

Studies on the structure of the mixed complex between the selector ligand and the dipeptides are in progress.

REFERENCES

1. W. Lindner, J. N. Le Page, G. Davies, D. E. Seitz, B. L. Kager, J. Chromatogr., **185**, 323 (1979).

2. G. Gübitz, J. Liq. Chromatogr., **9**, 519 (1986).

3. J. Florance, A. Galdes, Z. Konteatis, Z. Kosarych, K. Langer, and C. Martucci, J. Chromatogr., **414**, 313 (1987).

4. M. Hilton, and D. W. Armstrong, J. Liq. Chromatogr., **14 (20)**, 3673 (1991).

5. B. Esquivel, L. Nicholson, L. Peerey, J. High Resolut. Chromatogr., **14**, 816 (1991).

6. K. Günther, J. Martens, M. Schickedanz, Angew. Chem. Int. Ed. Engl., **25**, 278 (1986).

7. N. Oi, M. Horiba, H. Kitahara, H. Shimada, J. Chromatogr., **202**, 302 (1980).

8. M. H. Hyun, I.-K. Balk, W. H. Pirkle, J. Liq. Chromatogr., **11**, 1249 (1988).

9. M. G. Schmid, G. Gübitz, J. Chromatogr. A, **709**, 81 (1995).

10. G. Gübitz, W. Jellenz, F. Juffmann, Chromatographia, **16**, 103 (1982).

11. G. Gübitz, S. Mihellyes, G. Kobinger, A. Wutte, J. Chromatogr. A, **666**, 91 (1994).

12. G. Gübitz, W. Jellenz, W. Santi, J. Chromatogr., **203**, 377 (1981).

SYNTHESIS AND CHARACTERIZATION OF SILICA-IMMOBILIZED SERUM ALBUMIN STATIONARY PHASES FOR HPLC

V. Tittelbach,[1] M. Jaroniec, R. K. Gilpin

Separation and Surface Science Center
Department of Chemistry
Kent State University
Kent, Ohio 44242

[1]Current address:
Agricultural Research Division
American Cyanamid Company
Princeton, NJ 08543

ABSTRACT

Chiral HPLC stationary phases based on immobilized bio-polymers (i.e., proteins, enzymes, antibodies etc.) are of growing importance for the separation and purification of enantiomeric compounds, especially in the areas of biological, pharmaceutical, and clinical chemistry. In the work described in this paper, several silica-immobilized serum albumin phases were synthesized and characterized by a variety of techniques. Low-temperature nitrogen adsorption isotherms were measured and employed to evaluate the surface characteristics of the stationary phases as a function of both the immobilization matrix and the surface modification chemistry. Elemental analysis and high resolution thermogravimetry were used to evaluate the surface coverages at each stage of modification. Based on these results,

2943

surface parameters such as the specific surface area, pore size distribution, bonding density, etc. were calculated, as well as the changes of these parameters as a function of the modification chemistry were analyzed.   Different silicas of varying mean pore diameter from 30 nm to 400 nm were used.

INTRODUCTION

One of the fastest expanding areas of liquid chromatography is the separation of enantiomers using direct methods[1] (i.e., using chiral selective stationary phases).   While a large number of applications of protein phases have been published, a majority of the work has focused on more practical aspects of the separation.   On the other hand, mechanistic considerations often have not been elucidated fully.

In the field of chiral HPLC a significant improvement in the performance of protein based columns was achieved with the introduction of silica as the support matrix.[2]   The advantages of using silica,   compared to agarose and other commonly employed matrices for biochemical separations, are better mechanical stability and highly reproducible geometrical features, such as particle shape and diameter as well as pore size distribution. Likewise, the modification chemistry for altering the surface of the silica is well established. However, pH instability as well as chemical and energetic heterogeneity of silica-based stationary phases are potential problems.

It is important for the optimization of a separation , as well as for the development of new stationary phases, to fully understand the mechanisms which governs the solute's retention. Such knowledge makes it possible to take advantage of, or to exclude, certain forces in order to control the separation process.   This is particularly true for protein-based chiral stationary phases (CSPs) due to the intrinsically higher heterogeneity of this type of packing. Thus, the purpose of the current study has been to investigate various parameters that influence the physicochemical properties of a specific class of CSPs, silica-immobilized serum albumins.

There are a number of protein-based CSPs commercially available.   The most important ones are silica-based bovine and human serum albumin (BSA and HSA, respectively), α_1-acid glycoprotein (AGP), and ovomucoid (OVM) materials.   While AGP CSPs have the broadest utility,[3] immobilized serum albumins are considered to be more important proteins for the separation of neutral and acidic chiral species.[4]   Even though only a few different types of protein-based CSPs are commercially available, there are numerous accounts in

the literature which describe other protein phases, such those based on immobilized cellobiohydrolase (CBH-1),[5-7] avidin,[8] trypsin,[9] α-chymotrypsin,[10,11] lysozyme,[12,13] or ovotransferrin.[14] For a general review see Ref.[15]

Except for cases where the protein exhibits very strong interactions with the support matrix, it is necessary to covalently anchor the molecule to the surface.[16,17] Several different pathways of immobilization have been described in the literature. One of the commonly employed techniques involves the use of glutaric dialdehyde as bifunctional reagent to link proteins to amino-derivatized silica. This technique was used in the current study.

Investigations of parameters influencing the chromatographic performance of serum albumin based stationary phases have been reported by several groups. A series of studies have been carried out by Allenmark and coworkers over the years. While their first approaches utilized agarose-immobilized BSA,[16,18] the later work took advantage of the better chromatographic performance of silica-based stationary phases[19,21] and examined various modification techniques and cross-linking agents.[22-24] Other related investigations include the work of Aubel and Rogers,[25,26] who examined the influence of column pretreatment on the enantioselectivity of silica-immobilized BSA phases and that of Dabulis and Klibanov[27] who reported an increase in the binding properties of free BSA in non-aqueous media. However, Gilpin et al.[28] so far have published the only account which describes the use of silica-immobilized BSA in the normal-phase mode. They also found novel applications of this type of stationary phases for GC.[29,30] Additionally, the same group studied the influence of temperature, pH, solute concentration, and other parameters, upon the enantiospecific separation of tryptophan via BSA CSPs.[31-33]

Unlike the above studies which investigated the properties of protein-based CSPs under chromatographic conditions, the current work is focused on the effect of the immobilization chemistry upon the physicochemical properties of the silica matrix via nitrogen adsorption measurements.

MATERIALS

The LiChrospher Si 300 silica (particle diameter 10 μm), which was used to prepare most of the albumin phases, was purchased from EM Separations (Gibbstown, NJ, USA). The other silica samples tested (LiChrospher Si 500, LiChrospher Si 1000, LiChrospher Si 4000, and LiChrospher Si 300 WP), were donated by EM Separations . The γ-aminopropyl triethoxysilane was from

Hüls-America (Piscataway, NJ) and the glutaric dialdehyde (25% solution in water) was from the Aldrich Chemical Co. (Milwaukee, WI, USA). The different serum albumins (i.e., bovine, human, pig, sheep, and horse; essentially fatty acid free), the sodium cyanoborohydride, the sodium phosphate (reagent grade) were obtained from the Sigma Chemical Co. (St. Louis, MO). The deionized water was purified in-house using either a Milli-Q (Millipore, El Paso, TX, USA) or Ionpure Plus 150 (Ionpure, Lowell, MA, USA) reagent water system. All HPLC solvents (HPLC grade), the toluene (ACS specified grade), and the potassium chloride (reagent grade) were from Fisher Scientific (Pittsburgh, PA, USA).

METHODS

Synthesis of Stationary Phases

The silica-immobilized serum albumin stationary phases were prepared according to a modification of a previously reported three-step synthesis.[33] Each step in this procedure was monitored by microcombustion analysis in order to measure the carbon and nitrogen loadings. Initially, the silica was derivatized with γ-aminopropyl triethoxysilane to yield an amino functionality at the surface. An overview of the modification chemistry is given in Figure 1. For steric and probability reasons, most ligands are only anchored to the silica surface via one bond. However, cross-polymerization can yield multiple covalent linkages. For most cases, batches of five grams of each silica were modified at one time. In order to control the amount of physisorbed water at the silica surface, the starting silica was carefully hydrated, followed by a drying step. Specifically designed glass reaction flasks were employed. This was followed by the addition of the γ-aminopropyl triethoxysilane. In steps two and three, the amine surface was first activated, using glutaric dialdehyde as bifunctional reagent, and than the protein was anchored to the silica surface (see reaction scheme in Figure 1). At each step, the progress was monitored by taking a small sample for microcombustion analysis.

Column Packing

Stainless steel columns of dimensions of 15 cm x 0.21 cm I.D. were made from HPLC tubing purchased from Handy & Harman (Norristown, PA, USA). The column blanks were thoroughly cleaned, end fittings were attached and the modified silicas were packed into them using a iso-propanol slurry procedure described previously.[34]
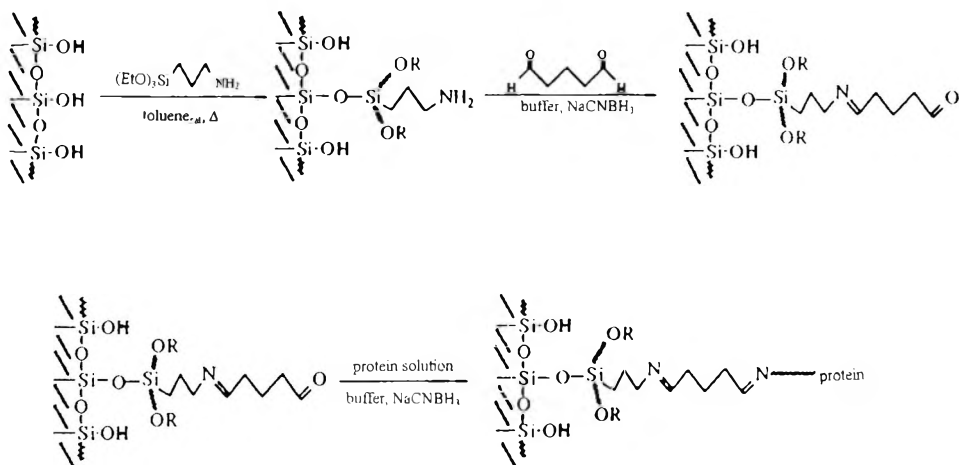
Figure 1. Silica modification chemistry.

The packing system was pressurized to about 6000 psi using a Haskel (Burbank. CA, USA) model DST-162-52 air driven fluid pump. Methanol was used as the carrier solvent, and the packing was continued for around two hours.

Surface Characterization

Each step in the surface modification process was monitored using microcombustion analysis that was carried out, first by Huffman Laboratories (Golden. CO. USA) and later in-house, using a LECO model CHNS-932 (LECO Co.. St. Joseph. MI, USA) elemental analyzer. In the latter case, usually three repeats were performed and the results averaged.

The physicochemical properties of the silica samples were evaluated by recording nitrogen adsorption isotherms. The instrument employed was an ASAP 2000 adsorption analyzer (Micromeritics Instrument Corporation, Norcross, GA. USA). Prior to each analysis, the sample tube was carefully washed and dried. About 400 mg of each sample were weighted out and degassed under high vacuum (around 2 μm Hg) for four hours at 100 °C. The final weight was determined after back-filling with analysis gas (dry nitrogen), and then the complete isotherm was recorded at the temperature of liquid nitrogen (i.e., 195.8°C).

Calculations of the BET specific surface area, monolayer capacity, pore size distribution, total pore volume and micropore volume were carried out using the manufacturer's software package.

High resolution thermogravimetric analysis (TGA), was carried out on the stationary phases studied over a range from ambient temperature to 1000 °C, and the degassing temperature was chosen on the basis of these measurements. In doing this, a TA 2950 high resolution analyzer (TA Instruments, Inc., New Castle, DE, USA) was used for studying the thermal properties of the samples.

Chromatographic Measurements

After the packing procedure was complete and prior to carrying out any chromatographic separations, all columns were conditioned overnight at a flow rate of 0.1 mL/min with the aqueous mobile phase. Then, before use, each of the columns was conditioned at the desired flow rate and temperature for another 30 minutes.

Different sets of chromatographic experiments were carried out on either one of two different HPLC systems. One of this was a Spectra Physics (San Jose, CA, USA) liquid chromatograph consisting of a model 8810 precision isocratic pump, a model spectra 100 series variable wavelength UV detector set to 254 nm, and a model 4400 Chromjet integrator, connected to a PC for data collection. The samples were injected using a Rheodyne (Berkeley, CA, USA) model 7125 six-port injection valve. equipped with a 20 μL sample loop and a position sensor that automatically started the runs.

The temperature of the column and the injection valve were controlled to ± 0.1 °C using a Fisher Scientific (Pittsburgh, PA, USA) model 9500 Isotemp refrigerated circulator bath. while the flow rate was monitored via a Phase Separation (Queensferry, Clwyd., UK) model F1080A digital flowmeter. The experiments were carried out by setting the pump to a value corresponding to a measured flow of 1.00 mL/min. (± 0.02).

The other system was a Varian (Walnut Creek, CA, USA) HPLC consisting of a model 9012 series inert gradient pump, a model 9050 programmable UV detector, and a model 9100 autosampler. The temperature of the column was controlled to 20 °C (± 0.2) using a water bath equipped with a Haake (Karlsruhe, Germany) model DC-1 immersion heater/circulator and a Neslab (Portsmouth, NH, USA) model EN-350 Flowthru Cooler.

The flow rate was monitored at the detector outlet, using a Varian Optiflow 1000 digital flow meter. The system was connected to a PC for system control, data collection and manipulation, using the vendor-provided software package.

RESULTS AND DISCUSSION

Elemental Analysis

In order to determine the qualitative and quantitative changes introduced during synthesis, elemental analysis for carbon and nitrogen was carried out and the resulting data were used to evaluate the degree of the surface coverage by using the following relationship:[35]

$$N_1 = \frac{\%C_1}{1200n_{c,1}(MW_1 - 1)} \tag{1}$$

where %C is the experimentally determined value, $n_{c,1}$ is the number of carbon atoms per attached ligand, MW_1 is the molecular weight of the ligand, and N_i is the number of moles of ligand attached in each step.

In doing this, it was assumed, that on average one ethoxy group remained attached to the silane silicon atom after the triethoxysilane reacted. Thus, the ligand introduced in the step 1 had the formula $-Si(OH)(OC_2H_5)(CH_2)_3NH_2$. The same notation is used for the second step (i.e., see Equation 2):

$$N_2 = \frac{\%C_2 N_1 (MW_1 - 1) - 1200N_1 n_{c,1}}{1200n_{c,2} - \%C_2 (MW_2 - 1)} \tag{2}$$

On average, the carbon load after the first step was 1.33%. Hence, the calculated surface coverage according to equation 1 was about 229 μmol ligands per gram sample.

Using the measured 60 m^2/g BET specific surface area of the silica and 8 μmol silanol groups/m^2, this value translates into a calculated coverage density I of about 47% of the available silanol groups. For mono-functional reagents this value is usually lower due to steric reasons.

Table 1

Physicochemical Properties for Serum Albumins

	BSA	HSA	SSA	PSA	ESA
# of C-atoms	2926	2908	2933	2981	2909
# of N-atoms	779	786	780	789	776
MW	66,236.6	66,410.6	66,263.1	66,536.2	65,593.0
% carbon	53.06	52.59	53.16	53.81	53.26
% nitrogen	16.47	16.58	16.49	16.61	16.57

For the second step of modification, the initial deposition of the amine ligand has to be taken into account. Equation 2 was used to calculate the subsequent conversion into the carbonyl intermediate phase. Based on solution reactivities, it was assumed that the activation via the aldehyde proceeded with almost quantitative yield. The average carbon load for the second step was 2.85%.

The amount of immobilized serum albumin was calculated using the differences between the carbon and nitrogen values prior and following the third modification step. These calculations were based on the data shown in Table 1 and can be found in Ref.[33]

Based on the values given in Table 1, the amount of protein immobilized in the third step averaged about 1 μmol per gram silica. The total carbon load for the silica-immobilized serum albumin stationary phases was between 6 and 7 %C, which is reasonable based on the relatively low specific surface area. Additionally, it was found previously[32] that maximizing the amount of protein anchored to the surface does not maximize the separation abilities of the resulting phase. This effect is shown in Figure 2, where the capacity factors for L-kynurenine and L-tryptophan are plotted vs. the normalized surface coverage. Clearly, an optimal protein coverage exists. This optimized modification procedure was used throughout the work.

Thermogravimetric Analysis

High resolution thermogravimetry (TGA) was employed for monitoring the progress of various synthetic steps. This method provides relatively fast results with good accuracy. Figure 3 shows a correlation between the weight
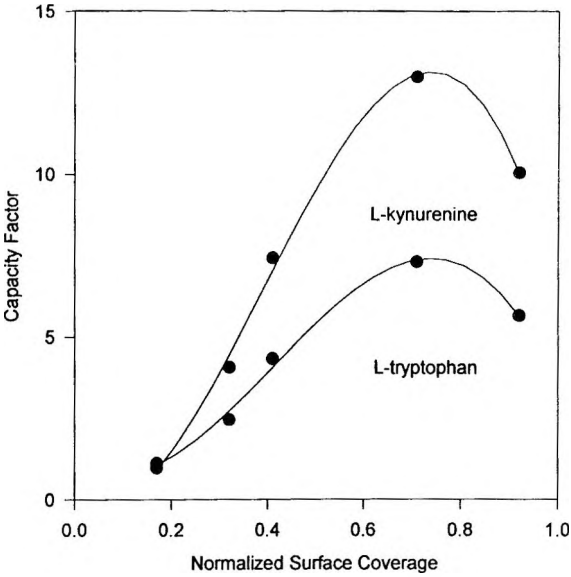
Figure 2. Influence of the BSA coverage on the solute's retention.
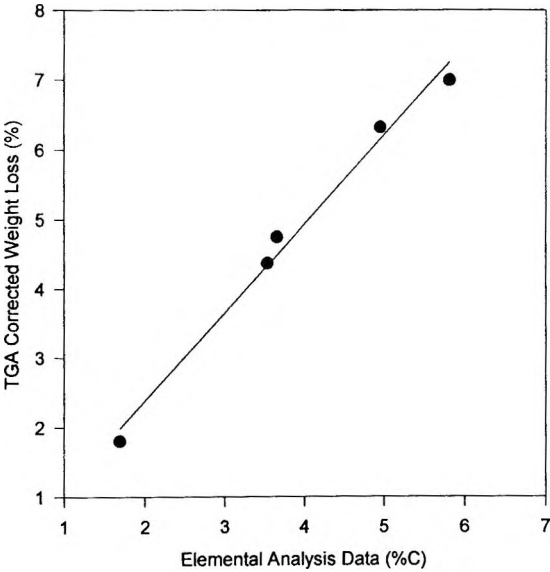
Figure 3. Correlation between the TGA data and elemental analysis.
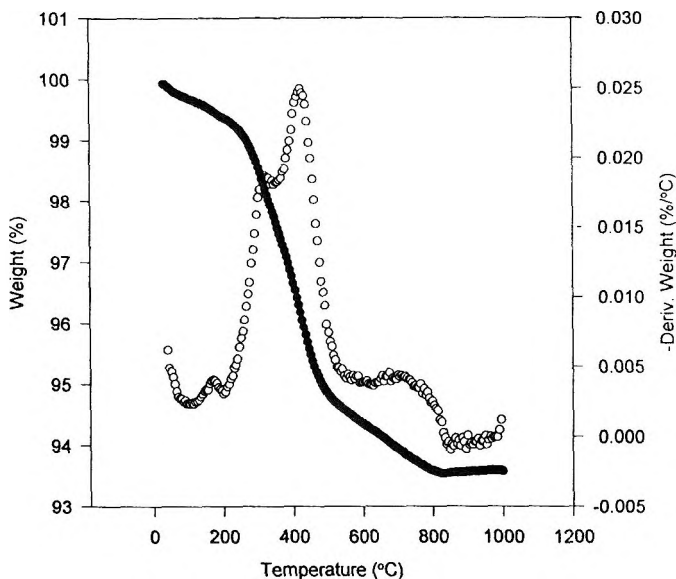
Figure 4. Typical thermogram for a silica-immobilized BSA phase, which contains the weight curve and its first derivative with respect to temperature.

loss, corrected for initial water loss, and the results from elemental analysis. An additional advantage of the TGA-based procedure was that it provides an estimate of the physically sorbed water. A typical thermogram is shown in Figure 4. Initially, up to 200 °C (under inert atmosphere), the physically adsorbed surface water was removed and then, the organic moiety burned off. The weight loss of this step was used to determine an approximate surface coverage, which needed a small correction for the weight loss due to the partial decomposition of residual surface silanols. The oxidation of the ligand was completed around 500 °C. The final loss was due to the condensation of the remaining surface silanol groups. Although this process overlaps the organic oxidation step, the error introduced by it is fairly small.

Influence of the Silica Characteristics on the Surface Coverage

For comparative purposes, four different silicas were used to immobilize BSA. In order to minimize size exclusion effects, all silicas had average pore diameters larger than 250 nm. All materials were modified using the methods described in the experimental section and the surface coverage for each step

was determined using elemental analysis. Additionally, the samples were evaluated via nitrogen adsorption in order to determine the BET specific surface areas. Applying the BET equation for the estimation of the specific surface area is by far the most widely used method.[36,37] By plotting the adsorption data for the relative pressure range of 0.05 to 0.30 according to the BET equation,[37] the monolayer capacity can be determined, which after multiplication by the molecular cross section of the probe molecule (i.e., nitrogen) and Avogadro's number gives the BET specific surface area. A summary of the resulting surface areas of the starting materials as well as the modified silica surfaces is shown in Table 2. All packings investigated were LiChrospher silicas. The Si 300, 1000 and 4000 silicas had an average particle diameter of 10 μm, and the remaining material was 5 μm. Furthermore, the LiChrospher Si 300 WP is a newer type of the 30 nm pore size material, that is called *wide pore* silica. Its specific surface area was slightly higher than the older materials. This increase may be due to the decrease in particle size and other factors.

Except for the Si 300 BSA material, the BET specific surface areas decreased following the BSA immobilization. One might expect that the surface area should increase after protein immobilization, since the BSA molecules might accommodate additional nitrogen molecules at their surface. However, the partial filling of pores (i.e., partial blocking of otherwise accessible surface area) seems to over-compensate this effect.

In addition to the BET specific surface areas, Table 2 contains the average pore sizes for the samples studied. There are different numerical methods available to calculate the average pore size from the nitrogen adsorption data. The values listed in Table 2 were calculated using the software package provided by the manufacturer of the adsorption instrument. These values were obtained on the basis of the pore size distributions calculated by using the BJH method that relates the volume adsorbed to the pore radius through the Kelvin equation.[38] The average pore diameter decreased, as expected, after modification with the exception of the Si 300 material. For the 100 and 400 nm materials, the average pore diameters could not be calculated, since the Kelvin equation is not applicable for materials that contain macropres..

The silica immobilized protein phases studied were tested chromatographically. The separation of D/L-tryptophan was used as a probe to evaluate the chromatographic performance of the synthesized phases. Chromatographic factors influencing that particular separation have been presented previously.[32,33] In the case of the 100 and 400 nm materials, this appears to be a surface area effect. Because of the low surface area available,

Table 2

Physicochemical Characteristics of Modified Silicas

Sample	%C	% N	S_{BET} [m^2/g]	$\overline{D}$ [nm]
Si 300	---	---	60	360
Si 300 amine	1.08	0.37	---	---
Si 300 aldeh.	2.97	0.44	---	---
Si 300 BSA	6.75	1.69	66	375
Si 500	---	---	68	390
Si 500 amine	1.64	0.63	---	---
Si 500 aldeh.	4.29	0.71	---	---
Si 500 BSA	5.81	1.30	66	320
Si 1000	---	---	27	---
Si 1000 amine	1.19	0.34	---	---
Si 1000 aldeh.	2.42	0.43	---	---
Si 1000 BSA	3.53	0.83	25	---
Si 4000	---	---	11	---
Si 4000 amine	0.43	0.09	---	---
Si 4000 aldeh.	1.05	0.13	---	---
Si 4000 BSA	1.69	0.35	9.7	---
Si 300 WP	---	---	84	340
Si 300 WP amine	1.82	0.61	---	---
Si 300 WP aldeh.	4.70	0.73	---	---
Si 300 WP BSA	4.95	1.02	72	280

the amount of immobilized BSA did not provide adequate numbers of binding sites required for enantiomeric separation (i.e., the columns were effectively overloaded). In the case of the 50 and 30 WP materials, it appears that synthesis conditions were not fully optimized. Since, the specific surface area of both starting materials are higher than for the standard 30 nm packing, it is reasonable to expect similar or higher protein coverage, i.e., better chromatographic performance. Also, the particle size of these materials was 5 μm and this factor should further enhance their chromatographic performance.

Interestingly, the coverage following the second modification step was much higher than expected for both silicas. However, the immobilization of the protein did not follow this trend. Contrary, the resulting BSA coverage was lower, compared to the "standard" 30 nm silica.

Influence of the Immobilization Chemistry

Although silica is both energetically and structurally heterogeneous,[39] it is further altered during the various modification steps. Changes in the pore size and energy distributions, which result from the protein modification, influence the chromatographic properties of the CSPs and they can be monitored via adsorption measurements.

Knowledge of the sorption and structural properties and their changes during modification is of great importance for understanding the mechanisms which govern the various chromatographic separations. A study of the sorption characteristics of serum albumin based CSPs was undertaken as an attempt to determine the physicochemical properties of the material at each step of the modification.

The complete (i.e., adsorption and desorption) isotherms shown in Figure 5 can be considered as type IV according to the common classification.[37] In the region of lower relative pressures, they reflect the formation of the monolayer, followed by multilayer adsorption. However, at high relative pressures (p/p_0 > 0.8) capillary condensation was observed. All of the isotherms show the same kind of hysteresis loop and its shape was not affected significantly by the subsequent steps of modification. The hysteresis loops resemble type H1, which has the adsorption and desorption branches almost vertical and nearly parallel over an appreciable range of relative pressures.[37] Type H1 of the hysteresis loop is observed for agglomerates made up of spheroidal particles of uniform size and shape. This is in good agreement with the manufacturer's claim of spherical particles with a narrow particle size distribution.

In order to examine the differences in the surface and structural properties of the unmodified silicas, intermediate materials and the final protein phases, a more detailed analysis of these isotherms was carried out. This analysis included the evaluation of the BET monolayer capacity (v_m), the BET specific surface area (S_{BET}), the total pore volume (V_t), the micropore volume (V_{mi}), and the average pore size ($\overline{D}$) for all surfaces. The results are shown in Table 3. The BET monolayer capacity and the BET specific surface area were calculated according to the BET equation by using the nitrogen adsorption data for the
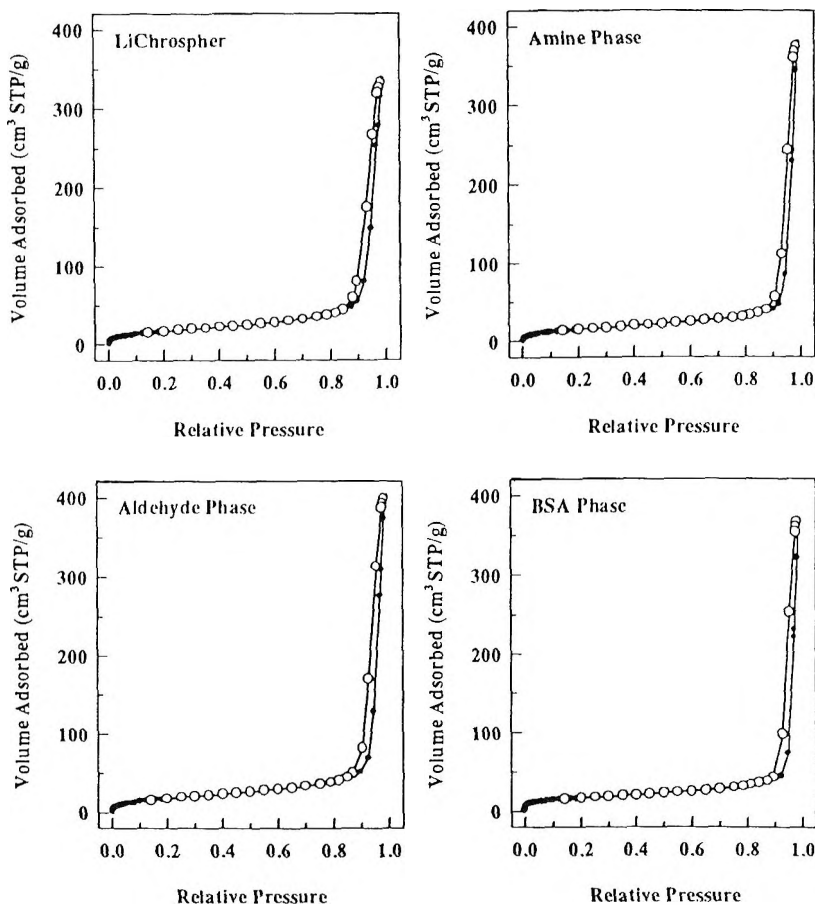
Figure 5. Complete isotherms for low temperature nitrogen adsorption on the starting material (LiChrospher 300), intermediate phases, and silica-immobilized BSA phase.

relative pressure range of 0.05 to 0.25. The total pore volume was evaluated from a single point measured at the relative pressure of about 0.975. The micropore volume, i.e., the volume of pores below 2 nm, was estimated by using the t-plot method,[37] which compares the adsorption isotherm studied with that measured on a nonporous reference material . For further discussion of the t-plot method see ref.[37] The average pore diameter ($\overline{D}$) was derived numerically from the adsorption isotherm using the BJH method developed by Barett, Joyner, and Halenda, which is based on the Kelvin equation.[38]
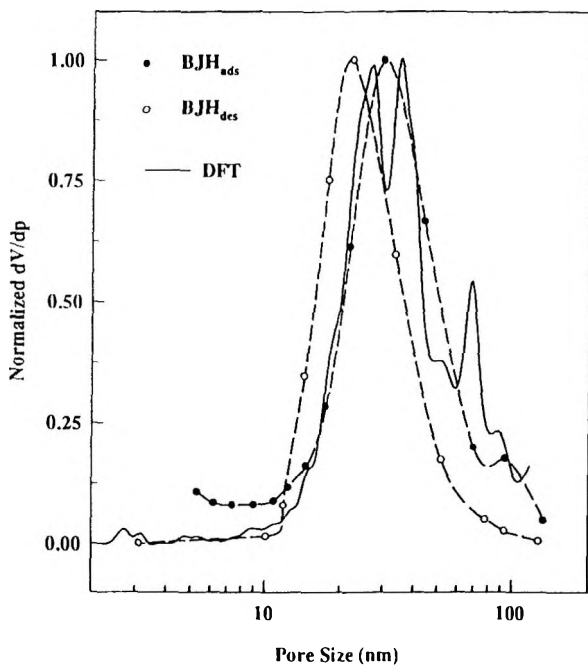
Figure 6. Normalized pore size distributions for Lichrospher Si 300

Table 3

Sorption Parameters of all Silica Surfaces Studies

Sample	V_m [cm^3 STP/g]	S_{BET} [m^2/g]	V_t [cm^3/g]	V_{mi} [cm^3/g]	$\overline{D}$ [nm]
LiChrospher Si 300	14.7	69	0.39	0.004	28.7
Amine Phase	12.8	56	0.35	0.004	25.3
Aldehyde Phase	15.6	68	0.43	0.005	25.1
BSA Phase	13.8	60	0.34	0.008	22.7
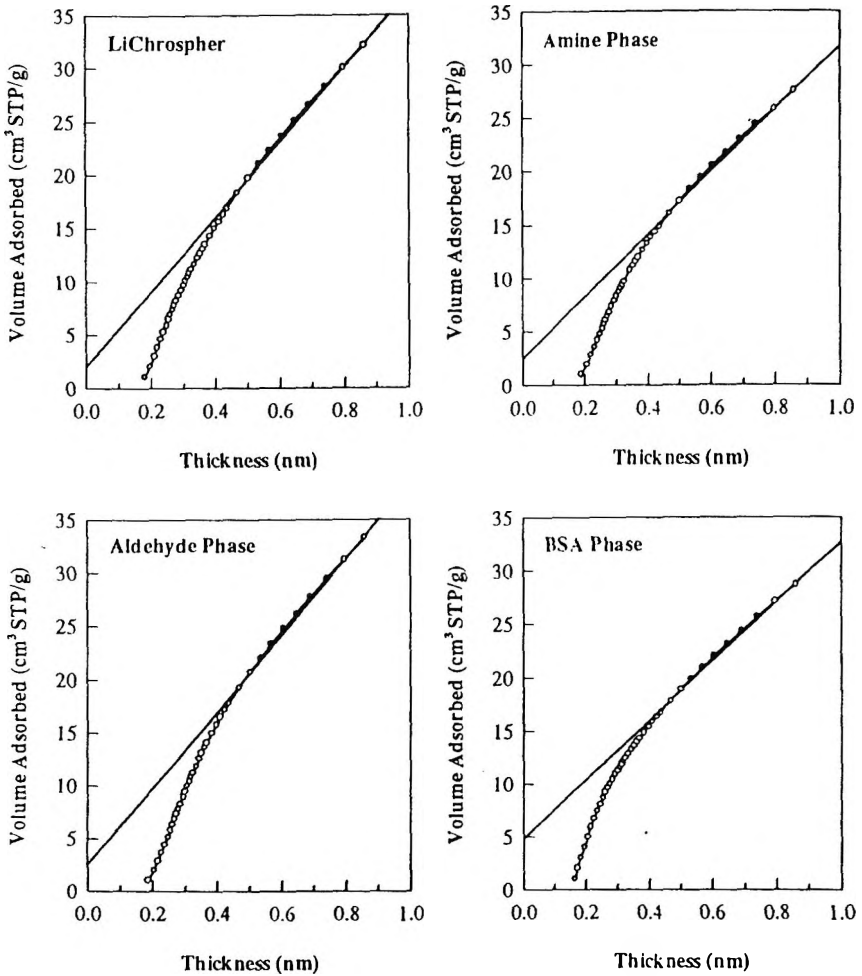
Figure 7. The t-plots for the starting material (LiChrospher 300), two intermediate phases and the BSA phase.

The data in Table 3 show that the micropore volume for all samples analyzed is negligible, as expected. Since the increase in this value for the BSA phase cannot be due to changes in the rigid structure of the support matrix, it has to be due to increased nitrogen adsorption capacity after protein immobilization. Since ligands were anchored to the surfaces during purification modification, the pore size was expected to decrease. The calculated values of the average pore diameter decrease as anticipated.
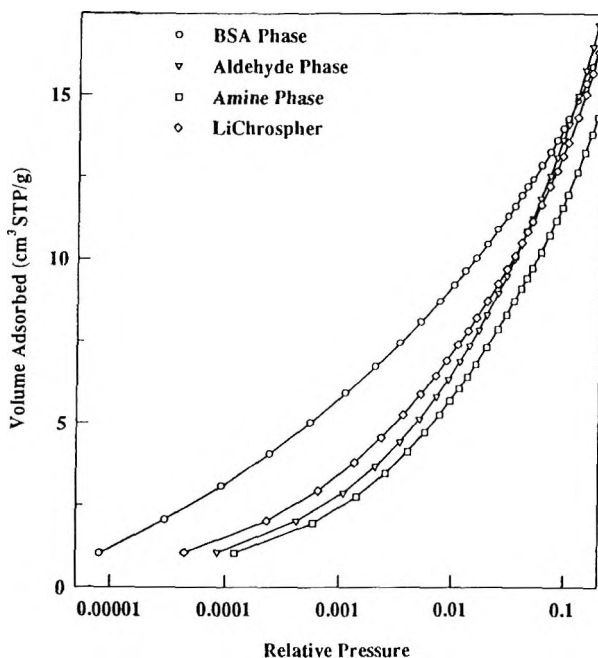
Figure 8. Low pressure branches of nitrogen adsorption isotherms for LiChrospher 300 and other phases studied

Accordingly, the pore diameter decreased from approximately 29 nm for the starting material (30nm according to the manufacturer's specification) to about 23 nm for the protein modified packings. In addition, the pore width data were estimated by an advanced computational method, which utilizes the incremental pore volume distribution obtained by combining the density functional theory (DFT) calculations for the local isotherm with a regularization method.[40]

The initial decrease in the BET surface area (and monolayer capacity) and the subsequent increase following the protein immobilization seem to be reasonable. However, the relatively high values of both parameters for the aldehyde phase cannot be explained conceivably.

Shown in Figure 6 is a comparison of the incremental pore volume distributions obtained by the BJH method with the DFT results for the starting silica matrix. Overall, there is a satisfactory agreement between the pore volume distributions obtained by various methods.
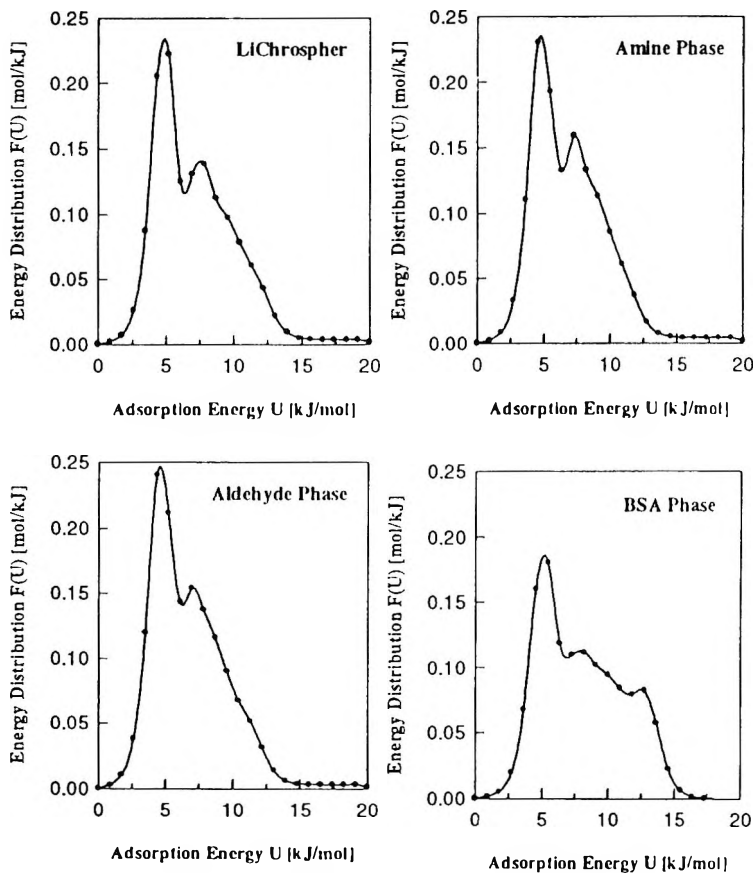
Figure 9. Adsorption energy distributions for LiChrospher 300 and other phases calculated from low temperature nitrogen adsorption isotherms.

It is important to note, however, that the DFT method was developed for the slit-like pore geometry, which is not optimal for sorbents like silica gels. The t-plot is a comparative method which was used to evaluate the microporosity of sorbents.[37] The t-plots for all phases studied are shown in Figure 7. There is no significant difference between these plots. A comparative plot of the low pressure regions for all four isotherms also is given in Figure 8. The branch corresponding to the BSA phase is distinctively different from the others. The amounts adsorbed by the BSA phase at very low
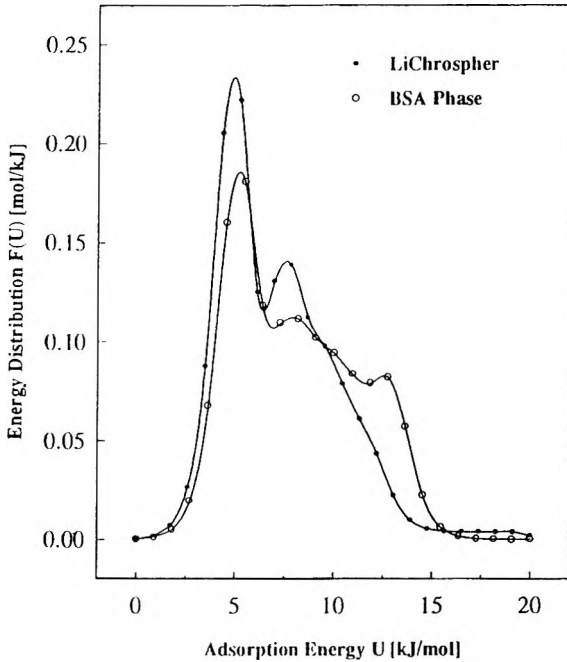
Figure 10. Energy distribution functions for the starting LiChrospher 300 silica (solid circles) and the BSA modified silica (hollow circles).

pressures are greater than those by the starting and intermediate phases. Although this observation can suggest high energetic heterogeneity of this phase, a quantitative comparison of the heterogeneity effects can be done by comparing the energy distributions for the systems studied.

The submonolayer adsorption data were utilized to calculate the adsorption energy distributions for all packings. Again, a regularization method was employed to invert the integral equation of adsorption with respect to the energy distribution.[41]

The energy distribution calculations were performed for the data points below the BET monolayer capacities given in Table 3. All parameters used were set according to previous studies.[42]

The resulting energy distributions for the four surfaces, as calculated from the low pressure nitrogen adsorption data, are shown in Figure 9. These graphs show, that the differences between the distribution curves for the starting silica,

the amine phase. and the aldehyde phase are very small. They have a distinct peak around 5 kJ/mol and a smaller one at about 8 kJ/mol. The smaller peak shows an almost linear tailing to approximately 13 kJ/mol, and a flat contribution in the energy range between 13 and 20 kJ/mol.

It is interesting, that the first and second steps of the silica modification do not change substantially its energetic heterogeneity with respect to nitrogen molecules. It appears. that the replacement of some silanol groups by either aminopropyl or aldehyde groups does not influence the nitrogen adsorption significantly. Other probe molecules could possibly be used to monitor this modification with respect to their adsorption affinities (i.e., argon. methane. benzene or others).

In contrast to the above observation, the BSA anchoring during the third modification step affects the adsorption energy distribution notably in its higher energy portion of the plot. while in the low energy portion it remains unchanged. Figure 10 shows an overlay of the energy distribution functions for the starting silica and the BSA modified silica. These distributions show a main peak around 5 kJ/mol for both phases, however the remaining part of the distribution function is significantly different. Although the smaller peak at 8 kJ/mol is still visible. its tailing is much more complex, exhibiting at least one more maxima at about 13 kJ/mol. A substantial portion of the fraction of sorption sites displaying higher adsorption energies (in the range from 8 to 13 kJ/mol) can be attributed to the energetically diverse structure of the protein. The disappearance of a small fraction in the energy range higher than 13 kJ/mol. however. possibly reflects the blocking of some high-energy silanol binding sites due to the third step of the modification.

REFERENCES

1. S. G. Allenmark in **Chiral Separations in Liquid Chromatography**, S. Ahuja (ed.). ACS Symposium Series, Washington, 1991. p. 471.

2. S. Allenmark, B. Bomgren. H. Borén, J. Chromatogr.. **264**. 63 (1983).

3. I. W. Wainer in **Drug Stereochemistry**, I.W. Wainer (ed.), Marcel Dekker, Inc., New York 1993.

4. H. J. Ritchie, Lab. Pract., **41 (12)**, 13 (1992).

5. P. Erlandsson, I. Marle, L. Hansson, R. Isaksson, C. Pettersson, G. Pettersson, J. Am. Chem. Soc., **112**, 4573 (1990).

6. I. Marle, P. Erlandsson, L. Hansson, R. Isaksson, C. Pettersson, G. Pettersson, J. Chromatogr., **586**, 233 (1991).

7. S. Hjertén, Y.-M. Li, J.-L. Liao, J. Mohammad, K. Nakazato, G. Pettersson, Nature, **356**, 810 (1992).

8. T. Miva, T. Miyakawa, Y. Miyake, J. Chromatogr., **457**, 227 (1988).

9. K. M. Kirkland, K. L. Neilson, D. A. McCombs, J. Chromatogr., **545**, 43 (19991).

10. I. W. Wainer, P. Jadaud, G. R. Schombaum, S. V. Kadodkar, M. P. Henry, Chromatographia, **25**, 903 (1988).

11. S. Thelohan, P. Jaduad, I. W. Wainer, Chromatographia, **28**, 551 (1989).

12. J. Haginaka, T. Murashima, C. Seyama, J. Chromatogr. A , **666**, 203 (1994).

13. W. Su, R. B. Gregory, R. K. Gilpin, J. Chrom. Sci., **31**, 285 (1993).

14. N. Mano, Y. Oda, T. Miva, N. Asakawa, Y. Yoshida, T. Sato, J. Chromatogr., **603**, 106 (1992).

15. S. Allenmark, S. Andersson, J. Chromatogr. A, **666**, 167 (1994).

16. S. Allenmark, B. Bomgren, H. Borén, J. Chromatogr., **237**, 473 (1982).

17. O. R. Zaborsky in **Immobilized Enzymes**, CRC Press, Cleveland 1973.

18. S. Allenmark, B. Bomgren, J. Chromatogr., **316**, 297 (1984).

19. S. Allenmark, B. Bomgren, H. Borén, J. Chromatogr., **316**, 617 (1984).

20. S. Allenmark, S. Andersson, J. Chromatogr. A, **351**, 231 (1994).

21. S. Allenmark, S. Andersson, J. Bojarski, J. Chromatogr., **436**, 479 (1988).

22. R. A. Thompson, S. Andersson, S. Allenmark, J. Chromatogr., **465**, 263 (1989).

23. S. Allenmark, S. Andersson, P. Erlandsson, S. Nilsson, J. Chromatogr., **498**, 81 (1990).

24. S. Andersson, R. A. Thompsson, S. Allenmark, J. Chromatogr., **591**, 65 (1992).

25. M. Aubel, L. B. Rogers, J. Chromatogr., **392**, 415 (1987).

26. M. T. Aubel, L. B. Rogers, J. Chromatogr., **408**, 99 (1987).

27. K. Dabulis, A. M. Klibanov, Biotech. Bioeng., **39**, 176 (1992).

28. W. Zhao, R. K. Gilpin, presented at the 46th Pittsburgh Conference, New Orleans, LA, 1995; paper 959.

29. L. Mayse, R. K. Gilpin, presented at the 46th Pittsburgh Conference, New Orleans, LA, 1995; paper 925.

30. L. Mayse, M.S. Thesis, Kent State University, Kent, OH, 1995

31. R. K. Gilpin, S.E. Ehtesham, R. B. Gregory, *Anal. Chem.*, **63**, 2825 (1991).

32. V. Tittelbach, R. K. Gilpin, Anal. Chem., **67**, 44 (1995).

33. V. Tittelbach, PhD. Dissertation, Kent State University, Kent, OH, 1995.

34. R. K. Gilpin, W. R. Sisco, J. Chromatogr., **194**, 285 (1980).

35. B. Buszewski, M. Jaroniec, R. K. Gilpin, J. Chromatogr. A, **673**, 11 (1994).

36. K. K Unger in **Packings and Stationary Phases in Chromatographic Techniques**, Chromatographic Science Series, vol. 47, K. K. Unger (ed.), Marcel Dekker, Inc., New York, 1990, p. 54.

37. S. J. Gregg, K. S. W. Sing in **Adsorption, Surface Area and Porosity**, Academic Press, London, 1982, p. 41.

38. E. P. Barett, L. S. Joyner, P. P. Halenda, J. Am. Chem. Soc., **73**, 373 (1983).

39. M. Jaroniec, R. Madey, **Physical Adsorption on Heterogeneous Solids**, Elsevier, Amsterdam 1988.

40. J. P. Olivier, W. B. Conklin, M. v. Szombathely, **Determination of Pore Size Distribution from Density Functional Theory: A Comparison of Nitrogen and Argon Results" in Characterization of Porous Solids III**, J. Rouquerol, F. Rodriguez-Reinoso, K. S. W. Sing, K. K. Unger (eds.), Elsevier, Amsterdam, 1992, p. 81.

41. M. v. Szombathely, P. Bräuer, M. Jaroniec, **J. Comput. Chem.**, **13**, 17 (1992).

42. M. Heuchel, M. Jaroniec, R.K. Gilpin, P. Bräuer, M. v. Szombathely, Langmuir, **9**, 2537 (1993).

LIPID MEMBRANE ANALOGUE-IMMOBILIZED SILICA GELS FOR SEPARATION WITH MOLECULAR RECOGNITION

Hirotaka Ihara,[1] Shoji Nagaoka,[2] Hideaki Tanaka,[1]
Sigeyoshi Sakaki,[1] Chuichi Hirayama[1]

[1] Department of Applied Chemistry & Biochemistry
Kumamoto University
Kurokami
Kumamoto 860, Japan

[2] Kumamoto Industrial Research Institute
Higashimachi
Kumamoto 862, Japan

ABSTRACT

The comb-shaped polymer (ODA$_n$) composed of a reactive terminal group and highly-orienting side-chain groups was prepared by telomerization using 3-mercaptopropyl trimethoxysilane and octadecylacrylate. The polymer was readily immobilized onto porous silica gels through a terminal reactive group. DSC indicated that the silica-supported polymer (Sil-ODA$_n$) underwent crystal-to-isotropic phase transition on silica gels at a temperature range of 28 - 47°C (in the case of n = 27) in methanol. Polarity microscopic observation of the polymer showed the phase transition included a nematic liquid crystalline state. The packed column showed a remarkably higher separation factor for mixtures of planar aromatics (e.g. triphenylene and *trans*-stilbene) and non-planar aromatics (e.g. *o*-terphenyl or *cis*-stilbene) at room temperatures than did the

2967

conventional hydrophobic stationary phases, i.e. octadecylated silica gels. In addition, the Sil-ODA$_n$ column showed remarkable temperature dependence on both retention capacity (k') and separation factor (α). The k'-temperature and α-temperature plots showed distinct bending at temperatures around the phase transition temperature of immobilized ODA$_n$. These results indicate that the selective retention for planar compounds is related to highly-orienting structure formed from long-chain alkyl groups. This paper discusses the molecular recognition mechanism using additional chromatographic behaviors and MOPAC calculation.

INTRODUCTION

Lipid membranes act as most important intermediaries for producing biofunctions including various chemical reactions and selective transportation. Immobilization of their functions on artificial carriers expands their possible applications, especially for separation chemistry purposes such as column chromatography. Therefore, various methods for stabilization and immobilization of lipid membranes have been developed, because lipid membranes are just aggregates which can be easily dissolved in organic media.

The polymerization of lipids[1-7] is a good technique for stabilizing lipid membranes. This polymerization is usually performed through introduction of polymerizable groups into either hydrophilic or hydrophobic moieties. In this technique, the molecular orientation of lipids can be maintained after polymerization, but causes remarkable suppression of molecular fluidity. Since membrane fluidity is an essential property for producing membrane functions, this loss is highly disadvantageous.

To alleviate this problem, Kunitake et al.[8] and Regen et al.[9,10] have developed lipid membrane systems containing polyions as counter ions. In this technique, the membrane stability was increased without damaging either molecular orienting or fluidity. Okahata et al. found that quartz-crystal microbalances covered with polyion-complexed lipid membranes could be used as sensing materials.[11,12] However, this stabilization technique is still not satisfactory for use as immobilized stationary phases for column and membrane separation processes because 1) it is impossible to prevent the elution of lipids to mobile phases and 2) the polyion complex system provides many complicated electrostatic interactions between immobilized phases and solutes, which lead to peak-broadening and abnormal adsorption in liquid chromatography.

Figure 1. Synthetic scheme of lipid membrane analogue (ODA$_n$) and illustration of the phase transition of immobilized ODA$_n$ on silica gels.

On the other hand, direct immobilization of lipids onto silica gels was reported by Pidgeon and Venkataram.[13] This was obtained by amidation of aminated silica gels with a dimyristoyl phosphatidylcholine derivative containing a terminal carboxylic group. Such chemically bonded lipids are more stable than polyion-complexed lipid membranes, but it may be impossible to reproduce molecular orientation and lateral diffusion of lipids on carrier particles.

Therefore, in order to introduce lipid membrane functions as silica-based stationary phases, it is necessary to develop a new approach for immobilization of lipid membranes. For this purpose, we have synthesized comb-shaped polymer ODA$_n$ (Fig. 1).[14-16] This polymer can be readily immobilized onto silica gels through a reactive terminal group, and the silica-supported polymer (Sil-ODA$_n$) shows several essential functions (highly-orienting structure, hydrophobicity and phase transition behavior) like those of lipid membranes. This is because the polymer is immobilized at the one side of terminal groups and still maintains molecular fluidity after immobilization. In this paper, we

demonstrate that the immobilized polymer does not form bilayer membrane structures in water, but shows unique retention behaviors for various aromatic compounds and steroids analogous to those of aqueous lipid membranes. In addition, the molecular recognition mechanism was discussed.

EXPERIMENTAL

Materials

The comb-shaped polymer (ODA_n, where n is the average polymerization degree) was prepared by telomerization of octadecylacrylate and 3-mercaptopropyltrimethoxysilane in ethanol. The synthetic procedure of ODA_{28} is as follows: octadecylacrylate and 3-mercaptopropyltrimethoxysilane (30 : 1 in the molar ratio) were dissolved in ethanol. Azobisisobutyronitrile (0.1 wt% for the monomer) was added to the solution at 80°C. The mixture was stirred for 6 h at 80°C under N_2 gas atmosphere. The white precipitates obtained were gathered by filtration, washed successively with methanol and acetone and dried in vacuo. The structure and polymerization degree of the polymer were determined by NMR spectroscopy: ^1H-NMR chemical shifts of ODA_n in $CDCl_3$ were follows: δ = 0.75 ppm ($SiCH_2$), δ = 2.28 ppm (CHCO), δ = 3.58 ppm ($SiOCH_3$), and δ= 4.15 ppm ($C(=O)OCH_2$).

ODA_n was readily introduced onto porous silica gels by mixing in tetrachloromethane at reflux temperature (12 h). YMC 120-S5 (diameter 5 μm, pore size 120 Å) were used as porous silica gels. Successive washing of the resulting gels with chloroform showed no change in weight. The amount of ODA_n introduced was determined by elemental analysis.

Measurements

Silica-supported ODA_n (Sil-ODA_n) was packed into a stainless steel column (4.6 mm I.D. x 250 mm) using a hexanol-chloroform (1 : 1) mixture and the liquid chromatographic property was examined using methanol or methanol-water as mobile phases. The chromatograph included a JASCO 880 PU pump, a Shimadzu UV-visible photodiode array SPD-M6A and a Shodex reflactomonitor SE-51. Five μL of the sample dissolved in methanol was injected through a Reodyne Model 7125 injector. Chromatography was carried out at flow-rate 0.5 mL min^{-1}. The retention capacity (k') was determined by (t_e
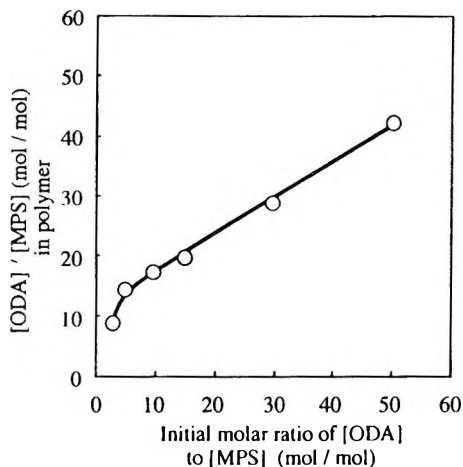
Figure 2. Relationship between the molar ratio ([ODA]/[MPS]) in the telomerization process and the polymer obtained. AOD: octadecylacrylate, MPS: 3-mercaptopropyl-trimethoxysilane.

- t_o) / t_o where t_e and t_o are retention time of samples and glycerol, respectively. The separation factor (α) was given by the ratio of retention capacity. DSC thermograms of ODA_n and $Sil-ODA_n$ were obtained using a heating rate of 1 °C min^{-1} with Seiko I & E SSC-580 with a DSC-10 instrument.

Calculations

The structures of ODA_n and aromatic compounds were estimated using Sony-Tektronix CAChe-mechanics (the optimization with MM2 parameters continued until the energy change was less than the 0.001 kcal mol^{-1}) or CAChe-MOPAC (Ver. 6, PM3 option) . The energy level of HOMO and log P were also estimated by CAChe-MOPAC with the PM3 and AM1 options, respectively.

RESULTS AND DISCUSSION

Polymerization Degree of ODA_n

The polymerization degree (n) of ODA_n was determined by ^{1}H-NMR spectroscopy (SiOCH$_3$: δ = 3.58 ppm, C(=O)OCH$_2$: δ = 4.15 ppm). The
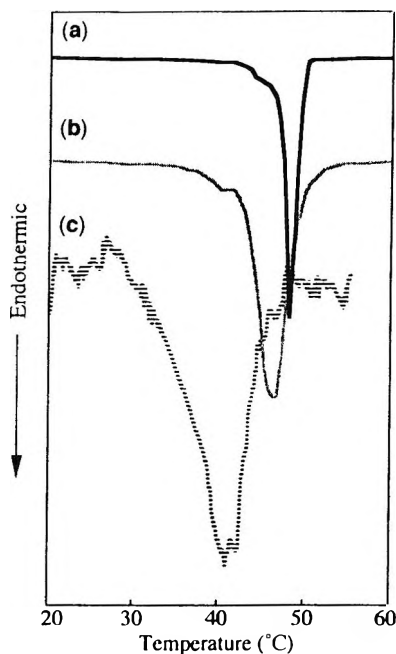
Figure 3. DSC thermograms of ODA$_{27}$ (a and b) and Sil-ODA$_{27}$. The thermogram **a** was observed in the absence of solvent. The thermograms **b** and **c** were obtained in the presence of methanol and methanol-water (7 : 3), respectively.

molecular weights of ODA$_n$ determined by ^{1}H-NMR corresponded to the values estimated by size exclusion chromatography (SEC) using a Shodex KF-803 column. For example, the molecular weight of ODA$_{28}$ was 9.3 x 10^3 as observed by NMR spectroscopy. SEC analysis of ODA$_{28}$ showed that M$_w$ = 1.3 x 10^4 and M$_n$ = 7.4 x 10^3. The small value of M$_w$/M$_n$ = 1.76 indicates that the distribution of the polymerization degree in ODA$_n$ is relatively narrow in spite of the radical polymerization. This may be related to the fact that an alkyl mercaptan is a good chain-transfer agent.

Supporting this, the plots of the polymerization degree (n) and the initial molar ratio show a good linearity (Fig. 2). In this study, ODA$_n$s with n = 9, 12, 14, 17, 22, 27, 28, 33 and 60 were synthesized by adjusting the initial molar ratio in the telomerization process.
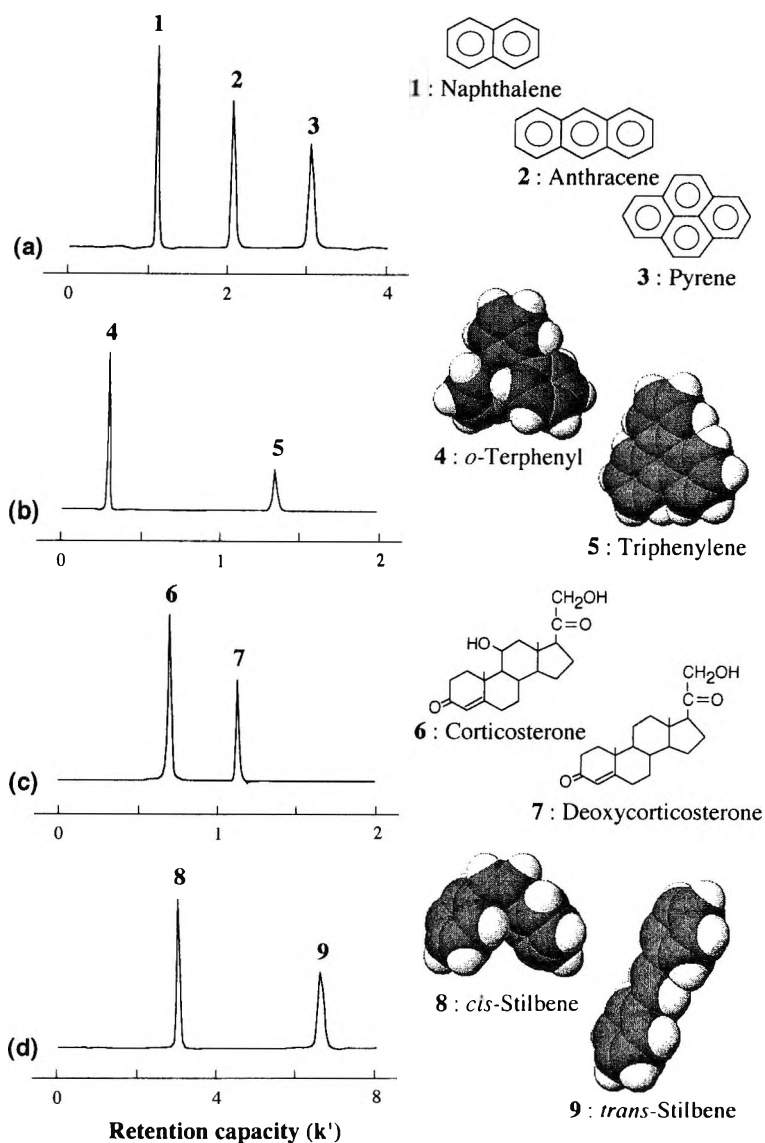
Figure 4. Typical chromatograms with Sil-ODA$_n$ columns (n = 27 in **a, b** and **d**; n = 17 in **c**) at 20°C. Mobile phases: methanol (**a** and **b**); methanol-2ater (7 : 3, **c** and **d**).

Phase Transition of ODA$_n$

The DSC thermograms of ODA$_n$ showed a sharp endothermic peak in both heating and cooling processes. For example, the peak-top temperature of ODA$_{27}$ was 49°C (T$_{C2}$) with a shoulder (T$_{C1}$) at 42 - 47°C in the heating process as shown in Fig. 3-a. Polarity microscopic observation indicated that T$_{C1}$ and T$_{C2}$ were assigned to crystal-to-liquid crystal and the liquid crystal-to-isotropic phase transition, respectively. This liquid crystalline state contains Shlieren issue which belonged to a nematic phase and was observed at a temperature range of 42 - 47°C. Similar phase transitions were also observed in methanol (or methanol-water) dispersions, accompanied by a slight decrease in temperature by about 2 - 4°C. This indicates that ODA$_n$ can form highly-ordered structures such as crystal states even in the presence of organic eluents used in the column chromatography process. Phase transitions were also observed in ODA$_n$ with n = 9 - 60, although T$_{C2}$ depended on n (for example, T$_{C2}$ = 41°C (n = 9), 44°C (n = 14), 45°C (n = 20), 49°C (n = 27), 49°C (n = 33) and 49°C (n = 60).

The ODA$_n$ was readily immobilized on silica gels. Successive washing of resulting gels with chloroform showed no change in weight: chloroform is a good solvent for ODA$_n$. In the case of ODA$_{27}$, the elemental analysis showed that 20.6 wt% (0.6 unit-mmol g^{-1}) of ODA$_{27}$ was introduced on the silica gels (YMC SIL-120). The amount of ODA$_n$ introduced was dependent on the type of silica gel as well as on the reaction time and the concentration of ODA$_n$ in the immobilization process (detailed results will be reported elsewhere). The immobilized ODA$_n$ (Sil-ODA$_n$) also showed an endothermic peak in their DSC measurements. Fig. 3 includes a DSC thermogram of Sil-ODA$_{27}$ in methanol-water (7 : 3). The thermogram shows about 8°C lowering of peak-top temperature (T$_C$) compared with T$_{C2}$ of original ODA$_{27}$. This indicates that silica gels influence the orientation of bound ODA$_{27}$, but the bonded phase can maintain oriented structures and undergo crystal-to-isotropic phase transition on silica gels (Fig. 1). Similar phase transition behavior was also observed in Sil-ODA$_n$ with n = 17, 28 and 33.

Retention Behavior for Polyaromatics

Fig. 4-a shows that the column packed with Sil-ODA$_{27}$ performs complete separation for a mixture of naphthalene, anthracene and pyrene. The theoretical plate number and the separation factor (α) at 20°C were about 18000 in pyrene and 3.4 for naphthalene and pyrene, respectively. The elution order was the same as those that were observed in conventional reversed phase
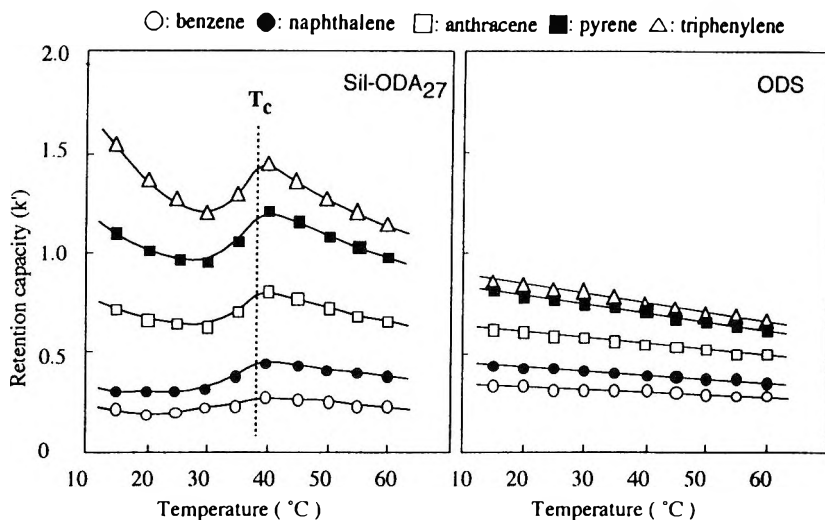
Figure 5. Temperature dependencies on retention capacity for polyaromatics with Sil-ODA$_{27}$ and ODS columns. Mobile phase: methnol, T$_C$ was determined in a methanol dispersion.
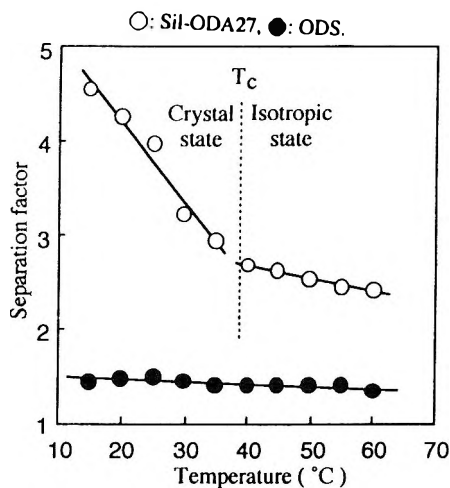
Figure 6. Temperature dependencies on separation factor (the ratio of retnetion capacity for triphenylene to o-terphenyl). T$_C$ was determined in a methanol dispersion. Mobile phase: methanol .

liquid chromatography (RPLC) packings, i.e. octadecylated silica gels (ODS: Inertsil ODS, 4.6 I.D. x 300 mm, GL Science Co., Ltd.). It was also confirmed that the retention capacity (k') increased with an increase in mobile phase polarity. These results indicate that the Sil-ODA$_{27}$ has a retention mode similar to RPLC and recognizes molecular hydrophobicity: log P values determined by MOPAC calculation were 3.47, 4.43 and 4.64 in naphthalene, anthracene and pyrene, respectively.

The performance of the Sil-ODA$_{27}$ column was unique in that it was characterized by temperature dependency. As shown in Fig. 5-a, the Sil-ODA$_{27}$ column showed distinct bending in the plots of temperature vs. k'. On the other hand, no similar temperature dependence was observed in ODS, but it must also be taken into account that the separation factor was much smaller in ODS (α = 1.8 at 20°C) than in Sil-ODA$_{27}$ (α = 3.4 at 20°C). As shown in the dotted line of Fig. 5-a, the T$_C$ of Sil-ODA$_{27}$ observed in the DSC (in a methanol dispersion) measurement almost agrees with the temperature of the bending point. This strongly suggests that the unusual temperature dependencies in Sil-ODA$_{27}$ occur at the crystal-to-isotropic phase transition temperature of the bonded phase.

Recognition of Molecular Planarity

The specificity of Sil-ODA$_n$ was emphasized by checking retention behaviors for triphenylene and o-terphenyl. These compounds have the same carbon number per molecule and thus the molecular hydrophobicity is similar.

The Sil-ODA$_{27}$ column showed complete separation for triphenylene and o-terphenyl as shown in Fig. 5-b. The separation factor (α) at 20°C was 4.2 in Sil-ODA$_{27}$ but 1.5 in ODS. The Sil-ODA$_{27}$ column provided remarkable temperature dependencies with respect to the retention capacity (k') for both samples. The k'-temperature plots show a distinct jump at 30 - 40°C similar to those of anthracene and pyrene. Remarkable temperature dependencies were also observed for the separation factor (Fig. 6). According to Fig. 6, the separation factor is much higher at the crystal state temperature than the isotropic state temperature: 4.7 at 15°C and 2.6 at 45°C. On the other hand, the ODS column showed almost no temperature dependence for the separation factor. Therefore, the enhancement of separation factor at the crystal state temperature cannot be explained only by hydrophobicity recognition. It is known that planar compounds such as triphenylene are more strongly incorporated to an oriented medium than non-planar compounds such as o-terphenyl.[17-19] For example, we have previously reported that poly (γ-methyl L-
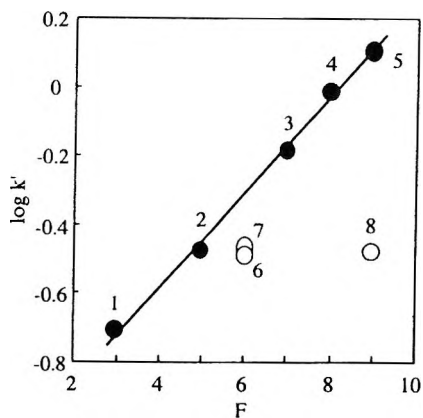
Figure 7 Relationship between retention capacity and correlation factor F with a Sil-ODA$_{27}$ column. mobile phase: methanol. Solutes: 1, benzene; 2, naphthalene; 3, anthracene; 4, pyrene; 5, triphenylene; 6, diphenyl; 7, fluorene; 8, o-terphenyl. F = number of double bonds + the number of primary and secondary carbons - 0.5 for a nonaromatic ring.[20]

glutamate) whose main chain is α-helical produces highly-oriented structures and shows unexpectable higher retention capacity for planar aromatics than for non-planar aromatics.[18,19] Therefore, it is presumed that Sil-ODA$_{27}$ also recognizes molecular planarity as well as molecular hydrophobicity. To support this assumption, when the retention capacity was plotted against the correlation factor F proposed by Schabron et al.,[20] whose parameter is related to molecular planarity, the experimental data point in planar aromatics such as benzene, naphthalene, anthracene, pyrene and triphenylene, are approximately on a straight line, but are not lined up in non-planar aromatics such as diphenyl, fluorene or o-terphenyl (Fig. 7).

Recognition of Molecular Bulkiness

It is shown that Sil-ODA$_n$ is sensitive to molecular bulkiness. Fig. 8 shows the temperature dependence of retention capacity for adamantane as a sterically bulky compound. The plots include a remarkable increase of retention capacity at temperatures around T$_C$. Especially, it should be noted that the retention capacity is much smaller at the crystal state temperature than at the isotropic state temperature. This indicates that a sterically bulky compound is hardly incorporated into the highly-oriented bonded phase.
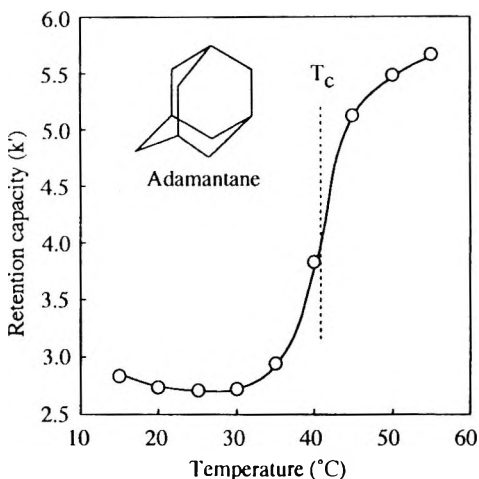
Figure 8. Temperature dependence on retention capacity for adamantane with a Sil-ODA$_{27}$ column. T$_C$ was determined in a methanol-water (7 : 3) dispersion. Mobile phase: methanol-water (7 : 3).

Retention Behavior for Rigid Hydrocarbons, Steroids

It is well-known that highly-oriented aggregates such as lipid bilayer membranes specifically incorporate rigid and hydrophobic compounds. For example, cholesterol can be easily incorporated into lipid bilayer membranes. Therefore, the retention behavior for cholesterol was examined using the Sil-ODA$_{27}$ column. The temperature dependence on the k' of cholesterol showed a critical bending point around T$_C$ and remarkable increase at temperatures below T$_C$: k' (in methanol) = 1.8 (60°C), 2.0 (50°C), 2.4 (40°C), 2.5 (30°C), 3.2 (20°C), and 4.3 (15°C). These results indicate that Sil-ODA$_{27}$ incorporates cholesterol specifically at temperatures below 30°C. Fig. 4-c shows a chromatogram of a mixture of steroid hormones, corticosterone and deoxycorticosterone. Complete separation (α = 1.6) was obtained in spite of small structural differences. In the case of ODS, the α was only 1.1.

Discussion on Recognition Mechanisms for Geometrical Isomers

Fig. 4-d shows complete separation for a mixture of *trans*- and *cis*-isomers of stilbene with the Sil-ODA$_{27}$ column. The separation factor was 2.2 at 20°C, although ODS provided a very small separation factor (α = 1.1 at 20°C). The

Figure 9. Temperature dependencies on retention capacities for geometrical isomers of stilbene (**a**, **b**, **g** and **h**), 1,2-bis(sulphonyl)ethylene (**c** and **d**) and 1,4-dichloro-2-butene (**e** and **f**). T_C was determined in a methanol-water (7 : 3) dispersion. Mobile phases: methanol-water = 7 : 3 (**a** and **b**), = 5 : 5 (**c** ~ **f**), 9 : 1 (**g** and **h**).

specificity of Sil-ODA$_{27}$ is emphasized by comparing the temperature dependence of Sil-ODA$_{27}$ to ODS. As shown in Fig. 9-g and -h, in the case of ODS, the k' values decreased with increase of temperature. Such negative slopes are commonly observed in usual RPLC packings.[21,22] These can be explained by increase of the solubility of solutes from stationary to mobile phases with increase of temperature.[21,22] Therefore, in the case of ODS, the separation factor should be independent of temperature, and is small and constant (1.04 - 1.07 at 15 - 55°C). This can be also expected by the fact that hydrophobicity of *cis*-stilbene (log P = 4.92) is very similar to that of *trans*-stilbene (log P = 4.88). On the other hand, Sil-ODA$_{27}$ provided critical bending points and positive slopes at temperatures between 35 and 45°C in their plots (Fig. 9-a and -b). These unusual temperature dependencies also include remarkable selectivity changes of 2.33 (15°C), 1.97 (25°C), 1.64 (35°C), 1.55 (40°C), 1.40 (45°C), 1.38 (50°C) and 1.35 (55°C). However, it is believed that the positive slope in the k'-temperature plots at 30 - 45°C and selectivity change are not due to the change of the retention mechanism. To explain this unusual phenomenon, we hypothesized the following: immobilized ODA$_{27}$ forms a mixed phase containing both crystalline and isotropic phases and the ratio of isotropic ODA$_{27}$ to crystalline ODA$_{27}$ increases with increase of temperature between 30 - 45°C. The retention capacity (k') also increases with increase of the ratio, because k' is larger in the isotropic state than in the crystalline state.

On the other hand, we also encountered retention phenomena which cannot be explained only by the above-mentioned molecular recognition mechanism. For example, Sil-ODA$_{27}$ showed geometrically selective retention for 1,2-bis(phenylsulphonyl)-ethylene isomers (α = 1.79 at 20°C, Fig. 9-c and -d), but showed small selectivity for geometrical isomers of 1,4-dichloro-2-butene (Fig. 9-e and -f), 2-hexenol and 1,2-dimethylcyclohexane. The selectivities were only 1.11, 1.09 and 1.05 at 20°C, respectively. Interestingly, however, the k'-temperature plots in all samples showed distinct jumps at temperatures around T_C. This indicates that the difference of bulkiness between *cis*- and *trans*-isomers is not always reflected in geometric selectivity.

On the basis of these results, our proposed mechanism for molecular recognition should be modified and developed as follows: (1) immobilized ODA$_{27}$ forms a highly-oriented structure at its crystal state temperature. A planar compound such as *trans*-stilbene can be more easily incorporated into this oriented polymer than a bulky non-planar compound such as *cis*-stilbene. This mechanism is analogous to the fact that cholesterol as a rigid and planar compound is readily incorporated into lipid bilayer membranes which form highly oriented structures. (2) Immobilized ODA$_{27}$ can interact with double

$$CH_3O - \underset{\underset{OCH_3}{|}}{\overset{\overset{OCH_3}{|}}{Si}} - (CH_2)_3 - S - (X)_n - H$$

X = CH$_2$ – CH
                |
                C = O
                |
                O – CH$_2$CH$_2$(CF$_2$)$_7$CF$_3$

X = CH$_2$ – CH
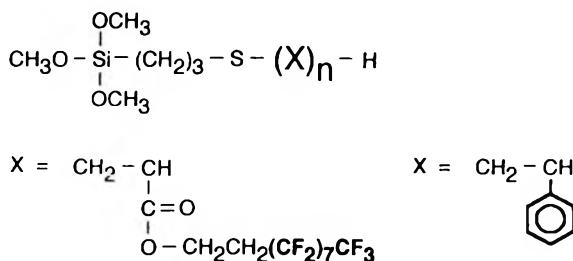
Figure 10. Poly(perfluoroalkylacrylate)[25] and poly(styrene)[26] with reactive terminal groups. Both polymers can be readily immobilized onto silica gels and show specific chromatographic separations.[25,26]

bonds of solutes with recognizing their π electron density. Perhaps this interaction is derived from the carbonyl π electrons of acrylate moieties which can work as electron-accepting groups. This assumption is supported by following facts: (i) it was confirmed that the selectivity with crosslinked poly(methyl acrylate) polymer (MA) particles as a reference showed higher selectivity for various isomeric aromatics was smaller than with Sil-ODA$_n$ but significantly higher than with ODS, although these MA particles provided comparably small k' values because there were no long-chain alkyl groups. This result indicates that the carbonyl groups of MA moiety play an important role for molecular recognition. The detailed date for MA particles were briefly reported.[23] (ii) Judging from the calculation of the HOMO (Highest Occupied Molecular Orbital) energy level in stilbenes, *trans*-isomers are more electron-donating (-8.63 eV) than *cis*-isomers (-9.06 eV). Bredas and Street have reported using computer calculations that similar interactions occur between benzene and formic acid.[24] On the other hand, geometrical isomerism for 1,4-dichloro-2-butene (-9.63 and -9.86 eV in *trans*- and *cis*-isomers) and 2-hexenol (-10.28 and -10.13 eV in *trans*- and *cis*-isomers) having non-conjugating substituent groups provides no significant difference in energy level of HOMO. In these cases, Sil-ODA$_{27}$ shows a small selectivity for retention of these isomers.

CONCLUSIONS

(1) A special polymer-bonded phase on silica gels was synthesized by one-step telomerization of octadecylacrylate using 3-mercaptopropyl-trimethoxysilane. The degree of polymerization was readily controlled by adjusting the initial molar ratio in the telomerization process.

(2)   By selecting monomers, various polymer-bonded phases can be prepared (Fig. 10) and show unique separations.   Detailed results have been reported elsewhere.[25-27]

(3)   The polymer (ODA_n) was readily immobilized onto silica gels with a reactive terminal group.   Therefore, the polymer still maintains flexibility after immobilization.

(4)   The immobilized polymer ($Sil\text{-}ODA_n$) underwent crystal-to-isotropic phase transition on silica gels.   The elution order for hydrophobic compounds in the packed column with $Sil\text{-}ODA_n$ usually agreed with the order expected as RPLC mode regardless of temperature.   However, $Sil\text{-}ODA_n$ at crystal state temperature provided exceptionally specific selectivity, recognizing for molecular planarity and bulkiness.   The driving force is clearly related to the highly oriented structures. The π electron due to the carbonyl group also plays an important role for molecular recognition.

(5)   The specificity of $Sil\text{-}ODA_n$ was drastically appeared by examining the temperature dependency.

REFERENCES

1. H. Ihara, M. Takafuji, C. Hirayama, D. F. O'Brien, Langmuir, **8**, 1548 (1992).

2. D. F. O'Brien, R. Ramasuwami, in **Encyclopedia of Polymer Science and Engineering**, 2nd ed.; J. Wiley & Sons: New York, 17, 108-135 (1989).

3. D. F. O'Brien, U. Liman, Angew. Makromol. Chem., **166 / 167**, 2761 (1989).

4. H. Ringsdorf, B. Schlarb, J. Venzmer, J. Angew. Chem., Int. Ed. Engl, **27**, 113 (1988).

5. S. L. Regen, in **Liposomes: From Biophysics to Therapeutics**; M. J. Ostro. Mercel Dekker: New York, 73 (1987).

6. J. H. Fendler, Science, **223**, 888 (1984).

7. T. Kunitake, N. Nakashima, K. Takarabe, M. Nagai, A. Tsuge, H. Yanagi, J. Am. Chem. Soc., **103**, 5945 (1981).

8. T. Kunitake. A. Tsuge, N. Nakashima, Chem. Lett., 1783 (1984).

9. H. Fukuda, T. Diem, J. Stefely, F. J. Kezdy, S. L. Regen, J. Am. Chem. Soc.. **108**, 2321 (1986).

10. S. L. Regen, J. Shin, K. Yamaguchi, J. Am. Chem.Soc., **106**, 2446 (1984).

11. Y. Okahata, H. Endo, K. Taguchi, J. Chem. Soc., Chem. Commun., 1363 (1987).

12. Y. Okahata, O. Shimizu, Langmuir, **3**, 1171 (1987).

13. C. Pidgeon, U. V. Venkataram, Anal. Biochem., **176**, 36 (1989).

14. C. Hirayama, H. Ihara. T. Mukai, Macromol., **25**, 6357 (1992).

15. H. Ihara, T. Fukumoto, C. Hirayama, Anal. Sci., **9**, 711 (1993).

16. T. Fukumoto, H. Ihara, S. Sakaki, H. Shosenji, C. Hirayama., J. Chromatogr., **672**, 237 (1994).

17. N. Tanaka, K. Hashizume, M. Araki, J. Chromatogr., **400**, 33 (1987).

18. C. Hirayama, H. Ihara, S. Nagaoka, T. Shono, Chem, Lett., 971 (1992).

19. H. Ihara, C. Hirayama, H. Hachisako, K. Yamada, **Functions and Recent Applications of High-orienting Materials,** IPC, Tokyo, 92, 1995.

20. J. F. Schabron, R. J. Hurtubise, H. F. Silver, Anal. Chem.. **49**, 2253 (1977).

21. J. H. Knox. G. Vasvari, J. Chromatogr., **83**, 181 (1973).

22. Separation Report, No. 077, Tosoh, Japan, p. 3.

23. C. Hirayama, H. Ihara, S. Nagaoka, K. Kato, K. Kashihara, Chromatographia, **33**, 473 (1992).

24. J. L. Bredés, G. B. Street, J. Chem. Phys., 90, 7291 (1989).

25. H. Ihara, H. Tanaka, C. Hirayama, Polym. Preprints Jpn., **44**, 689 (1995).

26. C. Hirayama, H. Ihara, S. Nagaoka, T. Wada, Polym. J., **26**, 499 (1994).

27. H. Ihara, N. Nakamura, S. Nagaoka, C. Hirayama, Anal. Sci., **11**, 739 (1995).

MULTIFUNCTIONAL ZWITTERION-EXCHANGE STATIONARY PHASE FOR HPLC

Tsong-Yung Chou,[1,4] Mei-Hui Yang*

Department of Chemistry
National Taiwan University
Taipei, 106, Taiwan

ABSTRACT

A zwitterion-exchange stationary phase (ZIXSP) was prepared for the separation of the mixture of organic bases, organic acids and amino acids by high performance liquid chromatography (HPLC). It was synthesized by the reaction of cyanuric chloride with sulfanilic acid and then bonded onto the silica gel on which the silane coupling agent was prebonded. The chromatographic behaviours of the prepared ZIXSP revealed that the capacity factors of each analyte varied with the pH value of the mobile phase. By applying the concept of acid-base equilibrium the correlation between the capacity factor on the ZIXSP and pH of the mobile phase could be explained reasonably. Based on our results, it is concluded that ZIXSP is a zwitterion exchanger that additionally provides π-π charge-transfer interaction and hydrophobic interaction functions.

INTRODUCTION

Knox[1,2] had found that the addition of zwitterionic pairing agents, i.e., 11-aminoundecanoic acid or 12-aminododecanoic acid, to the mobile phase could improve the efficiency of the C_{18} column (ODS Hypersil) for the separation of nucleotides. However, the addition of zwitterionic pairing agents to the mobile

2985

phase is not adapted to the preparative chromatography since it would contaminate the analytes. Later, Hartwick[3] prepared a zwitterion-exchange stationary phase (ZIXSP) by introducing both amino group and carboxylic acid group to the surface of silica gel. Since -COOH is a weak acid group and could not be dissociated into -COO⁻ and H⁺ at a lower pH value, the ZIXSP prepared by Hartwick would lose the properties of zwitterion-exchange at low pH value of mobile phase.

For separations of ionic organocompounds, contributions from forms of interaction other than ion exchange, such as H-bonding, π-π interaction or hydrophobic interaction, may be involved if the stationary phase provides the corresponding functional moiety.[4-6] The possibility of simultaneous separation of ionized/ionizable and non-ionic compounds with columns prepared by mixing together ion-exchange and reverse phase packing materials was confirmed by Wilson and co-workers.[7]

In our previous report,[8] multifunctional zwitterion phases containing aromatic moieties were prepared successfully and used to separate various weak organic acids and bases. In addition, we reported that the ion-exchanger which was synthesized through bonding aniline onto silica with 3-aminopropyltriethoxysilane and followed by sulfonation was an 1 : 1 mixed phase with 50% unsulfonated aniline-derived moiety. It was observed that this ion-exchanger was a zwitterion-exchanger that additionally provided hydrophobic-interaction and π-π charge-transfer interaction functions.

In our previous reports,[9,10] highly selective s-triazine-modified C_{18} phase and chiral phase were successfully prepared. The presence of an s-triazine ring in the bonded phase system not only led to a convenient reproducible synthetic way of introducing a desired organic moiety to the silica surface but also played an important role, possibly due to a π-π interaction with aromatic analytes, in the separation of aromatic hydrocarbons. Therefore, instead of the above process,[8] using s-triazine derivatization can be served as an alternative one for the preparation of an sulfonated ZIXSP.

In this study, we prepared a ZIXSP by introducing both sulfo- (-SO₃H) group and amino group through s-triazine derivative to the aminated silica gel. The chromatography behaviours of this ZIXSP with regard to the separation of the mixture of organic bases, organic acids and amino acids were explained by applying the concept of acid-base equilibrium.

Table 1

Characteristics of the Prepared Phase

| | Elemental Analysis | | | | Loading Capacity[a] | |
	C/%	N/%	H/%	Cl/%[b]	mmol/g	μmol/m^2
BS	6.94	2.78	1.57		0.99	2.84
ZIXSP	9.83	4.35	1.61	1.03	0.28	0.80

[a] Based on N%.

[b] By Carius method.[11]

EXPERIMENTAL

Chemicals

Silica gel (Nucleosil; pore size 100 Å, particle size 10 μm, surface area 350 m^2/g), was obtained from Macherey-Nagel and dried at 100 °C for 10 h. The chemicals used in the synthetic processes and analytes used in the chromatographic experiments were of reagent grade: N-(2-aminoethyl)-3-aminopropyltrimethoxysilane (AEAPS, Tokyo Kasei); p-sulfanilic acid (Riedel-Dehaen); Cyanuric chloride (Fluka). The solvents used for HPLC were LC-grade acetonitrile and deionized water.

Preparation of ZIXSP

To a solution of pre-dried silica gel (3 g) in 150 mL of toluene, AEAPS (6 mL) was added and refluxed for 15 h. This bonded silica gel (BS, Figure 1) was collected by filtration and washed with methanol, ether and then dried under vacuum in the presence of the drying agent, P$_2$O$_5$. The BS was characterized by elemental analysis (Table 1).

Sodium carbonate (0.02 mol) and p-sulfanilic acid (0.02 mol) were dissolved in 0-5 °C water (50 mL), then a solution of cyanuric chloride (0.02 mol) in acetone (10 mL) was added and stirred. Another portion of sodium carbonate (0.02 mol) in 20 mL water was dropply added within 30 min under 0-5 °C.

$(CH_3O)_3Si(CH_2)_3NH(CH_2)_2NH_2$ —$\xrightarrow{\text{Silica gel}}$

$-O-\underset{|}{\overset{|}{Si}}(CH_2)_3NH(CH_2)_2NH_2$ **BS**

$H_2N-\!\!\bigcirc\!\!-SO_3H$ + (cyanuric chloride) $\xrightarrow{Na_2CO_3}$ $^{\ominus}O_3S-\!\!\bigcirc\!\!-\overset{H}{N}-$(triazine-Cl₂)

$\xrightarrow{HCl}$ $HSO_3-\!\!\bigcirc\!\!-\overset{H}{N}-$(triazine-Cl₂)   **Cy-S**

BS + Cy-S ⟶

$-O-\underset{|}{\overset{|}{Si}}(CH_2)_3NH(CH_2)_2NH_2$ 5

⋮

$-O-\underset{|}{\overset{|}{Si}}(CH_2)_3NH(CH_2)_2NH-$(triazine-Cl)$-NH-\!\!\bigcirc\!\!-SO_3H$ 2
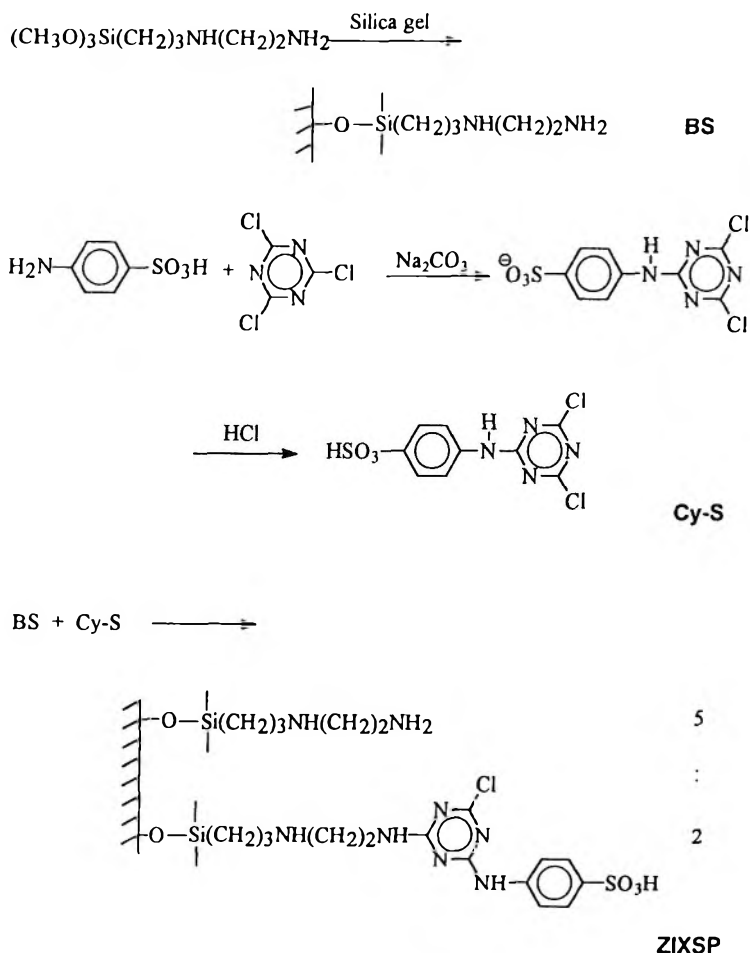
ZIXSP

Figure 1. Preparation of zwitterion exchange stationary phase ZIXSP

After the pH of the reaction mixture was adjusted to 1-2 with diluted hydrochloric acid, the derivative of cyanuric chloride was collected by filtration, washed with water and dried over P_2O_5 under vacuum. The product (Cy-S, Figure 1) was characterized by IR and ^{1}HNMR.

BS (3 g) was suspended in 150 mL of dimethylsulfoxide (DMSO). Cy-S (0.003 mol) was added and stirred at 50 °C for 2 h, NaOH (0.12 g) was then added and reacted for a further 24 hours.

The reaction mixture was filtered and the product (ZIXSP, Figure 1) was washed with water, acetone, methanol and ether. Characterization was done by elemental analysis (Table 1).

Chromatographic Studies

The chromatographic studies were carried out with a Waters liquid chromatographic system which consisted of a M-510 solvent-delivery system, a U6K injector and Spectroflow 757 variable-wavelength UV detector. Stainless-steel column (300 mm x 4 mm I.D.) was packed by the balanced density slurry method.

Results and Discussion

In this study, AEAPS which provides possible cation-exchange sites was used as a coupling agent. The AEAPS-derived silica phase (BS) then reacted with the s-triazine derivative of sulfanilic acid (Cy-S) to give the expected ZIXSP (Figure 1). Both the BS and ZIXSP were characterized by elemental analysis, and the data are shown in Table 1. It demonstrated that each gram of BS contained about 0.99 mmol of AEAPS, and each gram of ZIXSP contained about 0.28 mmol of Cy-S. Therefore, about seven molecules of AEAPS bonded on the silica gel was further bonded with two molecules of Cy-S.

Effective separation of the mixture of organic bases, organic acids and amino acids on the ZIXSP by HPLC was observed: Representative chromatogram is shown in Figure 2. The effect of the pH of mobile phase on the values of k' (capacity factor) for various analytes on this ZIXSP is shown in Figure 3. It was observed that the relationship between the capacity factor of analyte and the pH of mobile phase in the range pH 3 to 5 depended upon the nature of analytes.

For the organic bases, aniline and benzylamine, the k' values decreased as the pH of mobile phase increased. However, for the weak organic acids, 1-naphthylacetic acid and benzoic acid, the capacity factors increased before pH 5 and decreased after pH 5. as the pH of mobile phase increased. Interestingly, the k' of a strong organic acid, p-toluenesulfonic acid, decreased rapidly with increasing the pH value of mobile phase, while that of zwitterion compounds, phenylalanine, leucine and alanine, had a volcano at pH about 4.
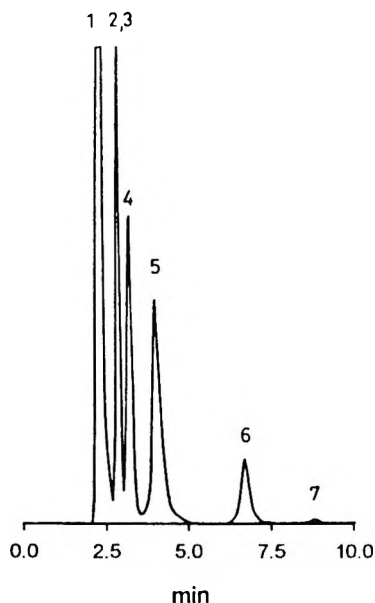
Figure 2. Chromatogram for the separation of organic bases, organic acids and amino acids on the ZIXSP. Mobile phase: CH_3CN-H_2O (2 : 1), $[KH_2PO_4]$: 1 mM, pH 7.0, flow rate: 1.1 mL/min, UV detection, room temperature. analytes: (1) p-toluenesulfonic acid, (2) benzylamine, (3) aniline, (4) benzoic acid, (5) 1-naphthylaectic acid, (6) phenylalanine, (7) aniline.

The result with respect to the effects of pH (Figure 3) of the mobile phase on the capacity factor revealed the possibly available contributions of zwitterion-exchange, π-π charge-transfer, and hydrophobic interactions by this ZIXSP to the separation process.

ZIXSP Behaves as a Cation Exchanger in the Separation of Amines

The correlation between the capacity factor on the ZIXSP and pH of the mobile phase can be explained by applying the concept of acid-base equilibrium, which was also applied by Horvath et al. for separating ionogenic substances on an alkyl phase.[12]
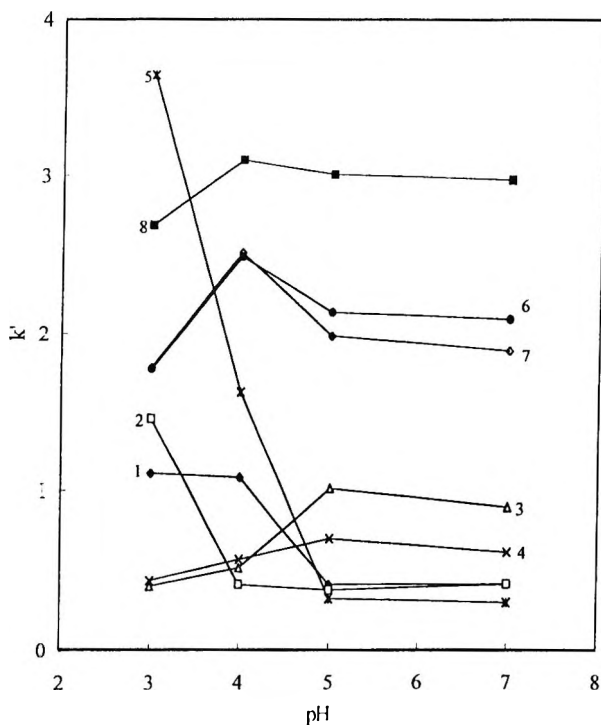
Figure 3. Effect of the pH of mobile phase on the values of k' for (1) aniline, (2) benzylamine, (3) 1-naphthylacetic acid, (4) benzoic acid, (5) p-toluenesulfonic acid, (6) phenylalanine, (7) leucine, (8) alanine on home-made ZIXSP. Mobile phase: CH_3CN-H_2O (2:1), $[KH_2PO_4]$: 1 mM, flow rate: 1.1 mL/min.

When the pH of mobile phase is less than 7, the organic base (B) will be protonated as eq. (1).

$$B + H^+ \underset{K_b}{\rightleftharpoons} HB^+ \tag{1}$$

Suppose HB^+ as it interacted with the stationary phase, would replace a counter ion (C^+) from the stationary phase as eq. (2).

$$HB^+_m + C^+_s \underset{K_c}{\rightleftharpoons} HB^+_s + C^+_m \tag{2}$$

The subscript characters of s or m, indicates the species which is in the stationary phase or in the mobile phase, respectively. In ion-exchange chromatography, the retention of an analyte on the organic stationary phase bearing ionic functional groups can be predicted as the result of two processes: (a) the distribution of an analyte between an aqueous mobile phase and the organic stationary phase and (b) the reaction of an analyte with the ionic sites of the stationary phase (i.e. ion exchange). Then, the capacity factor k' can be presented as eq. (3).

$$k' = \frac{V_s}{V_m} \times \frac{[B]_s + \left[BH^+\right]_s}{[B]_m + \left[BH^+\right]_m}$$

$$= \frac{V_s}{V_m} \times \frac{D_B + K_b[H^+]_m K_c \dfrac{[C^+]_s}{[C^+]_m}}{1 + K_b[H^+]_m} \tag{3}$$

where V_s is the volume of stationary phase within the column, V_m is the total volume of solvent within the column and D_B is the distribution coefficient of the unprotonated base between stationary phase and mobile phase ($[B]_s/[B]_m$).

In eq. (3), in the range pH 3 to 7, $K_b[H^+]_m$ could be neglected for aniline ($K_b = 4.2 \times 10^{-10}$) and benzylamine ($K_b = 0.2$). Since $[C^+]_s$ is about equal to the total exchange capacity[13] for the stationary phase, and $[C^+]_m \doteq [KH_2PO_4] = 1$ mM, eq. (3) would be simplified as:

$$k' = \frac{V_s}{V_m}(D_B + C[H^+]_m) \tag{4}$$

where C is a constant equal to $K_b K_c [C^+]_s [C^+]_m^{-1}$

If we are not concerned with the dependence of the D_B value on the pH of the mobile phase, according to eq. (4), the k' values of aniline and benzylamine would be linearly proportional to $[H^+]$ in the mobile phase. While Figure 3 exhibited that the k' values of aniline and benzylamine decreased with increasing the pH of the mobile phase in the range of pH 3 to 5 and remained constant as pH≥5. The chromatographic results indicated that beside the contribution of cation exchange, the distribution of the unprotonated organic

bases between the stationary phase and the mobile phase is important. The interactions between the unprotonated organic bases and stationary phase may be due to the π-π charge-transfer provided by the phenyl and/or s-triazine ring moiety and the hydrophobic character of this stationary phase. The roles of these interactions, compared to the function of cation exchange, became predominate interactions when the pH of the mobile phase increased.

ZIXSP Behaves as an Anion Exchanger in the Separation of Organic Acids

Suppose the organic acid in the mobile phase is in an equilibrium state as eq. (5)

$$AH \xrightleftharpoons{K_a} A^- + H^+ \tag{5}$$

and A^- as it interacted with the stationary phase, would replace a counter ion (C^-) from the stationary phase as eq. (6).

$$A^-_m + C^-_s \xrightleftharpoons{K'_c} A^-_s + C^-_m \tag{6}$$

Similarly, the capacity factor k' can be shown as:

$$k' = \frac{V_s}{V_m} \times \frac{[AH]_s + \left[A^-\right]_s}{[AH]_m + \left[A^-\right]_m}$$

$$= \frac{V_s}{V_m} \times \frac{D_{AH} + K'_c \dfrac{K_a}{\left[H^+\right]_m} \dfrac{[C^-]_s}{[C^-]_m}}{1 + \dfrac{K_a}{\left[H^+\right]_m}} \tag{7}$$

Where $D_{AH} = \dfrac{[AH]_s}{[AH]_m}$. Since $[C^-]_s$ is about equal to the total anion exchange capacity[7] for the stationary phase, and $[C^-_m] \doteq 0.001\ M$ in pH range 3 to 7, eq. (7) would be simplified as:

$$k' = \frac{V_s}{V_m} \times \frac{D_{AH} + \dfrac{C'}{\left[H^+\right]_m}}{1 + \dfrac{K_a}{\left[H^+\right]_m}} \tag{8}$$

where C' is a constant equal to $K_a K_c'[C^-]_s[C^-]_m^{-1}$.

In the case of weak acid, such as 1-naphthylacetic acid ($K_a = 5.8 \times 10^{-5}$)and benzoic acid ($K_a = 6.3 \times 10^{-5}$), the term of $K_a[H^+{}_m]^{-1}$ can be neglected at lower pH and eq. (8) could be simplified as:

$$k' = \frac{V_s}{V_m} \times \left(D_{AH} + \frac{C'}{\left[H^+\right]_m} \right) \tag{9}$$

However, since the value of $K_a[H^+{}_m]^{-1}$ would become quite larger than 1 with increasing the pH of the mobile phase in the range of pH 5 to 7 for 1-naphthylacetic acid and benzoic acid. Eq. (8) could be changed into:

$$k' = \frac{V_s}{V_m} \frac{D_{AH}\left[H^+\right]_m + C'}{K_a} \tag{10}$$

Indeed, it revealed that the k' of 1-naphthylacetic acid and benzoic acid increased with the pH of mobile phase before pH 5 (coincide with eq (9)) and tended to decrease with the pH of mobile phase after pH 5 (coincide with eq. (10)).

For the strong acid such as *p*-toluenesulfonic acid ($K_a = 0.020$), the value of K_a is large and in the whole investigated pH range of mobile phase $K_a[H^+{}_m]^{-1}$ is quite larger than 1. Therefore, eq. (8) could be simplified reasonably as eq. (10). Figure 3 also revealed that the k' of *p*-toluenesulfonic acid decreased rapidly with the pH of the mobile phase in the pH range 3 to 5 and leveled off in the pH range 5 to 7.

Since D_{AH} represented the distribution coefficient between the stationary phase and the mobile phase of undissociated organic acid, D_{AH} not being zero, implied that the additional factor(s) of undissociated organic acid in the stationary phase had contributed to the retention mechanism for this ZIXSP

towards the separation of these acids. This factor(s) may be due to the π-π charge-transfer and the hydrophobic interactions between the acid and the phenyl and/or s-triazine ring moiety of this stationary.

ZIXSP Behaves as a Zwitterion Exchanger in the Separate of Amino Acids

In the pH range 3 to 7, the amino acids, phenylalanine, leucine, and alanine, were mostly in the form of zwitterions. Therefore, the COO^- and H_3N^+ groups of amino acid would interact with the amino and sulfo- moieties of the stationary phase respectively. The force of the quadrupolar charge interaction[1,2] among each of the three amino acids and this ZIXSP was stronger than that of the dipolar charge interaction between the simple organic acid or organic base and this ZIXSP. This resulted in that the k' of these amino acids were apparently higher than that of the other five compounds as shown in Figure 3. The occurrence of a volcano at about pH 4 of the mobile phase for the k' of phenylalanine, leucine and alanine may result from the formation of this quadrupolar charge interaction occurred most efficiently at this pH range.

CONCLUSIONS

The present results indicate that a multifunctional ZIXSP containing a s-triazine derived aromatic moiety can be successfully prepared and used to separate various organic acids and bases. The chromatographic behaviour of the phases shows that the effective selectivity of this ZIXSP is due to the sulfo- ($-SO_3H$) group for the cation-exchange ability, the amino group(s) for the anion-exchange ability, the s-triazine as well as phenyl rings for the charge-transfer, and the organic moiety for the hydrophobic character.

ACKNOWLEDGEMENT

REFERENCES

1. J. H. Knox. J. Jurand. J. of Chromatogr., **203**, 85-92 (1981).

2. J. H. Knox, J. Jurand. J. of Chromatogr., **218**, 341-354 (1981).

3. L. W. Yu, T. R. Floyd, R. A. Hartwick, J. of Chromatogr. Sci., **24**, 177-182 (1986).

4. W. Funasaka, T. Hanai, T. Matsumoto, K. Fujimura, T. Ando, J. Chromatogr., **88**, 87 (1974).

5. L. M. Jahangir, L. Olsson, O. Samuelson, Talanta, **22**, 973 (1975).

6. L. M. Jahangir, O. Samuelson, Anal. Chim. Acta., **100**, 53 (1978).

7. P. J. Davis, R. J. Ruane, I. D. Wilson, Chromatographia, **37**, 60 (1993).

8. M. H. Yang, K. C. Chang, J. Y. Lin, J. of Chromatogr. A, **722**, 87-96 (1996).

9. M. H. Yang, C. E. Lin, J. K. Kan, Silicon Material Research Program (Monograph Series, No. 1), National Science Council, Taiwan 75 (1986).

10. J. Y. Lin, M. H. Yang, J. of Chromatogr., **644**, 277-283 (1993).

11. R. L. Shriner, D. Y. Curtin, R. C. Fuson, T. C. Morrill, **The Systematic Identification of Organic Compounds**, 2nd Ed. John Wiley & Sons, Inc., New York, 1980, p.202.

12. C. Horvath, W. Melander, I. Molnar, Anal. Chem. **49**, 142-154 (1977).

13. P. Jandera, J. Churacek, J. of Chromatogr., **91**, 207-221 (1974).

14. Present address: Department of Medical Technology, Hualien 970, Taiwan.

HIGH PERFORMANCE LIQUID CHROMATOGRAPHIC EVALUATION OF A LOW-TEMPERATURE GLASSY CARBON STATIONARY PHASE

C. T. Rittenhouse, S. V. Olesik

The Ohio State University
100 W Eighteenth Ave
Columbus, OH 43210

ABSTRACT

A low temperature glassy carbon (LTGC) stationary phase coated on porous glassy carbon and zirconium oxide is chromatographically evaluated and compared to an uncoated porous glassy carbon stationary phase. The curing temperature of the LTGC was chosen to produce a surface having a reversed phase type retention mechanism. The LTGC coating of the porous glassy carbon reduced retention due to dispersive interactions while maintaining a similar retention mechanism as the untreated porous glassy carbon phase. The LTGC-coated zirconia produced an efficient column with classical reversed-phase retention behavior.

INTRODUCTION

The most commonly-used stationary phases are based on bonded silanes or polysiloxane polymers supported on silica gel surfaces. These materials are not typically suitable for separations performed at high or low pH.

2997

The search for more stable stationary phases as well as alternative nonpolar stationary phases and supports for chromatographic separations is continuous. A surface containing only carbon atoms is often considered the nonpolar surface of choice due to its uniform chemical nature. Kieselev and his associates initiated and established the use of graphitic materials, such as carbon blacks, as adsorbents in gas chromatography.[1] Graphitic carbon black adsorbents are now used routinely for the separation of structural isomers of compounds by gas chromatography. These materials cannot be readily used in high performance liquid chromatography (HPLC) because of inadequate mechanical stability and surface area.

Glassy carbon was first prepared by Yamada and Sato in 1962 by high temperature pyrolysis of phenolic resins.[2] Glassy carbon is macroscopically amorphous, but contains the regional microstructures of graphite. Glassy carbon is less dense than graphite, which implies structural voids. These voids are apparently not connected since, glassy carbon is impermeable to gases. Glassy carbon is particularly well suited as an adsorbent or stationary phase material for HPLC because of its high mechanical, excellent chemical stability and high surface area ($150\text{-}200 \ m^2/g$).[3]

In 1982 Knox and Gilbert described the production and use of a glassy carbon adsorbent they call "porous glassy carbon" or "porous graphitic carbon" (PGC).[4] This material is produced by coating suitable phenolic resins on the surface of porous silica gel particles, polymerizing the resin in the pores, pyrolyzing the resin in N_2 (or Ar), dissolving the silica particle (template) and then heating the polymerized resin to 2000-2800°C to produce particles of "porous glassy carbon." These particles are now commercially available as Hypercarb.

The retention mechanism and the selectivity of solutes on porous glassy carbon in HPLC and SFC were studied by us[5-9] and others.[10-13] Glassy carbon, like graphite, is a hydrophobic, highly-polarizable solid. In reversed phase HPLC, it can be classified as an adsorbant where the glassy carbon surface acts as a Lewis base toward polar solutes and is involved in $\pi\text{-}\pi$ interactions and dispersive interactions with aromatic solutes. Porous glassy carbon (PGC) has the advantage of extreme pH stability. The highly ordered planar surface, on the molecular level, produces unique structural selectivity, with an amorphous macro structure that forms the porous particles necessary for high surface area. The homogeneous surface has fewer chromatographic active sites and provides good chromatography for basic compounds.

A method of producing glassy carbon at low temperatures (200-800°C) was recently reported.[14,15]   Poly-(phenylene diethynyl) compounds are first synthesized and then slowly heated to produce glassy carbon. The heat treatment of these oligomers results in small observable mass loss that allows the production of continuous low temperature glassy carbon (LTGC) films. Since poly-(phenylene diethynyl) oligomers are soluble in organic solvents, such as methylene chloride, standard coating procedures used to produce open tubular columns with polysiloxane stationary phases should be applicable for the production of open tubular columns with LTGC films.

Applications of LTGC-coated silica chromatographic stationary phases in HPLC and SFC were recently demonstrated.[6-8,16] LTGC stationary phases have been produced with a range of retention mechanisms. If the LTGC is cured at low processing temperatures (i.e., 200°C), then its surface specificity is similar to bonded phenyl polysiloxane stationary phases.[16]   As the processing temperature is increased, then conjugation within the LTGC increases and the dipolarity / polarizability of a solute becomes more important. At processing temperatures near 550°C, the LTGC has chemical specificity and retention very similar to that of PGC. At higher processing temperatures the importance of analyte dipolarity / polarizability on retention seems to increase further than that possible with PGC,[16] although this requires further study.

PGC has the disadvantage of being very retentive, and higher molecular weight solutes may not elute. Large molecule mobile phase additives, such as p-terphenyl, have been used to reduce retention and improve peak shapes.[3,4] The retentivity of LTGC increases with processing temperature. The retentivity of LTGC processed at 550°C is similar to that of PGC. At lower temperatures the retentivity is markedly decreased.

Because the LTGC can be produced at low temperatures (200-600°C), a variety of chromatographic support materials are possible. For example, silica, alumina, zirconia and PGC particles are all potential supports. To date, silica gel is the only LTGC support material studied. Zirconium oxide is stable over the entire (0 - 14) pH range and its use has been demonstrated in RP-HPLC.[11,17-22] Zirconia offers significant advantages to silica gel and is a worthy choice to investigate. The hydrophobic surface of PGC should be an advantage when coating with LTGC monomers dissolved in hydrophobic solvents and should result in a more uniform coating than a polar support. This paper compares the chromatographic characteristics of PGC (produced by the Knox method), LTGC coated on zirconia particles, and LTGC coated on PGC particles.

The final processing temperature of the LTGC in these studies was 400°C to supply retentivity and selectivity characteristics approximately in the middle of the range available for LTGC. The solvatochromic comparison method was used to evaluate the relative chromatographic selectivity of the three different column types studied.

MATERIALS

Reagents and Chemicals

Table 1 lists the test solutes (Aldrich Chemical Co.) used in this study. The 60:40 water: acetonitrile mobile phase was prepared using purified water (Millipore, Milford MA) and HPLC grade acetonitrile (Fisher Scientific, Fairlawn, NJ).

The oligomer precursor was synthesized in-house according to the procedure previously reported.[14]   The 5 μm zirconia was obtained from Keystone Scientific (State College, PA) and 5.5 μm Hypercarb® were obtained from Shandon HPLC (Runcorn, UK). For each type of chromatographic support, 100 mg of particles were slurried in 2 mL of a 10 mg/mL solution of oligomer in methylene chloride for 5 minutes, then the slurry was sonicated briefly (5 min.) under a vacuum. The coated particles were isolated by filtration without rinsing, and placed in the fluidized bed apparatus; argon flow was introduced and they were slowly heated at a rate of 1°C/ min over the temperature range of 50-400°C. The LTGC was cured at 400°C for 1 hr then cooled under argon to room temperature.

Columns

The particles were packed into 0.51 mm x 10 cm x 1/16" O.D. columns of Silcosteel tubing (Restek Corp., Bellefonte, PA, USA). A slurry of the PGC packing materials was prepared by sonicating the required amount of packing in 1.5 mL HPLC grade acetonitrile for approximately 30 minutes. The slurry was then transferred by syringe from the vial to a 4.6 mm id x 5 cm stainless steel reservoir connected directly to the head of the column. The reservoir connector was machined to form a funnel-like taper to the head of the column. The column was placed into a sonicator bath while the slurry was forced into the column at 4000 psi, using a syringe pump, for at least one hour. After one hour the column was allowed to depressurize to ambient before being removed.

Table 1

Solvatochromic Regression Data

Solute	$V/100^{24}$	π^{*24}	β^{24}	α^{24}	PGC	Log Ret. Factor LTGC/ Zirconia	LTGC/ PGC
1,3,5 trimethylbenzene[A]	0.769	0.43	0.13	0	1.564	0.284	1.052
3 xylene	0.668	0.51	0.12	0	1.122	0.060	0.738
benzene	0.491	0.59	0.10	0	0.228	-0.458	0.022
biphenyl	0.920	1.18	0.20	0	2.094	0.610	1.668
bromobenzene	0.624	0.79	0.06	0	0.941	-0.019	0.616
butylbenzene[A]	0.883	0.49	0.12	0	1.596	0.503	1.150
chlorobenzene	0.581	0.71	0.07	0	0.777	-0.125	0.331
ethylbenzene[A]	0.687	0.53	0.12	0	0.907	-0.010	0.564
iodobenzene	0.671	0.81	0.05	0	1.212	0.154	0.864
naphthalene	0.753	0.70	0.15	0	1.808	2.053	1.384
pentylbenzene	0.981	0.47	0.12	0	2.007	0.697	1.475
propylbenzene	0.785	0.51	0.12	0	1.252	0.218	0.865
toluene	0.592	0.55	0.11	0	0.658	-0.212	0.425
2 chloroaniline	0.652	0.83	0.40	0.25	0.636	-0.432	0.217
3 chlorophenol	0.626	0.77	0.23	0.69	0.613	-0.497	0.248
3 cresol[A]	0.634	0.68	0.34	0.58	0.305	-0.666	-0.050
3 phenyl 1 propanol	0.830	0.95	0.55	0.33	0.314	-0.760	-0.127
4 chlorophenol	0.626	0.72	0.23	0.67	0.599	-0.508	0.228
4 cresol	0.634	0.68	0.34	0.58	0.329	-0.666	-0.036
N ethylaniline[A]	0.758	0.82	0.47	0.17	0.849	-0.228	0.420
N methylaniline	0.660	0.73	0.47	0.12	0.471	-0.458	0.122
aniline	0.562	0.73	0.50	0.26	-0.125	-0.896	-0.144
benzanol[A]	0.634	0.98	0.52	0.39	-0.163	-1.028	-0.502
phenol	0.536	0.72	0.33	0.61	-0.132	-1.080	-0.416
N,N diethylaniline[A]	0.948	0.86	0.43	0	1.442	0.334	0.953
acetophenone	0.690	0.90	0.49	0.06	0.499	-0.550	0.210
anisole	0.630	0.73	0.32	0	0.546	-0.378	0.214
benzonitrile[A]	0.590	0.90	0.37	0	0.378	-0.586	0.005
butyrophrenone[A]	0.886	0.85	0.49	0.06	1.295	-0.067	0.742
hexanophenone[A]	1.092	0.83	0.49	0.06	2.161	0.461	1.46!
methylbenzoate	0.736	1.14	0.52	0	0.908	-0.299	0.453
nitrobenzene[A]	0.631	1.01	0.30	0	0.756	-0.038	0.375
phenotole	0.727	0.69	0.30	0	0.956	-0.154	0.539
propiophenone[A]	0.788	0.87	0.49	0.06	0.966	-0.280	0.471
valerophenone	0.984	0.83	0.49	0.06	1.702	0.182	1.078
hexane	0.648	-0.04	0	0			

[A] Solutes used in hexane mobile phase experiment

The zirconia packing was slurried with isopropanol to inhibit rapid settling of the denser particles, but otherwise handled the same. A 10 cm x 0.51 mm column should contain about 50 mg of the PGC packing and about 70 mg of the zirconia coated packing.

Equipment

The chromatographic system consists of an LC-2600 syringe pump (ISCO, Inc., Lincoln NE, USA), W-series high pressure injection valve with 200 nL loop (Valco Instruments, Houston TX), and Spectroflow 757 UV detector (Kratos Analytical Inst., Ramsey, NJ, USA) operated at 210 nm. The detector cell was prepared from 100 μm id fused silica with the polyimide coating removed.

The column temperature was maintained at 50°C with an HP 5890 GC oven (Hewlett-Packard, Avendale, PA, USA). The chromatographic data were collected with EZchrom Chromatography Data System V6.0 (Scientific Software, Inc., San Ramon, CA, USA) and analyzed by Peak Fit (Jandel Scientific, San Rafael, CA, USA).

RESULTS AND DISCUSSION

Loading Linearity

To achieve optimum efficiency in elution chromatography, the linear portion of an isotherm should be used. The variation of the retention factor (or capacity factor, k) with amount of solute injected was studied. Test solutes for the loading study were chosen for their different chromatographic properties.

The solute concentration ranges were chosen so that 0.08-1.64 μg was injected; the ethylbenzene concentration was slightly less due to solubility limits. The same volume (200 μL) of each sample solution was injected.

Figure 1 contains plots of the retention factor (k) versus the amount of solute injected. The tested amounts all gave constant retention factors and the subsequent chromatographic tests were performed by injecting approximately 0.2 μg of solute, well within the established linear loading range.
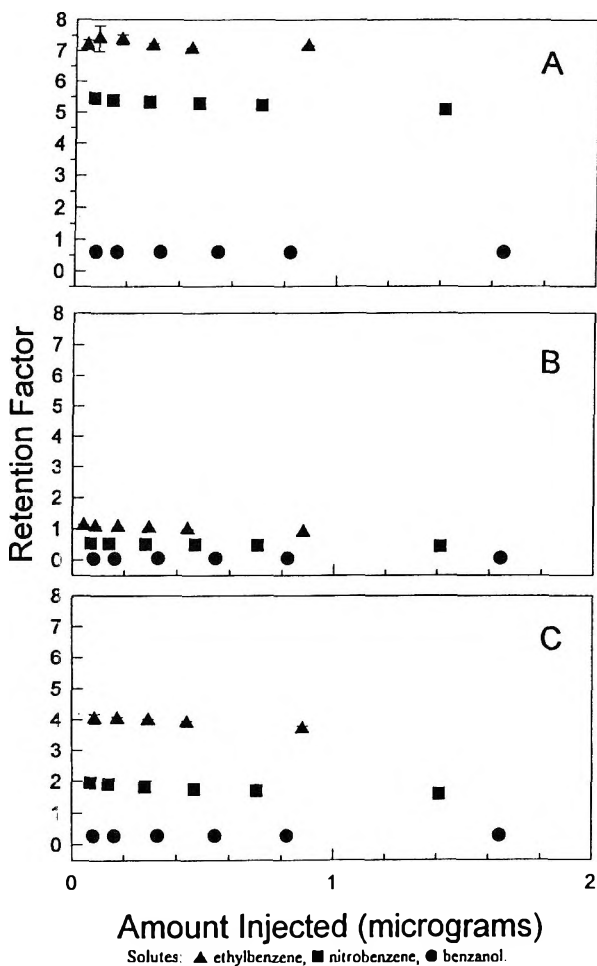
Figure 1. Loadability of stationary phases; A- PGC, B- LTGC-coated zirconia, C- LTGC-coated PGC. Solutes: ▲ ethylbenzene, ■ nitrobenzene, ● benzanol. Error bars are within the symbols if not visible.

Solvatochromic Comparisons Method

Many chromatographic processes have been investigated via the solvatochromic comparison method.[17,23-28] With this method (equation 1) a linear free energy model is used as a general equation to relate solute retention factors, log k, to the molecular level interactions occurring in solution and at

the stationary phase.[24]

$$\log k = SP_o + M(\delta_m^2 - \delta_s^2)\frac{V_2}{100} + S(\pi_s^* - \pi_m^*)\pi_2^* \tag{1}$$

$$+ A(\beta_s - \beta_m)\alpha_2 + B(\alpha_s - \alpha_m)\beta_2$$

The solute properties (subscripted 2) are multiplied by the difference in the complementary properties of the competing mobile and stationary phases, subscripted m and s, respectively. The first term, SP_0, is the intercept. The second term is a measure of the free energy needed to create space in the solvent for a solute molecule, where δ, the Hildebrand solubility parameter, measures the solvent's cohesiveness.[29]   To a first approximation, V, the van der Waals molar volume of the solute is proportional to the solute's dispersive interactions with the stationary phase. The molar volume is divided by 100 so the values are of the same magnitude as the other parameters. The last three terms are Kamlet-Taft terms, α and β are measures of H-bond donor ability, H-bond acceptor ability, and π^* measures dipolarity / polarizability.[30-32]   The coefficients of equation 1 (SP_0, M, S, A, B) are unknown, but can be determined by multifactor regression analysis.

In the studies described herein, the retention factors of the test solutes are measured for each stationary phase while the mobile phase conditions are held constant. Under these conditions, equation 1 simplifies to Equation 2.

$$\log k = SP_o + m\frac{V_2}{100} + s\pi_2^* + a\alpha_2 + b\beta_2 \tag{2}$$

The new coefficients, m, s, a and b, contain the information relating to the chemical nature of the mobile and stationary phases and also the original model coefficients. The sign of the coefficient represents whether the solute property is an exoergic or endoergic factor in the retention process.

The regression of the log k for the same solute set on various stationary phases under the same chromatographic conditions will give model coefficients that differ because of the stationary phase properties. Therefore a comparison of these coefficients shows the differences in the retention processes of the stationary phases under the mobile phase conditions and should give insight into the chemical nature of the stationary phase. The integrity of the data were determined using established guidelines for multivariable linear regression analyses.[33]   A cross correlation of the independent parameters produces a maximum correlation coefficient of 0.598
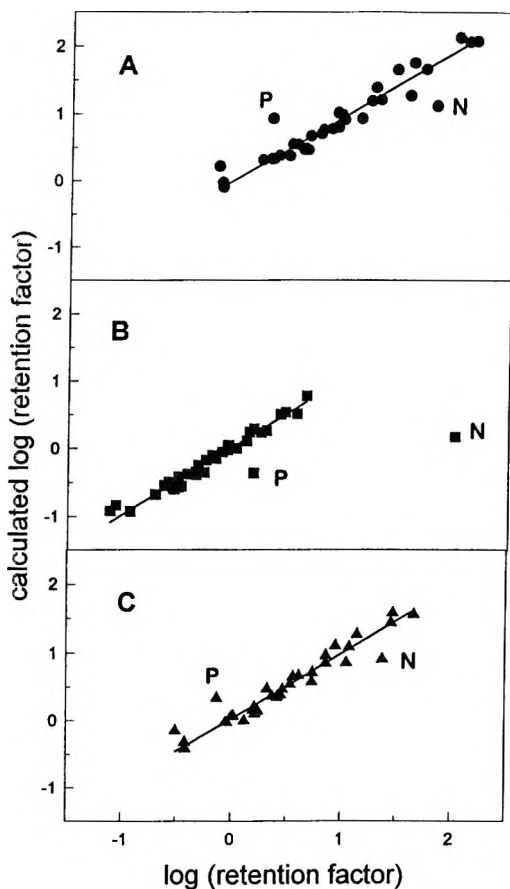
Figure 2. Solvatochromic regression plots of the solutes observed vs calculated log (retention factor) for the stationary phases; A- PGC, B- LTGC-coated zirconia, C-LTGC-coated PGC. The outliers phenyl propanol and naphthalene are not included in the regression but are designated P and N.

for β and π^* indicating that no significant correlative relationships exist between the independent variables. The F-test at the 95% confidence level was used to indicate whether the relationships in model equation was statistically significant. All models described here passed the F-test. The t-statistic of the coefficient was evaluated at the 95% confidence level to test for statistical significance.

The multivariable regression analysis was initially performed with all the independent variables. The significance of each independent parameter was evaluated at the 95% confidence level; those not meeting the requirements were omitted from the model.[34] The same data were also analyzed via the stepwise backward multiple regression analysis where one independent parameter was added to the model equation at a time in the order of most significant. Those independent parameters not improving the precision of the fitted equation were removed. The model equations from both regression methods for a given column and data set were the same.

The data used for the regression analysis are listed in Table 1. The chosen solute set consists of a range of solvatochromic parameter values to determine the significance of the corresponding interactions. Figure 2 illustrates the ability of the model to predict the retention factors for each column. Naphthalene and 3-phenyl-1-propanol are significant outliers in the LTGC-coated zirconia data (Figure 2B). These solutes are also outliers in the other data sets and are shown on all plots. These data were excluded from all regression analyses to maintain consistency between data sets. The omission of naphthalene and 3-phenyl-1-propanol improved the precision of the model equations in all cases. The retention models evaluate thermodynamic interactions of the solute with no consideration given to the shape of the molecule or its orientation to the stationary phase. The shape selectivity of chromatographic adsorbant stationary phases[13] is the most likely cause for the outliers.

Table 2 lists the summary of the regression results for the present study. Figure 3A is a plot of the table data comparing the coefficient values. The statistics show an excellent fit of the data using the solvatochromic model, Equation 2.

The results show that dispersive interactions, i.e., the m coefficient that scales with solute size, is the most important parameter in solute retention on all three supports. In all cases, the sign of the m coefficient is positive which shows as solute size increases so does its retention. A solute's ability to accept a hydrogen bond (b coefficient) was the next most important variable. In all cases the sign of the b coefficient was negative which indicates decreased retention with increasing H-bond accepting ability of the solutes. The s coefficient (dipolarity / polarizability) and the a coefficients (hydrogen bond donating ability) were of lesser importance but still affected solute retention on PGC and LTGC-PGC to approximately the same magnitude, but with opposite effects. Increasing π^* causes increased retention and increasing solute hydrogen bond donor ability, α, decreased retention. Interestingly, for the LTGC-coated zirconia the s coefficient (dipolarity / polarizability) was not
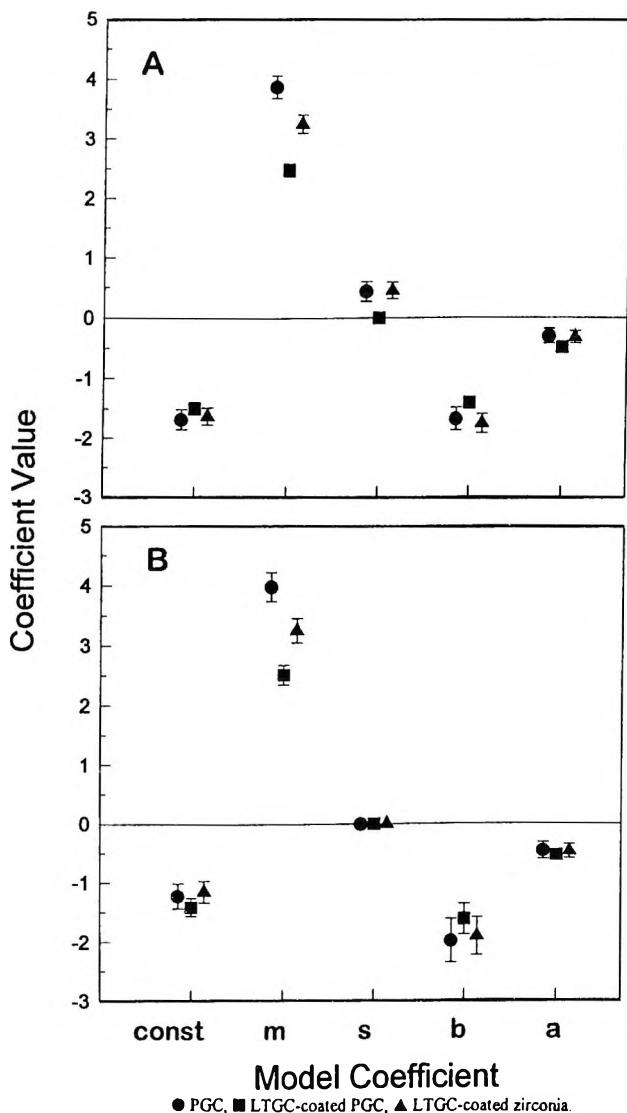
Figure 3. Comparison of the coefficient values from the solvatochromic regression using the aqueous mobile phase. ● PGC, ■ LTGC-coated zirconia, ▲ LTGC-coated PGC.

Solute groupings: A- all solutes, B- hydrogen bonding solutes. Error bars are within the symbols if not visible.

Table 2

Solvatochromic Model Coefficients using Water/Acetonitrile Mobile Phase with all Solutes

Column	Constant (s)[a]	m (s)	s (s)	b (s)	a (s)	Statistics		
						N[b]	R[2c]	F[d]
PGC	-1.68 (0.17)	3.88 (0.18)	0.44 (0.16)	-1.67 (0.19)	-0.30 (0.12)	33	0.957	157
LTGC-coated zirconia	-1.49 (0.08)	2.48 (0.11)	-[e]	-1.40 (0.09)	-0.48 (0.07)	33	0.972	332
LTGC-coated PGC	-1.62 (0.14)	3.26 (0.16)	0.45 (0.14)	-1.75 (0.16)	-0.32 (0.10)	33	.0960	166

[a] Standard Deviation. [b] Number of solutes. [c] Square of multiple correlation coefficient. [d] Calculated F value, all are statistically significant at the 95% confidence level. [e] not significantly correlated.

statistically significant; while the a coefficient (hydrogen bond donating ability of the solute) was even more significant than observed with PGC or LTGC-coated PGC.

The individual regression coefficients for PGC were compare to those from the LTGC-coated supports and tested for equality using the t-test at the 95% confidence level.[35] The m coefficients (dispersive interactions) were statistically different for all three supports and decreased in the order of PGC> LTGC-coated PGC > LTGC-coated zirconia. In general, the retentivity of the LTGC phases are less than that of the PGC mainly through a decrease in dispersive interactions; however, the s values determined for the PGC and the LTGC-coated PGC phases are statistically the same. These results suggest the LTGC coating does not diminish the dipolar / polarizability solute interactions with the PGC support. Statistically the s coefficient is 0 for the LTGC-coated zirconia which indicates the lack of solute dipolarity / polarizability interactions of the LTGC coating. The uncoated zirconia was found to have negligible retention of these solutes in an aqueous 10% acetonitrile mobile phase and would be expected to have no solute dipolar / polarizability interactions under the current conditions.[36]

Table 3

Solvatochromic Regression Coefficients using Water/Acetonitrile Mobile Phase with Nonpolar Solutes

Column	Constant (s)[a]	m (s)	s (s)	b (s)	a (s)	N[b]	Statistics R[2c]	F[d]
PGC	-1.62 (0.18)	3.43 (0.21)	0.51 (0.15)	-[e]	-[e]	12	0.969	141
LTGC-coated zirconia	-1.58 (0.090)	2.44 (0.14)	0.16 (0.08)	-1.22 (0.52)	-[e]	12	0.983	150
LTGC-coated PGC	-1.632 (0.19)	2.98 (0.23)	0.47 (0.16)	-[e]	-[e]	12	0.954	93

[a] Standard Deviation. [b] Number of solutes. [c] Square of multiple correlation coefficient. [d] Calculated F value, all are statistically significant at the 95% confidence level. [e] not significantly correlated

These data suggest that the LTGC coating (processed to 4000C) itself doesn't enhance or participate in π^* interactions. The a and b coefficients were statistically the same for all three supports.

A previous study of C_{18} bonded phase RP-HPLC revealed that solute size is the major factor in retention followed by its hydrogen bond acceptor ability with a minor dependence upon solute dipolarity / polarizability.[23] The same observations can be made here with the addition of a minor dependence upon the solute's hydrogen bond donor ability, especially in the case of the zirconium coated LTGC.

The data were also analyzed by solute class to highlight the differences in specific stationary phase interactions. The solutes were divided into the classes of nonpolar, hydrogen bond donors and hydrogen bond acceptors. The nonpolar compounds contain only aromatic solutes with aliphatic or halogen groups, and the results are presented in Table 3. The hydrogen bond donor solutes all contain donable protons and some have hydrogen bond acceptor sites as well. The hydrogen bond acceptor solutes had no donable protons. The hydrogen bond donor and acceptor solute data were combined and correlated

Table 4

Solvatochromic Model Coefficients using Water/Acetonitrile Mobile Phase HBD and HBA Solutes

Column	Constant (s)[a]	m (s)	s (s)	b (s)	a (s)	N[b]	Statistics R[2c]	F[d]
GPC	-1.22 (0.22)	3.98 (0.24)	-[e]	-1.99 (0.37)	-0.46 (0.14)	21	0.956	125
LTGC-coated zirconia	-1.41 (0.15)	2.52 (0.17)	-[e]	-1.62 (0.26)	-0.53 (0.10)	21	0.954	121
LTGC-coated PGC	-1.15 (0.19)	3.26 (0.20)	-[e]	-1.91 (0.32)	-0.47 (0.12)	21	0.954	119

[a] Standard Deviation. [b] Number of solutes. [c] Square of multiple correlation coefficient. [d] Calculated F value. all are statistically significant at the 95% confidence level. [e] not significantly correlated.

because separate analysis were yielding strong correlations with weak data set parameters. i.e. those with small ranges. The combined data set yields more conclusive information the statistical results are presented in Table 4. A comparison of the coefficient values determined for the hydrogen bond forming and nonpolar solutes are plotted in Figures 3B and 4A.

Only those observations which are unique to the solute classes are discussed. The retention of the nonpolar solutes on the LTGC-coated zirconia is strongly dependent upon solute dipolarity / polarizability interactions with the stationary phase. There is a strong stationary phase hydrogen bond donor interaction with the nonpolar solutes. The negative value of b indicates a decrease in retention and therefore a repulsive effect on the nonpolar solutes. The standard error is large. however the large b indicates a strong interaction. The hydrogen bonding solute retentions have no correlation with dipolarity / polarizability interactions with any stationary phase, which is surprising since the π^* values for the solute set cover a good range.
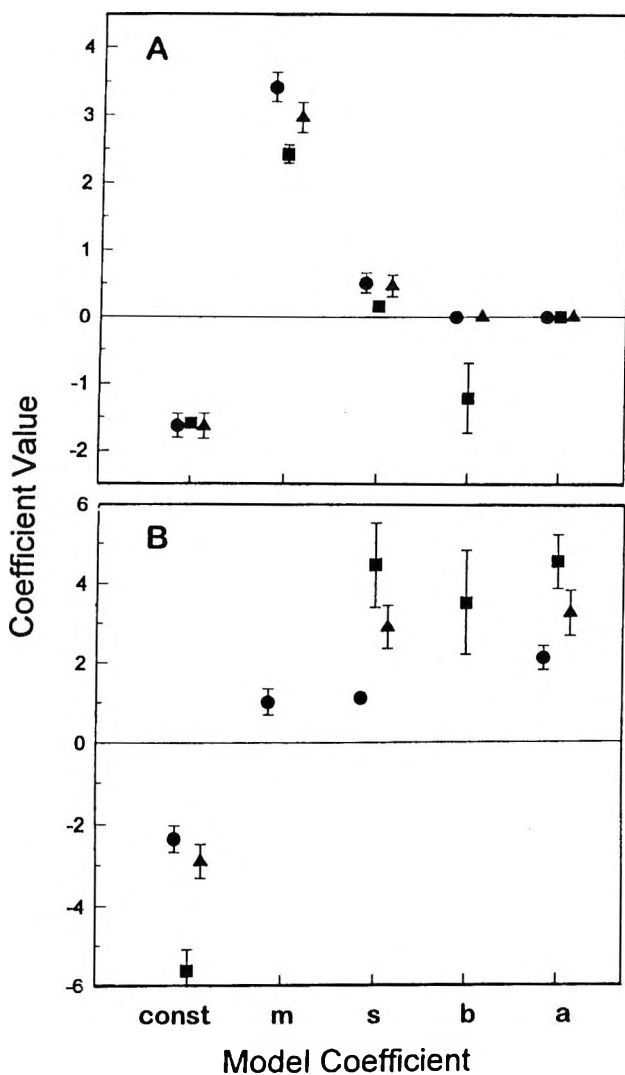
Figure 4. Comparison of the coefficient values from the solvatochromic regression of the stationary phases; ● PGC, ■ LTGC-coated zirconia, ▲ LTGC-coated PGC. Using: A- the nonpolar solutes with aqueous mobile phase, B- selected solutes with hexane mobile phase. Error bars are within the symbols if not visible.

The solvatochromic analysis of the entire and individual solute sets indicate the LTGC-coated PGC phase has the same retention mechanisms as the PGC phase with the exception of less dependence on solute dispersive interactions. Comparison of the PGC and the LTGC-coated PGC reveal no significant active site interactions are caused by the LTGC coating under the test conditions. The LTGC-coated zirconia results suggest much weaker dipolar / polarizable interactions with the nonpolar solutes which was not apparent in the analysis of the entire solute data set. Evidence of stationary phase hydrogen bond donor interactions with nonpolar solutes indicate stationary phase active sites capable of donating a hydrogen bond. It can be concluded that the strong dependence on solute β with LTGC-coated zirconia must be due to the presence of the zirconia.

Hexane Mobile Phase

The Hildebrand solubility parameter, δ, for hexane is very small relative to the aqueous acetonitrile mobile phase used earlier.[37] Unlike the aqueous mobile phase, hexane has a very large dispersive interaction with the solutes and a dispersive shielding effect on the stationary phase. The solvatochromic parameters for hexane, Table 1, indicate the absence of any hydrogen bonding ability. The negative π^* value shows there are slight repulsive dipolarity / polarizability interactions on the solute molecules. Chromatographic probing using a hexane mobile phase should enhance solute hydrogen bond interactions with the stationary phase.

The columns were flushed over night with acetonitrile at a column temperature of 80°C and then allowed to equilibrate with hexane for several hours. Both solvents were dried with a molecular sieve for at least three days. The column temperature was reduced to 50°C for the experiment. Each column was evaluated with a set of 13 solutes representative of those listed in Table 1 using hexane as the mobile phase.

The multiple correlation parameters were all 0.94 or greater which is a good fit for such a small diverse data set, Figure 5. Table 5 and Figure 4B lists the coefficients of the regression for comparison.

Only PGC retains a dependence upon dispersive interactions in the hexane mobile phase agreeing with the strong dispersive interactions observed in the reversed-phase system.
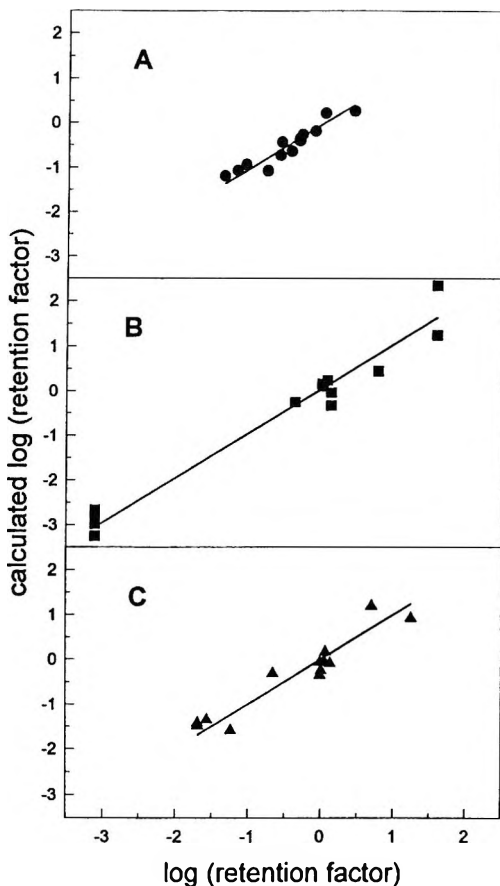
Figure 5. Solvatochromic regression plots using hexane mobile phase. A- PGC, B-LTGC-coated zirconia, C- LTGC-coated PGC.

The retention on LTGC-coated zirconia in hexane is strongly dependent upon the solute dipolarity / polarizability, hydrogen bond acceptor, and hydrogen bond donor interactions. Both PGC and LTGC-coated PGC had positive s and a coefficients, and b was statistically 0. The absence of solute hydrogen bond acceptor interactions (i.e., $b = 0$) with the PGC and LTGC-coated PGC stationary phases indicates there was no adsorbed water on the stationary phases.

Table 5

Solvatochromic Model Coefficients using Hexane Mobile Phase

Column	Constant (s)[a]	m (s)	s (s)	b (s)	a (s)	N[b]	Statistics R[2c]	F[d]
PGC	-2.35 (0.33)	1.02 (0.33)	1.12 (0.28)	-[e]	2.11 (0.31)	13	0.896	26
LTGC-coated zirconia	-5.62 (0.53)	-[e]	4.47 (1.07)	3.51 (1.30)	4.54 (0.68)	13	0.964	81
LTGC-coated PGC	-2.89 (0.42)	-[e]	2.91 (0.54)	-[e]	3.24 (0.57)	13	0.881	37

[a] Standard Deviation. [b] Number of solutes. [c] Square of multiple correlation coefficient. [d] Calculated F value, all are statistically significant at the 95% confidence level. [e] not significantly correlated.

High s values for all stationary phases can be attributed to the absence of dipolarity / polarizability competition with the mobile phase. However, the ordering of the s values (LTGC-coated zirconia > LTGC-coated PGC > PGC) is not readily explained, as it is contrary to the aqueous mobile phase results.

The stationary phase hydrogen bond acceptor strength is greatest for the LTGC-coated zirconia and least for the PGC. The oxide sites of the glassy carbon edge planes could cause these hydrogen bond acceptor interactions with the solutes. Greater solute hydrogen bond acceptor interaction with the LTGC-coated PGC may indicate more oxide formation during the polymer curing. The LTGC-coated zirconia has both strong hydrogen bond donor and hydrogen bond acceptor interactions with the solutes. This observation agrees with the nonpolar solutes - aqueous mobile phase observations. The stationary phase hydrogen bond donor interactions are therefore most likely due to the zirconia. The increased hydrogen bond acceptor interactions could also be from the zirconia. The presence of surface oxides on the zirconia is a known cause of chromatographic active sites.[21] Surface oxides in normal phase HPLC can cause polarization of large solutes.[38] This type of solute interaction should manifest as an increase in the s coefficient as was observed here.

This data is useful for discerning the surface of the stationary phases, however it is important to note that the "hexane mobile phase active sites" would most likely have little effect upon the reversed-phase retention mechanism.

Efficiency

The chromatographic efficiency of each column was determined by measuring the reduced plate height (h) for three chromatographically different test solutes, used previously in the loading study, over a range of mobile phase flow rates. Figures 6A through 6C show the results of this efficiency study.

The efficiency behavior between the columns varied. Both the LTGC-coated columns have much shallower slopes contrasted to the PGC column indicating faster mass transfer kinetics. The LTGC-coated zirconia column has the highest efficiency and a different ordering of the solute curves versus the other columns. That is, nitrobenzene yields the lowest efficiency curves with both the PGC and the LTGC-coated PGC phases, but ethylbenzene is the least efficient curve of the LTGC-coated zirconia plots. This switch in order of efficiency may be due to different retention mechanisms between the columns; however the order of analyte retention was the same for all three columns.

Scanning electron microscopy (SEM) was performed on the packing materials to further compare the packing materials. The range in particle diameters (2-8 μm) was substantial for PGC particles. The LTGC-coated PGC particles had the same size distribution as the PGC. Because the range of particle dimensions was so large for the PGC, the film thickness of the LTGC was not discernable. However, the uncoated particles had markedly smoother topology which indicated that the PGC particles were clearly coated with LTGC. Micrographs of both the PGC and the LTGC-coated PGC particles unexpectedly showed several broken shells of hollowed out spheres. The broken shells and the deeper pore structure of the LTGC-coated PGC would contribute to the lower column efficiency observed. The LTGC-coated zirconia also appeared smooth with a more uniform particle size distribution.

Homolog vs Log Retention Factor

The linear dependence of log k versus homolog carbon number, i.e., the number of repeating methylene units, is conventionally used to demonstrate reversed-phase retention behavior.[39] The first few homologs have been shown to deviate from linearity especially on adsorbant phases.[40]
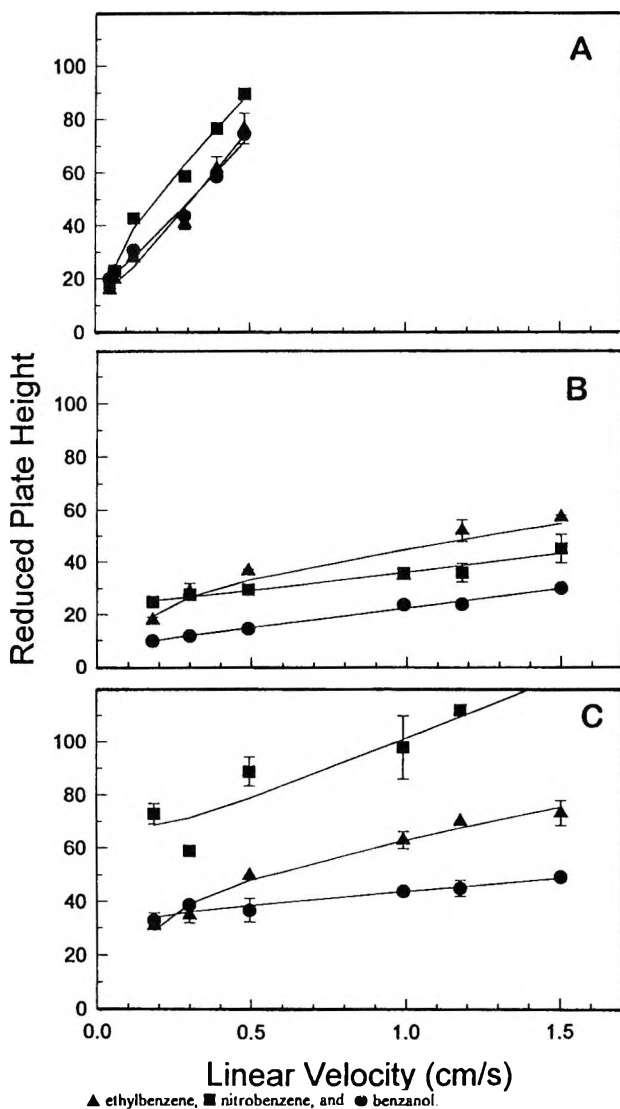
Figure 6 Reduced plate height vs linear velocity for ▲ ethylbenzene, ■ nitrobenzene, and ● benzanol. A- PGC, B- LTGC-coated zirconia, C- LTGC-coated PGC. Error bars are within the symbols if not visible.

Alkylbenzene and alkylphenone homologs were used in this study because they were previously used to characterize the selectivity on a carbon-clad zirconia support.[40]
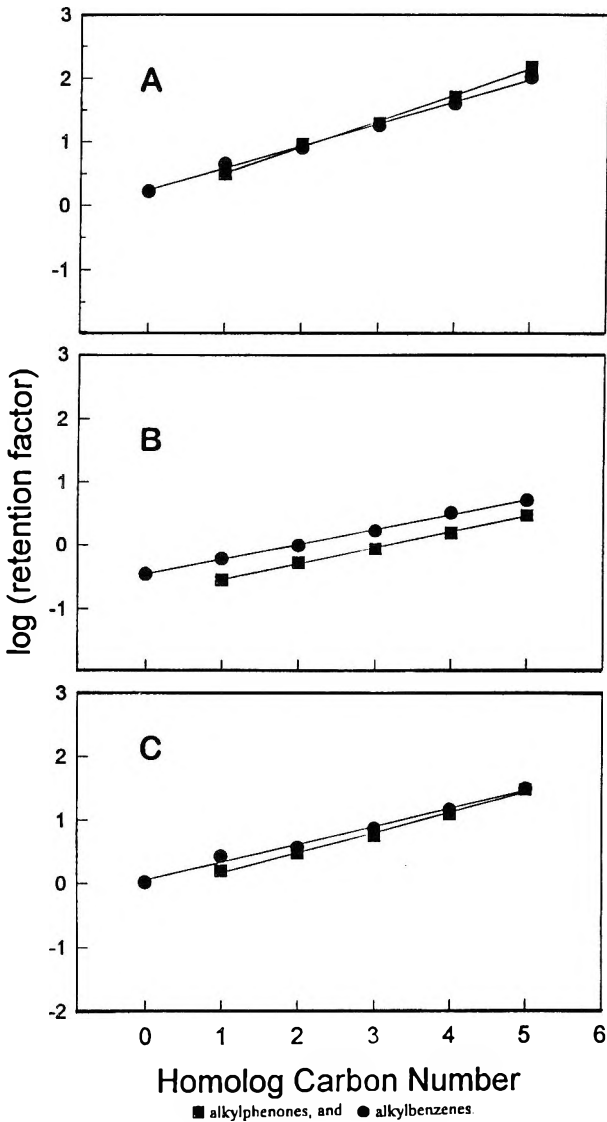
Figure 7. Log (retention factor) vs homolog carbon number for ■ alkylphenones, and ● alkylbenzenes. A- PGC, B- LTGC-coated zirconia, C- LTGC-coated PGC. Error bars are within the symbols if not visible.

Table 6

Stationary Phase	Alkylbenzene		Alkylphenone	
	Slope (s)	Intercept (s)	Slope (s)	Intercept (s)
PGC	0.34	0.25	0.41	0.11
	(0.011)	(0.03)	(0.012)	(0.042)
LTGC-coated PGC	0.28	0.06	0.31	-0.15
	(0.01)	(0.04)	(0.01)	(0.05)
LTGC-coated zirconia	0.23	-0.46	0.25	-0.80
	(0.01)	(0.02)	(0.01)	(0.02)

Figure 7A is a plot of the log (retention factor) for the alkylphenone and alkylbenzene homologs versus carbon number on the PGC column. The plot shows a crossover at carbon number 2 where the alkylphenones are more retained at carbon numbers greater than 2. The intercepts for both lines are positive as listed in Table 6.

Figure 7B is the homolog linearity plot of the LTGC-coated zirconia. The regression lines are almost parallel as indicated by the slopes demonstrating consistent selectivity throughout the tested range of carbon numbers. Both intercepts are negative with the alkylphenone being less retained.

The homolog plot of the LTGC-coated PGC stationary phase (Figure 7C) shows a crossover at 5 carbon numbers with the alkylbenzenes being more retained throughout the range 0 to 5 carbon numbers.

The intercepts confirm previous observations on retentivity with PGC being the most retentive and LTGC-coated zirconia being the least retentive. The differences in the slope between the three columns is very interesting.

The slope of the lines for the alkylphenones homolog was greater than that of the alkylbenzenes for all three columns. The difference in slope values between the alkylbenzene and the alkyl phenones decreased in the order of PGC> LTGC-coated PGC> LTGC-coated zirconia.

With conventional chemical-bonded reversed-phase supports, the alkylphenone homologs are retained less than the alkylbenzenes and the selectivity for a methylene group (slope) in the alkylbenzene and alkylphenones

is very similar. The selectivity of the LTGC-coated zirconia is very similar to that of conventional reversed phase supports. Marked differences between the slopes of alkybenzene and alkylphenone homologs were previously observed by Carr and coworkers[40] for a carbon-cladded surface. When a polybutadiene film was coated over the carbon-claded surface or the surface was exposed to hydrogen, the differences in the slopes decreased substantially. The cause of the different slopes was then attributed to active sites on the carbon cladded surface that were removed by exposure to hydrogen or covered with the polybutadiene. It stands to reason that active sites also cause the biggest difference in slopes with PGC and the LTGC coating diminished the problem.

The presence of active sites that polar compounds adhere to would also explain the difference in observed efficiency between the LTGC-coated zirconia and the LTGC-coated PGC or PGC. For purposes of comparison, the efficiency was also markedly lower for the alkylphenone homologs than the alkylbenzene homologs on PGC or LTGC-coated PGC; while the efficiency was approximately the same for the two homologous series on the LTGC-coated zirconia.

SUMMARY

The LTGC-coated PGC had less reverse phase retentivity than the uncoated PGC through decreased solute-stationary phase dispersive interactions. The both LTGC-coated phases had faster mass transfer kinetics than the PGC. The LTGC-coated zirconia had the lowest reversed phase retentivity and the highest efficiency column with good mass transfer, characteristic of its pellicular-like structure. The selectivity of the LTGC-coated zirconia was most like conventional reversed phase HPLC.

The LTGC-coated phase on either support provides advantages over the PGC phase and the choice support would depend upon the specific application. Further improvements in the chromatographic behavior and utility of the LTGC stationary phases can be accomplished through studies in the type and size of support, the coating amount, coating process, the curing temperature, and the chromatographic retention mechanism.

REFERENCES

1. A. A. Kiselev, Russ. J. Phys. Chem., **36**, 13 (1960).

2. S. Yamada, H. Sato, Nature, **193**, 261 (1962).

3. J. H. Knox, B. Kaur, **High-Performance Liquid Chromatography**, R. A. Hartwick, B. J. Brown, eds., (1989) pp. 189-222.

4. J. H. Knox, B. Kaur, G. R. Millward, J. Chromatogr., **352**, 3-25 (1986).

5. Y. Cui, S. V. Olesik, Anal. Chem., **63**, 1812-1819 (1991).

6. T. M. Engel, S. V. Olesik, Anal. Chem., **63**, 1830-1838 (1991).

7. T. M. Engel, S. V. Olesik, Anal. Chem., **62**, 1554-1560 (1990).

8. T. M. Engel, S. V. Olesik, J. High Res. Chromatogr., **14**, 99-102 (1991).

9. W. Larkins, Jr., S. V. Olesik, J. Microcol. Sep., **5**, 543-550 (1993).

10. B. J. Bassler, R. Kaliszan, R. A. Hartwick, J. Chromatogr., **461**, 139-147 (1989).

11. T. P. Weber, P. W. Carr, Anal. Chem., **62**, 2620-2625 (1990).

12. R. Kaliszan, K. Osmialowski, B. J. Bassler, R. A. Hartwick, J. Chromatogr., **499**, 333-334 (1990).

13. J. Kríz, E. Adamcová, J. H. Knox, J. Hora, J. Chromatogr., **663**, 151-161 (1994).

14. M. R. Callstrom, T. X. Neenan, R. L. McCreery, D. C. Alsmeyer, J. Am. Chem. Soc., **112**, 4954-4956 (1990).

15. N. L. Pocard, C. C. Alsmeyer, R. L. McCreery, T. X. Neenan, M. R. Callstrom, K. Mater. Chem., **2**, 771-784 (1992).

16. T. M. Engel, S. V. Olesik, M. R. Callstrom, M. Diener, Anal. Chem., **65**, 3691-3700 (1993).

17. T. P. Weber, PhD University of Minnesota at Minneapolis, 1991.

18. T. P. Weber, P. T. Jackson, P. W. Carr, Anal. Chem., **67**, 3042-3050 (1995).

19. U. Trudinger, G. Muller, K. K. Unger, J. Chromatogr., **535**, 111-125 (1990).

20. D. A. Hanggi. N. R. Marks, LC - GC, **11**, 128-138 (1993).

21. J. A. Blackwell. P. W. Carr, J. Chromatogr., **549**, 59-75 (1991).

22. M. P. Rigney, T. P. Weber, P. W. Carr, J. Chromatogr., **484**, 273-291 (1989).

23. P. C. Sadek, P. W. Carr, R. M. Doherty, M. J. Kamlet, R. W. Taft, M. H. Abraham, Anal.Chem., **57**, 2971-2978 (1985).

24. P. W. Carr, R. M. Doherty, M. J. Kamlet, R. W. Taft, W. Melander, C. Horváth, Anal. Chem., **58**, 2674-2680 (1986).

25. J. E. Brady, D. Byorkman, C. D. Herter, P. W. Carr, Anal.Chem., 56, 278-283 (1984).

26. J. H. Park, P. W. Carr, M. H. Abraham, R. W. Taft, R. M. Doherty, M. J. Kamlet. Chromatographia, **25**, 373-381 (1988).

27. L. R. Snyder, P. W. Carr, S. C. Rutan, J.Chrom., **656**, 537-547 (1993).

28. S. Pedigo, L. D. Bowers, J.Chrom., **499**, 279-290 (1990).

29. M. J. Kamlet, R. M. Doherty, M. H. Abraham, Y. Marcus, R. W. Taft, J.Phys. Chem., **92**, 5244-5255 (1988).

30. M. J. Kamlet, R. W. Taft, J. Am. Chem. Soc., **98**, 2886-2894 (1976).

31. M. J. Kamlet, J. L. Abboud, R. W. Taft. J. Am. Chem. Soc., **99**, 6027-6038 (1977).

32. M. J. Kamlet, R. W. Taft. J. Am. Chem. Soc., **98**, 377-383 (1976).

33. M. Charton, S. Clementi, S. Ehrenson, O. Exner, J. Shorter, S. Wold, S. Quant. Struct. Acta. Relat., **4**, 29 (1985).

34. J. H. Zar, **Biostatistical Analysis**, Prentice-Hall, Inc. Englewood. N.J. (1974) pp. 263-268.

35. J. H. Zar. **Biostatistical Analysis**, Prentice-Hall, Inc. Englewood, N.J. (1974) pp. 228-230.

36. C. T. Rittenhouse, S. V. Olesik [Unpublished] (1996) .

37. L. R. Snyder, J. J. Kirkland, **Introduction to Modern Liquid Chromatography**, John Wiley & Sons, Inc. New York (1979) pp. 259

38. L. R. Snyder, **Principles of Adsorption Chromatography**, Marcel Dekker, Inc. New York (1968) pp. 22-24.

39. C. F. Poole, S. K. Poole, **Chromatography Today**, Elsevier, Amsterdam (1991) pp. 395

40. T. P. Weber, P. W. Carr, E. F. Funkenbush, J. Chromatogr., **519**, 31-52 (1990).

LIQUID CHROMATOGRAPHIC STUDIES OF MEMORY EFFECTS OF SILICA IMMOBILIZED BOVINE SERUM ALBUMIN: I. INFLUENCE OF METHANOL ON SOLUTE RETENTION

R. K. Gilpin,* S. B. Ehtesham, C. S. Gilpin,
S. T. Liao

Department of Chemistry
Kent State University
Kent, OH 44242

ABSTRACT

Silica immobilized bovine serum albumin (BSA) has been synthesized and studied chromatographically using D,L-tryptophan and L-Kynurenine. Site specific and background interactions have been measured as a function of temperature and treatment with methanol. The results indicate that solvent entrapment in the interior hydrophobic region of the protein may lead to small changes in conformation and/or dynamics which influence the site specific binding of the protein and hence changes in chromatographic retention. The entrapped solvents appear to be thermodynamically and kinetically stable such that their influence on the protein persists at elevated temperatures and over hundreds of column volumes of aqueous buffer eluent.

INTRODUCTION

Although bovine serum albumin (BSA) is a very stable protein which is held together by 17 disulfide bridges, its tertiary structure is relatively dynamic and can undergo rapid changes between one of five conformational states as a function of pH.[1] The indigenous binding of BSA as a function of tertiary structure has been the subject of numerous investigations and has been reviewed extensively.[1,2]

The first reported work discussing the enantiomeric selectivity of BSA for D- and L-tryptophan was in 1958.[3] The ability of the protein to selectively bind the L-isomer over the D-isomer has been attributed to both charge interactions and hydrophobic interactions which occur near tyrosine-411 in domain III.[4] This same site will bind related degradation products such as L-kynurenine and other structurally similar compounds like L-thyroxin.

The application of immobilized bovine serum albumin as a chromatographic packing has been demonstrated often. In most cases, separations have been carried out using aqueous buffer eluents in order to take advantage of the protein's indigenous binding. Allenmark and co-workers were the first to resolve the enantiomers of N-aroylamino acids on a silica immobilized BSA support.[5] Subsequently, these same investigators,[6-13] as well as others,[14-22] have separated various chiral compounds using either chemically or physically immobilized BSA or fragments of the protein.

Although the emphasis of most liquid chromatographic studies have been application oriented, mechanistic questions also have been considered. The chromatographic characteristics of immobilized BSA supports have been studied as a function of pH and ionic strength of the mobile phase as well as when small amounts of organic and amphophilic modifiers are added to the mobile phase. Very subtle modifications in the eluent conditions often lead to dramatic changes in chromatographic properties of the support.

Because of this, reproducible separations are difficult to obtain between laboratories and suggested models to explain solute-solvent-protein-surface interactions often are marred by inconsistencies. For example, Aubel and Rogers[15] have noted that pretreatment of the BSA-surface with simple aliphatic alcohols, tetrahydrofuran, or acetonitrile increases solute retention and enhances enantiomeric resolution for racemic mixtures of N-benzoyl-D,L-valine and of N-benzoyl-D,L-phenylalanine. They have attributed this behavior to two possible mechanisms, the removal of impurities from the bound protein or conformational changes in the protein's tertiary structure.

The first mechanism was suggested as the favored and major contributor. Whereas, Allenmark and co-workers have reported opposite findings[10] to those of Aubel and Rogers.[15] However, in this latter investigation, the experimental results appear to be flawed because the control protein column, which was supposedly not treated with organic modifier, was actually exposed to hexane which contained small amounts (i.e., 1-6%) of 2-propanol as a modifier and then rinsed with acetone prior to use.

The literature contains other examples of differing opinions or inconsistencies in experimental observations and theoretical interpretations about immobilized bovine serum albumin as well as other immobilized proteins. Much of the confusion can be attributed to gross over simplifications of very complex problems in protein chemistry/dynamics and solution equilibria when immobilized proteins are used as chromatographic packings.

Differences in the: 1) chemistry used for immobilization, 2) matrix material, 3) amount of bound protein, 3) packing and preconditioning procedures, 4) binding sites, and 5) eluent conditions are often minimized, not recognized, or ignored. Thus, the need for more controlled and systematic studies, which address fundamental mechanistic questions about solute-solvent-protein-surface interactions, is clearly evident.

In a previous investigation,[22] the influence of temperature and pH on the native binding of silica immobilized BSA was studied using D- and L-tryptophan as probe solutes. Because the protein has a binding site for the L-isomer and not the D-isomer, it was possible to measure simultaneously both the background and site specific binding.

In the case of D-tryptophan, plots of the natural logarithm of the chromatographic capacity factor vs reciprocal temperature in K were linear as expected. However, similar plots for L-tryptophan were curved with a maximum in binding (i.e., largest k') at 20-22 °C. This behavior, which is not explainable by a simple retention mechanism, was attributed to a possible phenomenological change in the bound protein.

In an effort to help clarify and to extend the above observations,[22] the current study was undertaken. The thermal dependencies of the binding of L-tryptophan as well as its oxidative degradation product L-kynurenine have been used to investigate solvent memory effects of silica immobilized BSA first exposed to the packing solvents, 2-propanol/methanol, and later to binary mixtures of phosphate buffer and methanol.

EXPERIMENTAL

Materials

The 3-aminopropyltriethoxysilane was from Huls America (Piscataway, NJ, USA), the LiChrospher SI-300 silica from EM Separations (Gibbstown, NJ, USA) and the 25% solution of glutaric dialdehyde from the Aldrich Chemical Company (Milwaukee, WI, USA). Sodium cyanoborohydride, D- and L-tryptophan, potassium chloride, and dibasic sodium phosphate were purchased from the Sigma Chemical Company (St. Louis, MO, USA). L-kynurenine was obtained from ICN Biochemicals (Cleveland, OH, USA). The solvents were either HPLC grade (methanol and 2-propanol) or reagent grade (toluene and 85% phosphoric acid) and were purchased from Fisher Scientific (Pittsburgh, PA, USA). The deionized water was prepared in-house using a Millipore (El Paso, TX, USA) MilliQ reagent water system.

Synthesis

Five grams of silica were mixed with deionized water, the water removed, and the material dried for 12 hr at 110 °C. The silica and 200 mL of water-saturated toluene were placed in a specially designed reaction flask equipped a sintered glass filter and bubbling ports, and the contents were stirred for 3 hr using a stream of dry nitrogen. Subsequently, 100 mL of the toluene were removed, 20 mL of 3-aminopropyltriethoxysilane added and the mixture was refluxed overnight. The toluene was drawn off via suction, the modified silica was washed four times by refluxing it with 100 mL portions of water-saturated toluene for 1 hr, and then dried under nitrogen.

The BSA was immobilized to the above derivatized aminopropyl-silica as follows.[22-24] A 5% solution of glutaric dialdehyde (115 mL), which was buffered to pH 7.0 with 50 mM Na_2HPO_4, and 2.3 g of $NaCNBH_3$ were added to a 300 mL reaction flask and the contents stirred with nitrogen until the borohydride had dissolved completely. The aminopropyl-silica (4.5 g) was added slowly and the walls of the reaction vessel were rinsed with 115 mL of pH 7.0 phosphate buffer. The reaction was carried out for 3 hr while stirring with a stream of dry nitrogen. The silica was allowed to settle and the supernatant removed via suction.

The resulting activated support was washed with ten 100 mL portions of deionized water, dried with a stream of nitrogen, and 3.2 g of it and 72 mL of phosphate buffer were added to a 250 mL round bottom flask. The contents of the flask were gently stirred while adding 90 mg of $NaCNBH_3$. Subsequently, 60 mL of

a pH 7.0 buffered solution of BSA (4.0 mg/mL) were added in drop-wise fashion using a separatory funnel. The funnel was rinsed with 11 mL of buffer and another 90 mg of NaCNBH$_3$ were added directly to the reaction flask while stirring the mixture. The protein coupling reaction was allowed to proceed for 20 hr at room temperature. The BSA modified silica was transferred to a 50 mL conical tube, centrifuged at 500 G, and the supernatant was decanted off and saved for later analysis. The resulting silica was washed with 80 mL of 0.2 M KCl buffered to pH 7.0 with 50 mM Na$_2$HPO$_4$ followed by 120 mL of deionized water. The washing supernatants were combined with the initial protein reaction supernatant and the UV absorbance measured at 279 nm.

An initial estimate of the amount of BSA coupled to the surface was determined by comparing the absorbance of the original reaction solution with the final collection of supernatants. A value of 52 mg of protein/g of silica was obtained. Later, more quantitative procedures, microelemental analyses of carbon, nitrogen and sulfur, (Huffman Laboratories), were performed on the immobilized support. These measurements indicated a coverage of 59 mg of the bound protein/g of silica.

Column Packing

The 2.1 mm i.d. x 150 mm stainless steel column was slurry packed in upward fashion by the following procedure. Approximately 0.5 g of the BSA modified silica was added gradually to 30 mL of 2-propanol which was contained in a dynamic packing apparatus. The apparatus was sealed, pressurized to 6000 psi using a Haskel (Burbank, CA, USA) model DST-52 pump and methanol as the carrier solvent.

Equipment

The liquid chromatographic system consisted of a Spectra-Physics (San Jose, CA, USA) model SP8810 precision isocratic pump, model Focus UV detector, and model Chromjet integrator. Samples were injected using a Rheodyne (Berkeley, CA, USA) model 7125 valve with a 20 μl loop.

The column temperature was controlled by placing it in a Fisher Scientific (Pittsburgh, PA, USA) model Isotemp 9500 refrigerated circulator bath and the flow rate was monitored with a Phase Separation, LTD (Queensberry, Clwyd, UK) model FLOSOA1 flow meter connected to the detector outlet.

Liquid Chromatographic Measurements

The solute (D-tryptophan, L-tryptophan and L-kynurenine) solutions were made fresh daily at a concentration of 0.001 mg/mL in deionized water. The buffer which was used both by itself as a mobile phase and in combination with methanol (i.e., 2, 4, & 6% alcohol/buffer V/V) as mobile phases were prepared by adjusting the pH of a 50 mM solution of Na_2HPO_4 to 7.4 using phosphoric acid. Immediately following packing, the column was conditioned overnight with the pH 7.4 buffer at a flow rate of 0.5 mL/min. Further conditioning was carried out at each temperature studied to allow the column to attain thermal equilibrium. Usually this corresponded to at least 30 minutes or longer. After conditioning, the retention times for the three solutes were measured from approximately 0.5 °C to 35 °C at approximately 4-5 degree intervals. Solutes were injected at least twice at each temperature studied. Once reaching the maximum temperature, the column was rapidly cooled to ambient temperature.

This same evaluation procedure was used for the other mobile phases studied. Complete thermal curves as described above were generated by using different mobile phases in the following sequential order: 1) 100% buffer, 2) buffer with 2% methanol, 3) 100% buffer, 4) buffer with 2% methanol, 5) 100% buffer, 6) buffer with 4% methanol, 7) 100% buffer, 8) buffer with 4% methanol, 9) 100% buffer, 10) buffer with 6% methanol, 11) 100% buffer, 12) buffer with 6% methanol, 13) 100% buffer.

Following these sets of experiments, the column was rinsed with deionized water and then the original packing solvents (2-propanol/methanol). Subsequently, the column was reconditioned by using the original procedure that followed packing and a final set of thermal measurements carried out.

RESULTS AND DISCUSSION

The immobilized bovine serum albumin support was prepared via initially derivatizing LiChrospher SI-300 silica with aminopropyl groups and then linking the protein to the surface with glutaric dialdehyde.[23,24] This same procedure has been used previously to modify ICN-300 silica,[22] however, based on the elemental analysis of carbon, nitrogen and sulfur, the surface coverage of the material prepared in the current work was approximately 40% greater (i.e., 59 mg of protein/g of silica vs 42 mg/g). Subsequently, the influence of temperature on the specific binding of L-tryptophan and L-kynurenine was studied chromatographically. Similar studies also were carried out for D-tryptophan which served as a background control since there is not a specific binding site in BSA for this latter isomer.
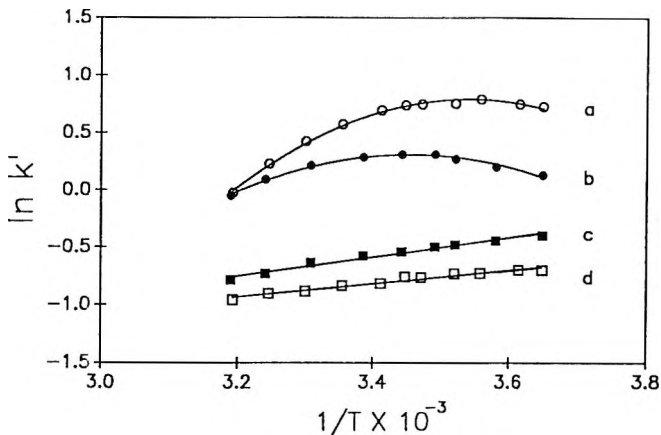
Figure 1. Influence of temperature on the binding properties of silica immobilized BSA. Solutes: Squares) D-tryptophan and Circles) L-tryptophan; Mobile phase: 50mM pH 7.4 phosphate buffer. Silica used for immobilization: Open symbols) LiChrospher-300; Closed symbols) ICN-300.

Plots of the natural logarithm of k' vs 1/T in K for both of the L-isomers were similar in shape to those obtained with the modified ICN-300 silica except they were offset to a lower temperature. This is illustrated in Figure 1 for L-tryptophan chromatographed using a 50 mM phosphate pH 7.4 buffer. Curve **a**, which is from the Merck derivatized silica, reaches a maximum in binding (largest k') at approximately 10 °C and curve **b**, which is from the ICN-300 immobilized BSA,[22] reaches a maximum in binding at approximately 20 °C. The initial increase in k' with increasing temperature at lower temperatures is thermodynamically inconsistent with a simple retention mechanism and has been attributed previously to a phenomenological change in the immobilized protein which increases either the number of specific binding sites or the strength of binding.[22] In the case of D-tryptophan, which does not specifically bind to BSA, plots of ln k' vs 1/T decreased linearly as a function of temperature (curves **c** and **d** for the ICN and Merck derivatized silica, respectively).

A further comparison of the L-isomer data obtained on the two BSA modified silicas (Figure 1) clearly demonstrates a difference in the specific binding characteristics of the two packings in region III where the L-tryptophan site is located. This may be due to either: 1) variations in the support material, 2) the amount of BSA bonded to the surface, or 3) both. In order to help clarify the reason for these differences, additional work is planned where various silica types, levels of coverage, and solutes which bind at other sites in the protein will be studied.
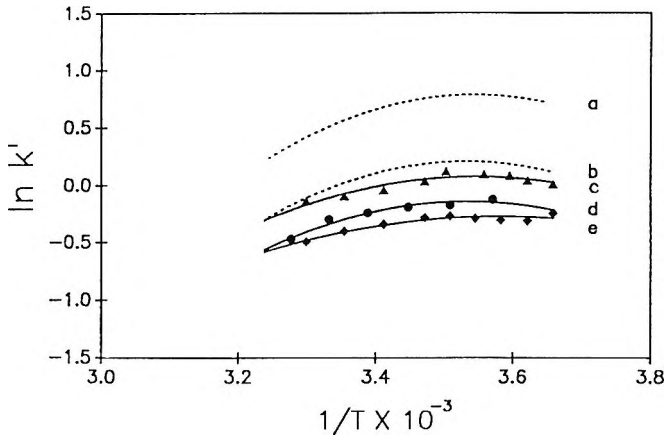
Figure 2. Influence of methanol on the binding of L-tryptophan by silica immobilized BSA. Mobile phase: 50mM pH 7.4 phosphate buffer a) immediately following packing, b) following exposure of column to the three different binary mobile phases containing methanol (i.e., those shown in curves **c-e**; c-e) with 2, 4, and 6% methanol added, respectively.
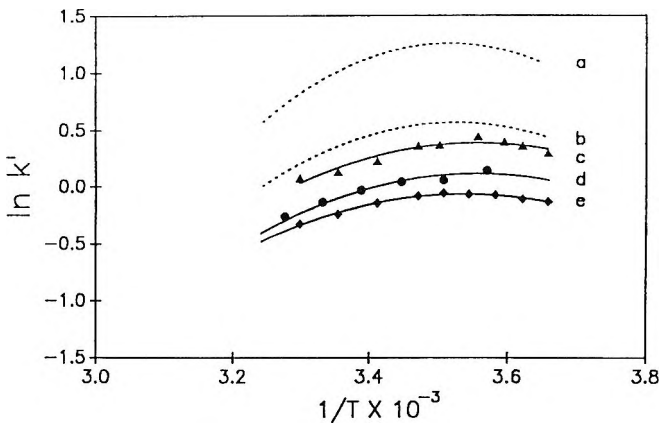
Figure 3. Influence of methanol on the binding of L-kynurinine by silica immobilized BSA. Mobile phase: same as Fig. 2.
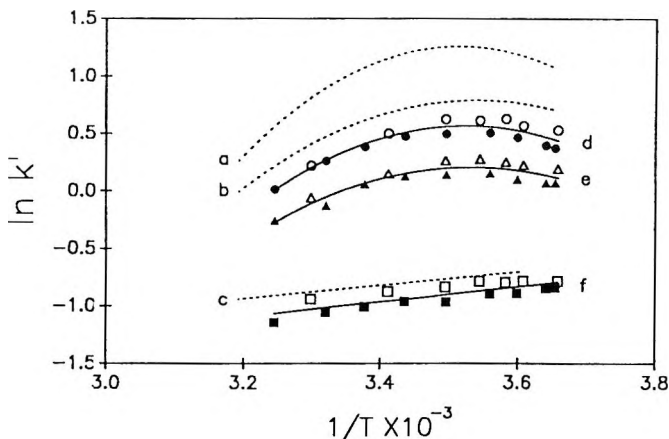
Figure 4. Influence of temperature on retention. Solutes: a & d) L-kynurenine b & e) L-tryptophan, c & f) D-tryptophan; Mobile Phase: 50mM pH 7.4 phosphate buffer; Evaluation: a-c) initial data, and d-f) post exposure to binary mobile phases containing methanol.

Following the initial thermal profile studies described above and which were carried out using 50mM Na_2HPO_4 pH 7.4 buffer as the eluent (Figure 1), a series of similar curves were generated by cycling between binary mobile phases consisting of the 50mM Na_2HPO_4 pH 7.4 buffer and small additions of methanol (2, 4, & 6%) and the original buffer. Each of the three methanol containing eluents was examined twice. Representative data from these studies are illustrated in Figures 2-4. Shown respectively in Figures 2 & 3 are the thermal curves as a function of varying additions of methanol for L-tryptophan and for L-kynurenine which also binds at the same site in the protein. The initial addition of 2% methanol resulted in the largest decrease (i.e., by a factor of approximately two) in the k' values for both the L-tryptophan and L-kynurenine (Curves **a** & **c** in Figures 2 & 3). When the column was reevaluated using the original buffer, the surface recovered only partially as illustrated by the curves **b** in Figures 2 & 3.

The excellent reproducibility of this partial recovery is demonstrated by the data summarized in Figure 4. The dotted curves, **a** & **b**, are second order regression fits of the initial data obtained using only the 50 mM phosphate buffer as the mobile phase for L-tryptophan and L-kynurenine, respectively. Whereas, solid curves **d** & **e** are the second order regression fits of the data obtained after the column had been exposed to 2% methanol (unfilled symbols) and after it had been cycled between all of the mixed mobile phases and buffer twice which represented a total of 9 complete thermal studies separating the two data sets (filled symbols). Also shown in Figure 4 for comparative purposes are the D-tryptophan data.
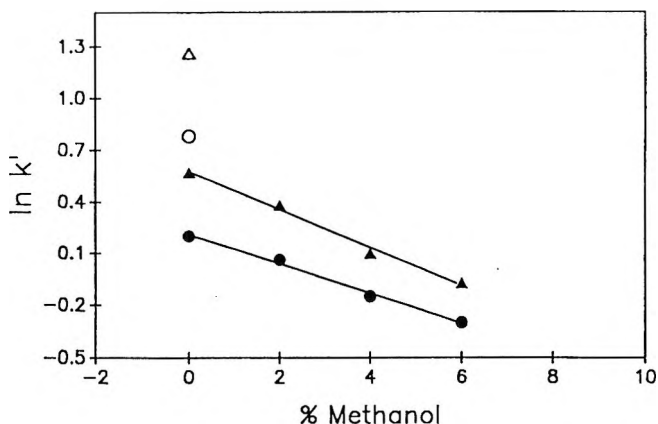
Figure 5. Retention as a function of methanol in the mobile phase. Temperature: 10 °C; Mobile phase: 50mM pH 7.4 phosphate buffer with 0-6% methanol added; Solutes: Triangles) L-kynurenine, Circles) L-tryptophan; Symbols: Unfilled) initial data following packing, filled) after exposure to 2% methanol.

A comparison of the reevaluation buffer data (curves **b** in Figures 2 & 3 and curves **d** & **e** in Figure 4), the 2% methanol data and the remaining curves for 4% methanol (curves **d** in Figure 2 & 3) and 6% methanol (curves **e** in Figure 2 & 3) show an approximate incremental drop in k' with addition of modifier. This relationship is illustrated further in Figure 5 for the maximum binding temperature, approximately 10 °C. Excluding the initial large decrease in k' (unfilled symbols in Figure 5), there is a linear relationship between the percentage of methanol in the mobile phase and ln k' (filled symbols in Figure 5). The regression coefficients for the two fits (solid lines) are both better than 0.99. The data in Figure 5 illustrate two important observations: 1) that the immobilized BSA can be alternated to a stable and reproducible form, and 2) that small additions of modifier, at least methanol, can be used to control retention in a predictable manner.

At this stage in the current work, it was believed that the above observations might be explained by one of two possible mechanisms, either loss of protein from the surface or a change in the protein's conformation which lead to reduced binding. In order to test these ideas and to better understand the changes which occurred in the immobilized BSA column (i.e., as noted by the large drop initially in retention) following its exposure to an eluent buffer containing small percentages of methanol, the column was reconditioned using the original packing solvents. In order to do this, the column first was washed overnight with deionized water at 0.5mL/min to eliminate residual buffer and then exposed to 2-propanol/methanol to simulate
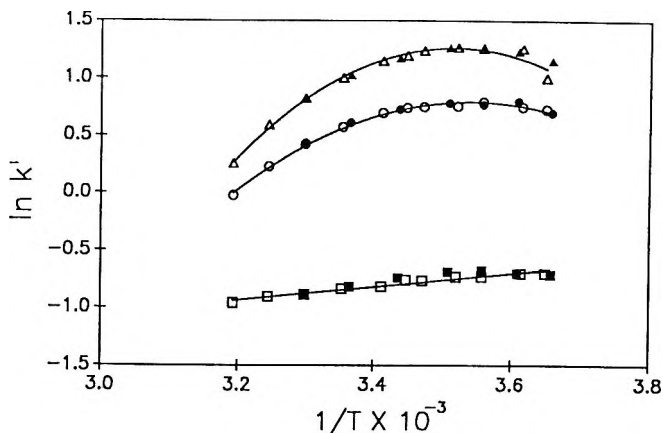
Figure 6. Protein recovery following treatment with 2-propanol/methanol. Mobile phase: 50 mM pH 7.4 phosphate buffer; Solutes: Triangles) L-kynurenine, Circles) L-tryptophan, and Squares) D-tryptophan; Curves: Unfilled symbols) initial set of data following packing, Filled symbols) last set of data following reconditioning with packing solvents.

packing conditions. Subsequently, the column was rinsed with 50 mM pH 7.4 phosphate buffer at a flow rate of 0.25 mL/min for 60 hours. Just prior to carrying out the final set of thermal experiments the column was further conditioned with the buffer mobile phase at 4 °C and a flow rate of 0.5 mL/min for one hour. Figure 6 shows the results of this experiment.

The data sets obtained in this latter experiment and the initial evaluation experiment which immediately followed packing are statistically identical for the three solutes and suggest that the initial change in the protein following exposure to the methanol-buffer mobile phase was not due to protein loss but to a stable yet switchable modification of the protein's structure.

CONCLUSION

The current work demonstrates that the binding properties of silica immobilized bovine albumin serum can be controllably altered using alcohol treatment. It is believed this may be due in part to solvent entrapment (i.e., in the current case, either 2-propanol and/or methanol) in the interior hydrophobic regions of the protein which leads to differences in binding at least at the L-tryptophan site which is located in region III near tyrosine-411. In the case of initial exposure of the immobilized BSA to mixtures of 2-propanol/methanol, binding was enhanced in the

aqueous buffer used as the mobile phase over that observed following exposure of the protein to binary mixtures of buffer and methanol. Such memory effects potentially may be useful in controlling the chromatographic behavior of immobilized BSA packing. Work is now in progress to explore these ideas.

ACKNOWLEDGEMENT

REFERENCES

1. T. Peters, Jr., in **Advances in Protein Chemistry**, Vol. 37, Ed. by C. B. Anfinsen, J. T. Edsall, F. M. Richards, Academic Press, New York, 1985, Vol. 37, p. 161.

2. V. M. Rosenoer, M. Oratz, M. A. Rothchild, **Albumin Structure, Function, and Uses**, Pergamon Press, New York, 1976.

3. R. H.McMenamy, J. L. Oncley, J. Biol. Chem., **233**, 1436 (1958).

4. L. Moravek, M. A. Saber, B. Meloun, Collect. Czech. Chem. Commun., **44**, 1657 (1979).

5. S. Allenmark, B. Bomgren, J. Chromatogr., **264**, 63 (1983).

6. S. Allenmark, B. Bomgren, H. Boren, J. Chromatogr., **316**, 617 (1984).

7. S. Allenmark, S. Anderson, J. Chromatogr., **351**, 231 (1986).

8. S. Allenmark, J. Liq. Chromatogr., **9**(2/3), 425 (1986).

9. S. Allenmark, S. Andersson, J. Bojarski, J. Chromatogr., **436**, 479 (1988).

10. S. G. Allenmark, **Chromatographic Enantioseparation Methods and Applications**, Halsted Press div. of John Wiley & Son, New York, 1988.

11. R. A. Thompson, S. Andersson, S. Allenmark, J. Chromatogr., **465**, 263 (1989).

12. S. Andersson, S. Allenmark, J. Liq. Chromatogr., **12**(3), 345 (1989).

13. S. Andersson, S. Allenmark, P. Erlandsson, S. Nilsson, J. Chromatogr., **498**, 81 (1990).

14. M. T. Aubel, L. B. Rogers, J. Chromatogr., **392**, 415 (1987).

15. M. T. Aubel, L. B. Rogers, J. Chromatogr., **408**, 99 (1987).

16. G. Gubitz, Chromatographia, **30**(9/10), 555 (1990).

17. I. W. Wainer, Trends Anal. Chem., **6**(5), 125 (1987).

18. S. Jacobson, S. Golshan-Shirazi, G. Guiochon, J. Am. Chem. Soc., **112**, 6492 (1990).

19. S. Jacobson, S. Golshan-Shirazi, G. Guiochon, Chromatographia, **31**(7/8), 323 (1991).

20. P. Erlandsson, S. Nilsson, J. Chromatogr., **482**, 35 (1989).

21. Z. Simek, R. Vespalec, J. High Res. Chromatogr., **12**, 61 (1989).

22. R. K. Gilpin, R. K., S. B. Ehtesham, R. B. Gregory, Anal. Chem., **63**, 2825 (1991).

23. H. H. Weetal, Methods Enzymol., **XLIV**, 134 (1976).

24. N. Jentoft, D. G. Dearborn, J. Biol. Chem., **254**(11), 4359 (1979).

EFFECT OF OCTADECYL-MODIFICATION ON RETENTION WHEN USING TITANIA AS A SUPPORT

K. Tani, Y. Suzuki

Department of Chemistry and Biotechnology
Faculty of Engineering
Yamanashi University
Takeda 4-3-11
Kofu 400, Japan

ABSTRACT

It is important to elucidate the effect of the support on retention when investigating the retention mechanism in reversed phase liquid chromatography. The objective of this research was to examine how octadecyl-modified phase can control the unique nature of Titania. Titania was synthesized in our laboratory by the sol-gel method. Octadecyl-modified Titania was prepared by silylation with a octadecyltriethoxysilane. By using anionic, cationic, acidic and basic solutes, the retention behaviours of the Titania and the octadecyl-modified Titania were determined under reversed phase conditions. In the use of aqueous methanol mobile phases containing acetic acid-sodium acetate or bicine-sodium hydroxide buffer, we observed that the Titania synthesized behaved as an amphoteric ion exchanger, and that the retention behaviours of the octadecyl-modified Titania were significantly influenced by octadecyl-modification. The effect of octadecyl-modification on retention was ascribed not only to octadecyl groups but also silanol groups, which were formed by silylation. The retention behaviour as a whole, however, was

clearly based on behaviour as an amphoteric ion-exchanger. Thus, we concluded that the octadecyl-modified phase, although it really influenced the retention behaviour, could not accomplish controlling the amphoteric ion exchange ability of the Titania in these experiments.

INTRODUCTION

It is generally accepted that the nature of the support can affect the chromatographic properties of bonded stationary phase. It is also necessary to have a detailed knowledge of the support when investigating the retention mechanism in reversed phase liquid chromatography. However, data on the supports cannot be obtained because no manufacturer provides full details. Therefore, we are starting an attempt to synthesize supports on a laboratory scale in order to investigate the effect of the supports on the chromatographic retention behaviour.

Titania has recently attracted interest as a new ceramic packing material, which possesses the desirable mechanical and physical properties of silica, and chemical stability superior to silica.[1-6] Titania is an amphoteric metal oxide and has anion-exchange properties in acidic pH and cation-exchange ones in alkaline pH.[7-8] although silica behaves as an only cation exchanger.[8] This means that the influence of the support on retention is worth further consideration when Titania is used as a support, because this unique nature of Titania would more strongly influence the retention behaviour than that of silica. To elucidate, the influence of the support on retention leads to reveal the function of bonded stationary phase. By octadecyl-modifying Titania, the unique nature, which is the amphoteric ion exchange ability, would be controlled. This degree of controlling the unique nature suggests the effect of octadecyl-modification. Thus, comparison of Titania and octadecyl-modified Titania on the retention behaviour is expected to give information about the function of octadecyl-modified phase.

We have already obtained silica on a laboratory scale,[9] from hydrolysis and polycondensation reactions of silicon alkoxide by the sol-gel method.[10-12] By this modified method, we have also obtained Titania on a laboratory scale.[13] The Titania obtained has been converted to reversed phase packings. To investigate how octadecyl-modified phase can control the unique nature of Titania, the retention behaviours of Titania and the octadecyl-modified Titania obtained, were examined by using aqueous methanol mobile phases containing acetic acid-sodium acetate or bicine-sodium hydroxide buffer as mobile phase.

We found that the Titania obtained behaved as an amphoteric ion exchanger and that the retention behaviours of the octadecyl-modified Titania were significantly influenced by octadecyl-modification. The effect of octadecyl-modification on retention was ascribed not only to octadecyl groups but also silanol groups, which were formed by silylation.

The retention behaviour as a whole, however, was clearly based on behaving as an amphoteric ion-exchanger. Consequently, the octadecyl-modified phase, although really influencing the retention behaviour, could not accomplish controlling the amphoteric ion exchange ability of the Titania in this experiments.

EXPERIMENTAL

Preparation

Titania was prepared and converted to reversed phase packing according to a previously described method,[13] of hydrolysis and polycondensation reaction of titanium isopropylate (Nacalai Tesque Inc., Kyoto, Japan) and by silylation with octadecyltriethoxysilane (Wako Pure Chemical, Osaka, Japan). Octadecyldimethylchlorosilane and octadecyltrichlorosilane were also used as reagents for octadecyl-modification of Titania.

The procedure was as follows: Dry Titania (1g) and silane(1mL) were slurred in 10mL of dry toluene; 5mL of pyridine was added to the reaction mixture to remove the acid generated (this procedure was eliminated in using octadecyltriethoxysilane); and the mixture was refluxed for 6h. The carbon content of modifying ligands was determined by CN-Corder MT-600 (Yanagimoto, Kyoto, Japan). The Titania and octadecyl-modified Titania obtained by silylation with octadecyltriethoxysilane (ODT-1) were slurry-packed in 30 X 4.6 mm I.D. stainless-steel tubes.

Characterization

The particle-size distribution was determined with Coulter Multisizer II (Coulter Electronics Limited, Luton, England). The physical properties of particle were determined by nitrogen adsorption measurement (Fuji-Silysia Chemical(Kasugai, Japan) on a home-made apparatus).

Chromatographic Use

The liquid chromatograph was constructed from a 880 PU pump (Jasco. Tokyo, Japan), a Rheodyne Model 7125 injector and a UVIDEC-100-II detector (254nm)(Jasco). A Model TM108M (Toyo, Tokyo, Japan) was used to maintain the column temperature at 30°C. The chromatograms were recorded on a chromatopac CR1A (Shimadzu, Kyoto, Japan).

Titania has anion-exchange properties in acidic pH and cation-exchange ones in alkaline pH. The objective of our research was to investigate how octadecyl-modified phase can control the unique nature of Titania as described above. In order to evaluate the effect of octadecyl-modification on retention, sodium p-toluenesulfonate(PT) and trimethylphenylammonium chloride(MP) were used as anionic and cationic test solutes. Benzoic acid(B, pKa=4.22) and benzylamine (BA, pKa=9.38) were used as acidic and basic test solutes. Titania and ODT-1 were tested under reversed phase conditions employing 0, 20 and 40 wt% methanol containing acetic acid-sodium acetate (pH4~7) or bicine-sodium hydroxide (pH7~9) buffer as the mobile phases. The buffers used were prepared by dilution with 0.1M acetic acid-0.1M sodium acetate and 0.1M bicine-0.1M sodium hydroxide, respectively, as described elsewhere.[14] The void volume was measured with methanol-d_4 in methanol and D_2O in water.

RESULTS

Preparation

The carbon content of modifying ligands was determined by elemental analysis. The carbon content of ODT-1 was 6.16 %. Attempts at converting Titania to octadecyl-modified Titania by using octadecyldimethylchlorosilane and octadecyltrichlorosilane were unsuccessful because the elemental analysis resulted in their being little carbon.

Characterization

The particle size distribution and the physical properties of Titania were determined with Coulter Multisizer and by nitrogen adsorption measurement. As a result, Titania had a mean particle diameter of 4μm, and the particle size distribution ranged from d_{1C} = 5.0 to d_{90} = 3.3μm, and had a surface area of 126 m²/g, a mean pore diameter of 11.1 nm and a mean pore volume of 0.3 mL/g.
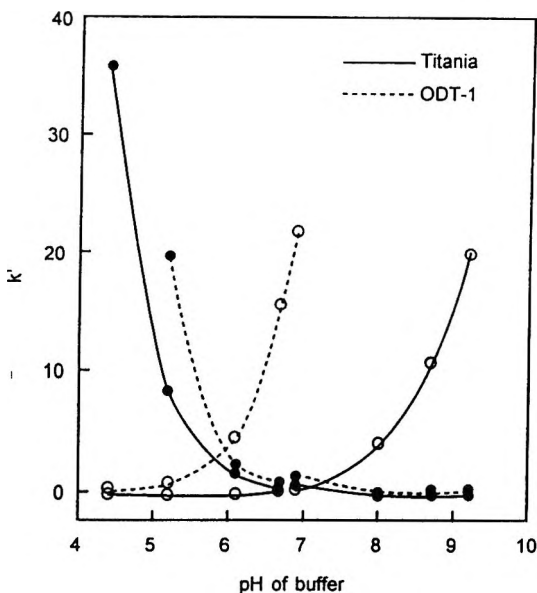
Figure 1. Retention behaviours of PT(●) and MP(○) versus the pH of the mobile phase on Titania and ODT-1.   Column, Titania and ODT-1, 30 X 4.6 mml.D.; mobile phase, acetic acid-sodium acetate and bicine-sodium hydroxide buffers; flow-rate, 1.0 mL/min.

Chromatographic Use

In order to investigate how octadecyl-modified phase can control the amphoteric ion exchange ability of Titania, PT and MP were used as anionic and cationic test solutes. B and BA were used as acidic and basic test solutes.

Use of Buffer as a Mobile Phase

The retention behaviours of the anionic and cationic test solutes on Titania and ODT-1 by using buffer as a mobile phase are shown in Fig. 1. The buffers used were acetic acid-sodium acetate and bicine-sodium hydroxide. As can be seen in Fig. 1, the retention of PT as an anion on Titania decreased steeply as the pH of the mobile phase was increased. On the contrary, that of MP as a cation on Titania increased rapidly as the pH of the mobile phase was increased. The retention behaviours of PT and MP against increasing pH of the mobile phase on ODT-1, were similar to those of PT and MP on Titania.
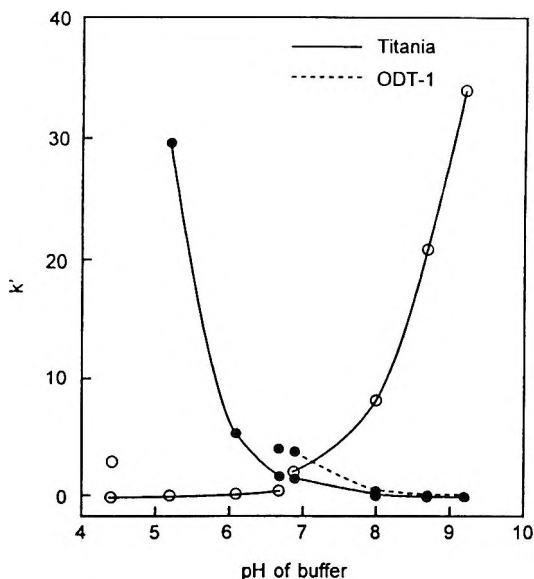
Figure 2. Retention behaviours of B(●) and BA(○) versus the pH of the mobile phase on Titania and ODT-1. Column, Titania and ODT-1, 30 X 4.6 mmI.D.; mobile phase, acetic acid-sodium acetate and bicine-sodium hydroxide buffers; flow-rate, 1.0 mI./min.

However, PT was more strongly retained on ODT-1, and the peak of PT at pH 4.4 was not detectable to be buried in the base line. Furthermore, the retention of MP on ODT-1 began at much lower pH than that of MP on Titania. Figure 2 shows the retention behaviours of the acidic and basic test solutes on Titania and ODT-1 by using buffer as a mobile phase.

As shown in Fig. 2, the retention of B as an acid on Titania decreased steeply as the pH of the mobile phase was increased, and that of BA as a base was reversed. The retention behaviours of B and BA against increasing pH of the mobile phase on ODT-1, could not be displayed entirely because the peaks of B below pH6 and BA above pH 5 were not detectable to be buried in the base line.

In comparison with Fig. 1, B was more strongly retained on Titania and ODT-1 than PT, and BA was also more strongly retained on Titania and ODT-1 than MP.
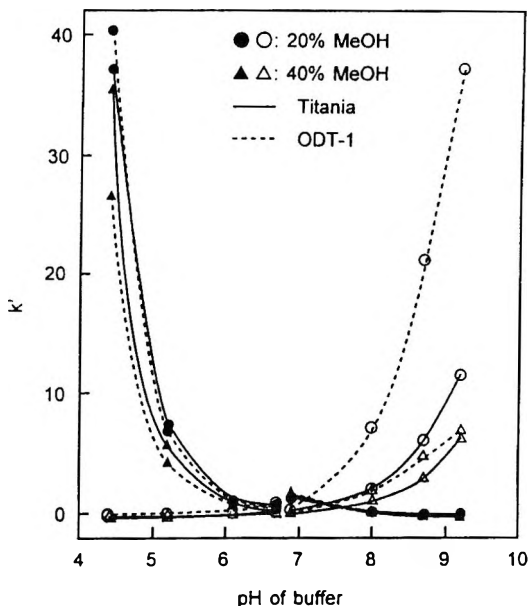
Figure 3. Retention behaviours of PT($\bullet$,$\blacktriangle$) and MP($\bigcirc$,$\triangle$) versus the pH of the mobile phase on Titania and ODT-1. Columns, Titania and ODT-1, 30 X 4.6 mmI.D.; mobile phase, 20%($\bullet$,$\bigcirc$) and 40%($\blacktriangle$,$\triangle$) methanol containing acetic acid-sodium acetate or bicine-sodium hydroxide buffer; flow-rate, 1.0 mL/min.

Use of Buffered Methanol as a Mobile Phase

The retention behaviours of PT and MP on Titania and ODT-1 by using 20 (20 % MeOH) and 40 % methanol containing buffer (40 % MeOH) as mobile phases, are shown in Fig. 3. Figure 3 indicates that the retention behaviour of FT against increasing pH of the mobile phase on Titania was similar to that of PT on ODT-1, although PT showed somewhat small retention as the amount of methanol increased.

On the other hand, the retention of MP on Titania, although increased gradually as the pH of the mobile phase was increased, decreased constantly with increasing amount of methanol. Furthermore, the retention of MP on ODT-1 showed remarkable decrease as the amount of methanol increased. Therefore, the retention behaviour of MP against increasing pH of the mobile phase varied from a steep increase in 20 % MeOH to a slight one in 40 % MeOH. On the whole, MP was more strongly retained on ODT-1 than on Titania.
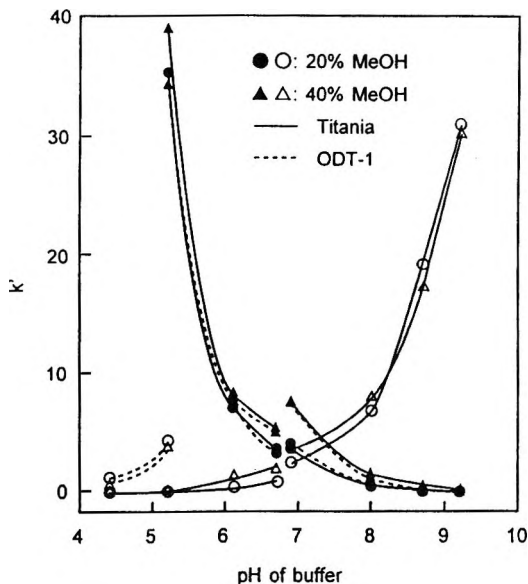
Figure 4. Retention behaviours of B(●,▲) and BA(○,△) versus the pH of the mobile phase on Titania and ODT-1. Columns, Titania and ODT-1, 30 X 4.6 mmI.D.; mobile phase, 20%(●,○) and 40%(▲,△) methanol containing acetic acid-sodium acetate or bicine-sodium hydroxide buffer; flow-rate, 1.0 mL/min.

In comparison with Fig. 1, the retention of PT in buffer and buffered methanol was similar to each other on Titania, and on ODT-1 the retention of PT in buffered methanol was smaller than that of PT in buffer. On the other hand, the retention of MP on Titania decreased constantly in changing from buffer to buffered methanol and that of MP on ODT-1 was shifted to higher pH. Figure 4 shows the retention behaviours of B and BA on Titania and ODT-1 by using 20 and 40 % MeOH containing buffer as mobile phases. As can be seen in Fig. 4, the retention behaviour of B against increasing pH of the mobile phase on Titania was similar to that of B on ODT-1, although B showed somewhat large retention as the amount of methanol increased. The peaks of B on Titania in both mobile phases below pH 5, and on ODT-1 in 20 % MeOH below pH 6 and in 40 % MeOH below pH 5, were not detectable to be buried in the base line. On the other hand, the retention behaviour of BA against increasing pH of the mobile phase on Titania was similar to each other in both mobile phases. The retention of BA on ODT-1 began at much lower pH than that of BA on Titania, and the peaks of BA above pH 6 were not detectable. In comparison with Fig. 3, B was more strongly retained on Titania and ODT-1 than PT, and BA was also more strongly retained on Titania and ODT-1 than

MP.   In comparison with Fig. 2, the retention of B in buffered methanol was larger than that of B in buffer on Titania.   On the other hand, the retention of BA on Titania was similar to each other in buffer and buffered methanol.   The retention of BA on ODT-1 decreased by changing from buffer to buffered methanol, although the retention began at same pH.

DISCUSSION

The focus of our research was to elucidate the effect of the support on retention for investigating the retention mechanism in reversed phase liquid chromatography.   To accomplish our objective, we have examined how octadecyl-modified phase could control the nature of the support.   Our investigation centered on Titania and octadecyl-modified Titania due to the unique nature of Titania, which shows anion-exchange properties in acidic pH and cation-exchange properties in alkaline pH although silica, which is widely used as a support, behaves only as a cation exchanger.   This is because the unique nature of Titania would more strongly influence the retention behaviour than that of silica.

Preparation and Characterization

The first stage of our investigation was to prepare Titania and octadecyl-modified Titania.   The Titania obtained had enough particle size distribution and physical properties to be used as a support.   The carbon content appeared to be comparable to that of well modified silica packing material, in view of the fact, that Titania had roughly one-third of the surface area of standard silica.   However, the evaluation of ODT-1 as a C_{18} silica packing material by the chromatographic characterization method, indicated that the surface coverage was poor, as described previously.[13]   Therefore, highly polymerized octadecyl groups seemed to be localized on the Titania surface.   The failure of octadecyl-modification by using chlorosilane means that Titania reacted easily with ethoxysilane and scarcely with chlorosilane.   We found that alkoxysilane was desirable for silylation of Titania.

Chromatographic Use

Use of Buffer as a Mobile Phase
Titania and ODT-1 were next investigated as the packing materials for evaluating the effect of octadecyl-modification on retention.   The retention behaviours of test solutes on Titania and ODT-1 were first examined by using buffer as a mobile phase.   As can be seen in Fig. 1, the retention of PT as an

anion on Titania decreased steeply as the pH of the mobile phase was increased. On the contrary, that of MP as a cation on Titania increased rapidly as the pH of the mobile phase was increased. This retention data suggest that Titania behaved as an amphoteric ion-exchanger, that is, Titania has anion-exchange properties in acidic pH and cation-exchange ones in alkaline pH. The fact that the retention of MP on ODT-1 began at much lower pH than that of MP on Titania, indicates that ODT-1 had stronger cation-exchange properties than Titania. It is accepted to be caused by the occurrence of cation-exchange with silanol groups because the groups were able to be formed by silylation for octadecyl-modification. Therefore, the retention of PT should be reduced by the ion exclusion effect of silanol groups. However, the retention of PT on ODT-1 actually increased compared to that of PT on Titania. The reason for this increase can be attributed to hydrophobic interaction between octadecyl groups and the hydrophobic residues of PT. Thus, the hydrophobic interaction of octadecyl groups more greatly influenced the retention of PT than the ion exclusion effect of silanol groups. Naturally, the retention of MP on ODT-1 should be influenced by the hydrophobic interaction of octadecyl groups, and this might be one of the causes that retention of MP on ODT-1 began at much lower pH than that of MP on Titania. The evidence for influence of silanol groups would be provided by preparing the octadecyl-modified Titania with octadecyldimethylethoxysilane, because the formation of silanol groups can be eliminated by using monofunctional alkoxysilane. In comparison between Fig. 1 and Fig. 2, B was more strongly retained than PT, and BA was also more strongly retained than MP. These increased retentions can also be ascribed to hydrophobic interaction between hydrophobic sites of Titania and the hydrophobic residues of B and BA, or between the octadecyl groups and the hydrophobic residues of B and BA, because the hydrophobicity of B and BA was higher than that of PT and MP. However, the retention behaviour as a whole, was clearly based on behaviour as an amphoteric ion-exchanger. Finally, the octadecyl-modified phase, although really influenced by the retention behaviour, could not accomplish controlling the amphoteric ion exchange ability of the Titania in this experiments. This may be because the evaluation of ODT-1 as a C_{18} silica packing material is indicated to have low surface coverage, although highly polymerized octadecyl groups seemed to be localized on the Titania surface.

Use of Buffered Methanol as a Mobile Phase

The retention behaviours of test solutes on Titania and ODT-1 were next examined by using buffered methanol as a mobile phase to enhance a function of the octadecyl group. The retention behaviour of MP was most sensitive to the addition of methanol and showed reversed phase chromatographic retention behaviour not only on ODT-1 but on Titania, as can be seen in Fig. 3. With an increasing amount of methanol, the retention of MP decreased constantly on

Titania. and showed remarkable decrease on ODT-1. The expected results were that MP was hardly retained in further increase in methanol because the retention of MP was hindered by the addition of methanol. Actually, MP showed only slight retention in 80 % buffered methanol as described previously.[13] The addition of methanol may contribute to either suppressing the ion exchange ability of Titania and ODT-1 or weakening that of MP. In the previous paper,[13] we predicted that the slight retention of MP was inhibited by the strong adsorption of buffer components on Titania. This prediction, however. resulted from the use of only 80 % methanol containing 0 1M acetic acid-0.1M sodium acetate. In the present paper, by using diluted buffer and low methanol content. two causes may offer a reasonable explanation for weakening the ion exchange ability of MP. One of the causes is that in changing from buffer to buffered methanol, the retention of MP on ODT-1 was shifted to higher pH for decreasing in cation-exchange interaction with silanol groups, whereas that of BA. which was cation-like in this experimental range, did not. Another. is that the retention behaviour of BA was not very sensitive to the addition of methanol and those of PT and B not either, compared with that of MP. Weakening of the ion exchange ability of MP seems to be caused by solvation of methanol. The unambiguous evidence for the weakening of the ion exchange ability of MP should be necessary to examine other cations. By the addition of methanol. however, the evidence for enhancing a function of octadecyl group was not given. The retention behaviours of PT between Titania and ODT-1 were similar to each other, although some difference was shown between 20 % and 40 % MeOH for hydrophobic interaction. The retention behaviours of B between Titania and ODT-1 were also similar to each other, although the retention of B was larger in 40 % MeOH than that of B in 20 % MeOH. The reason for the somewhat large retention of B as the amount of methanol increased was not clear. but it seemed to be attributed to Titania. Therefore. we concluded that the effect of octadecyl-modification on retention could not be clearly observed in buffered methanol.

The retention behaviour as a whole, was clearly based on behaviour as an amphoteric ion-exchanger. In conclusion, the octadecyl-modified phase, although really influencing the retention behaviour, could not accomplish controlling the amphoteric ion exchange ability of the Titania in this experiment. However. further examination for controlling the amphoteric ion exchange ability of Titania, can be made by the preparation of the octadecyl-modified Titania with various surface coverages because the evaluation of ODT-1 as a C_{18} silica packing material indicated that the surface coverage was poor. and the formation of silanol groups can be eliminated in using monofunctional alkoxysilane. The next stage of our investigation will be under way to improve the above. and to present the reason for the unambiguous evidence of weakening the ion exchange ability of MP.

ACKNOWLEDGMENTS

REFERENCES

1. R. M. Chicz. Z. Shi, F. E. Regnier, J. Chromatogr., **359**, 121-130 (1986).

2. M. Kawahara, H. Nakamura, T. Nakajima, Anal. Sci., **5**, 763-764 (1989).

3. H. Matsuda, H. Nakamura, T. Nakajima, Anal. Sci., **6**, 911-912 (1990).

4. H. Matsuda, M. Kawahara, H. Nakamura, T. Nakajima, Y. Asai and J. Sawa, Anal. Sci., **7**, 813-814 (1991).

5. M. Kawahara, H. Nakamura, T. Nakajima, J. Chromatogr., **515**, 149-158 (1990).

6. U. Trudinger, G. Muller, K. K. Unger, J. Chromatogr., **535**, 111-125 (1990).

7. K. A. Kraus, H. O. Phillips, J. Am. Chem. Soc., **78**, 249 (1956).

8. M. Abe, T. Ito, Nippon Kagaku Zasshi, **86**, 1259-1266 (1965).

9. K. Tani, Y. Suzuki, Chromatographia, **38**, 291-294 (1994).

10. K. Unger, J. Schick-Kalb, K.-F. Krebs, J. Chromatogr., **83**, 5-9 (1973).

11. K. Unger, B. Scharf, J. Colloid Interface Sci., **55**, 377-380 (1976).

12. H. Kozuha, S. Sakka, Chem. Mater., **1**, 398-404 (1989).

13. K. Tani, Y. Suzuki, J. Chromatogr., **772**, 129-134 (1996).

14. K. Tani, Y. Suzuki, manuscript in preparation.

CHARACTERIZATION AND HIGH PERFORMANCE LIQUID CHROMATOGRAPHIC EVALUATION OF A NEW AMIDE-FUNCTIONALIZED REVERSED PHASE COLUMN

Tracy L. Ascah, Krishna M. R. Kallury, Cory A. Szafranski,
Scott D. Corman, Francis Liu

Supelco, Inc.
Supelco Park
Bellefonte, Pennsylvania 16823

ABSTRACT

A new amide-functionalized silica stationary phase, Supelcosil ABZ$^+$ Plus, suitable for reversed phase HPLC applications, was characterized by X-ray photoelectron spectroscopy (XPS), solid-state ^{29}Si and ^{13}C CP/MAS NMR and FTIR. The degree of hydration of this material was found to be much higher compared to amide-functionalized silica phases prepared by acid chloride treatment of aminopropylsilylated silica reported earlier and also compared to conventional C_{18} reversed phase columns. The liquid chromatographic performance of this ABZ$^+$ Plus column was found to be superior to the C_{18} columns, especially for polar analytes. The enhanced selectivity and better peak shape with this ABZ$^+$ Plus material was attributed to greater compositional differences between the surface and mobile phases coupled with more effective shielding of residual silanols and a more oriented alkyl chain structure.

3049

INTRODUCTION

High performance liquid chromatography is an invaluable analytical tool that finds application in diverse areas which deal with the isolation, production and distribution of chemicals. Examples of such fields include environmental monitoring/control,[1] drugs/pharmaceutical production,[2] generation/purification of blood or plasma products,[3] biotechnological advances such as recombinant DNA-based proteins and other biochemicals[4,5] and food products,[6,7] to name a few. Silica-based C_8 and C_{18} columns are the most extensively used analytical probes for a vast majority of these applications.[8] Selection of a column most appropriate for a particular type of application depends upon the nature of the analyte(s). Thus, for the analysis of non-polar analytes such as small aromatic hydrocarbons, the choice is presumed to be the least complicated (although recent reviews[9-13] prove that even this is no trivial matter). However, the situation becomes extremely complex when analytes are polar or moderately polar small organic molecules with basic or acidic substituents, such as pharmaceuticals. Large differences are encountered by analysts dealing with such molecules, with respect to retention, selectivity and peak shape, even with ostensibly equivalent columns packed with C_{18} materials.[14]

Incomplete reaction of the silica surface silanols with a silanizing reagent or the formation of new silanols, when bi- or tri-functional modifiers are utilized, is a problem that continues to plague the area of liquid chromatography employing bonded phases, since these functionalities affect both retention and peak shape. Partial solutions for this problem consist of end-capping,[15] addition of organic modifiers to the mobile phase,[16] introduction of bulkier substituents on the silicon atom of the silane reagent in place of the methyl groups,[17-19] use of bidentate ligands,[20] formation of Si_{silica}-$C_{alkyl\ chain}$ bond in place of the normal siloxane bond between the silica and silane silicon atoms[21] and the use of mixed trifunctional silanes.[22] Nevertheless, the deleterious effect of surface silanols has not been resolved to the satisfaction of practising chromatographers.

A totally different approach towards minimizing the effect of residual silanols is to generate a functionality on the modified silica surface that can react with the silica silanols through electrostatic and/or hydrogen-bonding interactions. Of particular interest is the amide group which possesses attractive properties such as stability to bases, strong H-bond forming capabilities and non-reactivity with different chemical functionalities present on small polar organic molecules. The most convenient method of introducing the amide moiety is through the acylation of a pre-formed aminopropylsilylated silica surface. Tundo and Venturello[23] have adopted this approach as far back as 1979 to prepare silica-based phase transfer catalysts carrying the

acylaminoalkyl chain. An analogous surface modification procedure has been utilized by Oi and coworkers[24] in 1983 to prepare an acylaminoalkylsilylated silica stationary phase suitable for chiral liquid chromatography. Nomura and coworkers[25] subsequently investigated the acylation of aminopropylsilica with a variety of acid chlorides. This study was followed by the work of Buszewski and coworkers[26] with extensive solid-state NMR and chromatographic studies on similar acylamino-derivatized silicas, termed "peptide bond carrying silicas" by the authors. Similar amide-functionalized silicas were reported by Okahata et al.,[27] Boven et al.,[28] Yamamura et al.,[29] Pidgeon et al.,[30] Kallury et al.,[31] Ihara et al.,[32] Nagae et al.,[33] the Pirkle group[34] and by Meyerhoff and coworkers,[35] which were utilized for a variety of analytical and synthetic applications, besides liquid chromatography. An analogous functionalized silica surface carrying urethane functionalities instead of amide moieties has also been reported recently.[36]

The above brief summary reveals that although amide-functionalized silica phases have been synthesized and used for a wide range of applications, surface coverage data, the nature of interactions between the amide moiety and the surface silanols of the silica and retention mechanism studies have been scarce. The only reported surface coverage evaluations appear to be those from the Meyerhoff group dealing with a carboxytetraphenylporphyrin bound to aminopropylsilylated silica[35] and the Buszewski group on amide-functionalized silica surfaces prepared by a two-step procedure,[37] based on elemental analysis. In the current paper, X-ray photoelectron spectroscopy in combination with FTIR and ^{13}C and ^{29}Si CP/MAS NMR was utilized to probe the surface structure of Supelcosil ABZ$^+$ Plus, a new amide-functionalized silica stationary phase, and the surface characteristics of ABZ$^+$ Plus were compared with those of its precursor, ABZ, and a conventional C_{18} reversed phase silica. The chromatographic performance of this new amide-derivatized silica stationary phase ABZ$^+$ Plus was evaluated in the present work employing a wide selection of organic molecules widely differing in their polarities and it was demonstrated that this new LC column is superior to the conventional C_{18} reversed phase columns.

The chromatographic applications of Supelcosil ABZ, the other amide-functionalized stationary phase have been elaborated in several recent publications[38-41] and will not be discussed in the current work. The ABZ$^+$ Plus material was made by a single step surface attachment procedure, while the ABZ phase was made by a two-step protocol. The residual amino moieties on the ABZ phase were acetylated after the introduction of the longer acyl chain. The ABZ and ABZ$^+$ Plus materials contain the same number of carbon atoms in their alkyl chains as the C_{18} material.

EXPERIMENTAL

Materials

The analytes included in the present study were procured from either Aldrich or Sigma and were used as such. The solvents utilized were all HPLC grade and obtained from Baker. The chromatographic columns Supelcosil ABZ⁺ Plus, ABZ and LC-18DB were supplied by Supelco, Inc., Bellefonte, PA. The amide-functionalized stationary phase materials were generated from high purity silica with a surface area of 330 m^2/g and a pore volume of 0.6 cm^3/g.

Spectroscopic Analysis

The solid state ^{29}Si CP/MAS NMR spectra were recorded on a modified NT-270 Nicolet NMR spectrometer. Spectra were obtained in natural abundance at a frequency of 53.76 MHz employing a contact time of 10ms, high power proton decoupling during acquisition, a recycle delay of 3 sec and a spectral width of 20 kHz. MAS was carried out at 4.0 kHz. Cross-polarization (CP) and magic angle spinning (MAS) were performed using a multinuclear CP/MAS probe equipped to accommodate 7.0 mm spinners.

Typically, 4500 transients were accumulated. The ^{13}C CP/MAS NMR spectra were collected at 68.055 MHz with a contact time of 5 ms and MAS was carried out at 4.2 kHz. Typically, 3000 transients were collected for these spectra.

X-ray photoelectron spectra were recorded on a Kratos XSAM 800PCI using an unmonochromated Mg K$_\alpha$ source run at 14 kV and 20 mA. The samples were mounted on a gold-coated cup. The shape of the spectra indicated that no compensation for differential surface charging was needed. The binding energy scale was calibrated to 285.0 eV for the main C(1s) C-C feature. Spectra were run in both low resolution and high resolution modes (pass energy 40 eV) for the C(1s), N(1s), Si(2p) and O(1s) regions. Each sample was analysed at a 75° angle relative to the electron detector. An analysis area of 3 mm was used for rapid data collection.

Elemental compositions were calculated from the high resolution spectra normalized for constant transmission using the software supplied by the manufacturer. ATR-FTIR spectra were recorded on a Mattson 2020 infrared spectrometer in potassium bromide.

Table 1

X-Ray Photoelectron Spectroscopic Data on ABZ, ABZ$^+$ Plus and C$_{18}$ Silicas

	Elemental Composition (%)				High Resolution Data			
					C(1s)		N (1s)	
					Binding Energy (eV)	Area (%)	Binding Energy (eV)	Area (%)
	C (ls)	Si (2p)	O (ls)	N (1s)				
ABZ	43.1	22.3	32.4	2.2	285.0	94	399.7	69.9
					287.4	6	401.0	24.3
							402.9	6.8
ABZ$^+$ Plus	42.5	22.2	33.1	2.2	285.0	94	399.6	63.1
					287.0	6	400.6	28.1
							402.3	8.8
C$_{18}$	44.4	24.0	31.6	---	285.0	100	No nitrogen present	

Apparatus

The analytical system consisted of a HP 1090 Liquid Chromatograph, with UV detection at 254 nm and a flow rate of 2.0 mL/min. The mobile phase was 10mM potassium dihydrogen phosphate containing acetonitrile (70:30 or 60:40). Peaks were integrated by a HP3396 Series II integrator.

RESULTS AND DISCUSSION

Characterization of the Standard C$_{18}$, ABZ and ABZ$^+$ Plus Stationary Phases

The surface analytical techniques most extensively used for characterizing particulate materials are FTIR, solid-state CP/MAS NMR and X-ray photoelectron spectroscopy (XPS, also known as electron spectroscopy for chemical analysis, ESCA)[42]. The former two are invaluable in functional group analysis and in the evaluation of the motional dynamics of the alkyl chains on
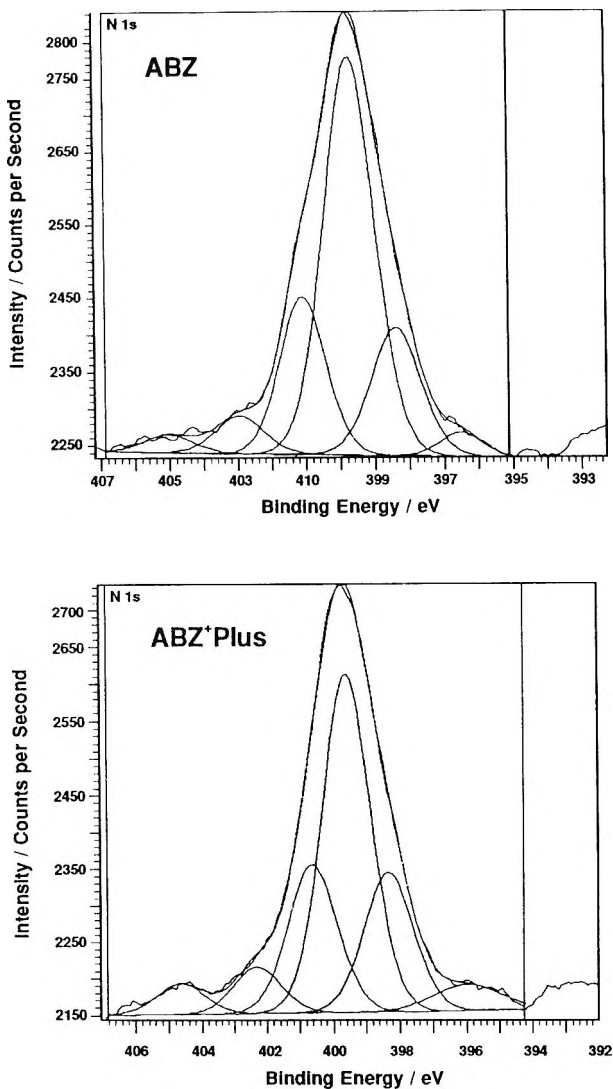
Figure 1. X-ray photoelectron spectra of Supelcosil ABZ and ABZ⁺ Plus amide-functionalized silicas: N(1s) binding energy region.

the silane silicon of the surface-treated silicas. XPS, on the other hand, is unique since it provides quantitative structural and functional group information from sub-monolayer level surface coverages to multi-layers up to a thickness of 10 nm, in addition to elemental composition data.
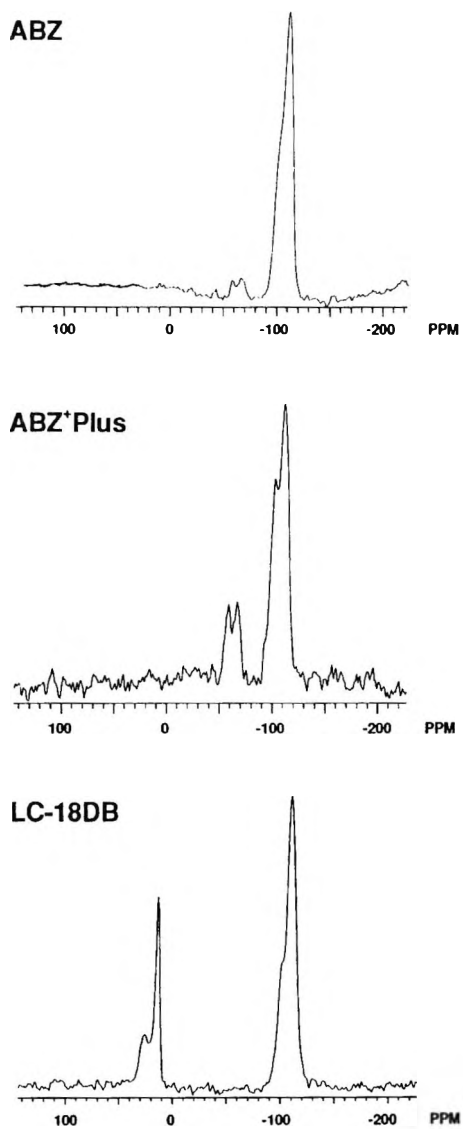
Figure 2. Solid-state ^{29}Si CP/MAS NMR spectra of Supelcosil ABZ, ABZ[+] Plus and LC-18DB silicas.

Consequently, XPS is a surface analysis tool as opposed to FTIR and NMR which are bulk analytical probes. The XP spectra of ABZ and ABZ⁺ Plus silica are included in Figure 1 and the elemental compositions of the two surfaces given in Table 1. Based on the carbon percentage derived from XPS data, surface coverage of an organic layer in general and of silane-modified silicas in particular can be calculated by Equation 1.[43]

$$\Gamma_{sox} = [10^{6}/S_{BET}] [(1201a_c/P_c) - M(Su) + \delta]^{-1} \qquad (1)$$

where, Γ_{scx}=surface concentration of the organic species on the silica surface in $\mu mol/m^2$; S_{BET}=specific surface area of untreated silica, a_c=number of carbon atoms on the organic species attached to the surface, P_c=percent of carbon on the modified silica surface, M(Su)=molecular weight of the silyl unit on the silica surface and δ=correction factor for desorbed water (usually taken as 5).

From Equation 1, the surface coverages of the ABZ⁺ Plus, ABZ and standard non-functional C_{18} silica could be calculated by substituting the values of carbon percentage P_c derived either from elemental analyses or from the XPS data. Employing the carbon percentages of 12.87, 12.01 and 11.87 for ABZ⁺ Plus, ABZ and C_{18}, respectively, obtained by elemental analyses, the surface coverages work out to 2.35, 2.15 and 2.12 $\mu mol/m^2$ for these three surfaces in that order. On the other hand, utilizing the atom percent values derived from the C(1s) binding energy peaks recorded in the XP spectra, the same surface coverages were computed as 14.86, 13.90 and 14.60 $\mu mol/m^2$, respectively. For computing the surface coverage of the non-functional monomeric C_{18} silica, data from earlier literature (44,45) was utilized. It is obvious that the surface coverage values obtained from the XPS data are about seven times greater than those measured from the elemental analysis data (and the carbon percentage values are 3-4 times greater for the XPS method compared to elemental analyses).

A similar discrepancy has been reported by Brown and coworkers,[46] who studied monomeric alkyl bonded phases by XPS and SIMS techniques. Their results show that the XPS-derived carbon percentages are higher by a factor of 2-3 than those obtained from elemental analysis. In our current study, the amide-functionalized silica surfaces are polymeric in nature and hence cross-linking is to be expected. If the XPS-derived carbon percentages are any indication, our polymeric surfaces contain nearly twice as much carbon as the monomeric C_{18} reported by Brown et al.[46] However, the elemental analysis data shows that the carbon percentages of our polymeric C_{18} surface (11.87) and their monomeric C_{18} surface (10.64) are not that different. Furthermore, Buszewski and coworkers[47] report that the carbon percentages obtained from

elemental analyses are 4.93 for monomeric aminopropyl bonded phase and 4.66 for polymeric aminopropyl bonded phase; for the corresponding AA_6 phases obtained by acylation with hexanolyl chloride, the carbon values are 9.93 and 9.47, respectively.

Our XPS results on the same monomeric and polymeric aminopropylsilylated silicas indicate that the carbon content of the latter is about twice that of the former.[48] FTIR spectroscopic data on all of the silica surfaces cited above support the fact that the carbon content of polymeric materials is much higher than the corresponding monomeric materials,[49] in spite of the fact that there are two additional methyl carbons on the silicon of the latter. It is thus clear that elemental analysis does not distinguish clearly between monomeric and polymeric alkylsilylated stationary phases with respect to their carbon contents. On the other hand, the XPS technique is more reliable since it probes only the top 5-10 nm of a surface with minimal interference from the bulk silica layers underneath and reflects the surface composition more accurately. Owing to the limited depth probing capability of the X-ray beam in XPS, the entire silane layer is scanned together with the silica underneath this layer to a depth of 3-4 nm. Therefore, the carbon content (and hence the surface coverage of the silane) appears to be higher than the silanol content which is computed to be around 8 μmol/m^2. Since the chromatographic properties of bonded phases are dependent primarily on the surface structure rather than the bulk structure of silica, it is reasonable to assume that XPS provides a more accurate measure of the chromatographic performance of a modified silica stationary phase than elemental analysis. From the XPS results registered in the current work, as well as those reported by others earlier, it is evident that about 90% of the total bound silane is present at the silica surface.

Both elemental composition and XPS data on the ABZ$^+$ Plus, ABZ and C_{18} surfaces indicate that there is no significant difference between the three types of silica (C_{18}, ABZ and ABZ$^+$ Plus) with respect to their surface coverages. However, both ABZ and ABZ$^+$ Plus carry the amide functionalities and obviously, there are bound to be differences in the nature of interactions these two surfaces exhibit with silica silanols as opposed to the non-functional C_{18} silicas. The non-functional C_{18} silica is hydrophobic (since it contains only the octadecyl chain and no other functionality) and shows only one C(1s) binding energy peak in its XPS at 285.0 eV which is assignable to the carbon atoms of the C_{18} alkyl chain. The amide-containing silicas exhibit two C(1s) binding energy peaks, at 285.0 and 287.2$\pm$0.2 eV, representing the hydrocarbon and amide carbons, respectively, in a 10:1 ratio (the theoretical value for this ratio is 9:1).
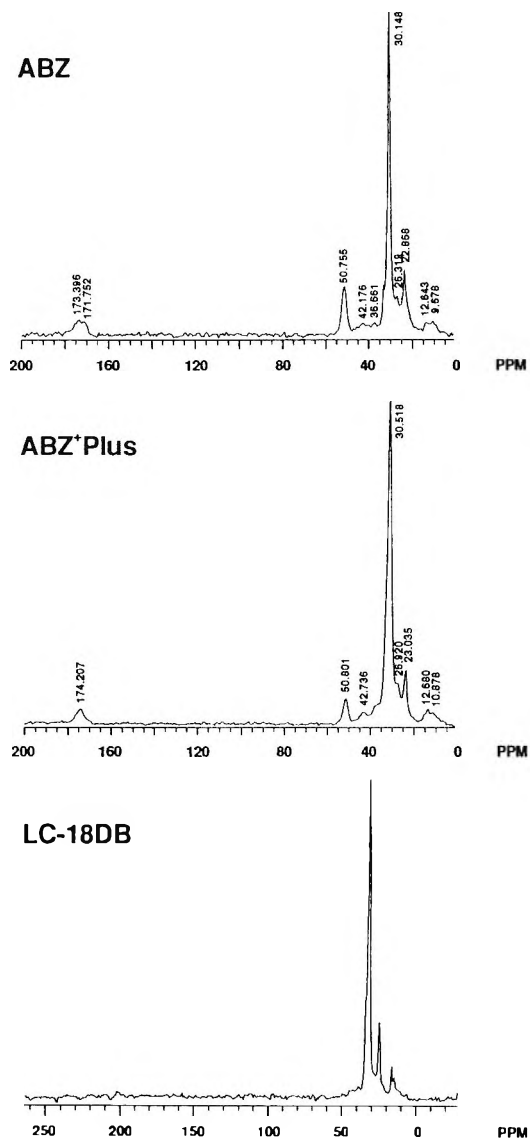
Figure 3.   Solid-state ^{13}C CP/MAS NMR spectra of Supelcosil ABZ, ABZ$^+$ Plus and LC-18DB silicas.

The N(1s) binding energy region (see Figure 1 and Table 1) throws significant light into the nature of interactions of the amide moiety in ABZ and ABZ$^+$ Plus with silica surface silanols. With both silicas, six peaks were registered in this region; however, two of them , which occur at the extremes of the binding energy scale, are due to charging and were not taken into account (these two account for only 5-6% of the total nitrogen). Two of the remaining four peaks were observed at approximately the same binding energy values, viz. 398.37±0.01 eV and 399.65±0.04 eV, respectively; with both silicas. The former is attributable to a more negative nitrogen atom resulting from strong H-bonding between the NH of the amide (to which this nitrogen belongs) and the carbonyl group of an adjacent amide moiety. The latter represents the non-hydrogen-bonded component of the amide functionality and is more prevalent with ABZ compared to ABZ$^+$ Plus. In addition, two other peaks were recorded for both silicas in the N(1s) binding energy region, at 400.8±0.2 and 402.6±0.3 eV, respectively. These two peaks form 24% of the total nitrogen with ABZ and 30% with ABZ$^+$ Plus silicas and represent the H-bonded fractions of the total amide moieties in either case.

Significantly, there is a 0.4 eV and 0.6 eV binding energy difference between the ABZ and ABZ$^+$ Plus amide functions with respect to the 400.8±0.2 and 402.6±0.3 eV peaks, respectively, indicating that the amide functionality in ABZ is more strongly hydrogen-bonded than in ABZ$^+$ Plus. This discrepancy is attributable to the variation in the moieties involved in H-bonding with the amide functionality on the two silica surfaces. Thus, in ABZ the amide groups appear to be H-bonded to the silica/silane silanols and in ABZ$^+$ Plus, they are H-bonded to water. This hypothesis derives strong support from the solid-state ^{29}Si CP/MAS spectra of the two amide-functionalized silicas (see Figure 2 for the spectra). The Q_3, T_3 and T_4 type[50] of ^{29}Si peaks for ABZ are shifted about 1.1 ppm downfield compared to the corresponding peaks in ABZ$^+$ Plus. The Q_3 peak in the ^{29}Si NMR spectrum of ABZ$^+$ Plus appears around the same frequency as for LC-18DB pointing to the same type of environment for this silica silicon atom in both samples; the LC-18DB sample contains an additional peak for the M_1 type of silicon (attached to two methyl groups and the C_{18} alkyl chain, with a single attachment to the silica surface) in its ^{29}Si NMR spectrum. However, there seems to be a significant difference in the degree of hydration of the ABZ$^+$ Plus and the LC-18DB silica surfaces, as evidenced by the higher oxygen content (about 4%) in the XPS of the former in comparison with the O(1s) peak intensity of the latter. It is to be noted that the Si(2p) binding energy peak intensities of ABZ$^+$ Plus and LC-18DB are about the same and the surface coverages are also roughly equal in the two samples. It is this water layer that contributes to the better chromatographic performance of the ABZ$^+$ Plus material than that observed with standard C_{18} reversed phase columns, as discussed in the next section.
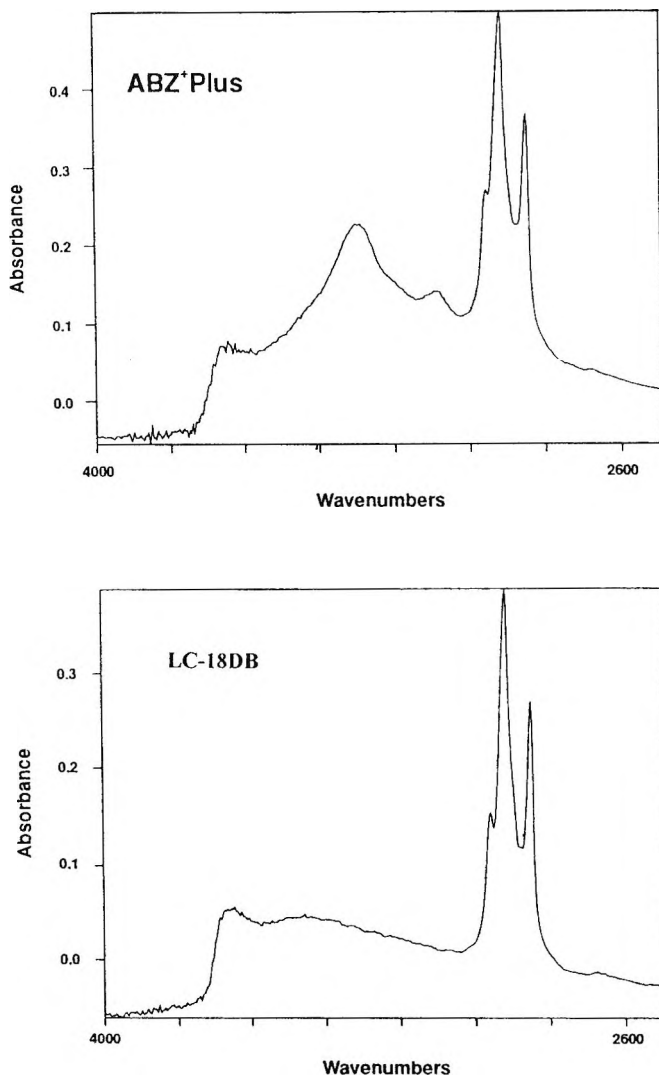
Figure 4. FTIR spectra of Supelcosil ABZ⁺ Plus and LC-18DB silicas.

Further confirmation of the difference in the H-bonding strengths of ABZ and ABZ⁺ Plus is obtained from the ^{13}C CP/MAS NMR spectra of the two surfaces (see Figure 3). The carbon β- to the silicon atom of the silane appears at 26.318 ppm with ABZ, while the same carbon in ABZ⁺ Plus is registered at 26.920 ppm.
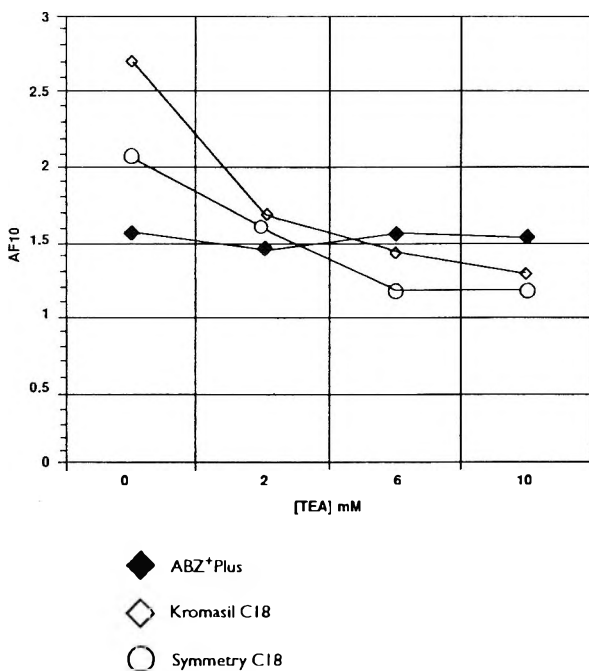
Figure 5. Asymmetry factor of the codeine peak as a function of triethylamine concentration for Supelcosil ABZ$^+$ Plus, Kromasil C-18 and Symmetry C-$_{18}$ columns.

It has been established earlier[51] that the β-carbon in aminopropylsilylated silica shifts from around 27 ppm to around 22 ppm upon hydration of the surface. In this instance, the mechanism proposed involves the protonation of the amino nitrogen with a proton from the silica surface silanol and stabilization of the charged species by the surface water. In the current context, the silane functionality in ABZ is the amide instead of the amine and the proton abstraction occurs through the carbonyl group of the amide with consequent stabilization by the surface water. Hence, the β-carbon in ABZ is upfield shifted in comparison with ABZ$^+$ Plus surface.

It is difficult to derive quantitative information from the ATR-FTIR spectra of the ABZ$^+$ Plus and ABZ surfaces (see Figure 4 for the FTIR spectrum of the former), but a clear distinction between ABZ$^+$ Plus and LC-18DB could be noticed both in the amide carbonyl region and the OH stretching region reflecting the structural differences between these two silica surfaces.
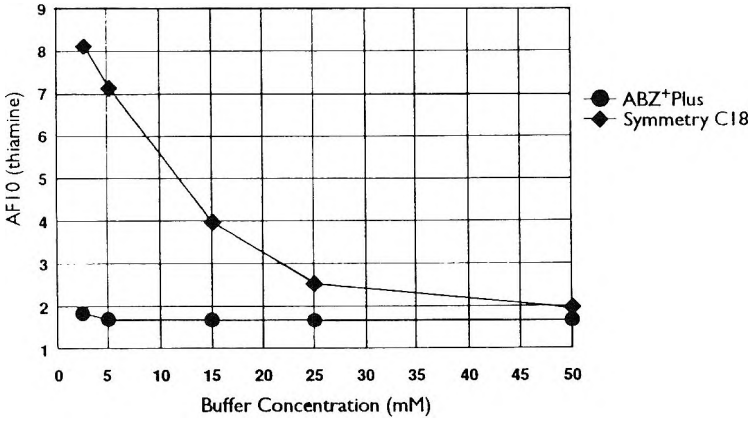
Figure 6. AF_{10} (thiamine) as a function of buffer concentration for Supelcosil ABZ^+ Plus and Symmetry C_{18} columns.
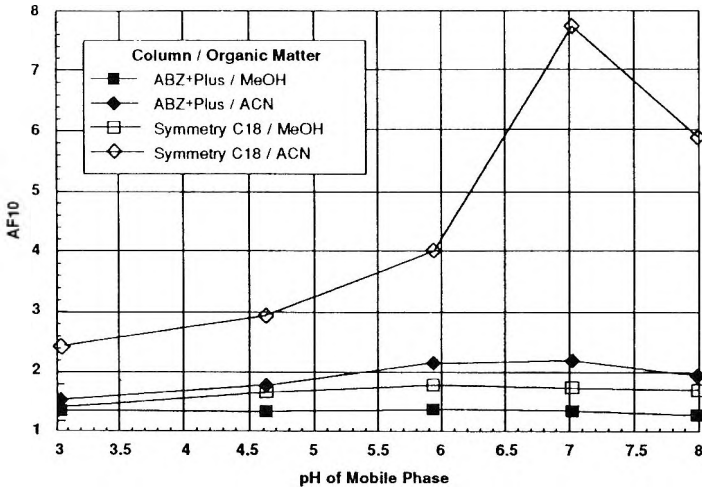
Figure 7. Effect of variation of mobile phase pH on peak shape of amytriptyline (without amine modifier) for Supelcosil ABZ^+ Plus and Symmetry C_{18} columns.
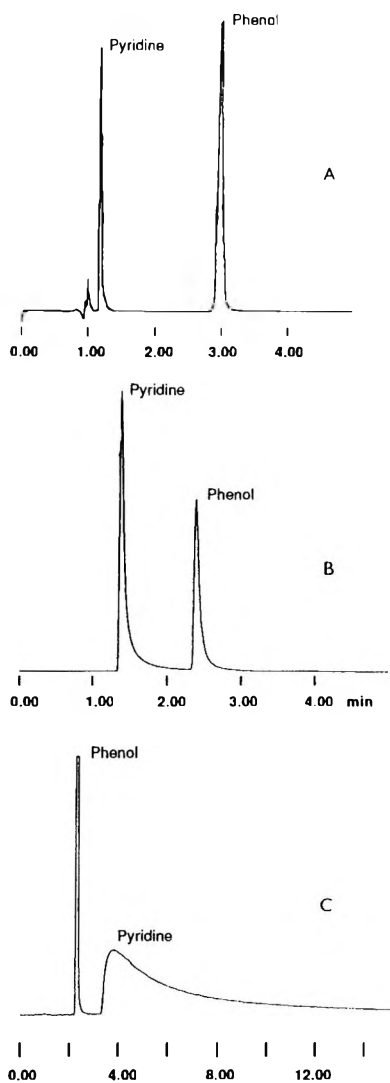
Figure 8. Comparison of the deactivation levels of Supelcosil ABZ⁺ Plus. LC-18DB and LC-18 columns for mixtures of phenol and pyridine.

Table 2

Comparison of Deactivated Columns for Chromatography and Resolution of Acids

Column	K'_{Sorbic}	$K'_{Benzoic}$	N_{sorbic} (Plates/m)	$N_{benzoic}$ (Plates/m)	AF_{10} Sorbic	AF_{10} Benzoic	Res
Supelcosil ABZ+Plus[a]	4.3	5.1	68,300	67,800	1.3	1.4	3.5
YMC-Basic[a]	2.2	2.4	68,200	69,300	1.2	1.4	0.9
LiChrosorb RP-Select B[b]	3.2	3.6	49,200	37,900	2.7	3.7	2.6
Intersil ODS-2[a]	2.6	2.7	50,500	50,400	1.2	1.3	0.8
Hypersil BDS-C18[a]	2.9	3.0	74,700	87,900	1.5	1.6	0.3
TSKgel ODS-80Ts[a]	2.8	3.0	109,600	110,900	1.2	1.2	1.5
Nucleosil 100-5 C18 AB[c]	2.6	2.7	53,900	60,000	2.2	2.0	0.4
Zorbax R_x[b]	3.8	4.2	82,900	94,300	1.3	1.3	2.6
Waters Symmetry C_8[a]	5.3	5.3	47,900	33,600	5.6	7.4	0.0
Waters Symmetry C_{18}[a]	4.9	5.0	62,900	60,900	2.0	2.2	0.5

Mobile Phase: acetonitrile: $25mM\ KH_2PO_4$ (pH 7.0), 25:75
Flow Rate: 1mL/min
[a] 15cm column
[b] 25cm column
[c] 10cm column

Comparison of the Liquid Chromatographic Behaviour of the ABZ⁺ Plus and the C_{18} Reversed Phase Columns

The inherent level of deactivation of the ABZ⁺ Plus stationary phase with respect to the conventional reversed phase C_{18} materials, when analytes such as codeine, thiamine or amitryptiline are subjected to liquid chromatographic analysis, is illustrated in Figures 5-7. In Figure 5, the asymmetry factor of the codeine peak at different concentrations of triethylamine was used as an index to assess the residual silanol effects. In all these experiments, the pH of the mobile phase was maintained at 7.0 so that the silanols are not protonated and their influence on the analyte elution profile could be more clearly visualized.

It is evident from Figure 5 that both types of C_{18} columns investigated show marked improvement in peak shape upon the addition of triethylamine, whereas this base additive had no influence on the codeine peak shape whatsoever with the ABZ⁺ Plus column. Similarly, Figure 6 shows that ionic strength had no effect on the peak shape of thiamine when analysed on the ABZ⁺ Plus column, while it exerts a significant effect on the peak shape with the C_{18} column.

Figure 7 demonstrates the influence of changing the mobile phase composition on the peak shape of amitryptiline in the absence of an amine modifier. In both acetonitrile and methanol, the peak shape on the ABZ⁺ Plus column is good; however, with pure-silica C_{18} the peak shape is poor at pH 7.0 indicating the influence of reactive silanol sites on this silica.

Figure 8 demonstrates the difference between a standard C_{18}, a conventional deactivated C_{18} and the ABZ⁺ Plus columns when a mixture of pyridine and phenol is eluted under identical conditions. Again, the best results are obtained with the ABZ⁺ Plus column which shows that both the acidic and basic silanol sites are shielded in this column. Table 2 shows the values of k', N and AF obtained for ten different columns with codeine under identical elution conditions. The data clearly indicate that Supelcosil ABZ⁺ Plus is the best column with respect to peak shape.

The selectivity achievable with the ABZ⁺ Plus column is illustrated in Figure 9 for a mixture of three basic drugs and for a mixture of acids, in comparison with Symmetry C_{18} column. The former were eluted at pH 7.0 and the latter at pH 2.3.

The superiority of the ABZ⁺ Plus columns over conventional C_{18} columns with respect to selectivity is readily recognized from the series of alkyl-benzenes, -anilines and -benzoic acids indicated in Figure 10. The retention
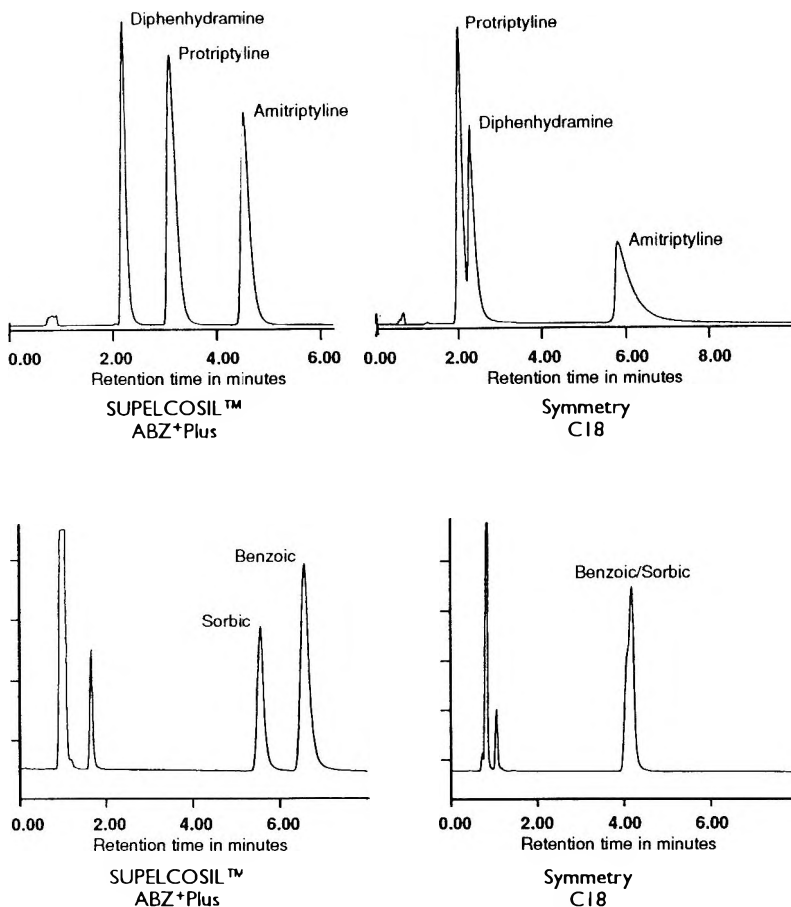
Figure 9. Comparison of the selectivities for three basic drugs and a mixture of sorbic and benzoic acids on Supelcosil ABZ$^+$ Plus and Symmetry C$_{18}$ columns.

times for alkylbenzenes and anilines were shorter with the ABZ$^+$ Plus column, while the acids were retained longer as compared to the C$_{18}$ column. This data clearly shows that the ABZ$^+$ Plus material is more polar than the C$_{18}$ stationary phase.

As indicated in the characterization section, the difference between ABZ$^+$ Plus and a conventional C$_{18}$ column is that in the former there is an amide group close to the silica surface coupled with the fact that there is a significant hydration layer at the surface. The ABZ$^+$ Plus organic surface layer is
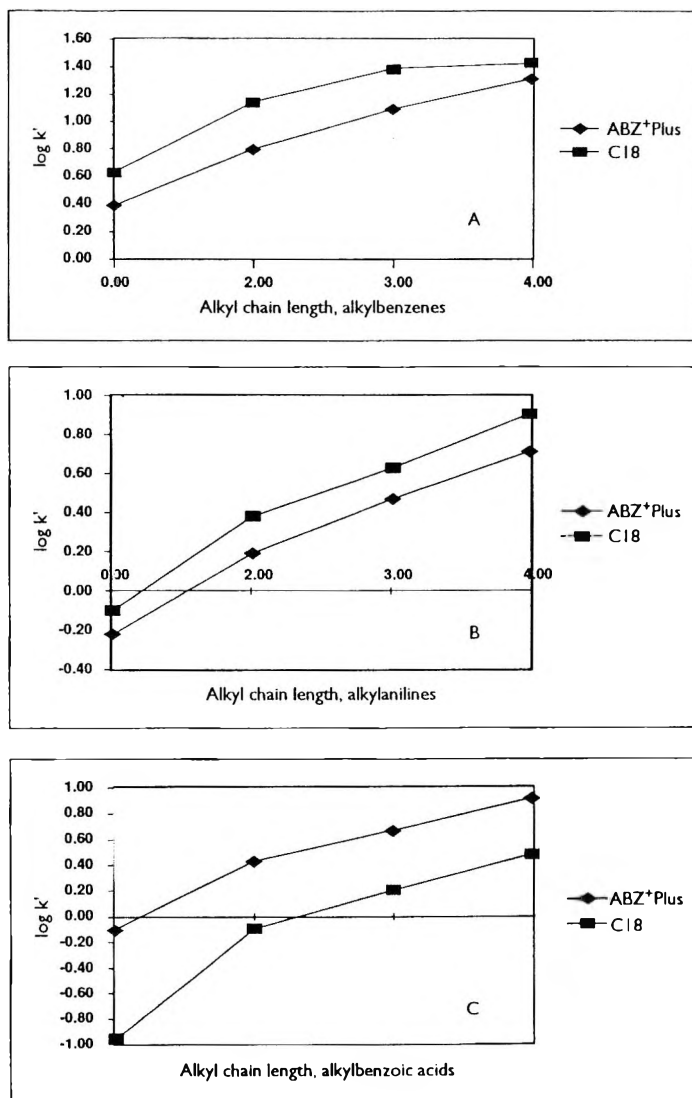
Figure 10. Selectivities of Superlcosil ABZ[+] Plus and C_{18} columns for alkyl-benzenes, -anilines and -benzoic acids.

amphiphilic with a polar functionality at the silica surface and a long alkyl chain extending into the stationary phase-mobile phase interface. This structural feature is analogous to a lipid membrane in a biological system which is known to be hydrated at the polar head group region.[52] Such surface-

immobilized structures were shown to interact with a variety of functionalized organic molecules through a partition mechanism, making use of electrochemical methods of analysis.[53] Similar partitioning mechanisms were proposed by Martire[54] and by Dill[55] through a unified molecular theory based on a lattice model and statistical-mechanical theory that takes into account bonded-chain reorganization energy, respectively, for solute retention on monomeric C_{18} bonded reversed phases.

Marshall and coworkers[56] have estimated through fluorescence measurements employing dansyl probes that the interfacial region of RP-18 stationary phase has an effective polarity comparable to that of methanol containing 10% water. It is presumed that the organic modifier in mixed organic-water mobile phases is preferentially adsorbed at this interface and thus the solvent composition of the stationary phase zone is different from that of the mobile phase varying with the distance from the silica surface. Partitioning of the solute takes place between the mobile phase and this zone and is dependent upon its polarity and dimensions.

Jaroniec[57] has recently pointed out that the composition of the solvents in the stationary phase significantly influences the solute's retention even in the the case of conventional bonded phases and that this effect is much stronger for silica-based packings with chemically bonded phases of specific properties. It has been demonstrated that the stationary phase plays a vital role in liquid chromatographic separations in RPLC in general and when the bonded reversed phase contains ligands carrying amide functionalities, in particular.[58-60] The factors that govern the thermodynamic equilibrium of solvent distribution between the mobile and stationary phases include the mobile phase composition, the chemical nature of the bonded ligands, their surface concentration and conformation. Furthermore, the hydrogen bonding interactions associated with the residual silanols on the modified silica also play a significant role in controlling the concentration of water molecules in the chemically bonded phase and consequently exert a profound effect on the composition of this phase. The pioneering work of the Jaroniec group[58-63] on the measurement of sorption excessess at the liquid-solid interface when aqueous-organic binary mobile phase systems are used in HPLC sheds considerable light on the liquid chromatographic behaviour of amide-functionalized stationary phases. Of particular interest is the observation that the sorption excess of water for the C_{18} and AA_3 (octadecanoylaminopropyl-silanized silica) reversed phases are similar and negative, while that for AA_2 (a shorter chain analogue of AA_3) it is positive. Both AA_3 and AA_2 exhibit good symmetry and peak shapes for polar molecules, especially basic compounds.

Hydration Layer on ABZ⁺Plus Phase
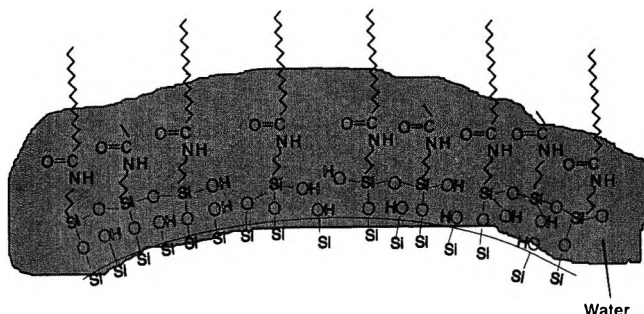
Figure 11. Structure of Supelcosil ABZ⁺ Plus stationary phase with its hydration layer.

With the current ABZ⁻ Plus material, we hypothesize that the combination of the surface amide functionalities and the larger hydration layer at the silica surface imparts a high degree of orientation to the alkyl chains of this stationary phase. When this phase is contacted by the binary water-acetonitrile mobile phase, the ensuing equilibration results in a profound difference between the solvent compositions of the stationary and mobile phases, which contributes to a more effective partitioning of a polar solute and results in greater selectivity. Moreover, the large hydration layer can also shield the residual silanols of the silica from the solute (see Figure 11) more effectively.

In contrast to the high degree of orientation of the ABZ⁺ Plus material, the alkyl chains on the conventional C_{18} reversed phase columns can fold back and block the solute from reaching the surface, under aqueous environments. Consequently, the water content of a reversed phase column seems to be a crucial factor in enhancing selectivity while simultaneously reducing residual silanol effects.

REFERENCES

1. J. Cadet, M. Weinfeld, Anal. Chem., **65**, 675A-682A (1993).

2. U. D. Neue, D. J. Phillips, T. H. Walter, M. Capparella, B. Alden, R. P. Fisk, LC-GC, **12**, 468-480 (1994).

3. G. W. Welling, R. van der Zee, S. Welling-Wester, "HPLC of Membrane Proteins", in **HPLC of Biological Macromolecules**, K. M. Gooding, F. E.Regnier, eds., Chromatographic Science Series, J. Cazes, ed., Marcel Dekker, New York, 1990, pp. 373-401.

4. W. S. Hancock, "HPLC in Biotechnology", in **HPLC in Biotechnology**, W. S. Hancock, ed., John Wiley, New York, 1990, pp. 1-19.

5. C. Schoneich, A. F. R. Huhmer, S. R. Rabel, J. F. Stobaugh, S. D. S. Jois, C. K. Larive, T. J. Siahaan, T. C. Squier, D. J. Bigelow, T. D. Williams, Anal. Chem., **67**, 155R-181R (1995).

6. S. K. C. Chang, E. Holm, J. Schwarz, P. Rayas-Duarte, Anal. Chem., **67**, 127R-153R (1995).

7. A. K. D. Liem, R. A. Baumann, A. P. J. M. de Jong, E. G. van der Velde, P. van Zoonen, J. Chromatogr., **624**, 317-339 (1992).

8. R. E. Majors, LC-GC, **12**, 890-898 (1994).

9. L.C. Sander, S.A. Wise, Anal. Chem., **67**, 3284-3292 (1995).

10. J. G. Dorsey, W. T. Cooper, Anal. Chem., **66**, 857A-867A (1994).

11. K. Tani,Y. Suzuki, J. Chromatogr. Sci., **27**, 698-703 (1989).

12. L. C. Sander, S. A. Wise, J. Chromatogr. A, **656**, 335-351 (1993).

13. K. Jinno, T. Ibuki, N. Tanaka, M. Okamoto, J.C. Fetzer, W.R. Biggs, P.R. Griffiths, J. M. Olinger, J. Chromatogr., **461**, 209-227 (1989).

14. R. Gill, D. Osselton, R. M. Smith, T.G. Hurdley, J. Chromatogr., **386**, 65-77 (1987).

15. L. C. Sander, S.A. Wise, Crit. Rev. Anal. Chem., **18**, 299-415 (1987).

16. S.O. Akapo, C.F. Simpson, Anal. Proc., **26**, 394-397 (1989).

17. P. Schneider, R. Cloux, K. Foti, E.sz. Kovats, Synthesis, 1027-1031 (1990).

18. J. J. Kirkland, J.W. Henderson, J. Chromatogr. Sci., **32**, 473-480 (1994).

19. R. Zhang. Z. Xie. R. Zhao. X. Li, G. Liu, M. Aguilar, M.T.W. Hearn, Anal. Chem., **63**, 1861-1867 (1991).

20. R. K. Gilpin. M.E. Gangoda. J. Chromatogr. Sci., **28**, 277-281 (1990).

21. J.E. Sandova:. J.J. Pesek. Anal. Chem., **61**, 2067-2075 (1989).

22. M.J. Wirth, H.O. Fatunmbi. Anal. Chem., **64**, 2783-2786 (1992).

23. P. Tundo. P. Venturello. J. Am. Chem. Soc., **101**, 6606-6613 (1979).

24. N. Oi. M. Nagase. Y. Inda. T. Doi. J. Chromatogr., **259**, 487-493 (1983).

25. A. Nomura. J. Yamada. K. Tsunoda, Anal. Sci., **3**, 209-212 (1987).

26. B. Buszewsk:, J. Schmid, K. Albert, E. Bayer, J. Chromatogr., **552**, 415-427 (1991).

27. Y. Okahata, K. Kimura, K. Ariga. J. Am. Chem. Soc., **111**, 9190-9194 (1989).

28. G. Boven, R. Folkersma, G. Challa, A.J. Schouten, Polymer Commun., **32**, 50-53 (1991).

29. S. Yamamura, T. Tamaki. T. Seki, M. Sakuragi, Y. Kawanishi. K. Ichmura. Chem. Lett., 543-546 (1992).

30. C. Pidgeon. U. V. Venkataram. Anal. Biochem., **176**, 36-45 (1989).

31. K. M. R. Kallury, M. Cheung. V. Ghaemmaghami. U. J. Krull. M. Thompson. Colloids Surfaces. **63**, 1-9 (1992).

32. T. Ihara, Y. Sugimoto, M. Asada, T. Nakagama, T. Hobo, J. Chromatogr., **694**, 49-56 (1995).

33. S. Nagae, T. Miyamoto. Y. Inaki. K. Takemoto, Polymer J., **21**. 19-33 (1989).

34. W. H. Pirkle, T. C. Pochapsky. Chem. Rev., **89**, 347-362 (1989).

35. C. E. Kibbey, M. E. Meyerhoff, J. Chromatogr., **641**, 49-55 (1993); Anal. Chem., **65**, 2189-2196 (1993).

36. J. E. O'Gara, B. A. Alden, T. H. Walter, J. S. Petersen, C. L. Niederlander, U. D. Neue, Anal. Chem., **67**, 3809-3813.

37. B. Buszewski, M. Jaroniec, R. K. Gilpin, J. Chromatogr., **673**, 11-19 (1994).

38. M. Alvinerie, J. F. Sutra, C. Eeckhoutte, P. Galtier, G. A. E. van't Klooster, A. S. J. P. A. M. van Miert, J. Chromatogr., **612**, 115-121 (1993).

39. R. J. M. Vervoort, M. W. J. Derksen, F. A. Maris, J. Chromatogr., **678**, 1-15 (1994).

40. D. Korakas, K. Valko, J. Liquid Chromatogr., **17**, 3571-3584 (1994).

41. J. Paesen, P. Claeys, E. Roets, J. Hoogmartens, J. Chromatogr., **630**, 117-122 (1993).

42. E. F. Vansant, P. Van Der Voort, K. C. Vrancken, "**Characterization and Chemical Modification of the Silica Surface**", Elsevier, Amsterdam (1995), pp. 489-510.

43. D. Amati, E. Kovats, Langmuir, **3**, 687-695 (1987).

44. M. L. Miller, R. W. Linton, S. G. Bush, J. W. Jorgenson, Anal. Chem., **56**, 2204-2210 (1984).

45. K. M. R.Kallury, M. Thompson, C. P. Tripp, M. L. Hair, Langmuir, **8**, 947-954 (1992).

46. V. A. Brown, D. A. Barrett, P. N. Shaw, M. C. Davies, H. J. Ritchie. P. Ross, A. J. Paul, J. F. Watts, Surface Interface Anal., **21**, 262-272 (1994).

47. B. Buszewski, P. Kasturi, R. K. Gilpin, M. E. Gangoda, M. Jaroniec, Chromatographia, **39**, 155-161 (1994).

48. K. M. R. Kallury, P. M. Macdonald, M. Thompson, Langmuir, **10**, 492-499 (1994).

49. K. M. R. Kallury, M. Thompson, C. P. Tripp, M. L. Hair, Langmuir, **8**, 947-954 (1992).

50. K. Albert, E. Bayer, J. Chromatogr., **544**, 345-370 (1991).

51. G. S. Caravajal, D. E. Leydon, G. R. Quinting, G. E. Maciel, Anal. Chem., **60**, 1776-1786 (1988).

52. H. Saint-Martin, I. Ortega-Blake, "The microscopic structure and dynamics of water at a surface", in "**Enzymes in Reverse Micelles Containing Phospholipids**", A. Darszon, L. Shoshani, eds., CRC Press, Boca Raton, 1992, pp. 35-65.

53. J. Wang, Z. Lu, Anal. Chem., **62**, 826-829 (1990).

54. D. E. Martire, R. E. Boem, J. Phys. Chem., **87**, 1045-1062 (1983).

55. K. A. Dill, J. Phys. Chem., **91**, 1980-1988 (1987).

56. Y. Men, D. B. Marshall, Anal. Chem., **62**, 2606-2611(1990).

57. M. Jaroniec, J. Chromatogr. A, **722**, 19-24 (1996).

58. B. Buszewski, M. Jaroniec, R. K. Gilpin, J. Chromatogr. A, **668**, 293-299 (1994).

59. P. Kasturi, B. Buszewski, M. Jaroniec, R. K. Gilpin, J. Chromatogr. A, **659**, 261-265 (1994).

60. M. Jaroniec, J. Chromatogr. A, **656**, 37-50 (1993).

61. M. Jaroniec, S. Lin, R. K. Gilpin, Chromatographia, **32**, 13-17 (1991).

62. R. K. Gilpin, M. Jaroniec, S. Lin, Anal. Chem., **63**, 2849-2852 (1991); **62**, 2092-2098 (1990).

63. M. Jaroniec, D. E. Martire, J. Chromatogr., **351**, 1-16 (1986); **387**, 55-64 (1987).

EDUCATION ANNOUNCEMENT

BASIC PRINCIPLES OF HPLC
AND HPLC SYSTEM TROUBLESHOOTING

A Two-Day
In-House Training Course

The course, which is offered for presentation at corporate laboratories, is aimed at chemists, engineers and technicians who use, or plan to use, high performance liquid chromatography in their work. The training covers HPLC fundamentals and method development, as well as systematic diagnosis and solution of HPLC hardware module and system problems.

The following topics are covered in depth:
- Introduction to HPLC Theory
- Modes of HPLC Separation
- Developing and Controlling Resolution
- Mobile Phase Selection and Optimization
- Ion-Pairing Principles
- Gradient Elution Techniques
- Calibration and Quantitation
- Logical HPLC System Troubleshooting

The instructor, Dr. Jack Cazes, is founder and Editor-in-Chief of the Journal of Liquid Chromatography & Related Technologies, Editor of Instrumentation Science & Technology, and Series Editor of the Chromatographic Science Book Series. He has been intimately involved with liquid chromatography for more than 35 years; he pioneered the development of modern HPLC technology. Dr. Cazes was Professor-in-Charge of the ACS Short Course and the ACS Audio Course on Gel Permeation Chromatography for many years.

Details of this course may be obtained from Dr. Jack Cazes, P. O. Box 970210, Coconut Creek, FL 33097, USA. E-Mail: jcazes@icanect.net.

LIQUID CHROMATOGRAPHY CALENDAR

1996

NOVEMBER 6 - 8: 31st Midwestern Regional Meeting, ACS, Sioux Falls, South Dakota. Contact: J. Rice, Chem Dept, S. Dakota State Univ, Shepard Hall Box 2202, Brookings, SD 57007-2202, USA.

NOVEMBER 6 - 9: 24th Biennial International Conference on Application of Accelerators in Research & Industry, Denton, Texas. Contact: J. L. Duggan or B. Stippec. University of North Texas, Physics Department, Denton, TX 76203, USA. Tel: (817) 565-3252; FAX: (817) 565-2227.

NOVEMBER 9 - 12: 48th Southeast Regional ACS Meeting, Hyatt Regency Hotel, Greenville, South Carolina. Contact: H. C. Ramsey, BASF Corp., P. O. Drawer 3025, Anderson, SC 29624-3025, USA.

NOVEMBER 10 - 13: 4th North American Research Conference on Organic Coatings Science & Technology, Hilton Head, South Carolina. Contact: A. V. Patsis, SUNY, New Paltz, NY 12561, USA. Tel: (914) 255-0757; FAX: (914) 255-0978.

NOVEMBER 10 - 14: 10th International Forum on Electrolysis in the Chemical Industry, Clearwater Beach, Florida. Contact: P. Kluczynski, Electrosynthesis Co, 72 Ward Road, Lancaster, NY 14086, USA. Tel: (716) 684-0513; FAX: (716) 684-0511.

NOVEMBER 10 - 15: AIChE Annual Meeting, Palmer House, Chicago, Illinois. Contact: AIChE, 345 East 47th Street, New York, NY 10017-2395, USA.

NOVEMBER 11 - 20: 2nd Latin-American Conference on Biomedical, Biopharmaceutical and Industrial Applications of Capillary Electrophoresis, Santiago, Chile. Dr. E. Guerrero, Servicio Medico Legal, Avenida de la Paz 1012. Santiago, Chile.

NOVEMBER 12 - 14: Plastics Fair, Charlotte, North Carolina. Contact: Becky Lerew. Plastics Fair, 7500 Old Oak Blvd, Cleveland, OH 44130, USA. Tel: (216) 826-2844; FAX: (216) 826-2801.

NOVEMBER 13 - 15: 13th Montreux Symposium on Liquid Chromatography-Mass Spectrometry (LC/MS; SFC/MS; CE/MS; MS/MS), Maison des Congres, Montreux, Switzerland. Contact: M. Frei-Hausler, Postfach 46, CH-4123 Allschwill 2, Switzerland. Tel: 41-61-4812789; FAX: 41-61-4820805.

NOVEMBER 18 - 20: 3rd International Conference on Chemistry in Industry, Bahrain, Saudi Arabia. Contact: Chem in Industry Conf, P. O. Box 1723. Dhahran 31311, Saudi Arabia. Tel: 966 3 867 4409; FAX: 966 3 876 2812.

NOVEMBER 17 - 22: Eastern Analytical Symposium, Garden State Convention Center, Somerset, New Jersey. Contact: S., Good. EAS, P. O. Box 633, Montchanin. DE 19710-0635, USA. Tel: (302) 738-6218; FAX: (302) 738-5275.

NOVEMBER 24 - 27: Industrial Research for the 21st Century, 1996 Biennial Meeting, Red Lion Resort, Santa Barbara, California. Contact: R. Ikeda. DuPont Central Research Dept., P. O. Box 80356, Wilmington, DE 19880-0356. USA. Tel: (302) 695-4382; FAX: (302) 695-8207.

DECEMBER 17 - 20: First International Symposium on Capillary Electrophoresis for Asia-Pacific, Hong Kong. Contact: Dr. S. F. Y. Li, Dept of Chemistry, National University of Singapore, Kent Ridge Crescent, Singapore 119260. Republic of Singapore.

1997

MARCH 16 - 21: PittCon '97, Atlanta, Georgia. Contact: PittCon '97, Suite 332. 300 Penn Center Blvd., Pittsburgh, PA 15235-5503, USA. Tel: (800) 825-3221; FAX: (412) 825-3224.

APRIL 13 - 17: 213th ACS National Meeting, San Francisco, California. Contact: ACS Meetings, ACS, 1155 16th Street, NW, Washington, DC 20036-4899, USA. Tel: (202) 872-6059; FAX: (202) 872-6128.

APRIL 14 - 19: Genes and Gene Families in Medical, Agricultural and Biological Research: 9th International Congress on Isozymes, sponsored by the Southwest Foundation for Biomedical Research, Hilton Palacio del Rio, San Antonio, Texas. Contact: Mrs. Janet Cunningham, Barr Enterprises, P. O. Box 279, Walkersville, MD 21793, USA.

MAY 5 - 9: 151st ACS Rubber Div Spring Technical Meeting, Anaheim, California. Contact: L. Blazeff, P. O. Box 499, Akron, OH 44309-0499, USA.

MAY 23 - 24: ACS Biological Chemistry Div Meeting, San Francisco, California. Contact: K. S. Johnson, Dept of Biochem & Molec Biol, Penn State Univ, 106 Althouse Lab, University Park, PA 16802, USA.

MAY 27 - 30: ACS 29th Central Regional Meeting, Midland, Michigan. Contact: S. A. Snow, Dow Corning Corp., CO42A1, Midland, MI 48686-0994, USA. Tel: (517) 496-6491; FAX: (517) 496-6824.

MAY 28 - 30: 31st ACS Middle Atlantic Regional Meeting, Pace Univ, Pleasantville, NY. Contact: D. Rhani, Chem Dept, Pace University, 861 Bedford Rd, Pleasantville, NY 10570-2799, USA. Tel: (914) 773-3655.

MAY 28 - JUNE 1: 30th Great Lakes Regional ACS Meeting, Loyola University, Chicago Illinois. Contact: M. Kouba, 400G Randolph St, #3025, Chicago, IL 60601, USA. Email: reglmtgs@acs.org.

JUNE 22 - 25: 27th ACS Northeast Regional Meeting, Saratoga Springs, New York. Contact: T. Noce, Rust Envir & Infrastructure, 12 Metro Park Rd, Albany, NY 12205, USA. Tel: (518) 458-1313; FAX: (518) 458-2472.

JUNE 22 - 26: 35th National Organic Chemistry Symposium, Trinity Univ., San Antonio, Texas. Contact: J. H. Rigby, Chem Dept, Wayne State Univ., Detroit, MI 48202-3489, USA. Tel: (313) 577-3472.

SEPTEMBER 7 - 11: 214th ACS National Meeting, Las Vegas, Nevada. Contact: ACS Meetings, 1155 16th Street, NW, Washington, DC 20036-4899, USA. Tel: (202) 872-4396; (202) 872-6128; Email: natlmtgs@acs.org.

SEPTEMBER 21 - 26: **Federation of Analytical Chemistry & Spectroscopy Societies (FACSS), Cleveland, Ohio.** Contact: J. A. Brown, FACSS, 198 Thomas Johnson Dr, Suite S-2, Frederick, MD 21702, USA. Tel: (301) 846-4797; FAX: (301) 694-6860.

OCTOBER 19 - 22: **49th ACS Southeast Regional Meeting, Roanoke, Virginia.** Contact: J. Graybeal, Chem Dept, Virginia Tech, Blacksburg, VA 24061, USA. Tel: (703) 231-8222; Email: reglmtgs@acs.org.

OCTOBER 21 - 25: **33rd ACS Western Regional Meeting, Irvine, California.** Contact: L. Stemler, 8340 Luxor St, Downey, CA 90241, USA. Tel: (310) 869-9838; Email: reglmtgs@acs.ord.

OCTOBER 26 - 29: **8th Symposium on Handling of Environmental & Biological Samples in Chromatography and the 26th Scientific Meeting of the Group of Chromatography and Related Techniques of the Spanish Royal Society of Chemistry, Almeria, Spain.** Contact: M. Frei-Hausler, IAEAC Secretariat, Postfach 46, CH-4123 Allschwill 2, Switzerland. FAX: 41-61-4820805.

OCTOBER 29 - NOVEMBER 1: **32nd ACS Midwest Regional Meeting, Lake of the Ozarks, Osage Beach, Missouri.** Contact: C. Heitsch, Chem Dept, Univ of Missouri-Rolla, Rolla, MO 65401, USA. Tel: (314) 341-4536; FAX: (314) 341-6033; Email: reglmtgs@acs.org.

NOVEMBER 11 - 15: **5th Chemical Congress of North America, Cancun, Mexico.** Contact: ACS Meetings, 1155 16th St, NW, Washington, DC 20036-4899, USA. Tel: (202) 872-6286; FAX: (202) 872-6128.

NOVEMBER 16 - 21: **Eastern Analytical Symposium, Garden State Convention Center, Somerset, New Jersey.** Contact: S. Good, EAS, P. O. Box 633, Montchanin, DE 19710-0635, USA. Tel: (302) 738-6218.

1998

MARCH 1 - 6: PittCon '98, New Orleans, Louisiana. Contact: PittCon '98, Suite 332, 300 Penn Center Blvd., Pittsburgh, PA 15235-5503, USA. Tel: (800) 825-3221; FAX: (412) 825-3224.

MARCH 29 - APRIL 2: **215th ACS National Meeting, Dallas, Texas.** Contact: ACS Meetings, 1155 16th Street, NW, Washington, DC 20036-4899, USA. Tel: (202) 872-4396; FAX: (202) 872-6128; Email: natlmtgs@acs.org.

JUNE 10 - 12: 53rd ACS Northwest Regional Meeting, Columbia Basin College, Pasco, Washington. Contact: K. Grant, Math/Science Div, Columbia Basin College, 2600 N 20th Ave, Pasco, WA 99301, USA. Email: reglmtgs@acs.org.

JUNE 13 - 19: 26th ACS National Medical Chemistry Symposium, Virginia Commonwealth Univ/Omni Richmond Hotel, Richmond, Virginia. Contact: D. J. Abraham, Virginia Commonwealth Univ, Dept of Med Chem, P. O. Box 581, Richmond, VA 23298, USA. Tel: (804) 828-8483; FAX: (804) 828-7436.

AUGUST 23 - 28: 216th ACS National Meeting, Boston, Massachusetts. Contact: ACS Meetings, 1155 16th Street, NW, Washington, DC 20036-4899, USA. Tel: (202) 872-4396; FAX: (202) 872-6218; Email: natlmtgs@acs.org.

SEPTEMBER 7 - 11: 15th International Symposium on Medicinal Chemistry, Edinburgh, Scotland. Contact: M. Campbell, Bath University School of Chemistry, Claverton Down, Bath, BA2 7AY, UK. Tel: (44) 1225 826565; FAX: (44) 1225 826231; Email: chsmmc@bath.ac.uk.

NOVEMBER 4 - 7: 50th ACS Southwest Regional Meeting, Resw Triangle Pk, North Carolina. Contact: B. Switzer, Chem Dept, N Carolina State University, Box 8204, Raleigh, NC 27695-8204, USA. Tel: (919) 775-0800, ext 944; Email: switzer@chemdept.chem.ncsu.edu.

1999

MARCH 7 - 12: PittCon '99, Orlando, Florida. Contact: PittCon '99, Suite 332, 300 Penn Center Blvd., Pittsburgh, PA 15235-5503, USA. Tel: (800) 825-3221; FAX: (412) 825-3224.

MARCH 21 - 25: 217th ACS National Meeting, Anaheim, Calif. Contact: ACS Meetings, 1155 16th Street, NW, Washington, DC 20036-4899, USA. Tel: (202) 872-4396; FAX: (202) 872-6128; Email: natlmtgs@acs.org.

AUGUST 22 - 26: 218th ACS National Meeting, New Orleans, Louisiana. Contact: ACS Meetings, 1155 16th Street, NW, Washington, DC 20036-4899, USA. Tel: (202) 872-4396; FAX: (202) 872-6128; Email: natlmtgs@acs.org.

OCTOBER 8 - 13: 51st ACS Southeast Regional Meeting, Knoxville, Tennessee. Contact: C. Feigerle, Chem Dept, University of Tennessee, Knoxville, TN 37996, USA. Tel: (615) 974-2129; Email: reglmtgs@acs.org.

2000

MARCH 5 - 10: PittCon 2000, Chicago, Illinois. Contact: PittCon 2000, Suite 332, 300 Penn Center Blvd., Pittsburgh, PA 15235-5503, USA.

MARCH 26 - 30: 219th ACS National Meeting, Las Vegas, Nevada. Contact: ACS Meetings, 1155 16th Street, NW, Washington, DC 20036-4899, USA. Tel: (202) 872-4396; FAX: (202) 872-6128; Email: natlmtgs@acs.org.

AUGUST 20 - 24: 220th ACS National Meeting, Washington, DC. Contact: ACS Meetings, 1155 16th Street, NW, Washington, DC 20036-4899, USA. Tel: (202) 872-4396; FAX: (202) 872-6128; Email: natlmtgs@acs.org.

2001

APRIL 1 - 5: 221st ACS National Meeting, San Francisco, Calif. Contact: ACS Meetings, 1155 16th Street, NW, Washington, DC 20036-4899, USA. Tel: (202) 872-4396; FAX: (202) 872-6128; Email: natlmtgs@acs.org.

AUGUST 19 - 23: 222nd ACS National Meeting, Chicago, Illinois. Contact: ACS Meetings, 1155 16th Street, NW, Washington, DC 20036-4899, USA. Tel: (202) 872-4396; FAX: (202) 872-6128; Email: natlmtgs@acs.org.

2002

APRIL 7 - 11: 223rd ACS National Meeting, Orlando, Florida. Contact: ACS Meetings, 1155 16th Street, NW, Washington, DC 20036-4899, USA.

SEPTEMBER 8 - 12: 224th ACS National Meeting, Boston, Mass. Contact: ACS Meetings, 1155 16th Street, NW, Washington, DC 20036-4899, USA.

2003

MARCH 23 - 27: 225th ACS National Meeting, New Orleans, Louisiana.
Contact: ACS Meetings, 1155 16th Street, NW, Washington, DC 20036-4899,
USA. Tel: (202) 872-4396; FAX: (202) 872-6128; Email: natlmtgs@acs.org.
SEPTEMBER 7 - 11: 226th ACS National Meeting, New York City.
Contact: ACS Meetings, 1155 16th Street, NW, Washington, DC 20036-4899,
USA. Tel: (202) 872-4396; FAX: (202) 872-6128; Email: natlmtgs@acs.org.

2004

**MARCH 28 - APRIL 1: 227th ACS National Meeting, Anaheim,
California.** Contact: ACS Meetings, 1155 16th Street, NW, Washington, DC
20036-4899, USA. Tel: (202) 872-4396; FAX: (202) 872-6128: Email:
natlmtgs@acs.org.

**AUGUST 22 - 26: 228th ACS National Meeting, Philadelphia,
Pennsylvania.** Contact: ACS Meetings, 1155 16th Street, NW, Washington,
DC 20036-4899, USA. Tel: (202) 872-4396; FAX: (202) 872-6128; Email:
natlmtgs@acs.org.

2005

MARCH 13 - 17: 229th ACS National Meeting, San Diego, California.
Contact: ACS Meetings, 1155 16th Street, NW, Washington, DC 20036-4899,
USA. Tel: (202) 872-4396; FAX: (202) 872-6128; Email: natlmtgs@acs.org.

**AUGUST 28 - SEPTEMBER 1: 230th ACS National Meeting,
Washington, DC.** Contact: ACS Meetings, 1155 16th Street, NW,
Washington, DC 20036-4899, USA. Tel: (202) 872-4396; FAX: (202) 872-
6128: Email: natlmtgs@acs.org.

The **Journal of Liquid Chromatography & Related Technologies**
will publish, at no charge, announcements of interest to scientists in every issue
of the journal. To be listed in the Liquid Chromatography Calendar, we will
need to know:

      a) Name of the meeting or symposium,
      b) Sponsoring organization,
      c) When and where it will be held, and
      d) Whom to contact for additional details.

Incomplete information will not be published. You are invited to send announcements to **Dr. Jack Cazes, Editor, Journal of Liquid Chromatography & Related Technologies, P. O. Box 970210, Coconut Creek, FL 33097, USA.**

Ion Exchange and Solvent Extraction

VOLUME **12**

edited by
JACOB A. MARINSKY
State University of New York at Buffalo
YIZHAK MARCUS
Hebrew University of Jerusalem, Israel

March, 1995
456 pages, illustrated
$195.00

Volume 12 of this unique series continues in the tradition of its widely received predecessors, presenting **current** developments in the theory and practice of ion exchange.

This authoritative reference provides interdisciplinary coverage of contemporary topics, including

■ the nature of metal-ion interaction with oppositely charged sites of ion exchangers

■ high-pressure ion-exchange separation of rare earth elements

■ the commercial recovery of valuable minerals from seawater and brines by ion exchange and sorption

■ the kinetics of ion exchange in heterogeneous systems

■ the ion-exchange equilibria of amino acids

■ and much more!

The *Ion Exchange and Solvent Extraction Series* treats ion exchange and solvent extraction both as discrete topics and as a unified, multidisciplinary study—presenting new insights for researchers in many chemical and related fields. The volumes in this now classic series are of major importance to analytical, coordination, process, separation, surface, organic, inorganic, physical, and environmental chemists; geochemists; electrochemists; radiochemists; biochemists; biophysicists; hydrometallurgists; membrane researchers; and chemical engineers.

Contents

ISBN: 0—8247—9382—X

This book is printed on acid-free paper.

Marcel Dekker, Inc.

Solvent Extraction and Ion Exchange

Editors: **KENNETH L. NASH** and **RENATO CHIARIZIA**
Chemistry Division, Argonne National Laboratory
9700 South Cass Avenue, Argonne, Illinois 60439-4831

1995 Volume 13, 6 Numbers
Institutional rate: $650.00
Individual rate: $325.00

Solvent Extraction and Ion Exchange, an international journal, provides current, in-depth, comprehensive coverage of advances and developments in all areas of the field—covering subjects ranging from agriculture, biology, and chemistry through engineering, metallurgy, medicine, and geology. *Solvent Extraction and Ion Exchange* publishes original research articles, notes of work in progress, critical reviews, and letters to the editor, as well as reviews of new books, a bibliography section, and notices of meetings. Some of the major topics discussed include adsorption and extraction chromatography, separations using liquid membranes and related techniques, separation materials, underlying principles, and all other aspects of solvent extraction and ion exchange.

Subscribe Today!

LIBRARIANS: Make sure the agricultural, analytical, and physical chemists; engineers; geologists; hydrometallurgists; and research physicians you serve find *Solvent Extraction and Ion Exchange* on your bookshelves. Order your subscription today either from your subscription agency or directly from Marcel Dekker, Inc.

CALL FOR PAPERS: *Solvent Extraction and Ion Exchange* welcomes manuscript contributions. Those papers accepted will be published promptly. For complete details regarding manuscript preparation and submission, please contact the editors directly.

ISSN: 0736—0299

Contents

INSTRUCTIONS TO AUTHORS

The *Journal of Liquid Chromatography & Related Technologies* is published in the English language for the rapid communication of research results in liquid chromatography and its related sciences and technologies.

Directions for Submission
One complete original manuscript and two (2) clear copies, with figures, must be submitted for peer review. After all required revisions have been completed, and the final manuscript has been accepted, the author will be asked to provide, if possible, a 3½" or 5¼" PC-Compatible computer diskette containing the complete manuscript. Microsoft Word, Word for Windows, WordPerfect, WordPerfect for Windows and ASCII are preferred formats. Text, including tables, and figures, if in electronic format, should be saved in separate files on the diskette. Label the diskette with the corresponding author's last name, the title of the manuscript and the file number assigned to the manuscript

Submission of a manuscript on diskette, in a suitable format, will significantly expedite its publication.

Manuscripts and computer diskettes should be mailed to the Editor:

Dr. Jack Cazes
Journal of Liquid Chromatography & Related Technologies
P. O. Box 970210
Coconut Creek, FL 33097

Reprints
Due to the short production time for papers in this journal, it is essential to order reprints immediately upon receiving notification of acceptance of the manuscript. A reprint order form will be sent to the author with the letter of acceptance for the manuscript. Reprints are available in quantities of 100 and multiples thereof. Twenty (20) free reprints will be included with orders of 100 or more reprints.

Format of the Manuscript
NOTE: Failure to adhere to the following guidelines will delay publication of a manuscript.

1. The preferred dimensions of the printed area of a page are
   6" (15.2 cm) width by 8.5" (21.6 cm) height.
   Use Times Roman 12 point font, if possible.

The general organization of the manuscript should be:

Title
Author(s)' names and full addresses
Abstract
Text Discussion
References

2. **Title & Authors**: The entire title should be in bold-face capital letters and centered within the width of the printed area, located 2 inches (5.1 cm) from the top of the page. This should be followed by 2 lines of space, then by the names and addresses of the authors, also centered, in the following manner:

A SEMI-AUTOMATIC TECHNIQUE FOR THE SEPARATION AND DETERMINATION OF BARIUM AND STRONTIUM IN WATER BY ION EXCHANGE CHROMATOGRAPHY AND ATOMIC EMISSION SPECTROMETRY

F. D. Pierce. H. R. Brown
Utah Biomedical Test Laboratory
520 Wakara Way
Salt Lake City, Utah 84108

3. **Abstract**: The heading **ABSTRACT** should be typed boldface, capitalized and centered, 2 lines below the addresses. This should be followed by a single-spaced, concise abstract. Allow 2 lines of space below the abstract before beginning the text of the manuscript.

4. **Text Discussion**: Whenever possible, the text discussion should be divided into major sections such as

INTRODUCTION
MATERIALS
METHODS
RESULTS
DISCUSSION
ACKNOWLEDGMENTS

These **major headings** should be separated from the text by two lines of space above and one line of space below. Each major heading should be typed boldface, in capital letters, centered.

Secondary headings, if any, should be placed flush with the left margin, and have the first letter of main words capitalized. Leave two lines of space above and one line of space below secondary headings.

5. The **first line of each paragraph** within the body of the text should be indented a half inch.

6. **Acknowledgments**, sources of research funds and address changes for authors should be listed in a separate section at the end of the manuscript, immediately preceding the references.

7. **References** should be numbered consecutively and placed in a separate section at the end of the manuscript. They should be typed single-spaced, with one line space between each reference. Each reference should contain names of all authors (with initials of their first and middle names); do not use *et al.* for a list of authors. Abbreviations of journal titles will follow the American Chemical Society's Chemical Abstracts List of Periodicals. The word **REFERENCES**, in boldface type, should be capitalized and centered above the reference list.

Following are acceptable reference formats:

Journal:

1. D. K. Morgan, N. D. Danielson, J. E. Katon, Anal. Lett., 18, 1979-1998 (1985).

Book:

1. L. R. Snyder, J. J. Kirkland, **Introduction to Modern Liquid Chromato-graphy**, John Wiley & Sons, Inc., New York, 1979.

Chapter in a Book:

1. C. T. Mant, R. S. Hodges, "HPLC of Peptides," in **HPLC of Biological Macromolecules**, K. M. Gooding, F. E. Regnier, eds., Marcel Dekker, Inc., New York, 1990, pp. 301-332.

8. Each page of manuscript should be numbered lightly, with a light blue pencil, at the bottom of the page.

9. Only standard symbols and nomenclature, approved by the International Union of Pure and Applied Chemistry (IUPAC) should be used. **Hand-drawn characters are not acceptable.**

10. Material that cannot be typed, such as Greek symbols, script letters and structural formulae, should be drawn carefully with dark black India ink. Do not use any other color ink.

Additional Typing Instructions

1. The manuscript must be prepared on **good quality white bond paper**, measuring approximately 8½ x 11 inches (21.6 cm x 27.9 cm). International paper, size A4 is also acceptable. The typing area of the first page, including the title and authors, should be 6" (15.2 cm) wide by 8.5" (21.6 cm) height.

2. All text should be **typed single-spaced**.

3. It is essential to use **dark black** typewriter or printer ribbon so **that clean, clear, solid characters** are produced. Characters produced with a dot/matrix printer are not acceptable, even if they are "near letter quality" or "letter quality." Erasure marks, smudges, hand-drawn corrections and creases are not acceptable.

4. **Tables** should be typed as part of the text, but in such a way as to separate them from the text by a 2-line space above and below the table. Tables should be inserted in the text as close to the point of reference as possible. **A table may not be longer than one page.** If a table is larger than one page, it should be divided into more than one table. The word **Table** (followed by an Arabic number) should precede the table and should be centered above the table. The title of the table should have the first letters of all main words in capitals. Table titles should be typed single line spaced, across the full width of the table.

5. **Figures** (drawings, graphs, etc.) should be professionally drawn in black India ink on separate sheets of white paper, and should be placed at the end of the text. They should not be inserted into the body of the text. They should not be reduced to a small size. Preferred size for figures is from 5 inches x 7 inches (12.7 cm x 17.8 cm) to 8½ inches by 11 inches (21.6 cm x 27.9 cm). Photographs should be professionally prepared, black and white, *glossy* prints. A typewriter or lettering set should be used for all labels on the figures or photographs; they may not be hand drawn.

Captions for figures should be typed single-spaced on a separate sheet of white paper, along the full width of the type page, and should be preceded with the

word **Figure** and an Arabic numeral. All figures and lettering must be of a size that will remain legible after a 20% reduction from the original size. Figure numbers. name of senior author and an arrow indicating "top" should be written in light blue pencil on the back of the figure. Indicate the approximate placement for each figure in the text with a note written with a light blue pencil in the margin of the manuscript page.

6. The reference list should be typed single-spaced. A single line space should be inserted after each reference. The format for references should be as given above.

Manuscripts which require correction of English usage will be returned to the author for major revision.